AD-A100 490 SCIENTIFIC SERVICE INC REDWOOD CITY CA F/G 13/13
UPGRADING OF EXISTING STRUCTURES. PHASE III. SHELTER DESIGN OPT--ETC(U)
MAY 81 R S TANSLEY, B L GABRIELSEN EMW-C-0153
UNCLASSIFIED SSI-8012-6 NL

1 OF 3
AD A
100490

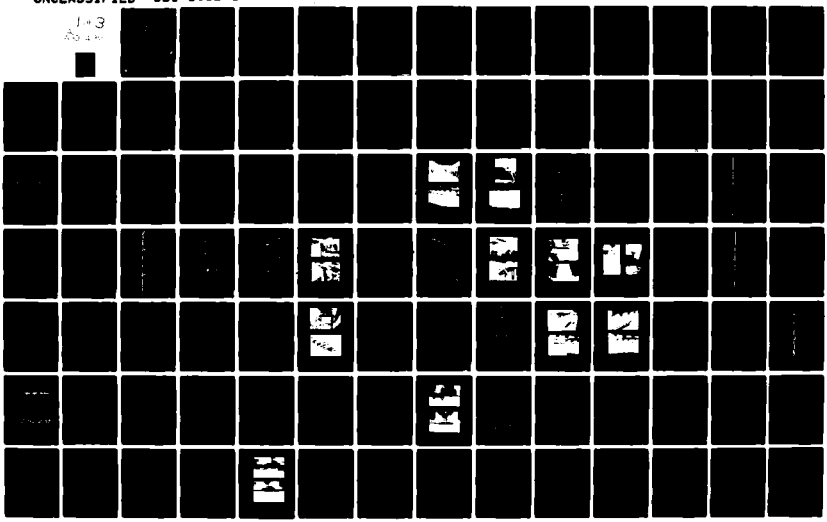

LEVEL II

(12)

BS

SSI 8012-6

May 1981

Upgrading of Existing Structures
Phase III
Shelter Design Options

AD A100490

FINAL REPORT

DTIC
ELECTE
JUN 23 1981
S D
A

DTIC FILE COPY

Approved for public release;
distribution unlimited

Contract No. EMW-C-0153
Work Unit 1128A

SCIENTIFIC SERVICE, INC.

81 6 22 109

Unclassified

SECURITY CLASSIFICATION OF THIS PAGE (When Data Entered)

REPORT DOCUMENTATION PAGE	READ INSTRUCTIONS BEFORE COMPLETING FORM
1. REPORT NUMBER: SSI-8012-6	2. GOVT ACCESSION NO.: AD-100480
	3. RECIPIENT'S CATALOG NUMBER
4. TITLE (and Subtitle): UPGRADING OF EXISTING STRUCTURES, PHASE III, SHELTER DESIGN OPTIONS	5. TYPE OF REPORT & PERIOD COVERED: Final Report
	6. PERFORMING ORG. REPORT NUMBER
7. AUTHOR(s): R.S. Tansley, B.L. Gabrielsen, and G.J. Cuzner	8. CONTRACT OR GRANT NUMBER(s): EMW-C-0153
9. PERFORMING ORGANIZATION NAME AND ADDRESS: Scientific Service, Inc. 517 East Bayshore, Redwood City, CA 94063	10. PROGRAM ELEMENT, PROJECT, TASK AREA & WORK UNIT NUMBERS: Work Unit 1128A
11. CONTROLLING OFFICE NAME AND ADDRESS: Federal Emergency Management Agency Washington, D.C. 20472	12. REPORT DATE: May 1981
	13. NUMBER OF PAGES: 262
14. MONITORING AGENCY NAME & ADDRESS (if different from Controlling Office)	15. SECURITY CLASS. (of this report): Unclassified
	15a. DECLASSIFICATION/DOWNGRADING SCHEDULE

16. DISTRIBUTION STATEMENT (of this Report)

Approved for public release; distribution unlimited

17. DISTRIBUTION STATEMENT (of the abstract entered in Block 20, if different from Report)

18. SUPPLEMENTARY NOTES

19. KEY WORDS (Continue on reverse side if necessary and identify by block number)

blast upgrading; Civil Defense; crisis relocation planning; failure prediction; shelters

20. ABSTRACT (Continue on reverse side if necessary and identify by block number)

This report presents the results of an investigation of blast upgrading of existing structures, which consisted of developing failure prediction methodologies for various structure types, both in "as built" and in upgraded configurations, and verifying these prediction techniques with full-scale load tests.

These upgrading schemes were developed for use as shelters in

DD FORM 1 JAN 73 1473 EDITION OF 1 NOV 65 IS OBSOLETE

Unclassified

SECURITY CLASSIFICATION OF THIS PAGE (When Data Entered)

Block 20: Abstract (contd)

support of Civil Defense crisis relocation planning. Structure types investigated included wood, steel, and concrete floor and roof systems.

The results of this study are being used in the development of a shelter manual presenting the various upgrading concepts in an illustrative workbook form for use in the field.

Accession For
NTIS GRA&I ☑
DTIC TAB ☐
Unannounced ☐
Justification
By
Distribution/
Availability Codes
Dist | Avail and/or Special
A

(DETACHABLE SUMMARY)

SSI 8012-6 Final Report
May 1981

Approved for public release;
distribution unlimited

UPGRADING OF EXISTING STRUCTURES

PHASE III

SHELTER DESIGN OPTIONS

by

R.S. Tansley, B.L. Gabrielsen, and G.J. Cuzner

for

Federal Emergency Management Agency
Washington, D.C. 20472

Contract No. EMW-C-0153, Work Unit 1128A
Dr. Michael A. Pachuta, Project Officer

FEMA REVIEW NOTICE:

This report has been reviewed in the Federal Emergency Management Agency and approved for publication. Approval does not signify that the contents necessarily reflect the views and policies of the Federal Emergency Management Agency.

Scientific Service, Inc.
517 East Bayshore, Redwood City, 94063

(Detachable Summary)

UPGRADING OF EXISTING STRUCTURES PHASE III

SHELTER DESIGN OPTIONS

This report presents a summary of the technical work performed during Phase III of a program to develop upgrading techniques for existing structures. This investigation has included the development of failure prediction methodologies for the most common construction types, in both "as built" and upgraded configurations. The prediction methodologies are founded on engineering mechanics, limit theory, and statistical approaches to failure analysis that enable realistic assessment to be made of failure probabilities based on the combined effects of statistical variation in materials, structural elements, and construction practices. These analysis and prediction techniques have been applied to wood, steel, and concrete roof and floor systems; both full- and small-scale verification tests, to failure, have been performed statically, dynamically, and in combination.

To date, Scientific Service, Inc., has conducted full-scale loading tests to failure on 16 wood joist floors, 3 one-way reinforced concrete floors, 15 prestressed concrete hollow-core slabs, and 3 open-web steel joist floors with metal decking and structural concrete topping. Each type of construction tested included a minimum of one base case test; that is, "as built" without any upgrading. The additional tests in each group incorporated various upgrading schemes appropriate to the construction type.

These full-scale tests have been complemented by a variety of small-scale tests that investigated punching shear of concrete floors and the contribution of the metal decking and structural concrete topping on open-web steel joist floors.

The results of the analytical and experimental program have been used to develop a preliminary survival matrix for floors, which is presented in Table 7-1. This matrix indicates the overpressure, in psi, at which 95% of the floor systems are better than the rating provided; i.e., it has been assumed that a 5% probability of collapse is an acceptable risk level. The test values obtained from the experimental program are indicated on the matrix. Also included is a preliminary survival matrix for roofs (Table 7-2). The roof matrix does not contain any test values.

The survival pressures indicated for the various types of construction were determined by assuming the dead loads (load of structure itself) and increasing the design live loads by the safety factors required for the design, as outlined in the applicable codes, for the particular construction considered.

Although the overpressure values indicated do not consider any superimposed live loads, it is assumed that some radiation protection would be required. Accordingly, the survival overpressures included the fallout radiation protection necessary to achieve a protection factor (P_f) of 100; i.e., 18 inches of earth (assumed density = 100 pcf) or other materials of comparable density. The weight of this radiation protection has been deducted from the survival overpressure when the floor or roof is in both the shored and the "as built" configurations. The test values (*italics)* have also been reduced for comparison purposes to include this radiation protection.

The basic construction type groups in Table 7-1 for floors are further divided into categories of light, medium, and heavy. These categories are based on the allowable live loads for types of occupancy, as specified in the building codes, and are defined as follows:

Light	40 to 60 psf
Medium	80 to 125 psf
Heavy	150 to 250 psf

The midspan, one-third span, and one-quarter span shoring may be lines of shoring, such as posts and beams or stud walls, placed transverse to one-way structural systems (open-web josts, double tees, etc.), or it may be post shores, located symmetrically under two-way structural systems (flat slabs, waffle slab, etc.). The king post truss shoring consists basically of cables or rods secured parallel to joists or beams and tensioned to form a king post truss configuration. The flange system consists of attaching bottom flanges to wood joists, while the boxed beam system involves "boxing" the entire ceiling system (wood joists) by attaching a plywood diaphragm, secured to the joists, under the entire ceiling.

The results of this Phase III effort have confirmed some of the survival estimates in Table 7-1 (which was first published in 1978) and have caused some modification to others.

A program summary section of this report includes charts and data from a number of reports and manuals developed by Scientific Service, Inc., as part of the overall program.

TABLE 7-1: PRELIMINARY SURVIVAL MATRIX FOR FLOORS

Overpressure at Which 95% of Floors Will Survive "As Built" and With Various Types of Shoring
(All values in psi.)

Type of Floor Construction and Dead Load	As Built		Shoring Required											
			Midspan		1/3 Span		1/4 Span		King-Post Truss		Flange		Boxed Beam	
	Pred.	Test	Pred	Test	Pred	Test	Pred	Test	Pred	Test	Pred	Test	Pred	Test
WOOD D.L. = 20 psf														
Light — Joist, Glulam*	†	*0.4*	3.3	*6.8*	8.6	*9.2*	—		1.6	*1.8*	1.1	*1.1*	1.1	*2.1*
Medium — Joist, Glulam	0.9	*1.5*	6.7	*8.1*	16.4	*12.9*	—		3.8		2.8		2.8	
Heavy — Plank	2.6		13.7		32.1		—		8.2		—		—	
STEEL, LIGHT D.L. = 30 psf														
Light — Open-Web Joist	0.2	*0.3*	1.0	*1.2*	2.8	*3.5*	—		1.0		—		—	
Medium — Open-Web Joist	1.4	*1.6*	3.0	*3.4*	6.6	*8.0*	—		2.5		—		—	
STEEL, HEAVY D.L. = 80 psf														
Light — Beam and Slab	0.1		3.1		7.9		—		—		—		—	
Medium — Beam and Slab	0.8		5.5		13.3		—		—		—		—	
Heavy — Beam and Slab	2.0		10.3		24.0		—							

Note: Overpressure values assume radiation protection equal to a P_f of 100 (18 in. of earth or equivalent) superimposed on floor. Assumed density of earth = 100 pcf.

* Glulam not tested.

† — Required radiation protection ($P_f = 100$) would cause floor to collapse.

TABLE 7-1: PRELIMINARY SURVIVAL MATRIX FOR FLOORS (contd)

Overpressure at Which 95% of Floors Will Survive "As Built" and With Various Types of Shoring
(All values in psi.)

Type of Floor Construction and Dead Load	As Built		Shoring Required											
			Midspan		1/3 Span		1/4 Span		King-Post Truss		Flange		Boxed Beam	
	Pred.	Test	Pred	Test	Pred	Test	Pred	Test	Pred	Test	Pred	Test	Pred	Test
CONCRETE D.L. = 100 psf														
Light – Single and Double Tees, One-Way Joists	0.6		4.7		11.7		–		–		–		–	
Light – Hollow-Core Slabs	0.6	*0.6*	4.8	*6.2*	11.7	*16.1*	–		–		–		–	
Light – One-Way Solid Slabs	0.9		5.0		12.0		–		–		–		–	
Light – Flat Slab, Flat Plate - Two-Way	0.9		5.0		12.0		21.7		–		–		–	
Light – Waffle Slab	0.6		4.7		11.7		21.4		–		–		–	
Medium – Single and Double Tees, One-Way Joists	1.3		7.6		18.0		–		–		–		–	
Medium – Hollow-Core Slabs	1.5	*2.2*	7.8	*10.2*	18.2	*19.8*	–		–		–		–	
Medium – One-Way Solid Slabs	1.7		8.0		18.4		–		–		–		–	
Medium – Flat Slab, Flat Plate - Two-Way	1.7		8.0		18.4		33.0		–		–		–	
Medium – Waffle Slab	1.3		7.6		18.0		32.6	*43.0**	–		–		–	

Note: Overpressure values assume radiation protection equal to a P_f of 100 (18 in. of earth or equivalent) superimposed on floor. Assumed density of earth = 100 pcf.

* Waterways Experiment Station Test

TABLE 7-1: PRELIMINARY SURVIVAL MATRIX FOR FLOORS (contd)

Overpressure at Which 95% of Floors Will Survive "As Built" and With Various Types of Shoring
(All values in psi.)

Type of Floor Construction and Dead Load	Shoring Required													
	As Built		Midspan		1/3 Span		1/4 Span		King-Post Truss		Flange		Boxed Beam	
	Pred.	Test	Pred	Test	Pred	Test	Pred	Test	Pred	Test	Pred	Test	Pred	Test
CONCRETE D. L = 100 psf														
Heavy — Single and Double Tees, One-Way Joists	2.8		13.2		30.6		—		—		—		—	
Heavy — Hollow-Core Slabs	3.0	*5.3*	13.4	*19.9*	30.8	*30.1*	—		—		—		—	
Heavy — One-Way Solid Slabs	3.3	*5.9*	13.7	*17.7*	31.1	*36.2*	—		—		—		—	
Heavy — Flat Slab, Flat Plate - Two-Way	3.3		13.7		31.1		55.4		—		—		—	
Heavy — Waffle Slab	2.8		13.2		30.6		54.9		—		—		—	

Note: Overpressure values assume radiation protection equal to a P_f of 100 (18 in. of earth or equivalent) superimposed on floor. Assumed density of earth = 100 pcf.

TABLE 7-2: PRELIMINARY SURVIVAL MATRIX FOR ROOFS

Overpressure at Which 95% of Roofs Will Survive
"As Built" and With Various Types of Shoring. All values in psi.

Type of Roof Construction and Dead Load	As Built	Shoring Required		
		Midspan	1/3 Span	1/4 Span
WOOD D.L. = 15 psf				
Joist, Glulam	†	0.6	2.7	–
STEEL, LIGHT D.L. = 25 psf				
Open-Web Joist, Plywood Deck	†	†	0.2	–
STEEL, HEAVY D.L. = 60 psf				
Open-Web Joist, Metal Deck	†	†	0.8	–
CONCRETE D.L. = 80 psf				
Single & Double Tees, One-Way Joists	0.0	2.2	6.0	–
Hollow-Core Slabs	0.0	2.3	6.1	–
One-Way Slabs	0.2	2.5	6.4	–
Flat Plate & Flat Slabs	0.2	2.5	6.4	11.7
Waffle Slabs	0.0	2.2	6.0	11.4

Note: Overpressure values assume radiation protection equal to a P_f of 100 (18 in. of earth or equivalent) superimposed on roof. Assumed density of earth = 100 pcf.

All values are predicted values.

† – Required radiation protection (P_f = 100) would cause roof to collapse.

SSI 8012-6 Final Report
May 1981

Approved for public release;
distribution unlimited

UPGRADING OF EXISTING STRUCTURES

PHASE III

SHELTER DESIGN OPTIONS

by

R.S. Tansley, B.L. Gabrielsen, and G.J. Cuzner

for

Federal Emergency Management Agency
Washington, D.C. 20472

Contract No. EMW-C-0153, Work Unit 1128A
Dr. Michael A. Pachuta, Project Officer

FEMA REVIEW NOTICE:

This report has been reviewed in the Federal Emergency Management Agency and approved for publication. Approval does not signify that the contents necessarily reflect the views and policies of the Federal Emergency Management Agency.

Scientific Service, Inc.
517 East Bayshore, Redwood City, 94063

ACKNOWLEDGEMENTS

This report describes some upgrading concepts designed to provide shelter from nuclear weapons effects, develops practical techniques for structural upgrading prediction, and attempts to substantiate the concepts and predictions by test. The authors wish to take this opportunity to thank all those involved in completing this project. We particularly wish to thank Dr. Michael A. Pachuta of the Federal Emergency Managment Agency for his contributions to overall project direction; Dr. T.C. Zsutty of San Jose State University for his contribution; and the support staff, Larue Wilton, Evelyn Kaplan, Maureen Ineich, and Michael Reeder for their patience as well as their talents. A special thanks to A.B. Willoughby for his thorough and helpful technical review.

Table Of Contents

	Page
Acknowledgements	iii
List of Figures	vii
List of Tables	xv
Metric Conversion Table	xvi
Section	
1 Introduction	1-1
2 Open-Web Steel Joist Tests	2-1
3 Prestressed Concrete Hollow-Core Slab Tests	3-1
4 Wood Floor Tests	4-1
5 Concrete Slab Punching Shear Tests	5-1
6 Summary of Phase III	6-1
7 Program Summary	7-1
8 References	8-1
Appendix	
A Open-Web Steel Joist Floor Test Failure Prediction	A-1
B Prestressed Concrete	B-1

List Of Figures

Number		Page
2-1	18H8 Open-Web Steel Joist	2-2
2-2	Test Assembly Under Construction	2-9
2-3	Test Assembly Under Construction	2-10
2-4	Construction Details	2-11
2-5	Construction Details	2-12
2-6	Loading Configuration for Test No. 79-1	2-14
2-7	Load vs Deflection, Test No. 79-1	2-15
2-8	Load vs Stress in Web Member 35, Test No. 79-1	2-16
2-9	Loading and Shoring Details, Test No. 79-2	2-18
2-10	Shoring Details, Test No. 79-2	2-19
2-11	Shoring Details, Test No. 79-2	2-20
2-12	Photographs of Shoring Details, Test No. 79-2	2-21
2-13	Load vs Deflection, Test No. 79-2	2-22
2-14	Load vs Stress, Test No. 79-2	2-23
2-15	Posttest Photographs, Test No. 79-2	2-24
2-16	Posttest Photographs, Test No. 79-2	2-25
2-17	Posttest Photographs, Test No. 79-2	2-26
2-18	Test Configuration, Test No. 79-3	2-28
2-19	Shoring Details, Test No. 79-3	2-29
2-20	Shoring Details, Test No. 79-3	2-30
2-21	Shoring Details, Test No. 79-3	2-31

2-22	Load vs Deflection, Test No. 79-3	2-32
2-23	Load vs Compressive Stress in Member 22, Test No. 79-3	2-33
2-24	Load vs Compressive Stress in Member 27, Test No. 79-3	2-34
2-25	Posttest Photographs, Test No. 79-3	2-35
2-26	Test Configuration for Test No. 80-1	2-38
2-27	Posttest Photographs, Test No. 80-1	2-39
2-28	Posttest Photographs, Test No. 80-1	2-40
2-29	Load vs Deflection, Test No. 80-1	2-41
2-30	Load vs Compressive Stress in Member 22, Test No. 80-1	2-42
2-31	Fundamental Period of Test Specimen 80-1	2-43
2-32	Fundamental Period of Web Member 22, Test No. 80-1	2-44
2-33	Test Configuration, Test No. 80-2	2-48
2-34	Test Configuration, Test No. 80-3	2-49
2-35	Load vs Deflection, Test Nos. 80-2 and 80-3	2-50
2-36	Posttest Photographs, Test No. 80-2	2-51
2-37	Test Configuration for Test No. 80-4A and 80-4B	2-55
2-38	Load vs Deflection for Test No. 80-4A	2-56
2-39	Load vs Deflection for Test No. 80-4B	2-57
2-40	Sketch Showing Location of Flexural Cracks, Test No. 80-4B	2-58
2-41	Test Arrangement for Test No. 80-5	2-60
2-42	Load vs Deflection for Test No. 80-5	2-61
2-43	Posttest Photographs, Test No. 80-5	2-62
2-44	Failure Prediction of Top Chord Assembly Loaded in the Transverse Direction	2-64

3-1	Design Properties of 4-inch Prestressed Precast Hollow-Core Plank	3-3
3-2	Design Properties of 8-inch Prestressed Precast Hollow-Core Plank	3-4
3-3	Design Properties of 10-inch Prestressed Precast Hollow-Core Plank	3-5
3-4	Loading Configuration - Base Case, 4-inch Slab, Test Nos. 1 and 2	3-8
3-5	Uniform Load vs Deflection, Test No. 1, Base Case, 4-inch Slab	3-9
3-6	Uniform Load vs Deflection, Test No. 2, Base Case, 4-inch Slab	3-10
3-7	Pre- and Posttest Photographs of 4-inch Slabs, Test Nos. 1 and 2	3-11
3-8	Test No. 1, After Test	3-12
3-9	Test No. 2, During Test	3-12
3-10	Test No. 2, After Test	3-13
3-11	Loading Configuration - Shored at Midspan, 4-inch Slabs, Test No. 3	3-15
3-12	Uniform Load vs Deflection, Test No. 3, Shored at Midspan 4-inch Slab	3-16
3-13	Pre- and Posttest Photographs, Test No. 3	3-17
3-14	Negative Moment Tension Crack, Test No. 3, After Test	3-18
3-15	Loading Configuration - Shored at One-Third Points, 4-inch Slab, Test No. 4	3-20
3-16	Uniform Load vs Deflection, Test No. 4, One-Third Shoring, 4-inch Slab	3-21
3-17	Shoring Details, Test No. 4, Before Test	3-22
3-18	Posttest Photographs, Test No. 4	3-23
3-19	Loading Configuration, Base Case, 8-inch Slab, Test No. 5	3-25
3-20	Uniform Load vs Deflection, Test No. 5, Base Case, 8-inch Slab	3-26

3-21	Pre- and Posttest Photographs, Test No. 5	3-27
3-22	Posttest Photographs, Test No. 5	3-28
3-23	Test No. 6, Steel Shore	3-30
3-24	Test No. 7, Timber Shore With 1½-inch Gap	3-30
3-25	Loading Configuration - Shored at Midspan, 8-inch Slabs, Test Nos. 6 and 7	3-31
3-26	Uniform Load vs Deflection, Test No. 6, Midspan Shoring, 8-inch Slab	3-33
3-27	Pre- and Posttest Photographs, Test No. 6	3-34
3-28	Posttest Photographs, Test No. 6	3-35
3-29	Uniform Load vs Deflection, Test No. 7, Midspan Shoring 8-inch Slab	3-37
3-30	Pre- and Posttest Photographs, Test No. 7	3-38
3-31	Left and Right Span Failures, Test No. 7	3-39
3-32	Loading Configuration - Two Shores, 8-inch Slabs, Tests Nos. 8 and 9	3-41
3-33	Uniform Load vs Deflection, Test No. 8, One-Third Point Shores, 8-inch Slab	3-43
3-34	Pre- and Posttest Photographs, Test No. 8	3-44
3-35	Posttest Photographs, Test No. 8	3-45
3-36	Uniform Load vs Deflection, Test No. 9, One-Quarter Point Shores, 8-inch Slab	3-47
3-37	Test No. 9 After Test, Showing Center Span Failure	3-48
3-38	Left and Right Span Failures, Test No. 9	3-49
3-39	Loading Configuration - Base Case, 10-inch Slab, Test No. 10	3-51
3-40	Uniform Load vs Deflection, Test No. 10, Base Case, 10-inch Slab	3-52
3-41	Test No. 10, Before Test	3-53
3-42	Test No. 10, During Test	3-53

3-43	Test No. 10, After Test	3-54
3-44	Closeup Photographs of Test No. 10 After Test	3-55
3-45	Steel Shore (Test No. 11) and Timber Shore (Test No. 12) Prior to Test	3-57
3-46	Loading Configuration - Shored at Midspan, 10-inch Slabs, Tests Nos. 11 and 12	3-58
3-47	Uniform Load vs Deflection, Test No. 11, Midspan Shoring, 10-inch Slab	3-60
3-48	Pre- and Posttest Photographs, Test No. 11	3-61
3-49	Posttest Photographs, Test No. 11	3-62
3-50	Uniform Load vs Deflection, Test No. 12, Midspan Shoring, 10-inch Slab	3-64
3-51	Test No. 12, During and After Test	3-65
3-52	Closeup Photographs of Test No. 12 After Test	3-66
3-53	Loading Configuration - Shored at One-Third Points, 10-inch Slab, Test No. 13	3-68
3-54	Uniform Load vs Deflection, Test No. 13, One-Third Point Shoring, 10-inch Slab	3-69
3-55	Pre- and Posttest Photographs, Test No. 13	3-70
3-56	Test No. 13, Failure Near Left and Right Support	3-71
3-57	Test No. 13, After Test	3-72
3-58	Loading Configuration - Two Shores, 10-inch Slabs, Tests Nos. 14 and 15	3-74
3-59	Uniform Load vs Deflection, Test No. 14, Shored at One-Third Points, 10-inch Slab	3-76
3-60	Pre- and Posttest Photographs, Test No. 14	3-77
3-61	Posttest Photographs, Test No. 14	3-78
3-62	Uniform Load vs Deflection, Test No. 15, Shored at One-Quarter Points, 10-inch Slab	3-80
3-63	Pre- and Posttest Photographs, Test No. 15	3-81
3-64	Posttest Photographs, Test No. 15	3-82

4-1	Framing Detail for All Floor Assemblies	4-2
4-2	Construction Details for All Floor Assemblies	4-3
4-3	Flooring Details for All Floor Assemblies	4-4
4-4	Loading Configuration - Base Case, Assembly No. 14	4-7
4-5	Uniform Load vs Deflection, Assembly No. 14	4-8
4-6	Assembly No. 14 After Test	4-9
4-7	Failed Joist Looking Toward Sill and Initiation of Crack, Assembly No. 14	4-10
4-8	Failed Joist Looking in Direction of Crack Propagation, Assembly No. 14	4-10
4-9	Shore Used at Midspan, Assembly No. 15	4-12
4-10	Loading Configuration, Shored at Midspan, Assembly No. 15	4-13
4-11	Uniform Load vs Deflection, Assembly No. 15	4-14
4-12	Assembly No. 15 Before Test	4-15
4-13	Shore Before Test, Assembly No. 15	4-15
4-14	Shore After Test, Showing Bearing Failure of Horizontal Member, Assembly No. 15	4-16
4-15	Midspan Flexural Failure, Assembly No. 15	4-16
4-16	Shores Used at One-Third Span, Assembly No. 16	4-18
4-17	Loading Configuration, Shored at One-Third Span, Assembly No. 16	4-19
4-18	Uniform Load vs Deflection, Assembly No. 16	4-20
4-19	Assembly No. 16, Before Test	4-21
4-20	Shore Before Test, Assembly No. 16	4-22
4-21	Shores After Test, Assembly No. 16	4-22
4-22	Failed Joist, Assembly No. 16	4-22
5-1	Load Conditions for Shore-Supported Roof Slab and Slab on Grade	5-2
5-2	Test Slabs, Reinforcing Steel Layout	5-4

5-3	Forms Prior to Casting	5-5
5-4	Typical Test Setup With Load and Support Conditions	5-8
5-5	Timber Post Setup	5-9
5-6	Steel Plate Test Setup	5-10
5-7	Posttest Photographs, Test Nos. 1 and 2	5-11
5-8	Posttest Photographs, Test No. 3	5-12
5-9	Posttest Photographs, Test Nos. 4 and 6	5-13
5-10	Posttest Photographs, Test Nos. 7 and 8	5-14
5-11	Posttest Photographs, Test Nos. 9 and 10	5-15
A-1	Load vs Deflection, Test No. 80-1	A-3
A-2	Computer Model Analysis Results of 18H8 Open-Web Joist (Failure Load, w_u = 1,070 plf/joist)	A-5
A-3	Load vs Deflection, Test No. 79-2	A-6
A-4	Computer Model Analysis Results for a Doubled Shored 18H8 Open-Web Steel Joist (Ultimate Failure Load, w_u = 3,300 plf/joist)	A-8
A-5	Load vs Deflection, Test No. 79-3	A-9
A-6	Computer Model Analysis Results for a Single Shored 18H8 Open-Web Steel Joist (Ultimate Failure Load w_u = 1,750 plf/joist)	A-11
B-1	Design Properties of 4-inch Prestressed Precast Hollow-Core Plank	B-2
B-2	Design Properties of 8-inch Prestressed Precast Hollow-Core Plank	B-3
B-3	Design Properties of 10-inch Prestressed Precast Hollow-Core Plank	B-4
B-4	Description of Failure Modes	B-12
B-5	Relation of Average Bond Stress to Strand Embedment Length	B-16

List Of Tables

Number		Page
2-1	Performance Predictions	2-4
2-2	Preliminary Predictions Compared with Test Data	2-5
2-3	Revised Performance Predictions Compared with Test Data	2-7
2-4	Ultimate Moment Capacity of Fluted Metal Deck with Concrete Topping	2-63
2-5	Decking Load-Carrying Capacity in the Transverse Direction	2-65
3-1	Prestressed Concrete Hollow-Core Slabs - Summary of Test Data	3-83
4-1	Wood Floors - Summary of Test Data	4-24
5-1	Punching Shear Tests	5-7
5-2	Summary of Slab Strength Predictions and Test Results	5-19
7-1	Preliminary Survival Matrix for Floors	7-3
7-2	Preliminary Survival Matrix for Roofs	7-6
7-3	Survival Pressure Matrix for Walls	7-7
7-4	Expedient Shelter Survival Matrix	7-10
7-5	Punching Shear Tests	7-13
A-1	Revised Performance Predictions Compared With Test Data	A-13
B-1	Notation	B-5
B-2	Calculated vs Actual Failure Mode Capacities	B-19

METRIC CONVERSION TABLE

Conversion Factors for U.S. Customary
to Metric (SI) Units of Measurement

To convert from:	To:	Multiply by:
inch	meter (m)	2.540×10^{-2}
foot	meter (m)	0.3048
yard	meter (m)	0.9144
square inch	meter^2 (m^2)	6.452×10^{-4}
square foot	meter^2 (m^2)	9.290×10^{-2}
pound	kilogram (kg)	0.4536
pounds per linear foot (plf)	newtons per meter (N/m)	14.5939
kip	newton (N)	4.448×10^3
kips per foot	kilonewtons per meter	14.5932
pressure (psi)	pascal (Pa)	6.894×10^3
pounds per square foot (psf)	pascal (Pa)	47.88
ksi	pascal (Pa)	6.894×10^6
kips per square foot (KSF)	pascal (Pa)	4.788×10^3
inch-pounds	meter-newtons	0.1129848
inch-pounds per foot	meter-newtons/meter	0.370682
degrees Fahrenheit	degrees Celsius	$(t_{oF} - 32)/1.8$

Section 1
INTRODUCTION

BACKGROUND

Current Civil Defense planning in the United States is based on the policy of "Crisis Relocation." This policy presumes that a period of crisis buildup or international tension would precede any future major war. This period of crisis would allow time — a few days or weeks — to accomplish a number of activities to protect the civilian population and industry from attack. These activities include:

1) Evacuation of most of the population out of risk areas to host areas where only fallout and possibly low-level blast protection would be required.

2) Development of shelter in the risk area for a relatively small contingent of key workers who would remain behind to maintain necessary services — fire protection, communications, military production, etc.

3) Hardening and protection of industry.

Scientific Service, Inc., is conducting three interrelated programs in support of crisis relocation planning. These programs, which are sponsored by the Federal Emergency Management Agency, include: the development and testing of an industrial hardening manual, the development and implementation of shelter plans for three test communities, and this effort, which is the development of shelter design options.

There were several parts to this program: a combined analytical

and experimental effort to determine the as-built failure strength of structural systems and also to develop a range of upgrading techniques for three structural systems; the development of a preliminary working draft of a key worker shelter manual (Ref. 1) and supplying revisions for the Host Area Shelter Manual (Ref. 2), which was developed under Phase II of this effort. This report presents the results from the analytical and experimental portions of this effort.

REPORT ORGANIZATION

This is the technical report for Phase III of a program to develop criteria for upgrading of existing structures. The Phase I and Phase II reports (Refs. 3 and 4) contain much of the backup material and preliminary test data necessary to an understanding of the results of the program conducted this year. To minimize the inconvenience of undue reference to these previous reports, some of that material has been summarized and included in this report.

The remainder of this report is organized as follows:

Section 2	Open-Web Steel Joist Tests
Section 3	Prestressed Concrete Hollow-Core Slab tests
Section 4	Wood Floor Tests
Section 5	Concrete Slab Punching Shear Tests
Section 6	Summary of Phase III
Section 7	Program Summary
Section 8	References
Appendix A	Open-Web Steel Joist Floor Test Failure Prediction
Appendix B	Prestressed Concrete

Section 2
OPEN-WEB STEEL JOIST TESTS

INTRODUCTION

During the previous two phases of the program, effort was devoted to predicting the behavior of upgrading techniques for floor and roof systems constructed with open-web steel joists. These joists, which are widely used for roofs and light to medium design (up to 125 psf) floors, basically consist of top and bottom chords made up of two light angles, two bars, or a tee, and web members made from a continuous round bar bent back and forth between the chords (to form the webs) and welded to the chords. The joists used in this program were type 18H8 and consisted of two back-to-back angles top and bottom (see Figure 2-1). The 18H8 joist was chosen because of its common use, and a 20-ft length span was chosen because it was a typical span and would only require one row of bridging in order to be consistent with the Steel Joist Institute recommendations. Accordingly, the selected joist and span combination represents an upper bound for maximum unbraced length for the lower chord.

Under normal service conditions, the top chords of open-web steel joists are subjected to axial compression and are restrained laterally by the floor slab or roof deck above. The bottom chords are subjected to axial tension. The web members develop both tension and compression, with compression being the most critical because of the slenderness of the member. The mode of failure for a given joist is a function of the span and loading.

The procedure used in this program is to make predictions based on conventional truss analysis and validate these predictions by laboratory

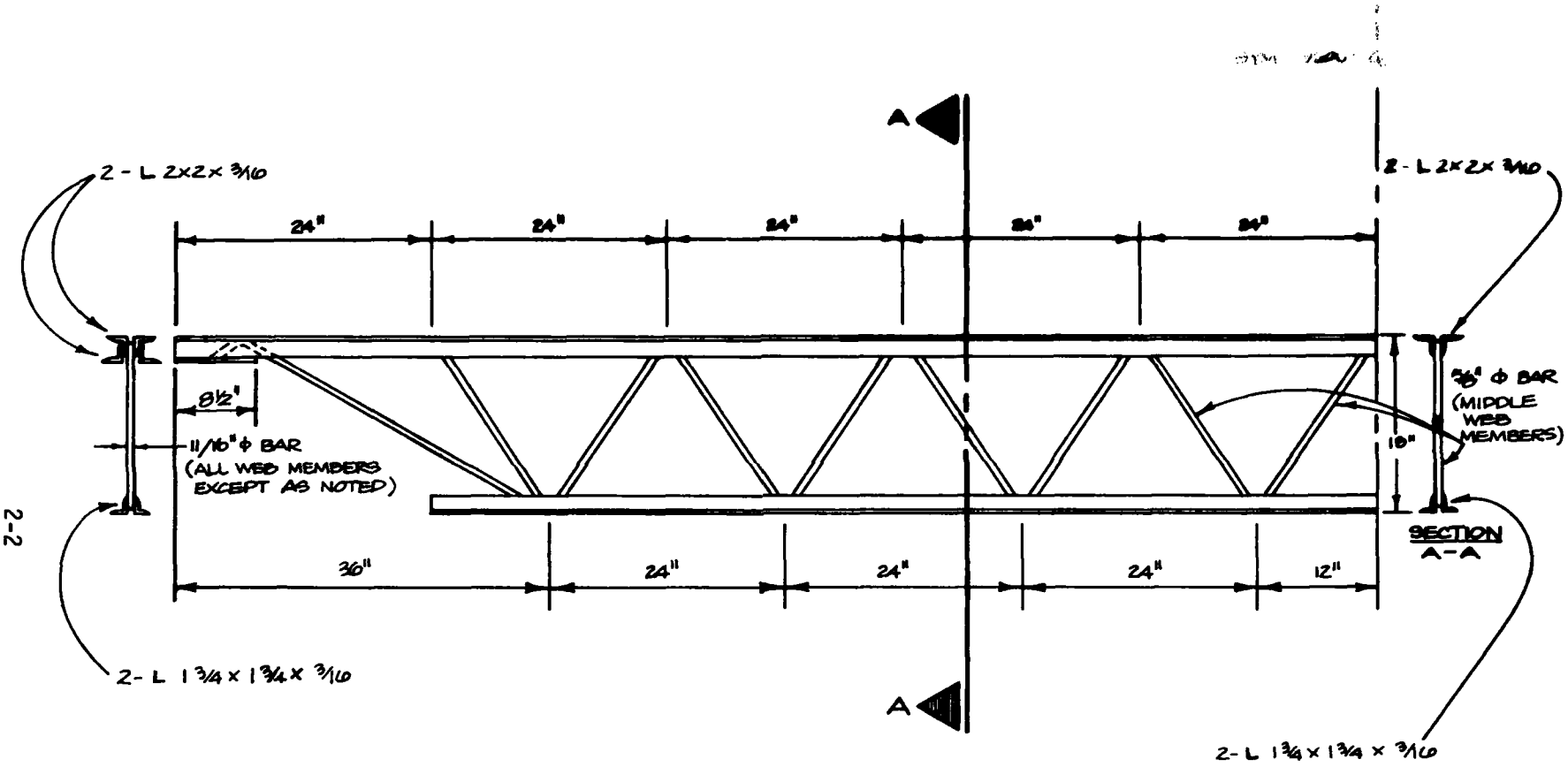

Fig. 2-1. 18H8 Open-Web Steel Joist.

tests conducted by Scientific Service, Inc., at San Jose State University and data from other sources, such as the Waterways Experiment Station. By using this approach of alternating laboratory tests with data review and prediction analysis, and then modifying the laboratory test program, it is possible to predict the behavior of the majority of these system types with a minimum of full-scale testing.

Prior to the initiation of the test program, performance predictions were made for a range of upgrading options involving shoring (Ref. 3). Because of lack of test data, many simplifying assumptions were made in these predictions, the most significant of which was to neglect the contribution of the metal and concrete decking. These predictions are presented in Table 2-1. It will be noted that both rigid shores and shores with a gap are considered.

TEST PROGRAM SUMMARY

During Phase II, conducted in 1978 and 1979 (Ref. 4), a series of three full-scale tests of open-web steel joist floor systems was conducted. These tests were as follows:

Number	Description
79-1	Case 1 — base case, no shoring (not tested to failure)
79-2	Case 3a — shores at third points with 1/8-inch gap
79-3	Case 2b — shore at midspan with 1/4-inch gap

The results of these tests are summarized and compared with the predictions from Table 2-1 in Table 2-2. It will be noted that the test failure loads are higher than the preliminary predicted values, suggesting strongly that the decking, which was not considered in the preliminary predictions, contributed significantly to the system's overall performance.

TABLE 2-1: PERFORMANCE PREDICTIONS

Open-Web Joist, H-Series, 18H8, 20-ft Span, Simply Supported

Case No.	Type of Shoring	Calculated Safe Load (plf)	Calculated Ultimate Load (plf)	(psi)**	Predicted Type of Failure	Percent of Case No. 1
1	None - Base Case	441*	794	1.84	Web buckling	100%
2	Rigid shore at center of span	425	765	1.77	Web buckling	96%
2a	Shore at center with 1/8-in. gap	615	1,107	2.56	Web buckling	139%
2b	Shore at center with 1/4-in. gap	805	1,449	3.35	Web buckling	182%
3	Rigid shores at the third points	991	1,784	4.13	Bottom chord buckling	225%
3a	Shores at the third points with 1/8-in. gap	1,028	1,850	4.28	Web buckling	233%
3b	Shores at the third points with 1/4-in. gap	1,028	1,850	4.28	Web buckling	233%

* Determined using the actual joist dimensions and assuming the web members to be pinned at both ends.

** Calculated for typical 3 ft joist spacing.

TABLE 2-2: PRELIMINARY PREDICTIONS COMPARED WITH TEST DATA

Open-Web Joist, H-Series, 18H8, 20-ft Span, Simply Supported

Test No.	Type of Shoring	Preliminary* Predicted Ultimate Failure Load (plf)	Tested Ultimate Failure Load (plf)	Relative Error of the Predicted Failure Load (%)
80-1	None — Base Case	794	1,160	- 32
79-3	Shore at center with 1/4-in. gap	1,449	1,928	- 24
79-2	Shores at third points with 0.11-in. gap	1,850	3,920	- 53

* See Ref. 4, Table 2-1.

This led to the Phase III program, conducted in 1980, where it was determined that it would be desirable to conduct a base case test to failure and then use sections of previously tested specimens for a series of four smaller scale tests, directed specifically to obtaining performance data on the decking and to determining the ultimate moment capacity of the top chord of the open-web joist and its contribution to the full-scale floor system's strength and stiffness. These tests were as follows:

Number	Description
80-1	Case 1 — base case, no shoring (tested to failure at 1,160 plf)
80-2	Small scale, longitudinal direction loading
80-3	Small scale, longitudinal direction loading
80-4	Small scale, transverse direction loading
80-5	Small scale, transverse direction loading

A finite element analytical model (described in Appendix A) was then developed, which with the data from the test program was used to make revised performance predicitons. These predictions are presented in Table 2-3.

The remainder of this section presents a brief description of the test procedures and the test results for each of the 1979 and 1980 tests.

TABLE 2-3: REVISED PERFORMANCE PREDICTIONS COMPARED WITH TEST DATA

Open-Web Joist, H-Series, 18H8, 20-ft Span, Simply Supported

Test No.	Type of Shoring	Predicted Ultimate Failure Load (plf/joist)	Tested Ultimate Failure Load (plf/joist)	Relative Error of Predicted Failure Load (%)	Increased Load-Carrying Capacity Over Base Case* (%)
80-1	None — Base Case	1,070	1,160	- 8	0
79-3	Shore at center with 1/4-in. gap	1,750	1,928	- 9	66
79-2	Shores at third points with 0.11-in. gap	3,300	3,920	-16	238

* Based on test data

FULL-SCALE TESTS OF OPEN-WEB JOIST FLOOR SPECIMENS

Test Arrangement

Four full-scale tests on open-web joist floor systems have been conducted to date. All of the test specimens have an overall dimension of 6 feet by 20 feet, and consist of three open-web steel joists (18H8), spaced 2 feet on center, and supporting VERCO, type B-30 FORMLOK®, 1½-inch deep, 22-gauge fluted metal deck with a 4½-inch maximum concrete topping. The concrete topping was 3 inches in depth above the flutes and was reinforced with 6x6—W1.1xW1.4 welded wire fabric. The metal decking was attached to the joists with plug welds in accordance with the manufacturer's recommendations, and the concrete strength was greater than 4,000 psi at the time of testing.

Photographs of the test assemblies under construction are shown in Figures 2-2 and 2-3, and details are shown in Figures 2-4 and 2-5.

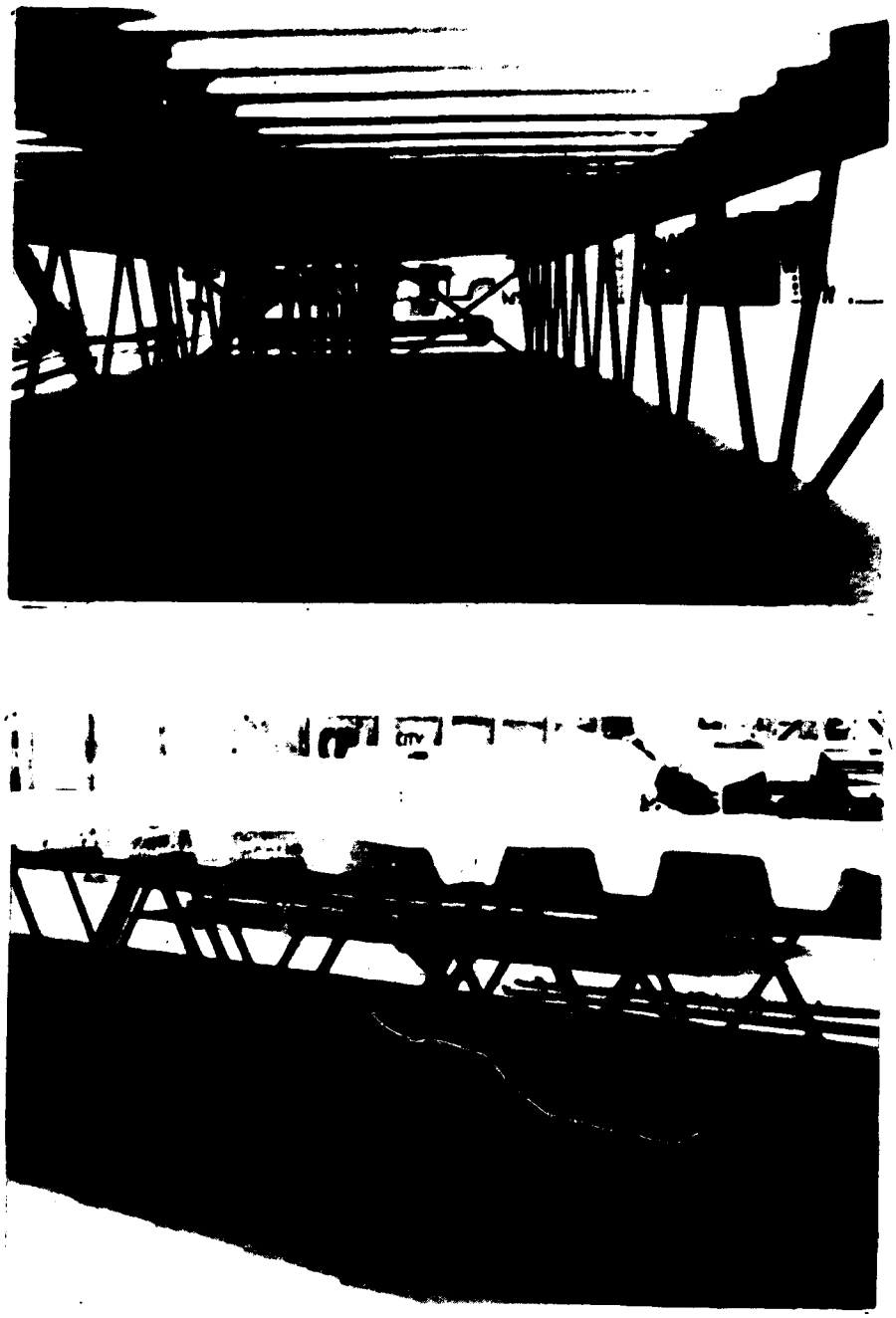

Fig. 2-2. Test Assembly Under Construction.

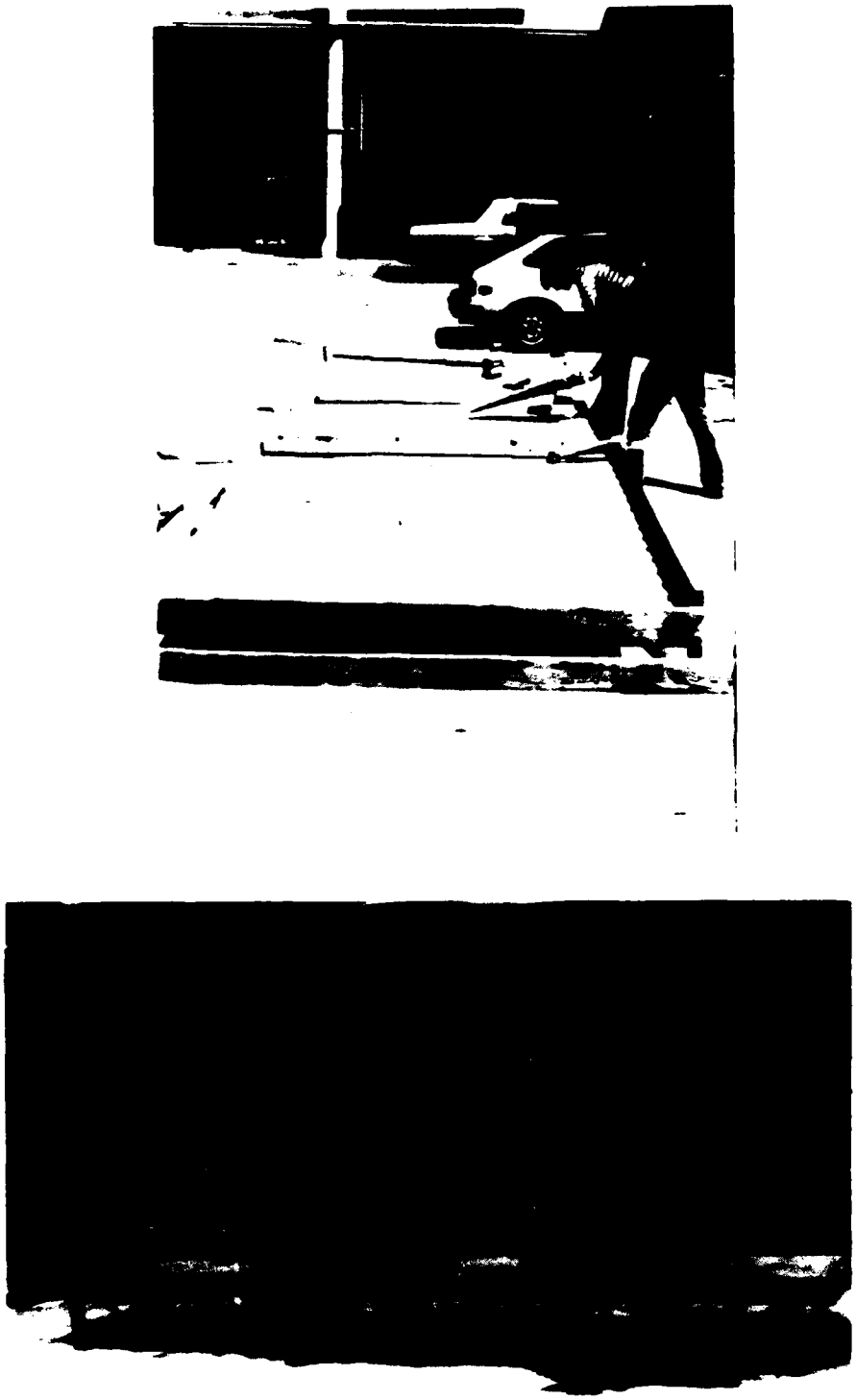

Fig. 2-3. Test Assembly Under Construction.

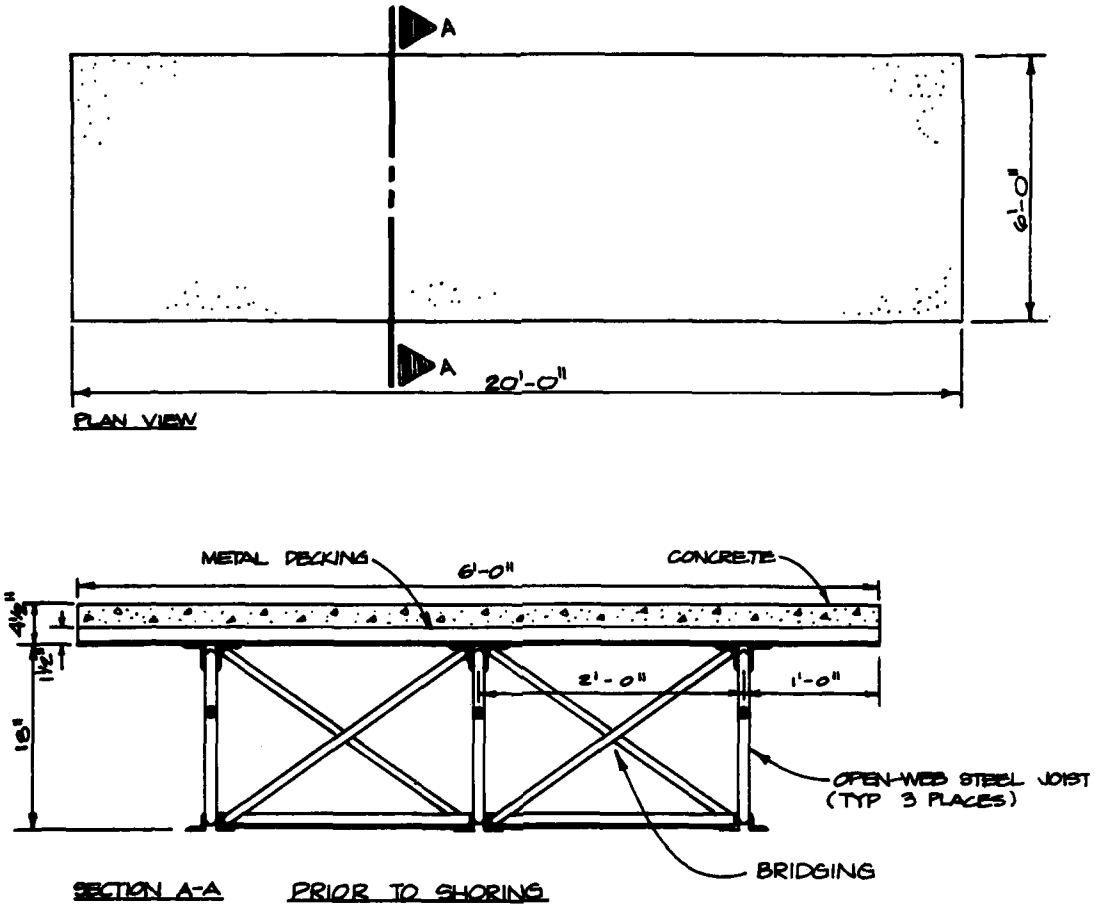

Fig. 2-4. Construction Details.

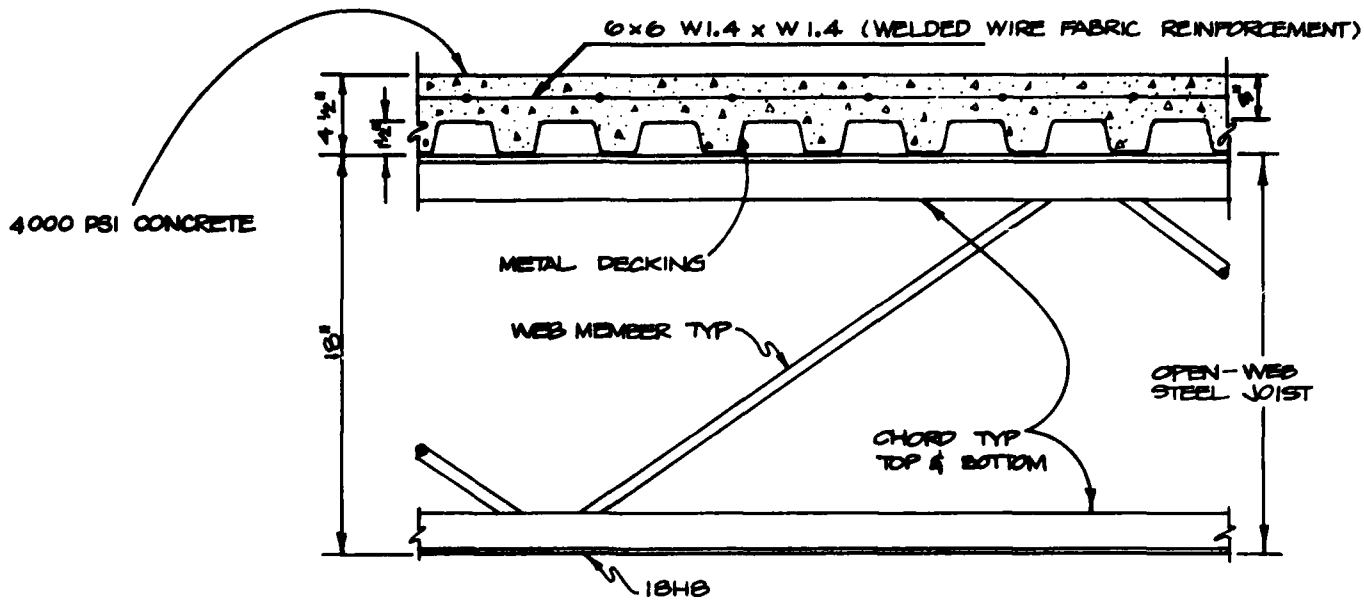

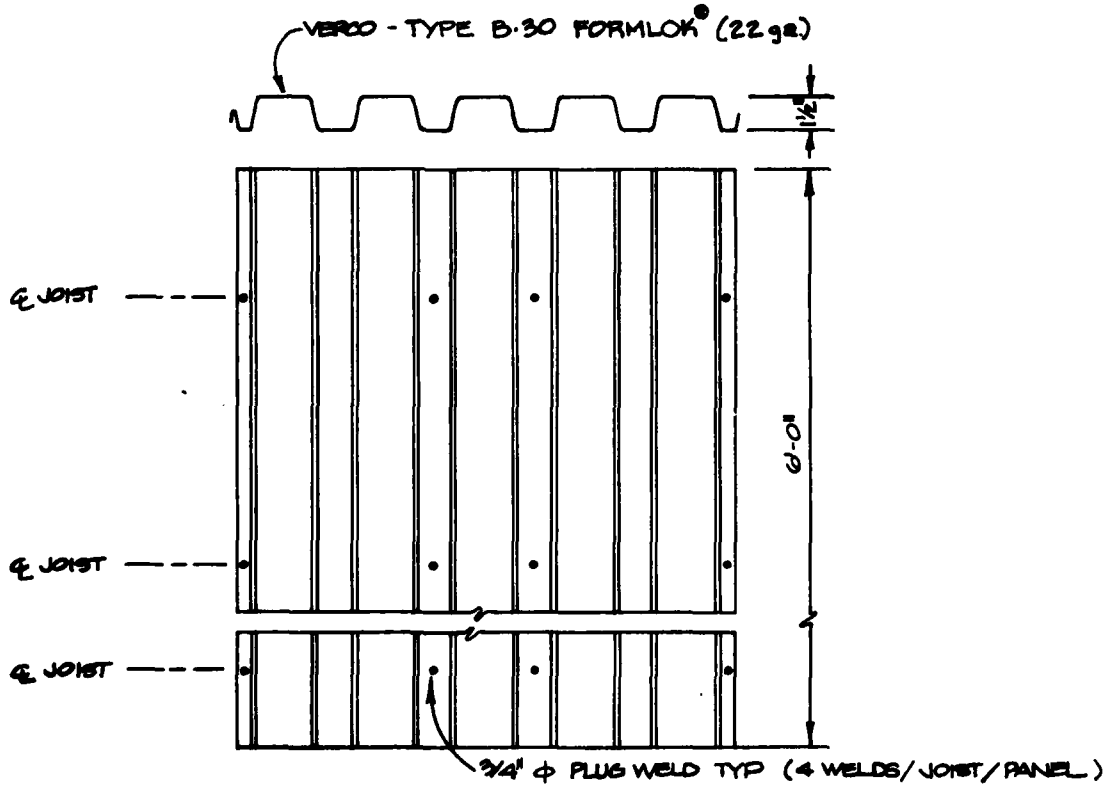

Fig. 2-5. Construction Details.

Test No. 79-1 (Base Case)

This test was conducted without any shoring or upgrading modification. The test specimen was not loaded to failure, but was tested to obtain load deflection data in the elastic domain. Loading was applied to the test specimen by hydraulic rams at eight locations, spaced equally along the length of the test sample to simulate, as closely as possible, a uniform load. The loading configuration is shown in Figure 2-6.

The load was applied at a slow rate of 1,000 lb/ram increments with deflection and strain data recorded at each load increment. The test was terminated at 7,500 lb/ram, or 595 plf/joist,* in order to preserve the structural integrity of the assembly, since it was to be used again in Test No. 79-3.

A plot of applied load per joist vs midspan deflection for Test No. 79-1 is shown in Figure 2-7, and a plot of applied load per joist vs compressive stress in web member 35 is shown in Figure 2-8. A review of this data shows it to be linear and within the elastic range, indicating that no permanent structural damage had been done.

* Includes 95 plf/joist dead load.

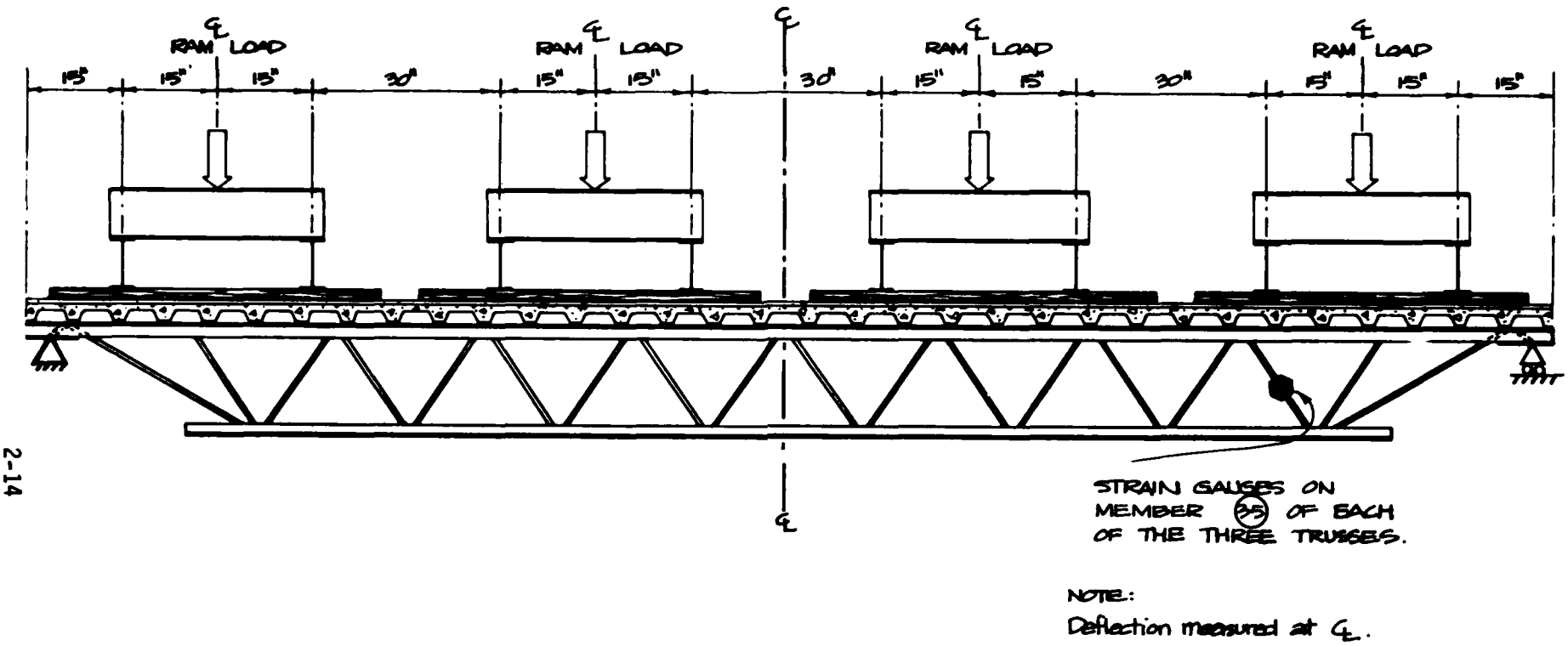

Fig. 2-6. Loading Configuration for Test No. 79-1.

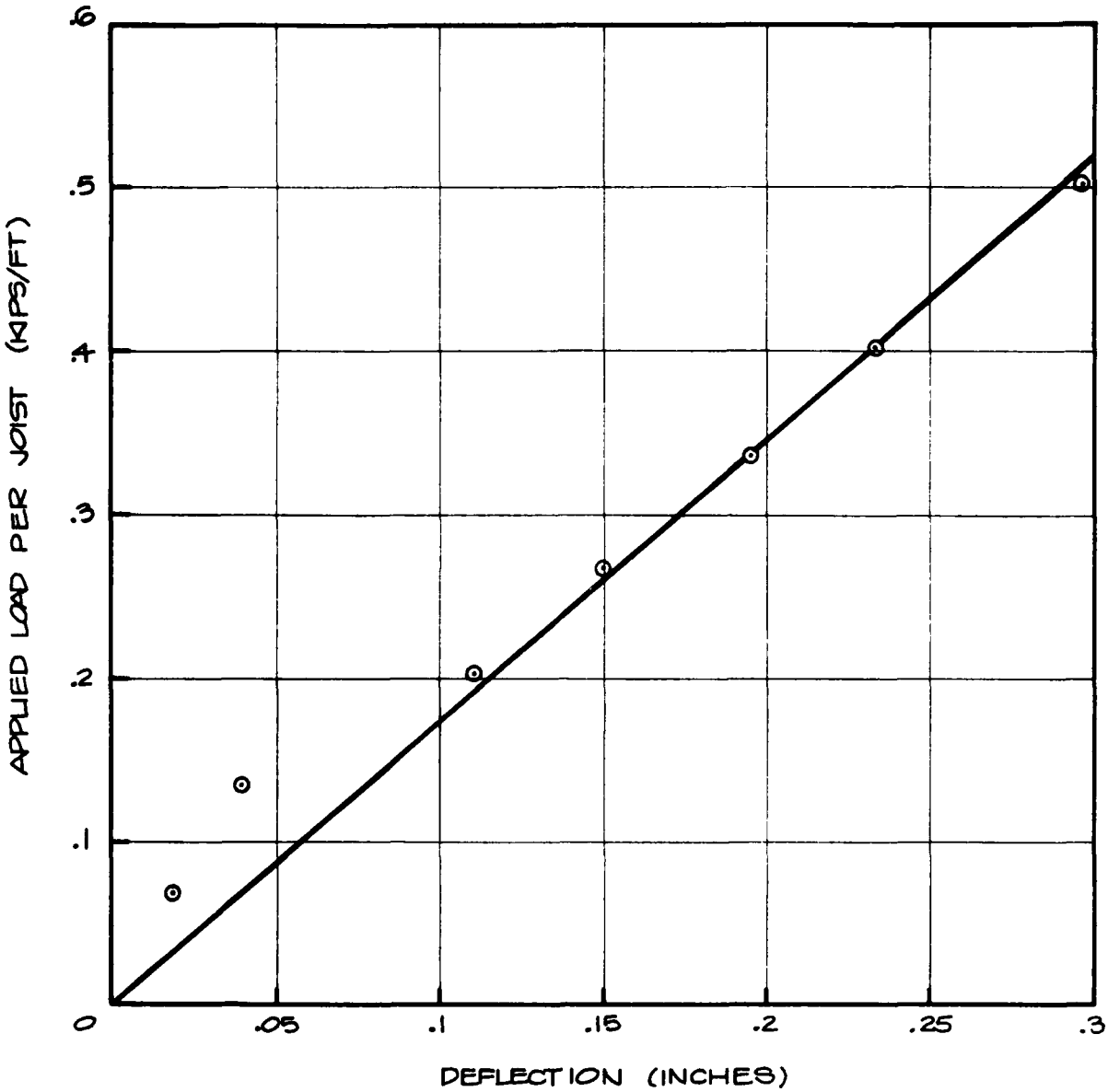

Fig. 2-7. Load vs Deflection, Test No. 79-1.

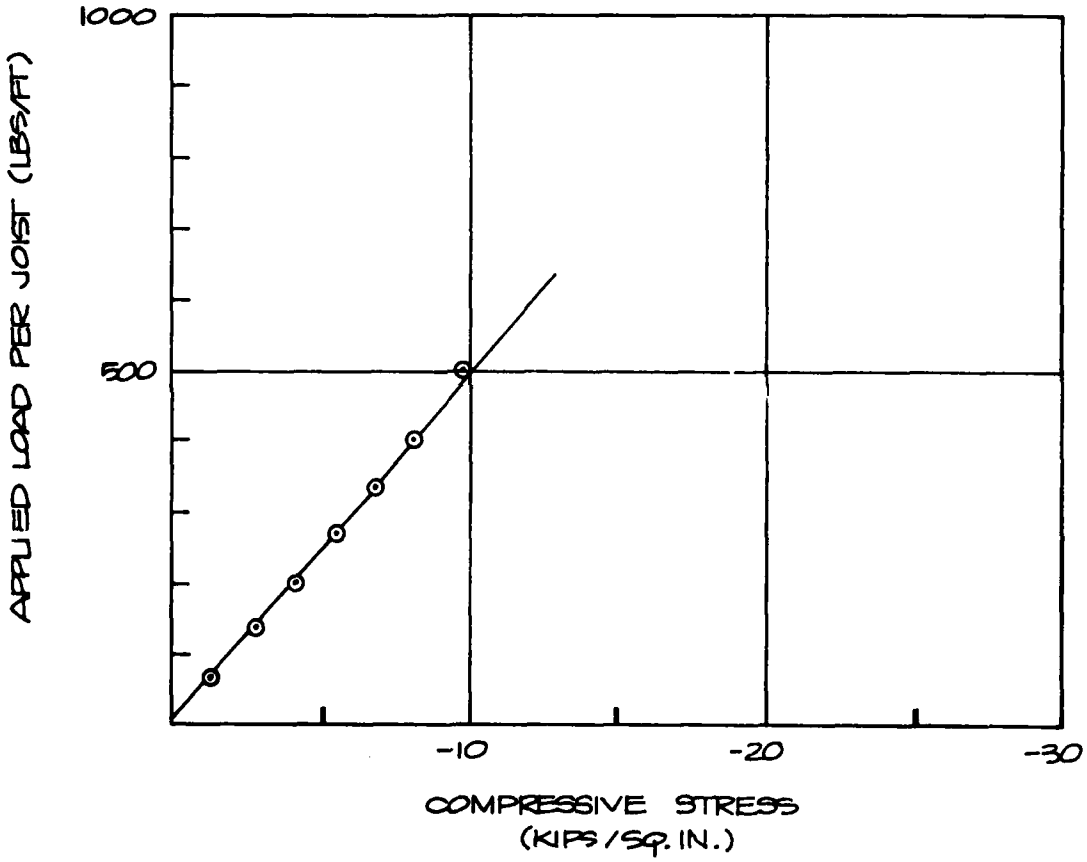

Fig. 2-8. Load vs Stress in Web Member (35), Test No. 79-1.

Test No. 79-2 (Shored at Third Points)

The test configuration and loading arrangement was essentially the same as in Test No. 79-1. Two rows of shoring were installed approximately at the third points of the floor system. A 0.11-inch stress control gap was left between the top of the shores and the joist (see Figures 2-9, 2-10, 2-11, and 2-12 for shoring location and details).

In addition to dial gauges measuring deflection at midspan, two dial gauges were placed on the decking directly over the left shore. Three strain gauges were placed on the open-web joist and were located on members 31, 35, and 19.

Load was applied slowly at 5,000 lb/ram load increments, with deflection and strain data recorded at each increment. The load was increased to approximately 50,000 lb/ram, at which point load cell recording devices had reached full scale, and the load was removed. The load cell recording device's scale range was increased, and a second load test was performed, but deflection and strain data were not taken. Load was increased to approximately 30,000 lb/ram and then ramped to failure. Failure occurred at 57,300 lb/ram, or 3,820 plf/joist. When dead load is included, the ultimate failure occurred at 3,920 plf/joist. Plots of load vs deflection are shown in Figure 2-13 and load vs stress in members 35, 31, and 19 in Figure 2-14.

A posttest examination of the floor system indicated that two failures had occurred. One of the failures occurred at the left shoring support (see Figure 2-15). Load was transferred between the floor system and the shore through steel bearing plates atop a horizontal wood beam. A bearing failure occurred here in the wood, which ultimately led to the shear failure in the horizontal wood beam. The other failure was at the left support where web member 20 had undergone considerable elongation due to strain hardening, as evidenced by the cracked and chipped paint along the length of the member. Additionally, the concrete deck and double angle top chord rotated a few inches away from the left support and ultimately caused a flexural failure in the concrete deck, which is shown in Figures 2-16 and 2-17.

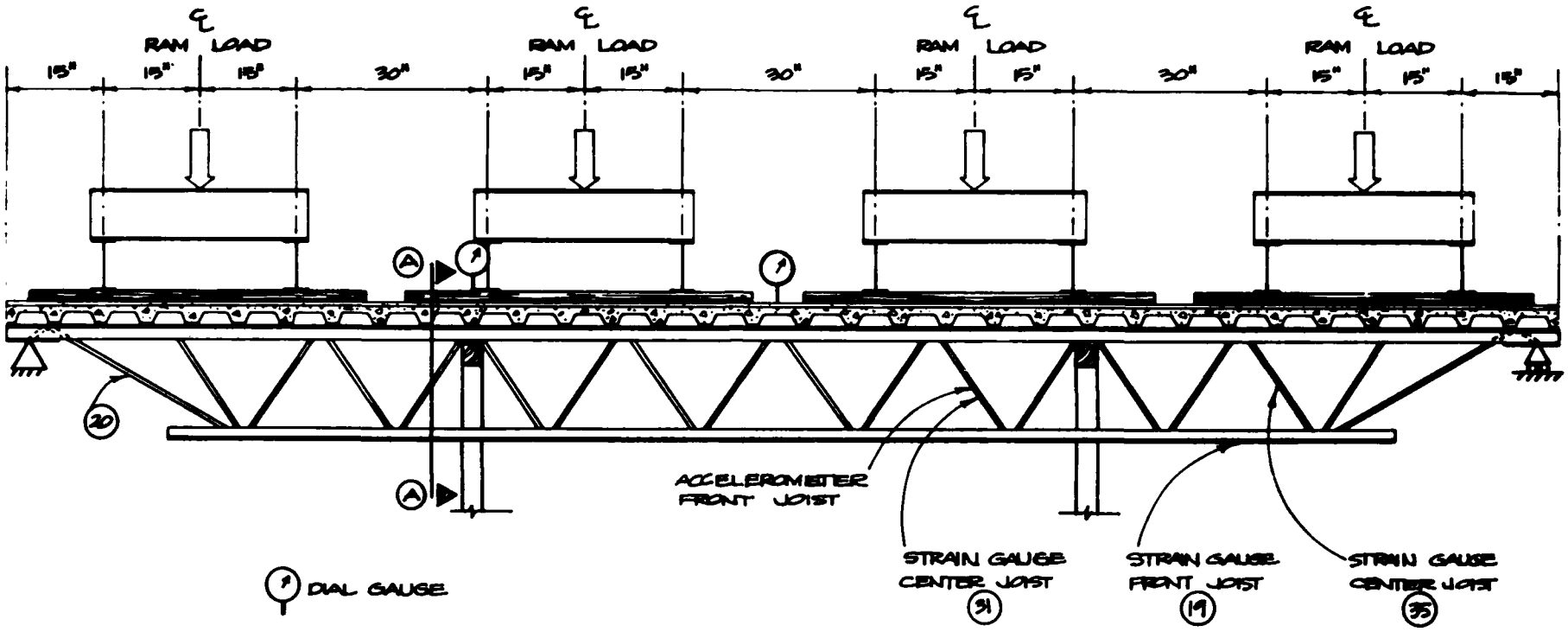

Fig. 2-9. Loading and Shoring Details, Test No. 79-2.

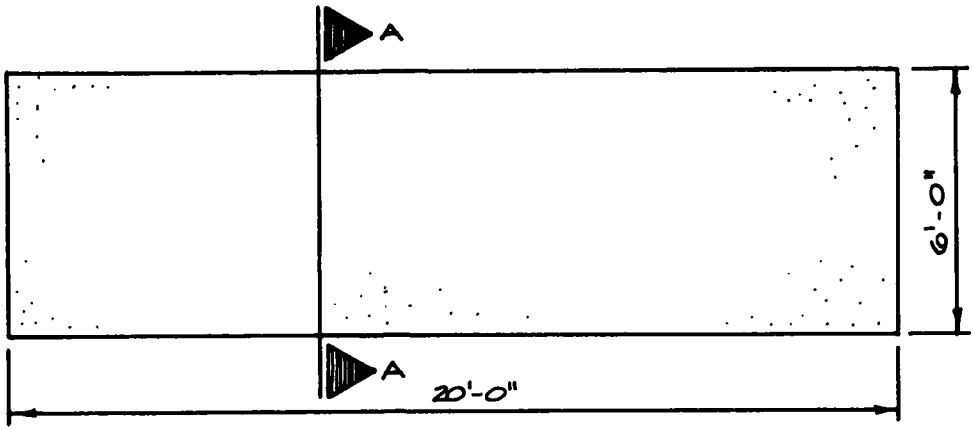

PLAN VIEW

DETAIL 1

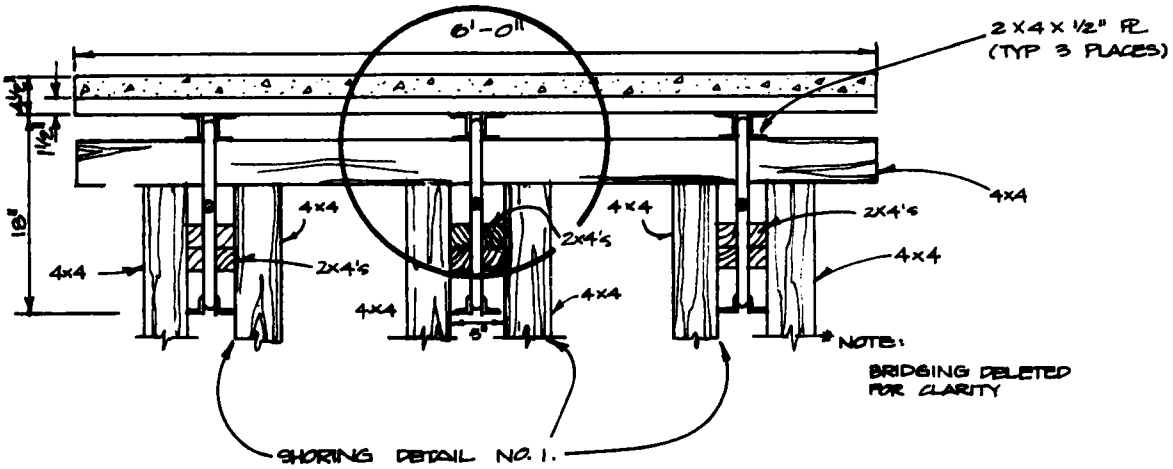

Fig. 2-10. Shoring Details, Test No. 79-2.

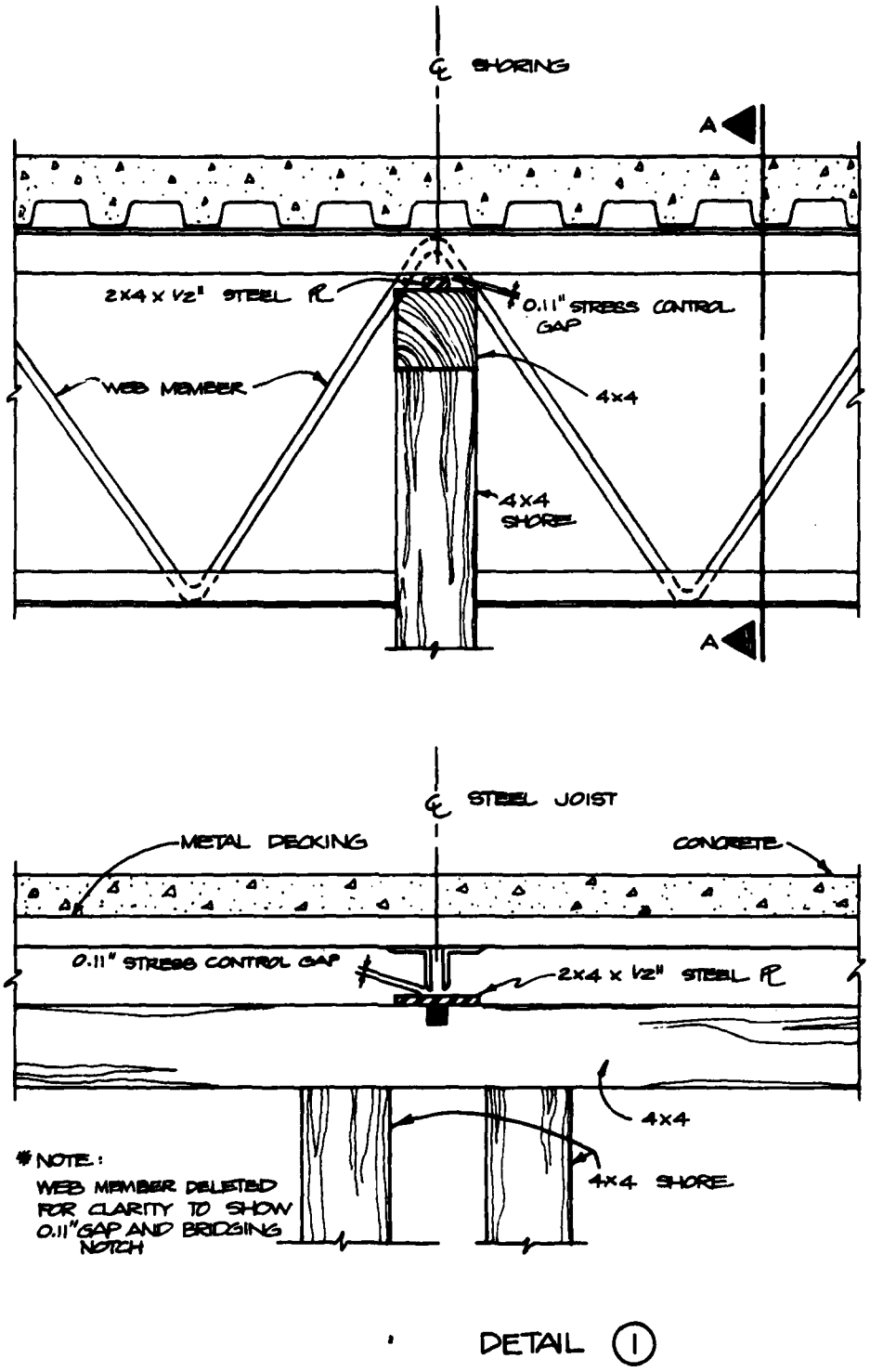

Fig. 2-11. Shoring Details, Test No. 79-2.

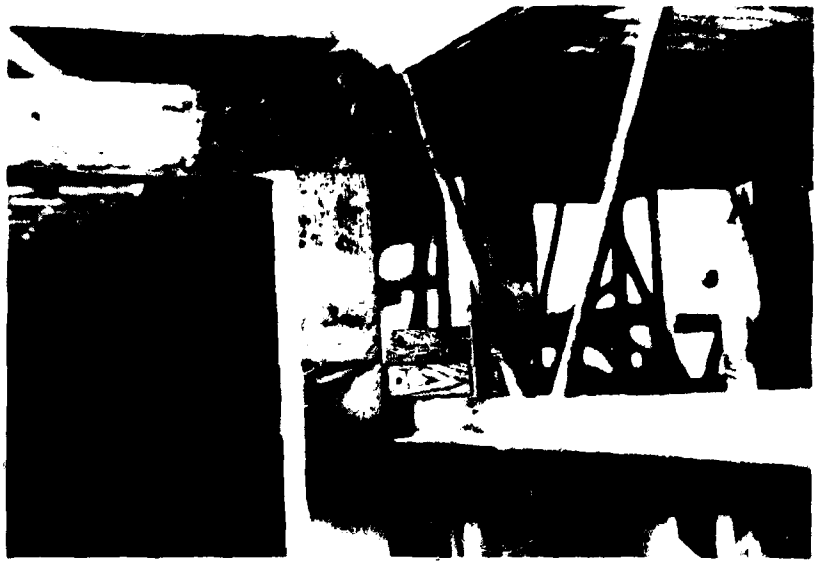

Fig. 2-12. Photographs of Shoring Details, Test No. 79-2.

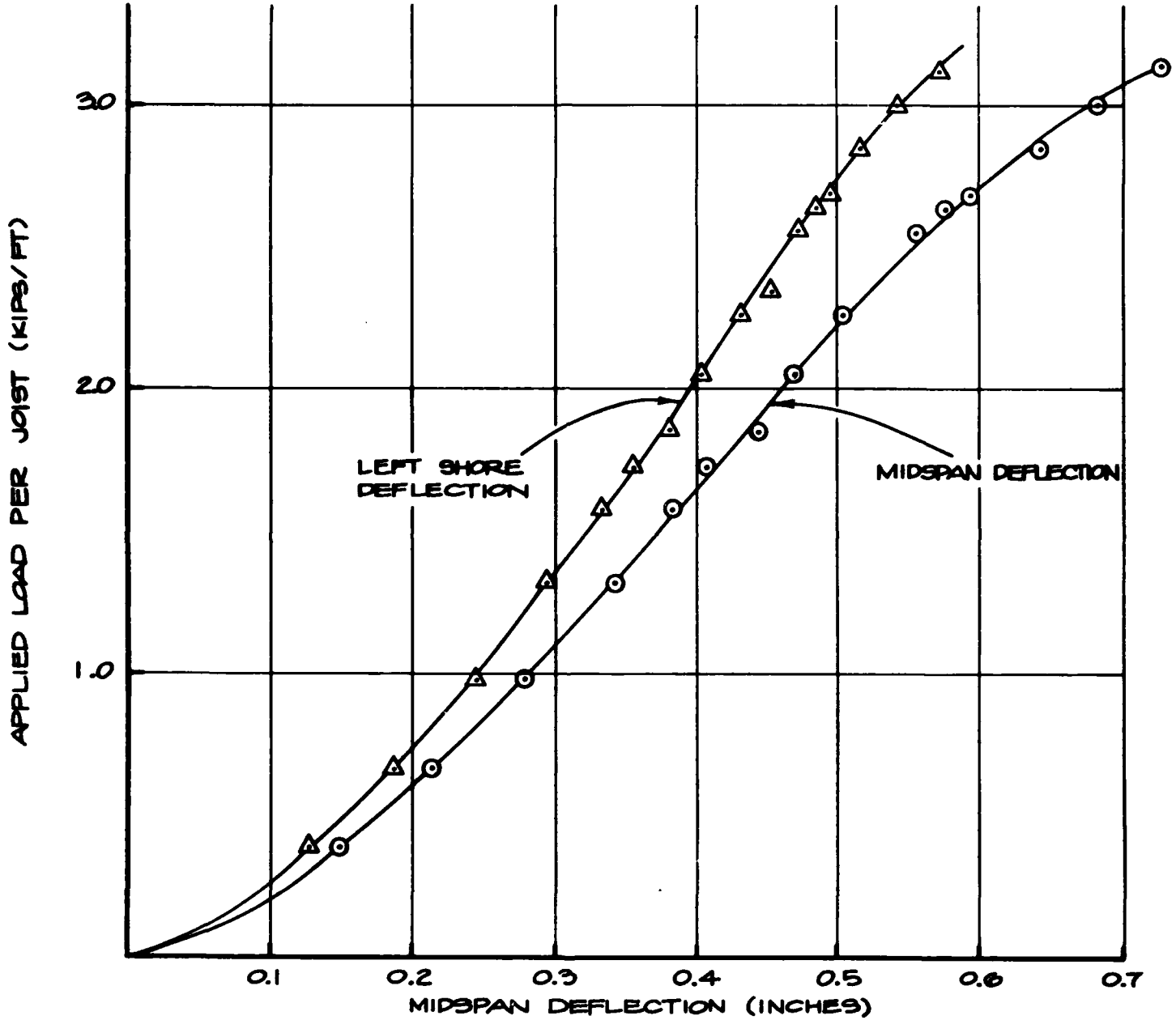

Fig. 2-13. Load vs Deflection, Test No. 79-2.

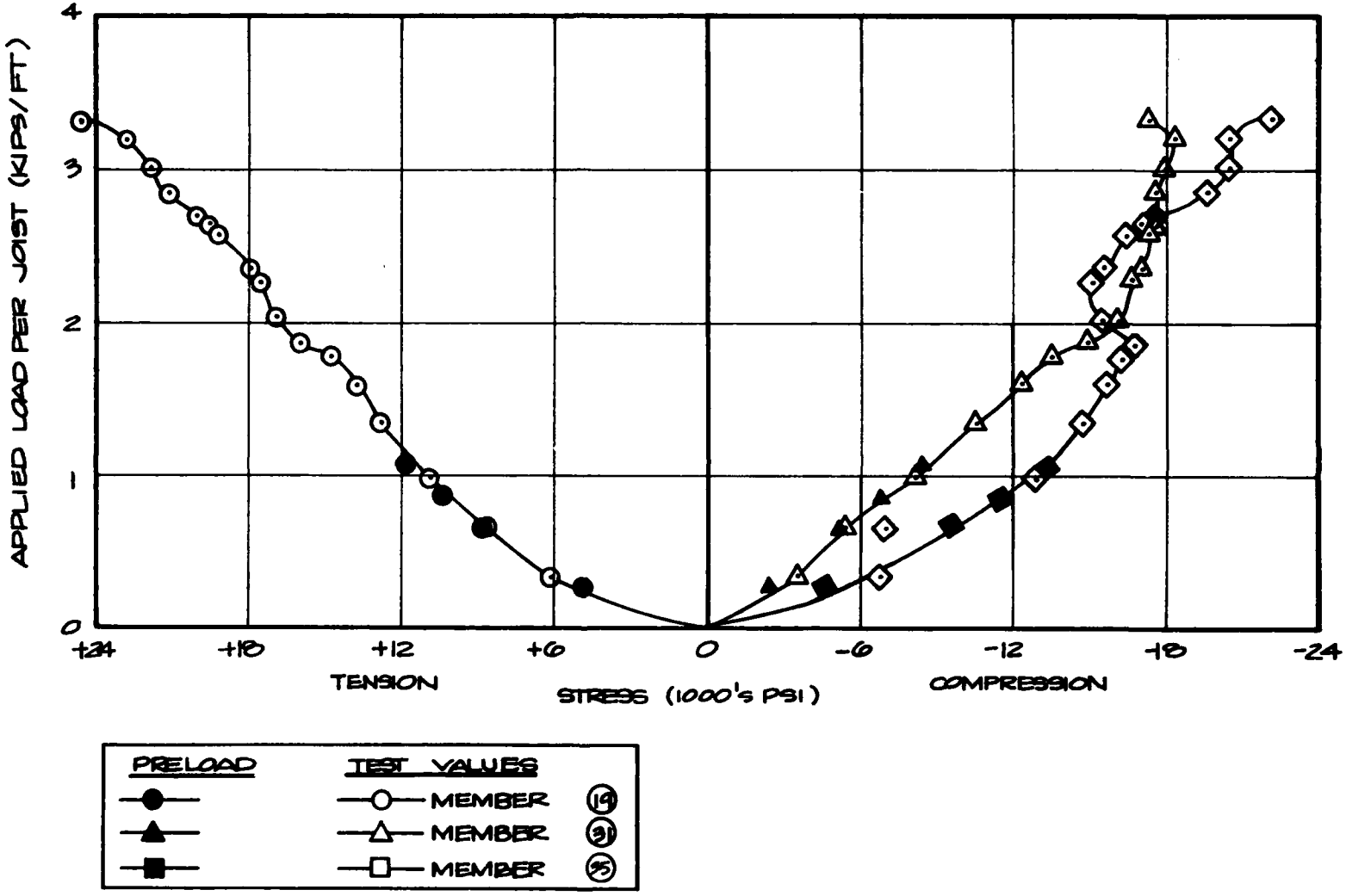

Fig. 2-14. Load vs Stress, Test No. 79-2.

Fig. 2-15. Pos+test Photographs, Test No. 79-2.

Fig. 2-16. Posttest Photographs, Test No. 79-2.

Fig. 2-17. Posttest Photographs, Test No. 79-2.

Test No. 79-3 (Shored at Midspan)

The test configuration and loading arrangement remained the same as in the previous tests (see Figure 2-18). A single row of shoring was installed at midspan with a 0.25-inch stress control gap between the top of the shore and the joists (see Figures 2-19, 2-20, and 2-21 for details).

Dial gauges were placed at midspan to measure deflection over the shores. Additionally, strain gauges were applied to web members 22 and 27 (see Figure 2-18 for member locations).

Loads were applied in 2,500 lb/ram increments. Deflection and strain data were recorded at each load increment. The load was increased to 27,500 lb/ram, or 1,833 plf/joist. With the dead load included, the ultimate load was 1,928 plf/joist.

A plot of load vs deflection is shown in Figure 2-22; load vs stress in web members 22 and 27 is shown in Figures 2-23 and 2-24, respectively.

Failure occurred at two locations. The first failure occurred at the midspan shore where the 4x4 beam atop the shores failed in flexure directly over the shores (see Figure 2-25A). The failure of the 4x4 led to the buckling failure of web member 22 (Figure 2-25B) in all three joists. The last recorded midspan deflection prior to failure was 0.595 inches at 25,000 lb/ram (1,761 plf/joist).*

* Includes 95 plf/joist dead load.

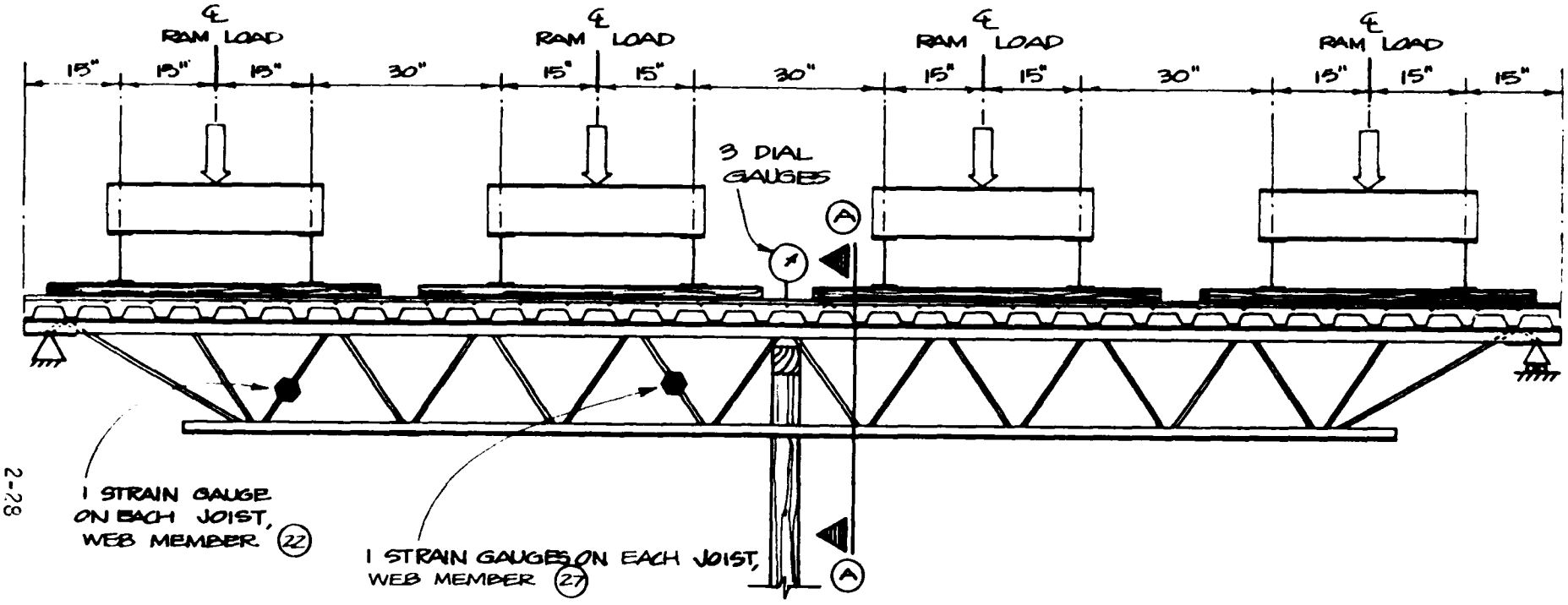

Fig. 2-18. Test Configuration, Test No. 79-3.

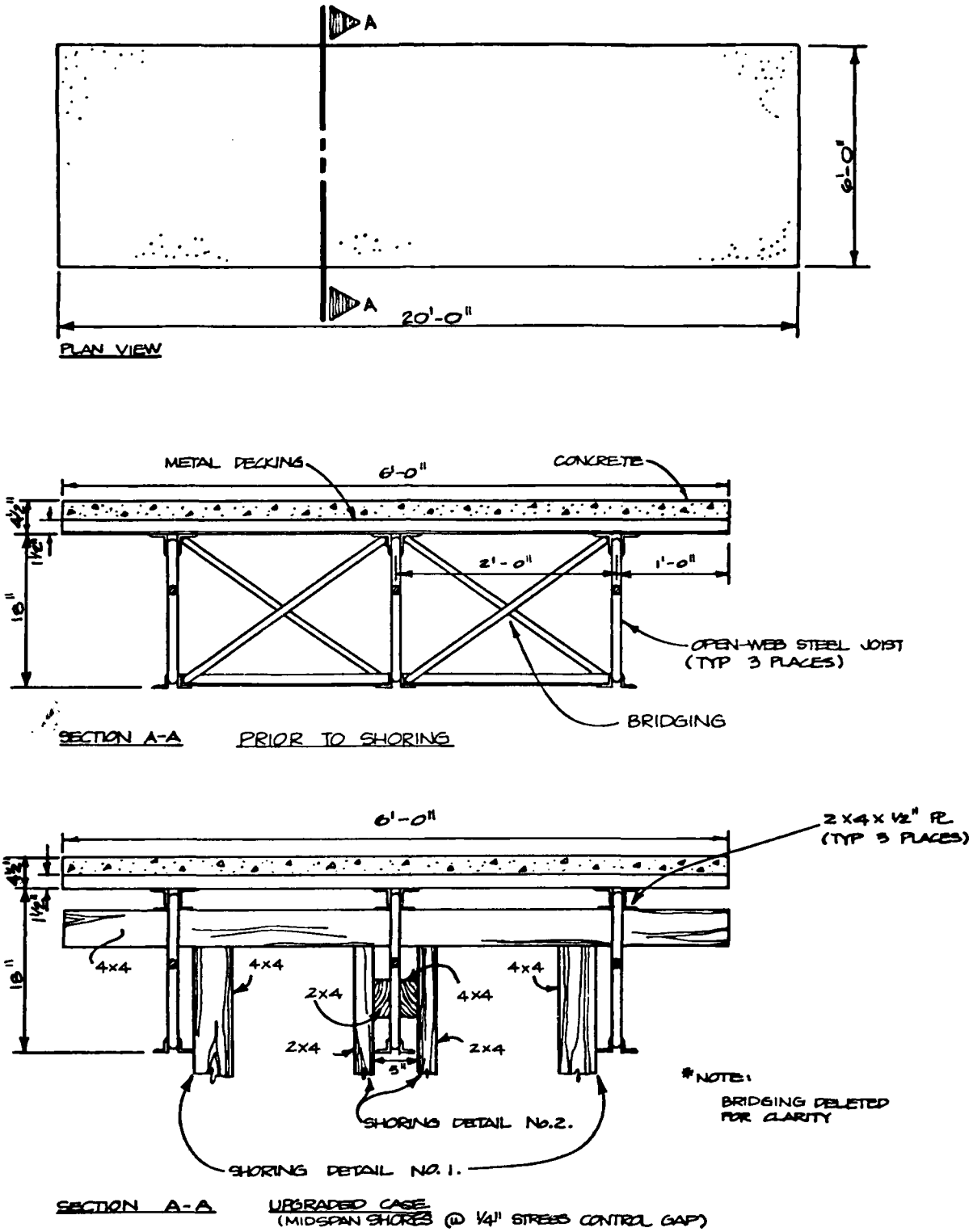

Fig. 2-19. Shoring Details, Test No. 79-3.

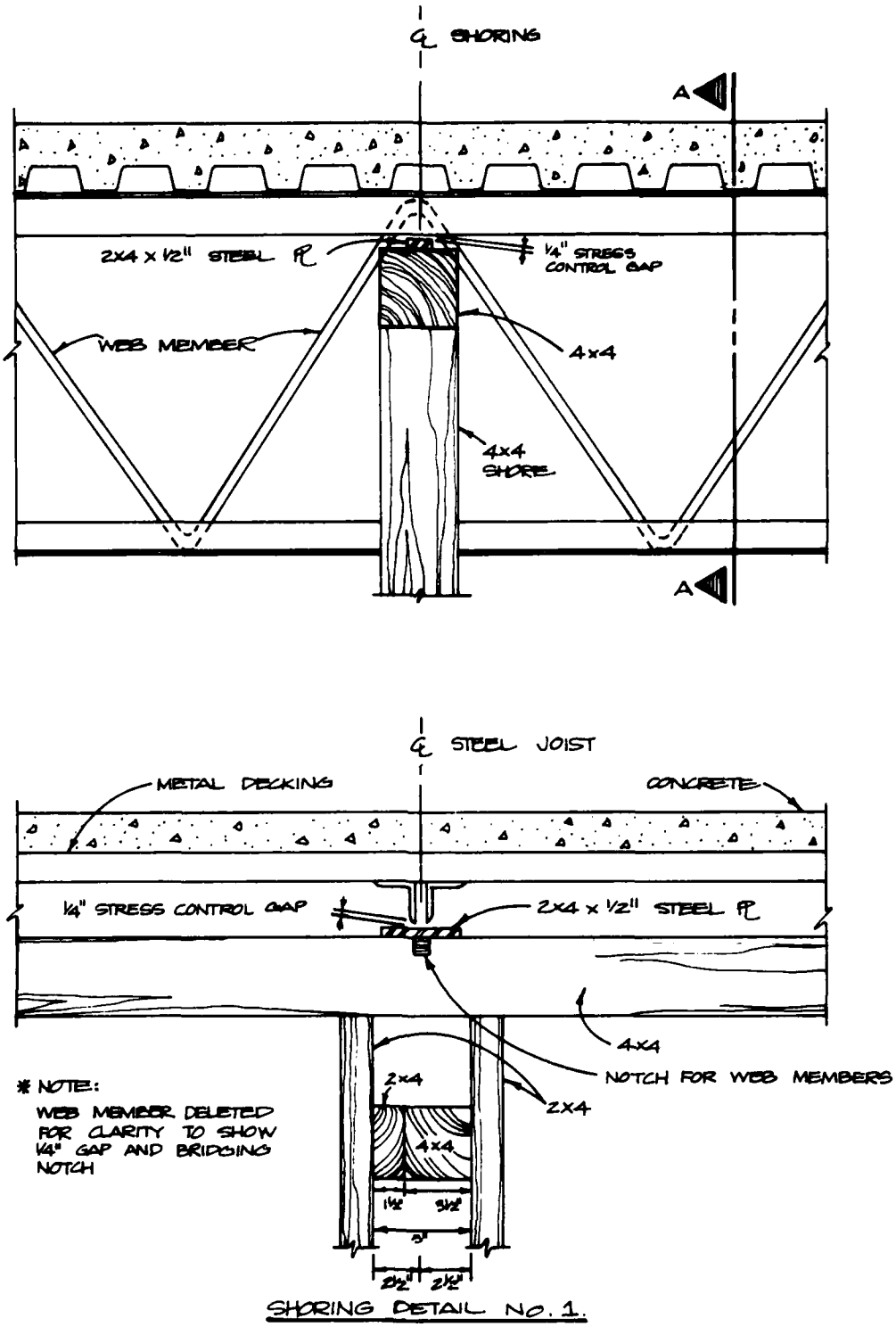

Fig. 2-20. Shoring Details, Test No. 79-3.

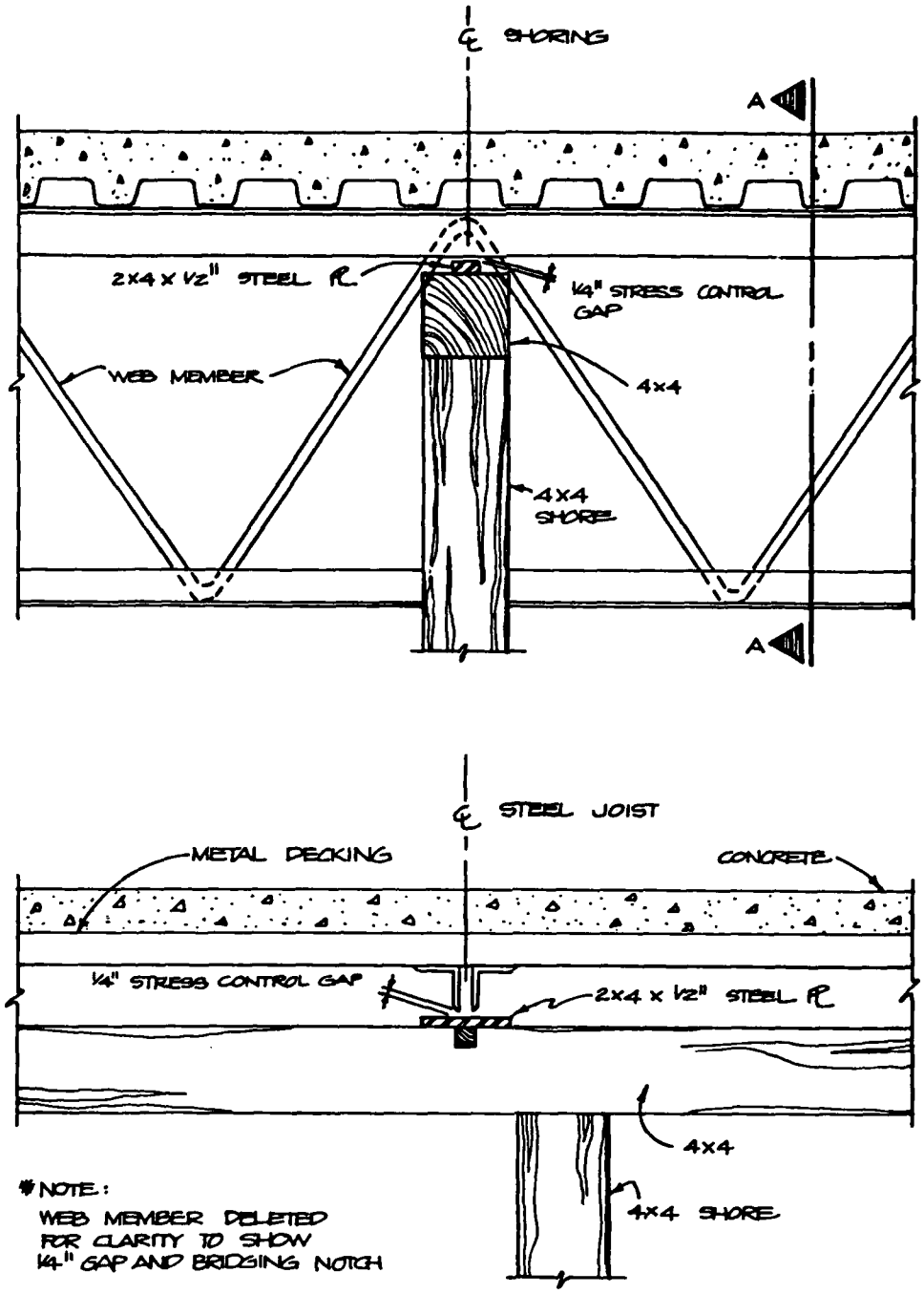

SHORING DETAIL No. 2

Fig. 2-21. Shoring Details, Test No. 79-3.

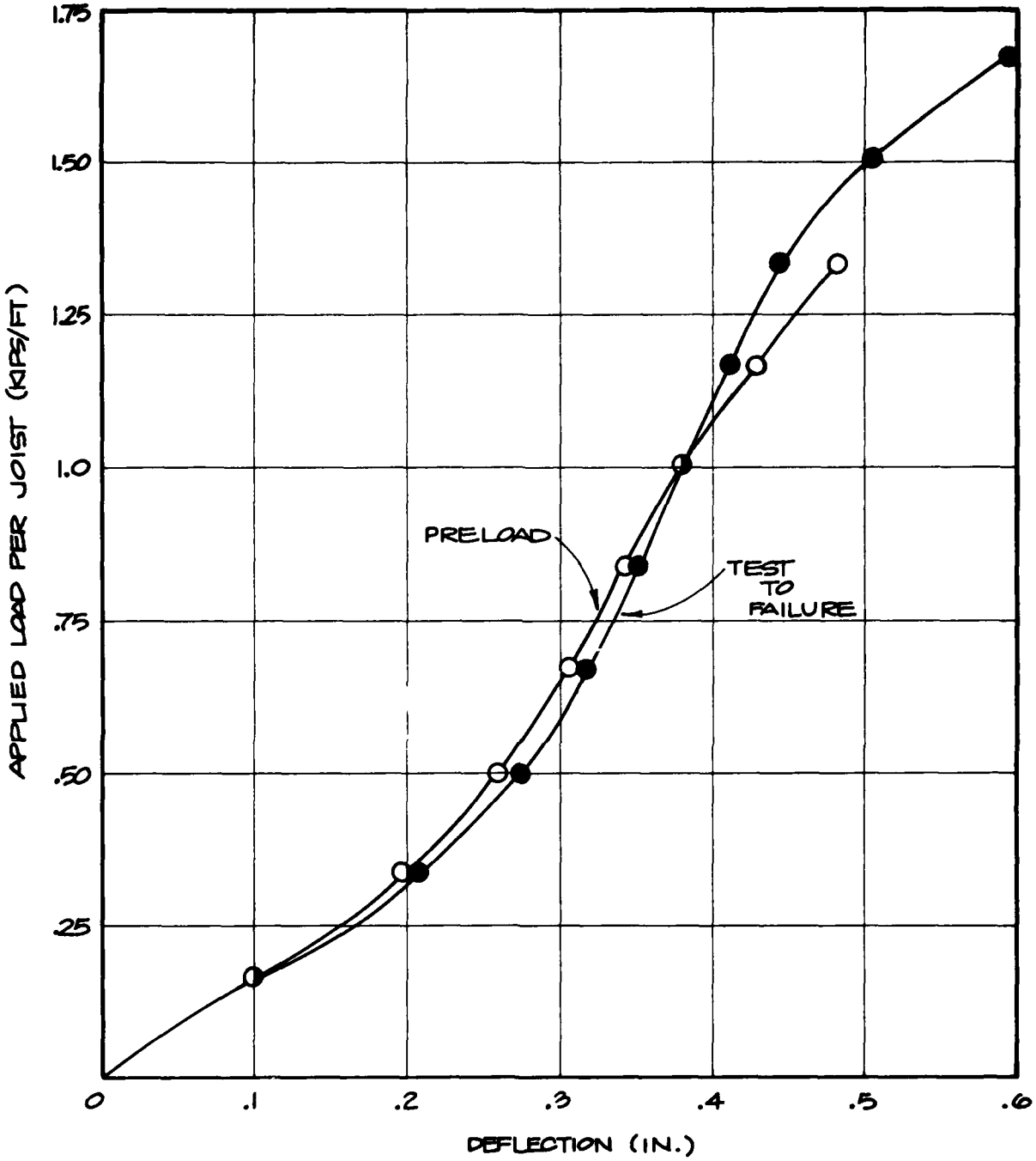

Fig. 2-22. Load vs Deflection, Test No. 79-3.

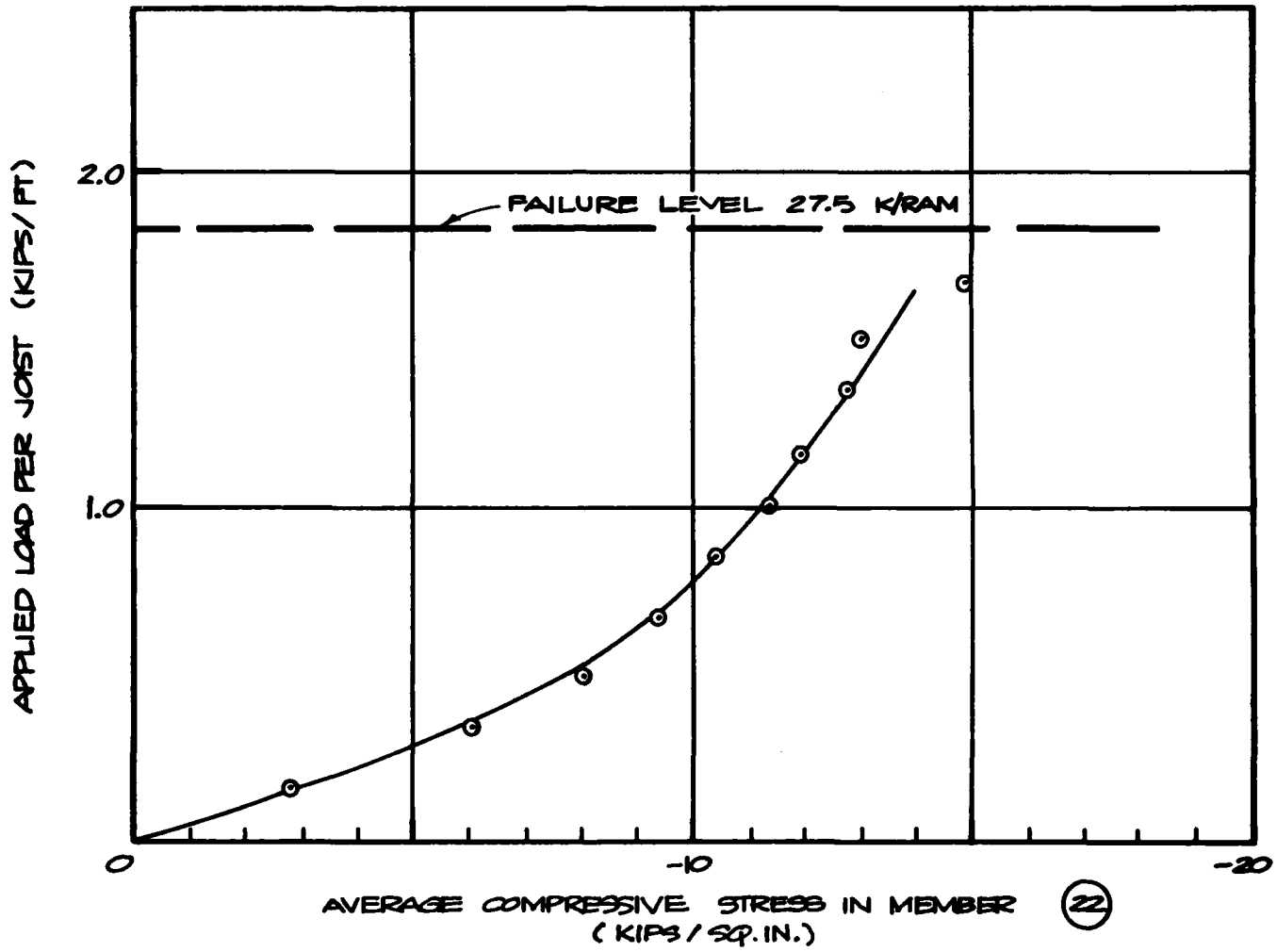

Fig. 2-23. Load vs Compressive Stress in Member 22, Test No. 79-3.

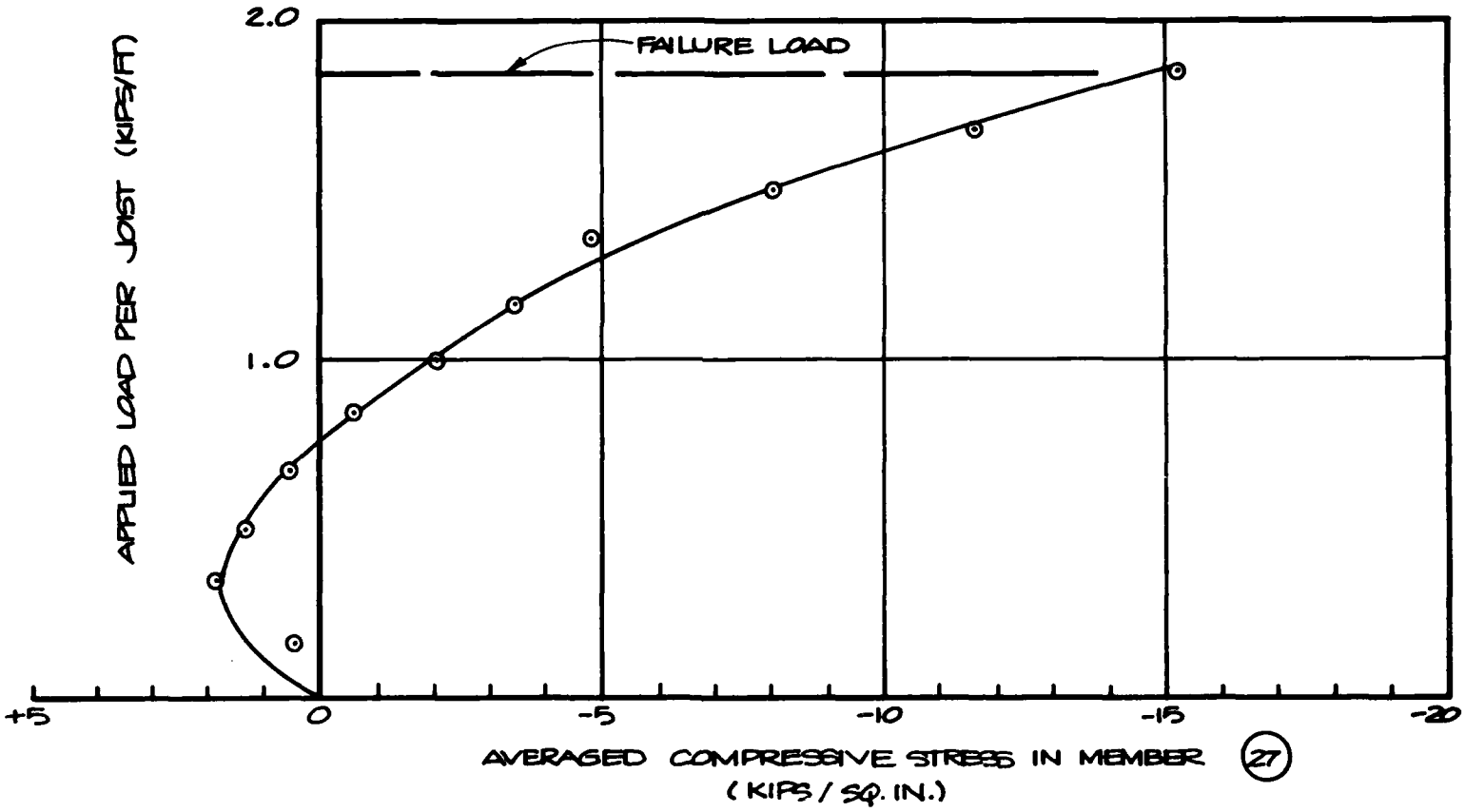

Fig. 2-24. Load vs Compressive Stress in Member 27, Test No. 79-3.

A. Center Joist Shore After Failure.

B. Web Member (22) After Failure.

Fig. 2-25. Posttest Photographs, Test No. 79-3.

Test No. 80-1 (Base Case)

This test was a base case test to failure on a simply supported open-web joist floor system. The loading arrangement and configuration were the same as that used in Test No. 79-1 (see Figure 2-26). In addition to dial gauges at midspan and strain gauges on web member 35, two accelerometers were used. One accelerometer was placed at midspan to measure the natural frequency of the entire floor system simply supported at its ends and loaded with its own dead weight. The second accelerometer was placed on web member 22 to measure its natural frequency.

Unlike Test No. 79-1, this test was loaded slowly in 2,000 lb/ram increments, with deflection and strain data recorded at each increment, to failure. Failure occurred at 15.9 kips/ram, or 1,060 plf/joist. When the dead weight of the floor system is included, the ultimate load is 1,160 plf/joist. Failure occurred when web member 22 buckled in all three joists. The buckling of web member 22 was immediately followed by the buckling failure of web members 21 and 24 (see Figure 2-26 for web member locations). Photographs of this area after failure are shown in Figures 2-27 and 2-28).

A plot of load per joist vs midspan deflection is shown in Figure 2-29, and load per joist vs compressive stress in member 22 is shown in Figure 2-30.

The midspan accelerometer provided a means to evaluate the fundamental period of vibration of the entire floor system under its own dead weight. The fundamental, or natural, period was found to be 0.074 seconds per cycle (see Figure 2-31).

A second accelerometer on web member 22 was used in two positions. The first position measured the fundamental period of the web member in the plane of the open-web joist (longitudinal direction). A second test was conducted with the accelerometer rotated 90 degrees to measure the

fundamental period perpendicular to the plane of the open-web joist (transverse direction). These two periods were 0.0043 seconds per cycle and 0.00630 seconds per cycle, respectively. Plots of acceleration vs time are shown for both tests in Figure 2-32.

Note that the last recorded midspan deflection just prior to failure (1,160 plf/joist) was 0.0625 inches. In comparison, Test No. 79-3 (shoring at midspan) had a midspan deflection of 0.595 inches just prior to failure (1,928 plf/joist).

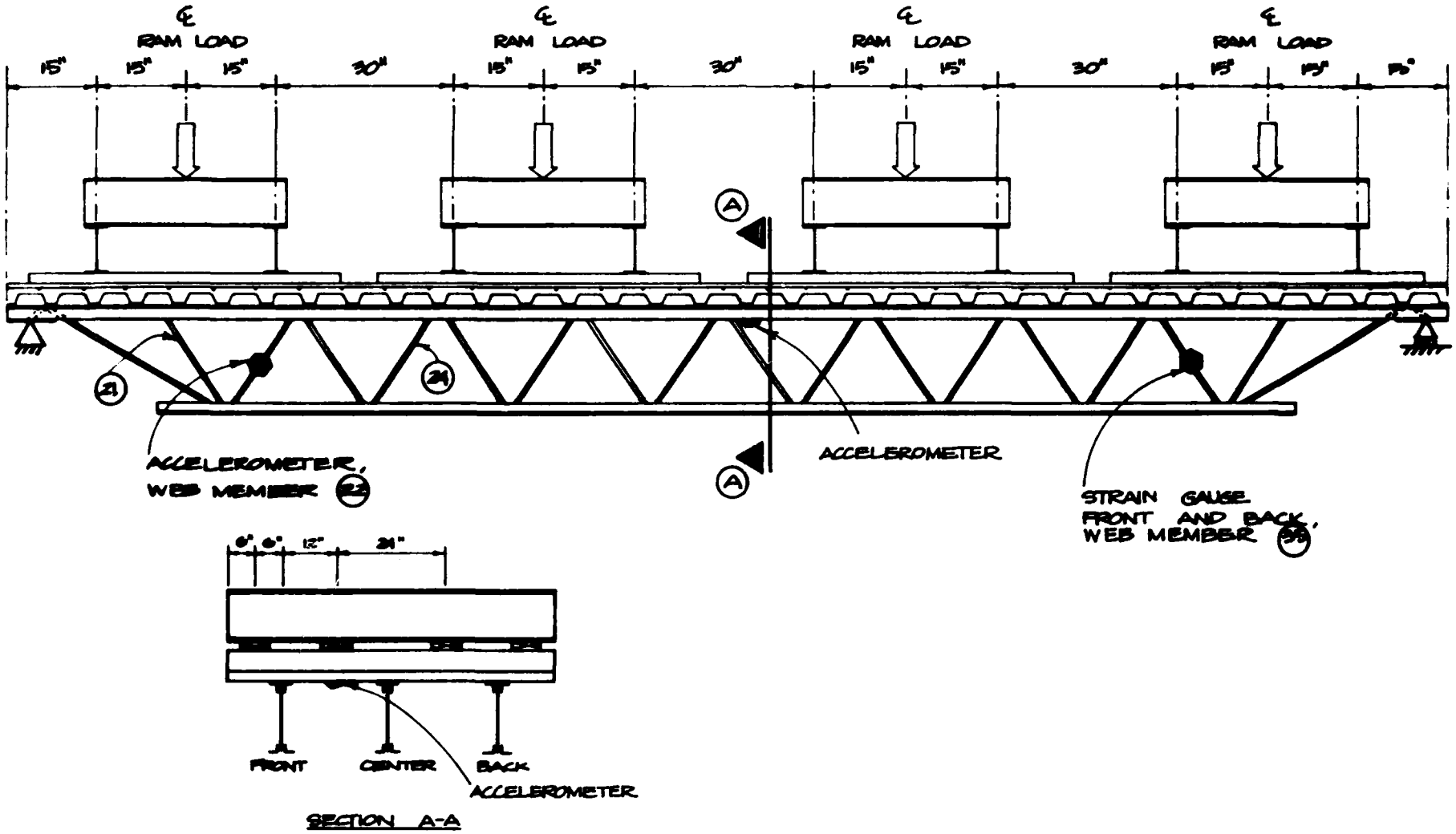

Fig. 2-26. Test Configuration for Test No. 80-1.

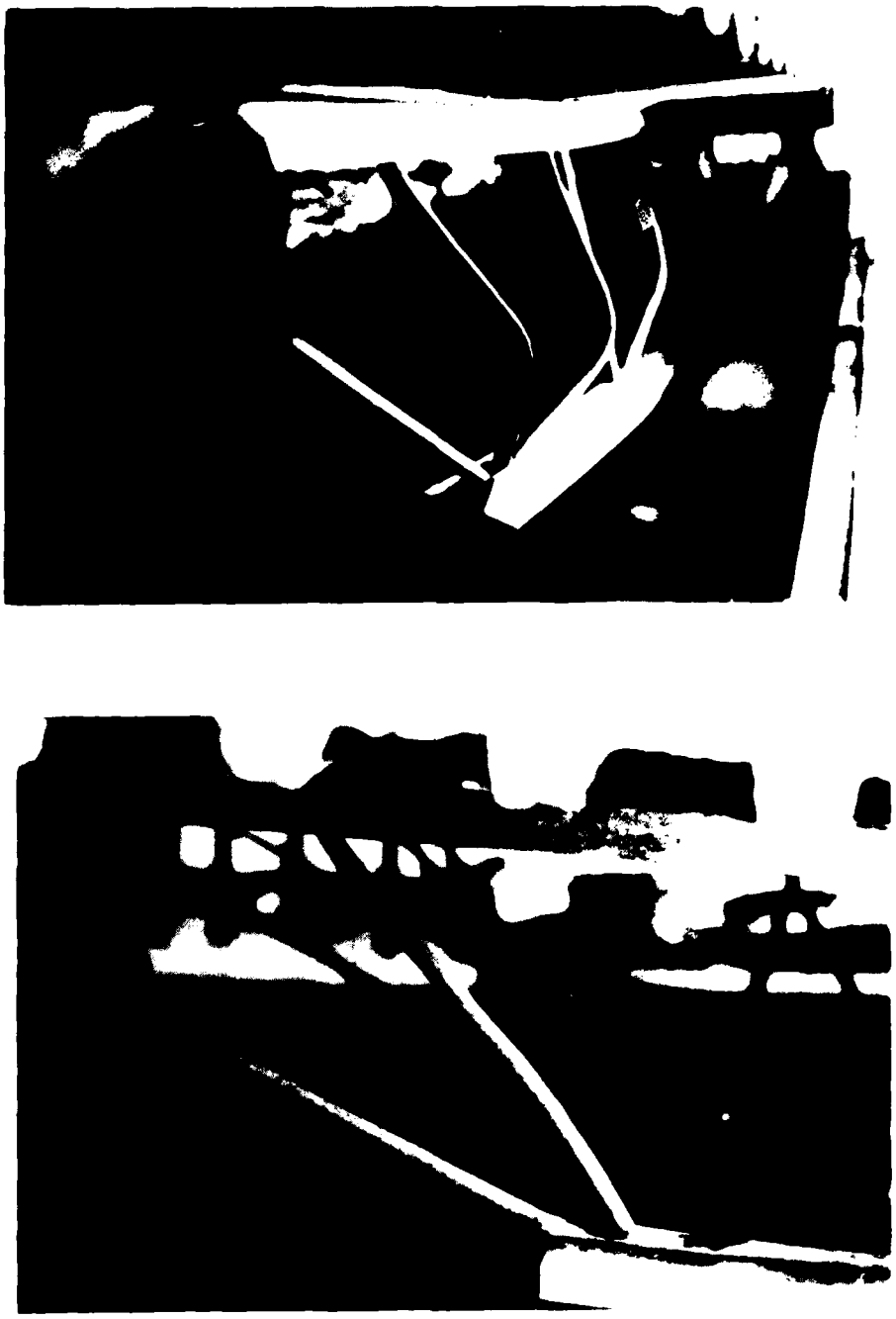

Fig. 2-27. Posttest Photographs, Test No. 80-1.

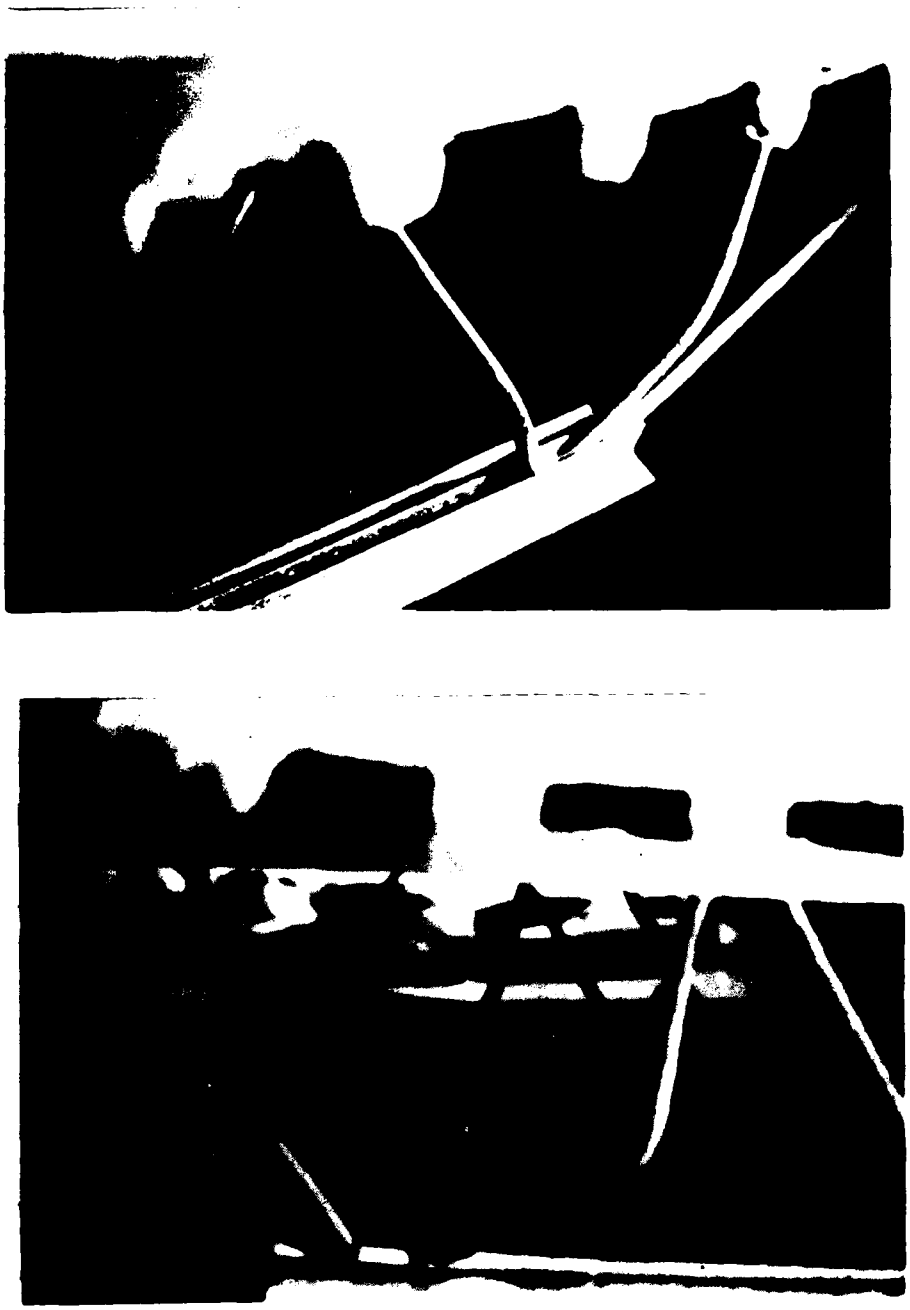

Fig. 2-28. Posttest Photographs, Test No. 80-1.

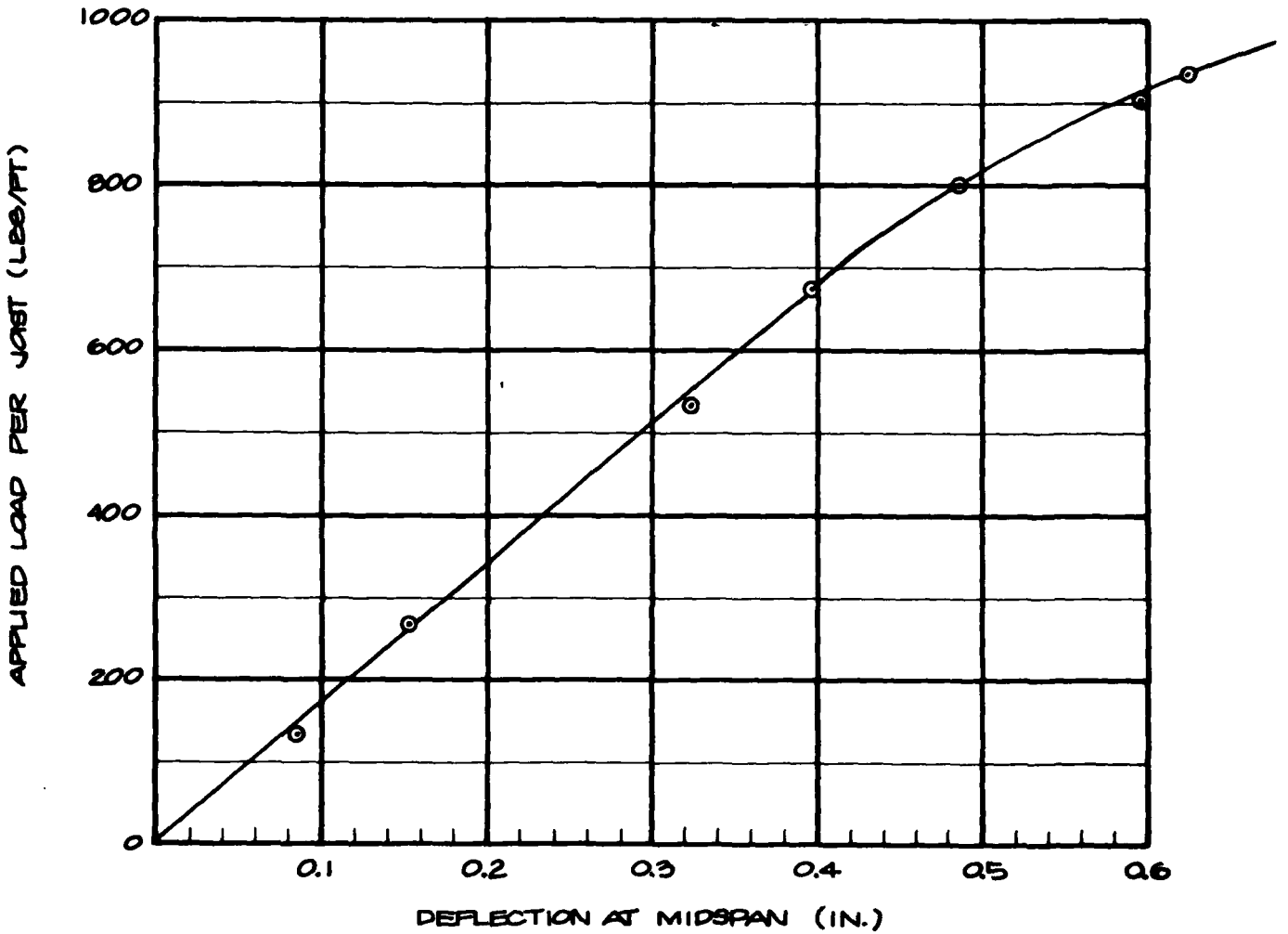

Fig. 2-29. Load vs Deflection, Test No. 80-1.

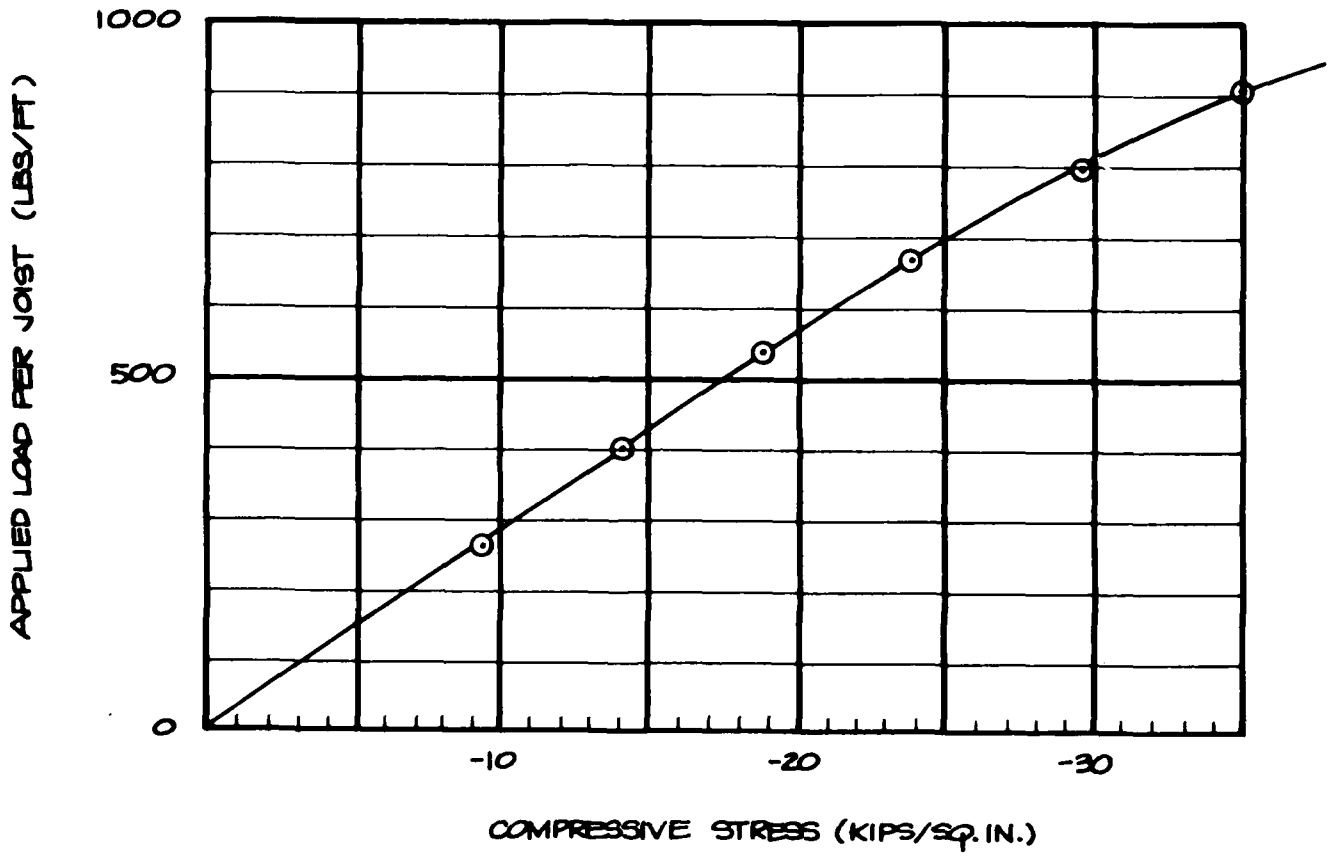

Fig. 2-30. Load vs Compressive Stress in Member (22), Test No. 80-1.

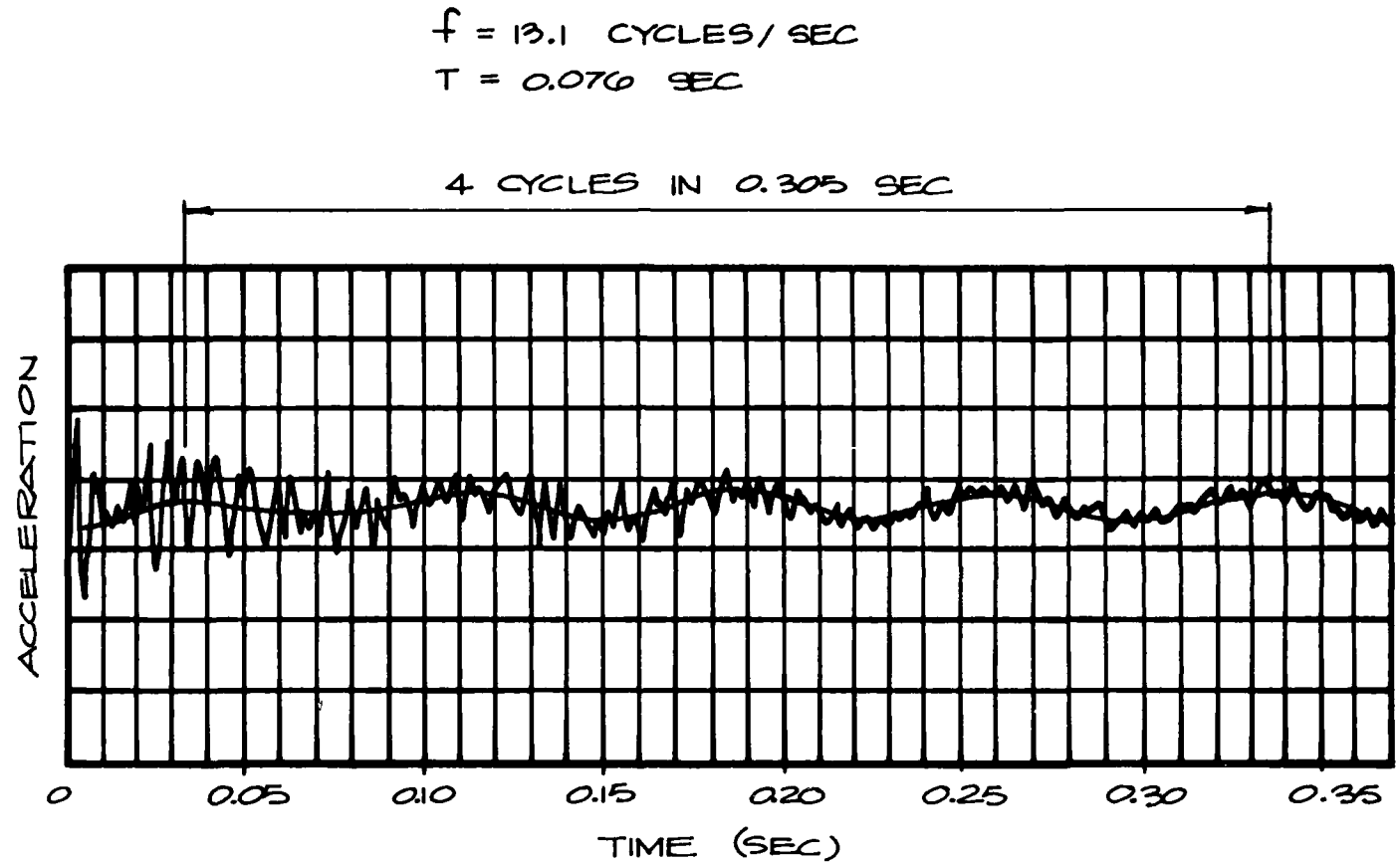

Fig. 2-31. Fundamental Period of Test Specimen 80-1.

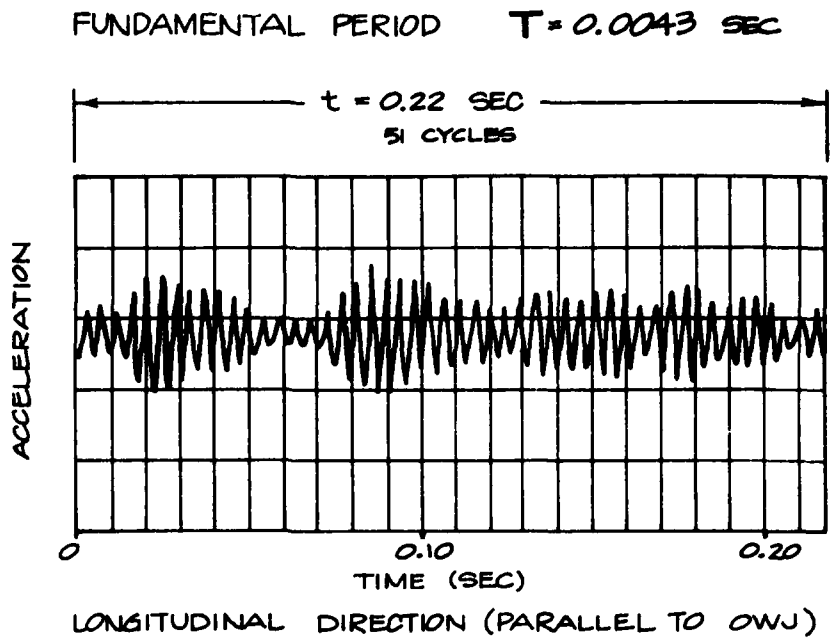

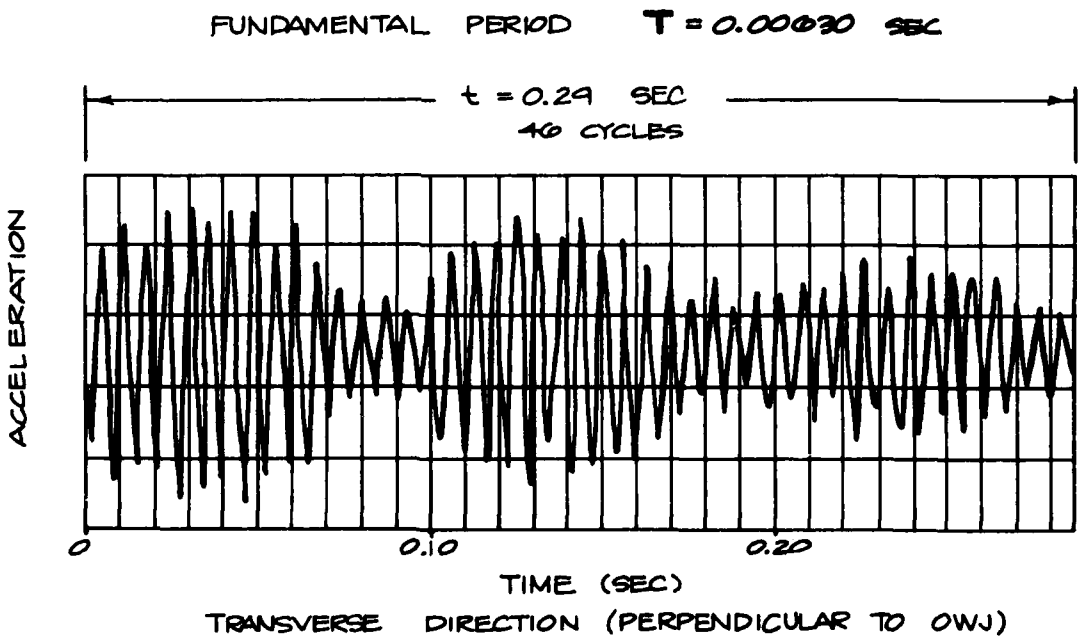

Fig. 2-32. Fundamental Period of Web Member (22), Test No. 80-1.

TOP CHORD ASSEMBLY TESTS

Introduction

The primary objective of the test program was to determine the upgrading potential of open-web joist floors using various shoring arrangements. With an upgraded open-web joist floor a secondary failure can occur in which the slab carrying load to the open-web joists collapses prior to the failure of the open-web joist. The top chord assembly test program examined this secondary failure mechanism to determine what the load-carrying capacity for the particular top chord assembly was and to develop a failure prediction scheme for a broad range of floor systems of this type.

Typical floors found in commercial structures of this type are constructed of metal decking attached via puddle welds to the top chord of the open-web joists. A layer of concrete is poured atop the decking to complete the floor. The concrete is poured in depths ranging from 2½ to 6 inches, depending on the type of decking used, superimposed live loads, and the spacing of the supporting open-web joists.

The metal decking and concrete topping serve a dual purpose in this type of floor system. They serve primarily as a slab carrying load to the supporting open-web joists and secondarily providing continuous lateral support to the top chord of the open-web joist, thus preventing a lateral buckling failure for this member.

Objective

These tests were performed to determine at a relatively minor cost the top chord assembly's* ultimate moment capacity in both the longitudinal and transverse directions (parallel and perpendicular to the open-web joists,

---

* The top chord assembly consists of 4½ inches of reinforced concrete topping, fluted metal decking, and the double angle top chord of the 18H8 open-web joist.

respectively). The ultimate moment capacity of the top chord assembly tested in the longitudinal direction (see Tests Nos. 80-2 and 80-3) was used in the analysis process to determine if the top chord assembly was at or near failure during any of the full-scale floor tests. The ultimate moment capacity of the top chord assembly tested in the transverse direction (see Tests Nos. 80-4 and 80-5) enabled determination of its ultimate load-carrying capacity.

Top Chord Assembly Test Specimens

Four sections of concrete decking were removed from previous full-scale open-web joist floor specimens. A concrete saw was used to cut the floors into sections. A gas torch was then used to cut the web members off the open-web joist.

The test specimens appeared to have suffered no permanent damage from their previous loading. The damage and failure in the previous tests was in the buckling of web members and subsequent damage to the lower chord. The concrete topping, fluted metal decking, and double angle top chord (i.e., top chord assembly) of the open-web joist were not damaged. The puddle welds connecting the double angles to the fluted metal deck, because of their inaccessibility, could not be inspected, and a few may have failed during the floor tests.

Tests Nos. 80-2 and 80-3

Test specimens 80-2 and 80-3 were tested to determine the ultimate moment capacity of the top chord assembly in the longitudinal direction (i.e., parallel to the joists). The test configuration and loading arrangement for these tests are shown in Figures 2-33 and 2-34.

Load was slowly applied in 2,000 lb increments to failure. Load and deflection data were recorded at each load increment. A plot of load vs midspan deflection is shown in Figure 2-35.

Test specimen 80-2 failed at a load of 32,000 lb, and specimen 80-3 failed at 28,000 lb. Test specimen 80-3 was much stiffer than specimen 80-2 at loads below about 14,000 lb, but note that both test specimens attained approximately the same ultimate load of 28,000 lbs, which corresponds to an ultimate moment of

$$M_u = 224 \text{ kip-in.} = 74.7 \text{ kip-in./joist.}$$

Failure was caused by a transverse crack in the concrete at midspan (see Figure 2-36). This is a positive moment, flexural crack in the concrete.

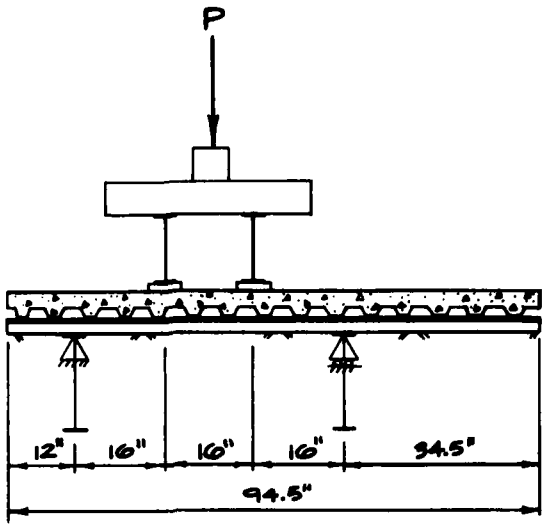

SIDE VIEW

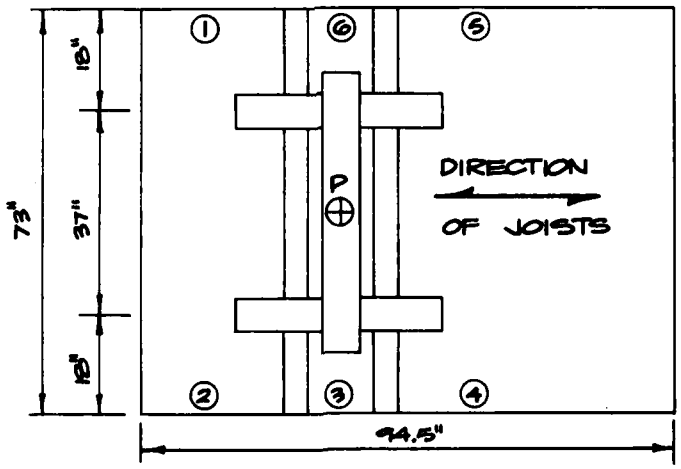

NOTE:
DIAL GAUGES ARE POSITIONED IN THE NUMBERED CIRCLES

PLAN VIEW

Fig. 2-33. Test Configuration, Test No. 80-2.

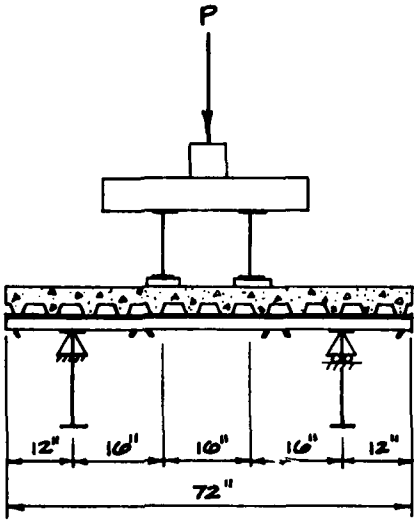

SIDE VIEW

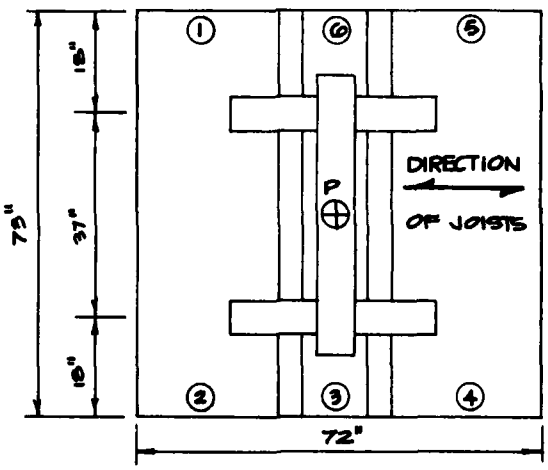

PLAN VIEW

NOTE:

DIAL GAUGES ARE POSITIONED IN THE NUMBERED CIRCLES

Fig. 2-34. Test Configuration, Test No. 80-3.

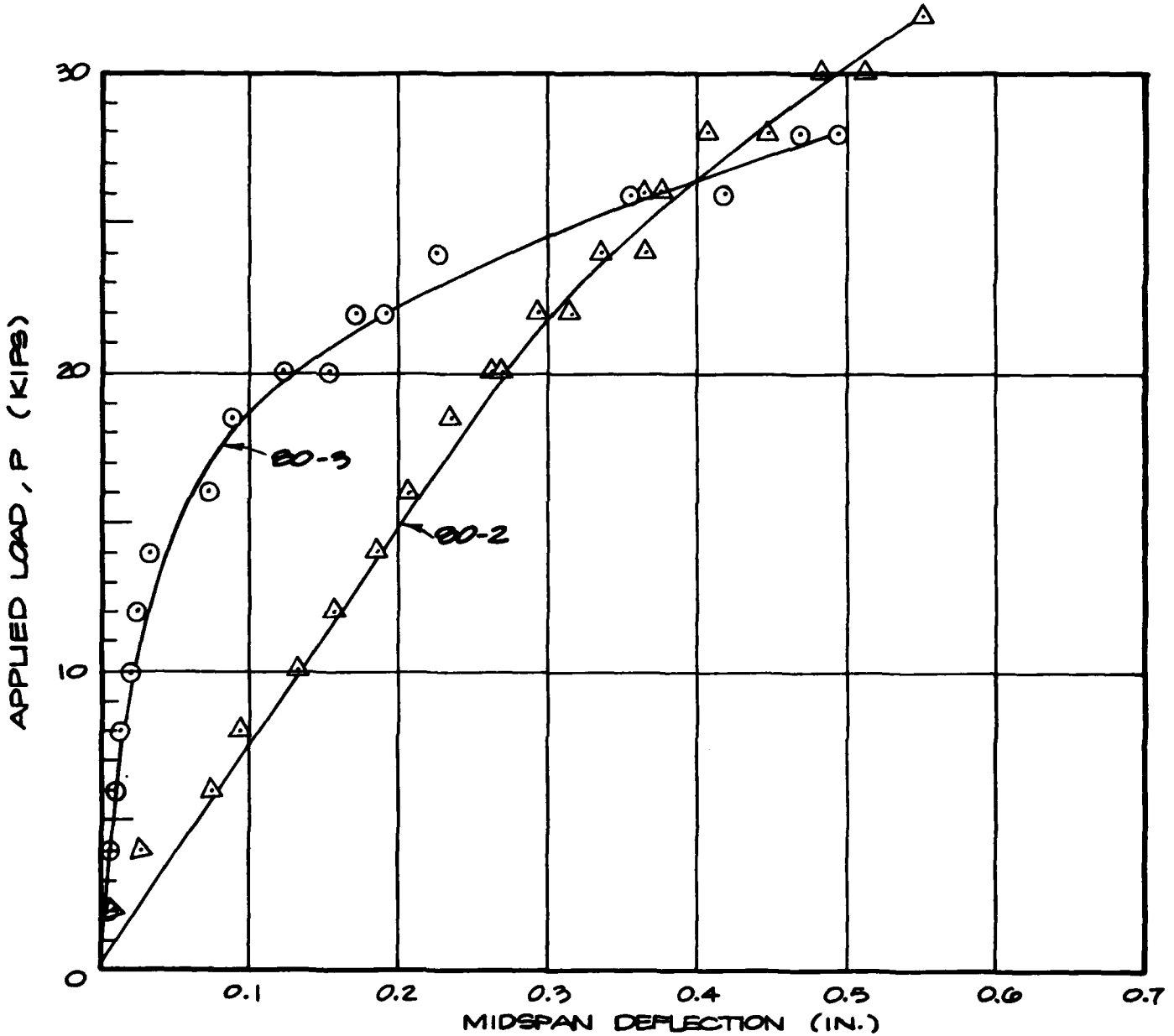

Fig. 2-35. Load vs Deflection, Tests Nos. 80-2 and 80.3.

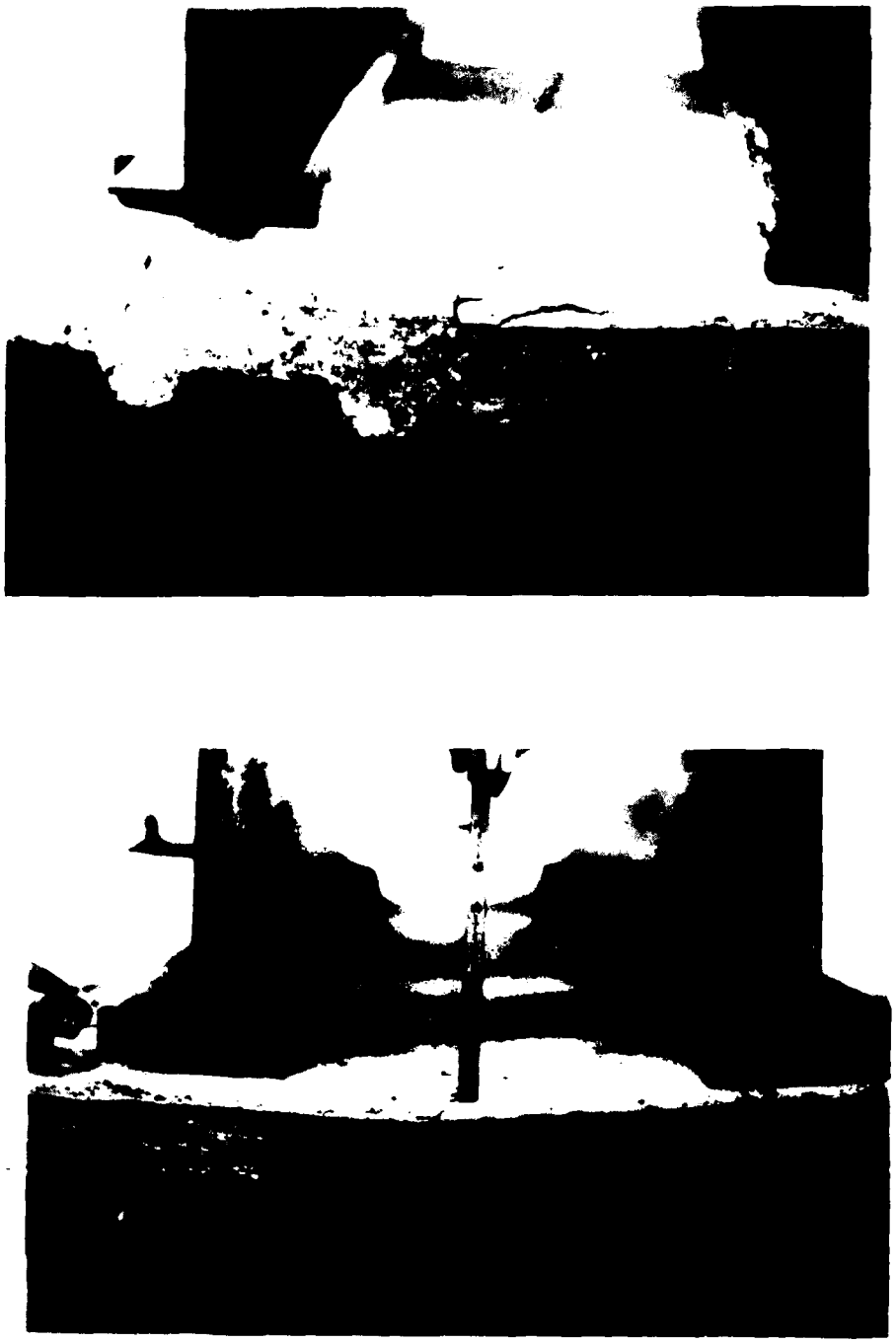

Fig. 2-36. Posttest Photographs, Test No. 80-2.

Tests Nos. 80-4 and 80-5

These specimens were tested to measure the ultimate moment capacity of the top chord assembly in the transverse direction.

The sketch below shows the applied load in the transverse direction and the regions of positive and negative moment.

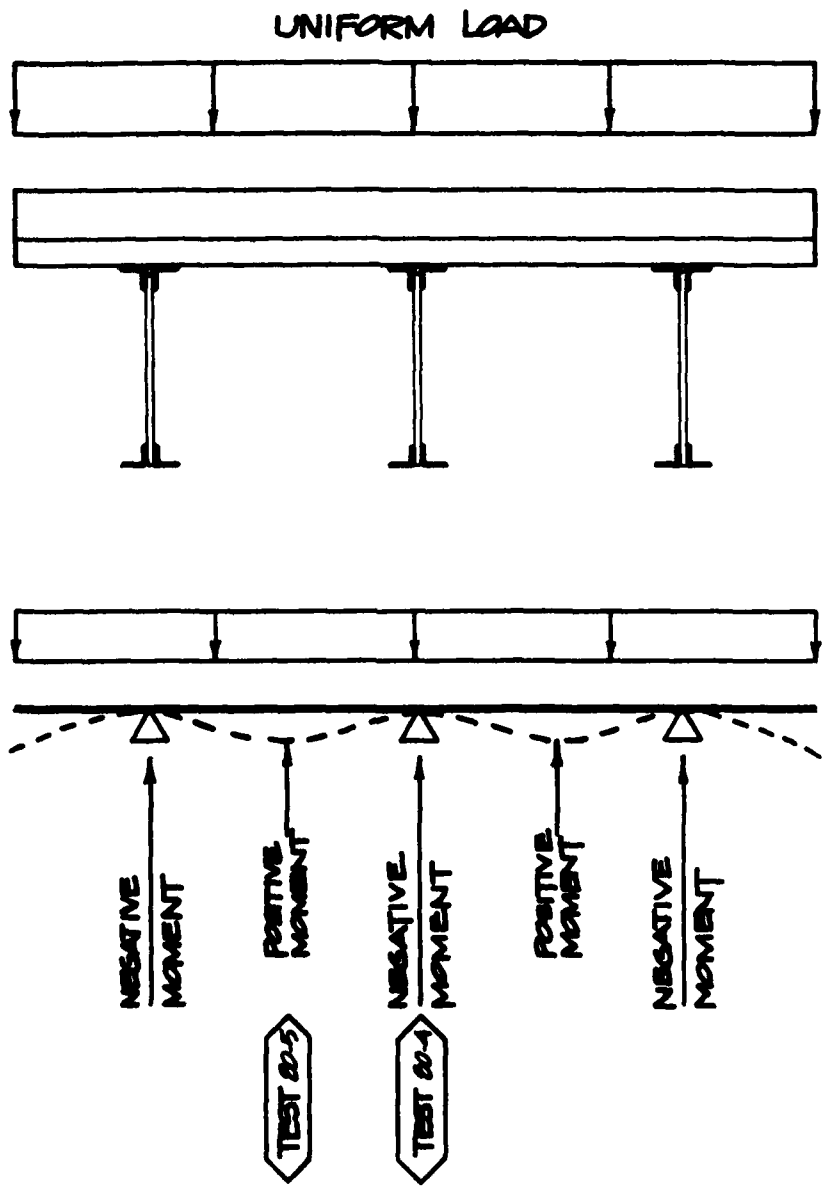

Specimen 80-4. — The test configuration and loading arrangement for test specimen 80-4 are shown in Figure 2-37. The objective of this test was to determine the ultimate negative moment capacity (tension on the top and compression on the bottom fibers of the section) of the composite deck (concrete and fluted metal decking).

Two load tests were conducted: the first (80-4A) was a preload of 500 lb increments to a total applied load (P) of 9,000 lb; the second test (80-4B) was a test to failure at 1,000 lb load increments to failure. Load and deflection data were recorded at each load increment. The test specimen failed in the second test at P = 20,000 lb. Below is a sketch of the applied load and moment diagram at failure.

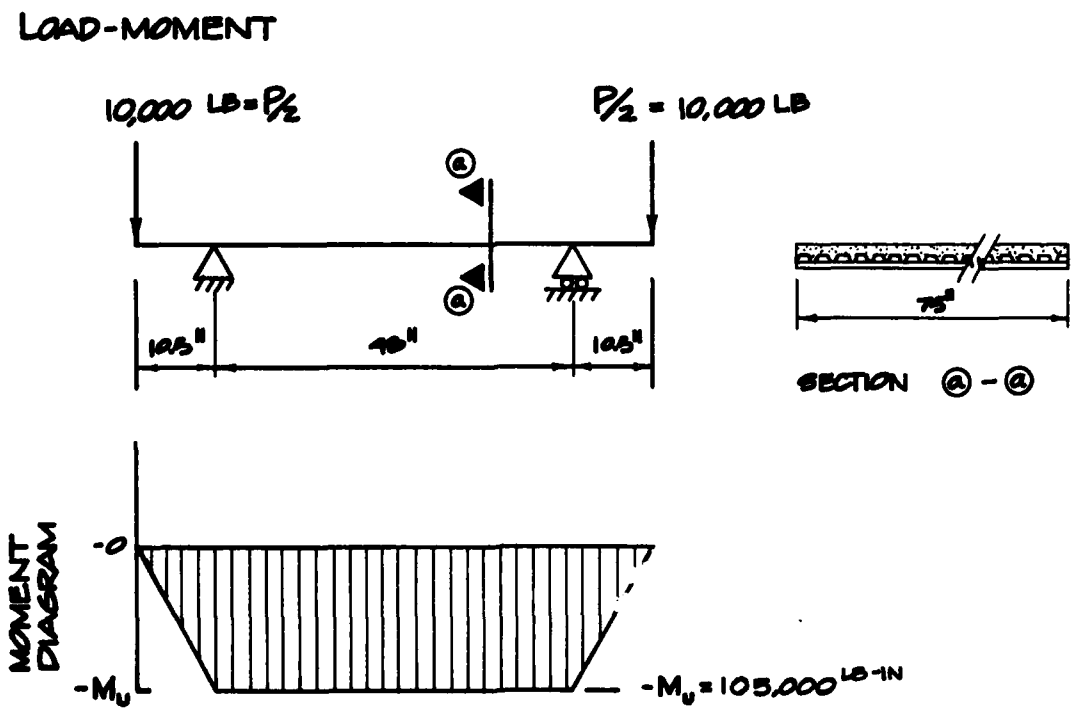

The corresponding ultimate negative moment capacity of the decking is:

$$-M_u = 105{,}000 \text{ lb-in.} = 1400 \text{ lb-in./in.}$$

Plots of load vs deflection for both the preload test and the load to failure test are shown in Figures 2-38 and 2-39.

Failure occurred as expected with flexural cracks in the top tension fibers of the section in the region of maximum moment (ie., between supports). See Figure 2-40 for crack location.

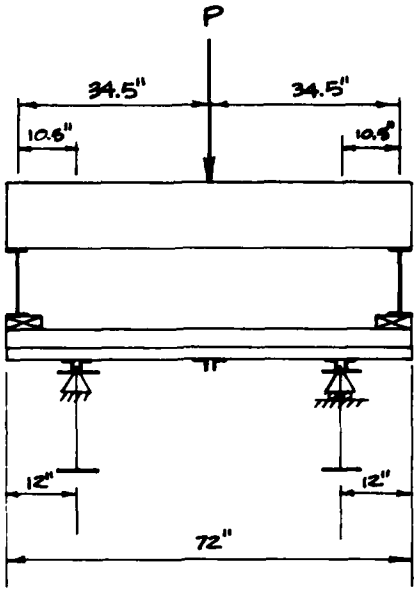

SIDE VIEW

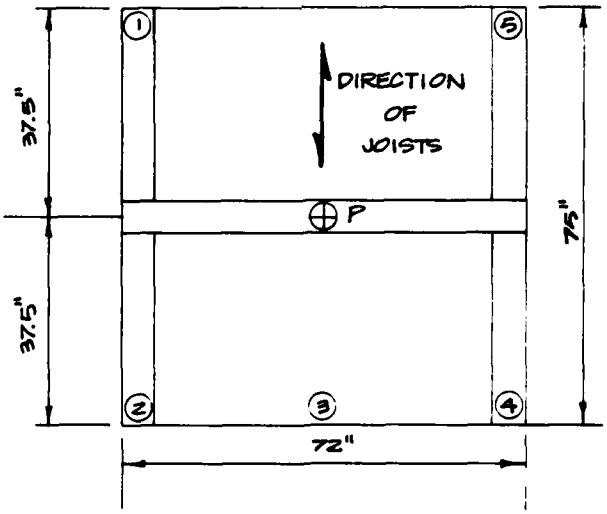

NOTE:

DIAL GAUGES ARE POSITIONED IN THE NUMBERED CIRCLES

TOP VIEW

Fig. 2-37. Test Configuration for Test No. 80-4A and 80-4B.

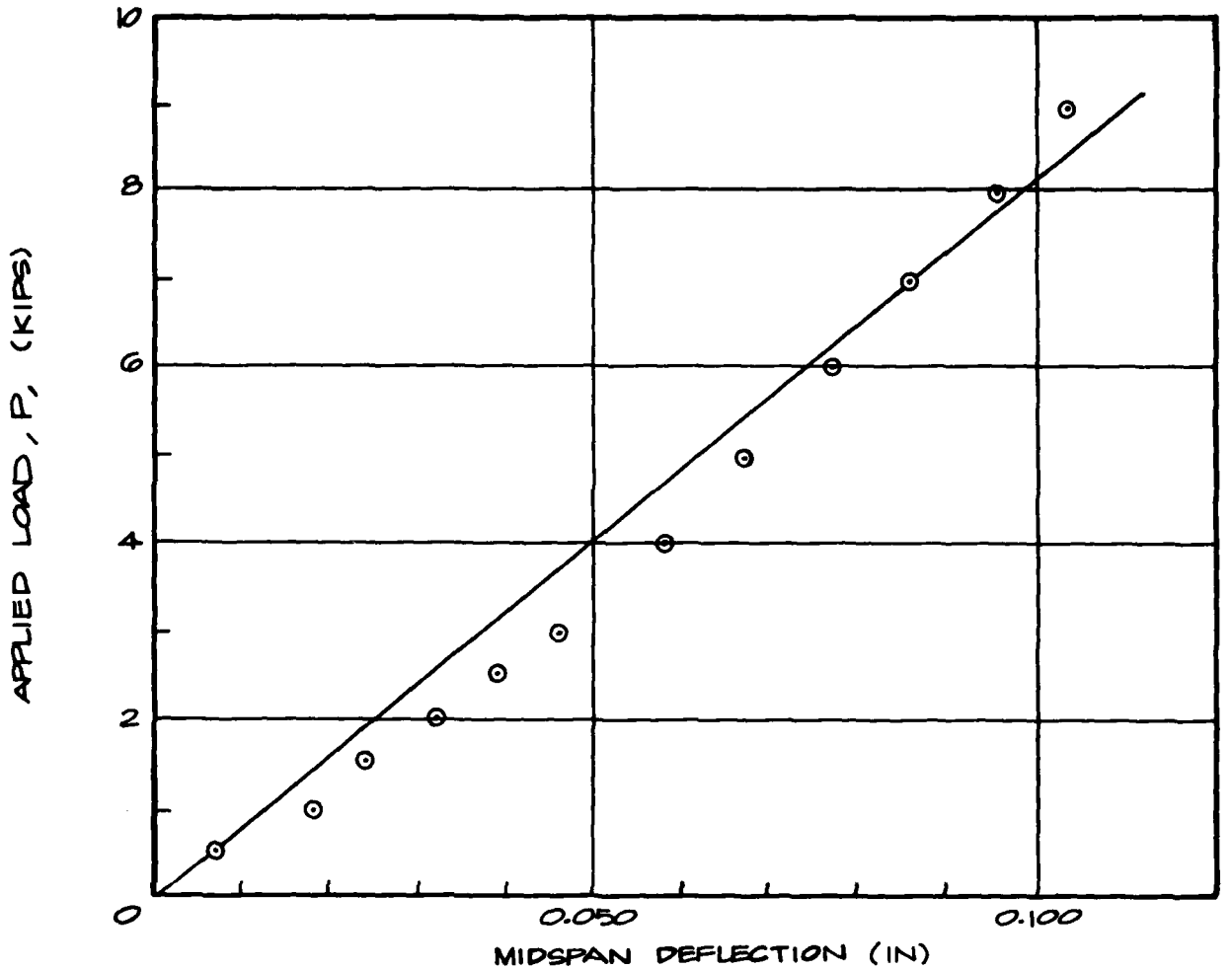

Fig. 2-38. Load vs Deflection for Test No. 80-4A.

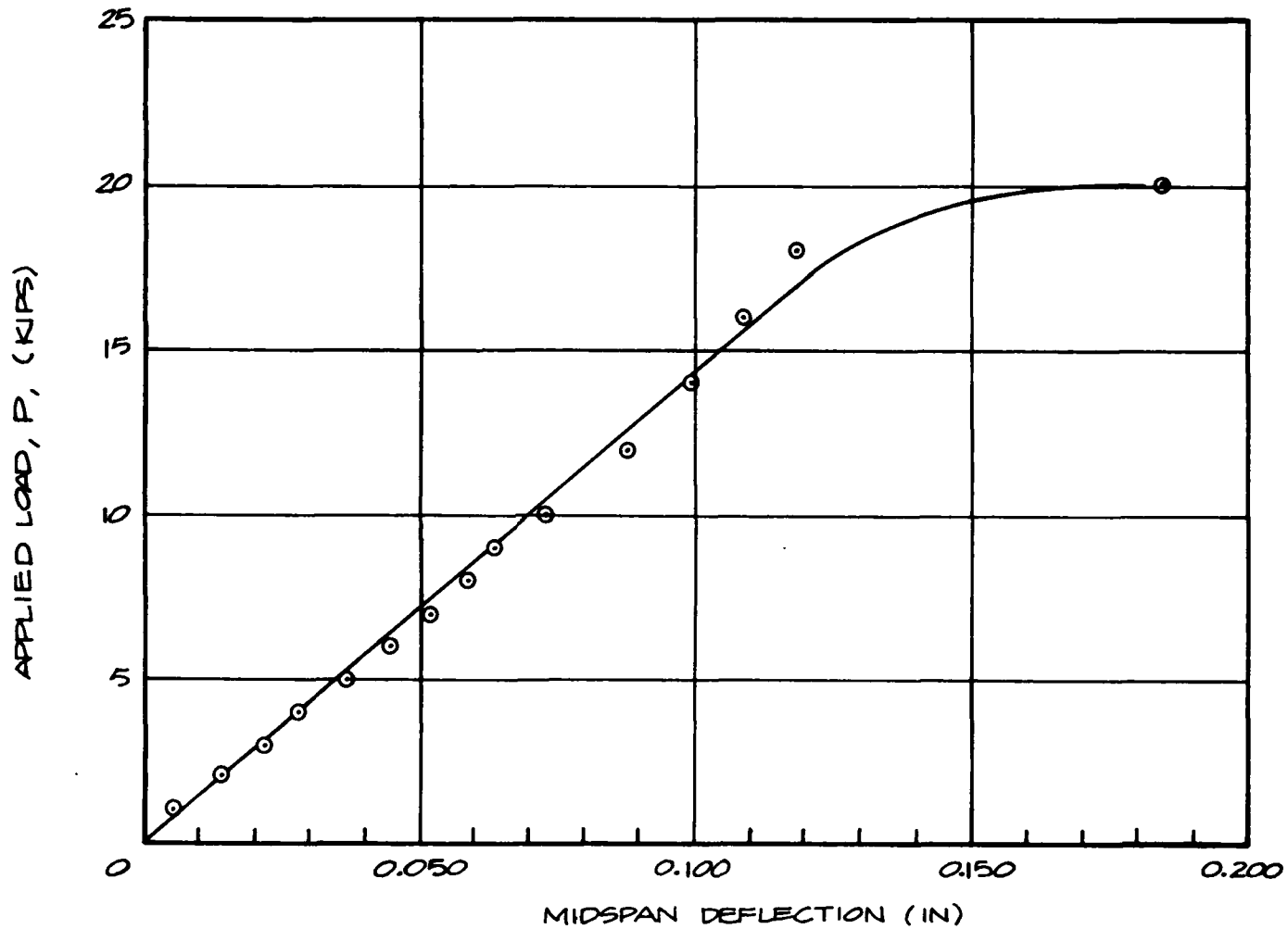

Fig. 2-39. Load vs Deflection, Test No. 80-4B.

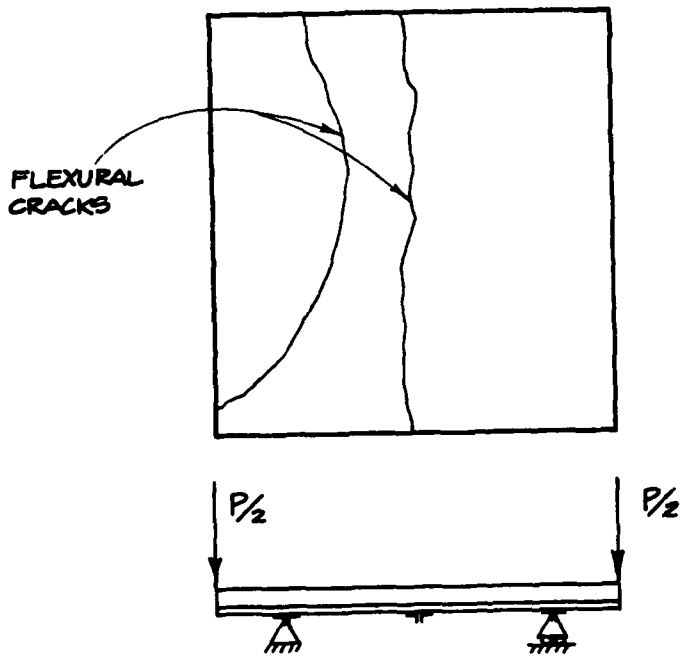

Fig. 2-40. Sketch Showing Location of Flexural Cracks, Test No. 80-4B.

Specimen 80-5. — The test configuration and loading arrangement for specimen 80-5 is shown in Figure 2-41. This test was conducted to determine the ultimate positive moment capacity of the composite deck.

Load was applied in 4,000 lb increments to failure. Ultimate failure occurred at an applied load of 30,000 lb. Below are sketches of the loading and moment diagram at failure.

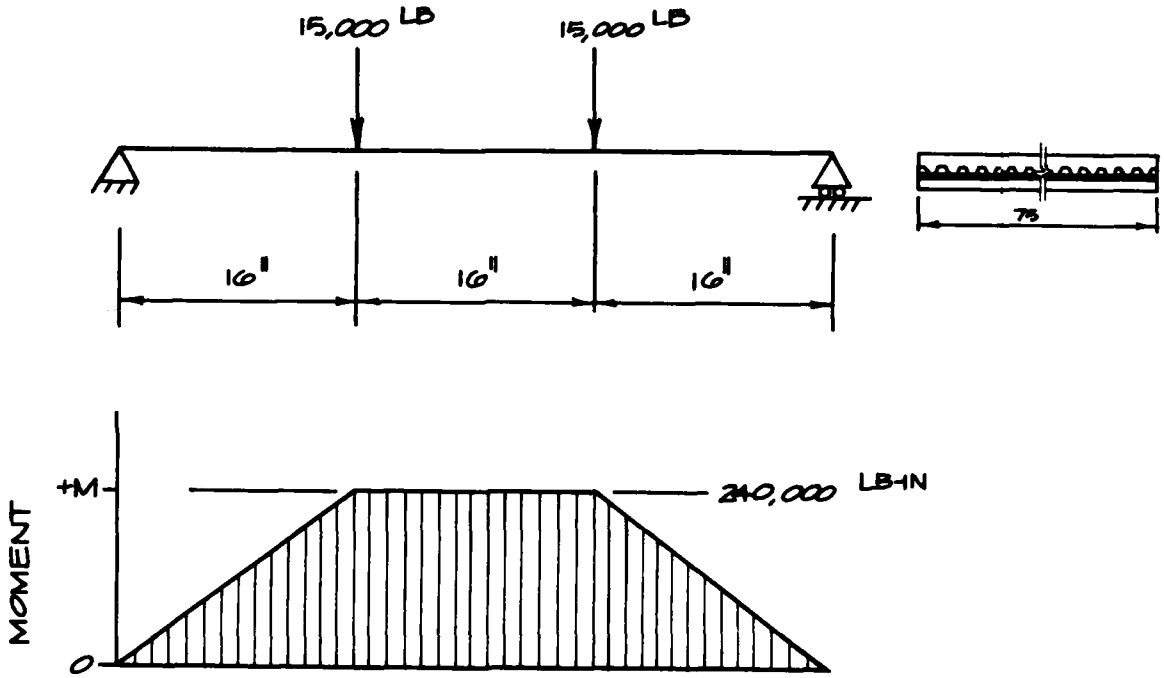

At 30 kips, the maximium positive moment is

$$M_u = 240 \text{ kip-in.} = 3200 \text{ lb-in./in.}$$

A plot of load vs deflection for specimen 80-5 is shown in Figure 2-42. Figure 2-43 shows the positive moment flexural crack in the section of the deck under maximum positive moment.

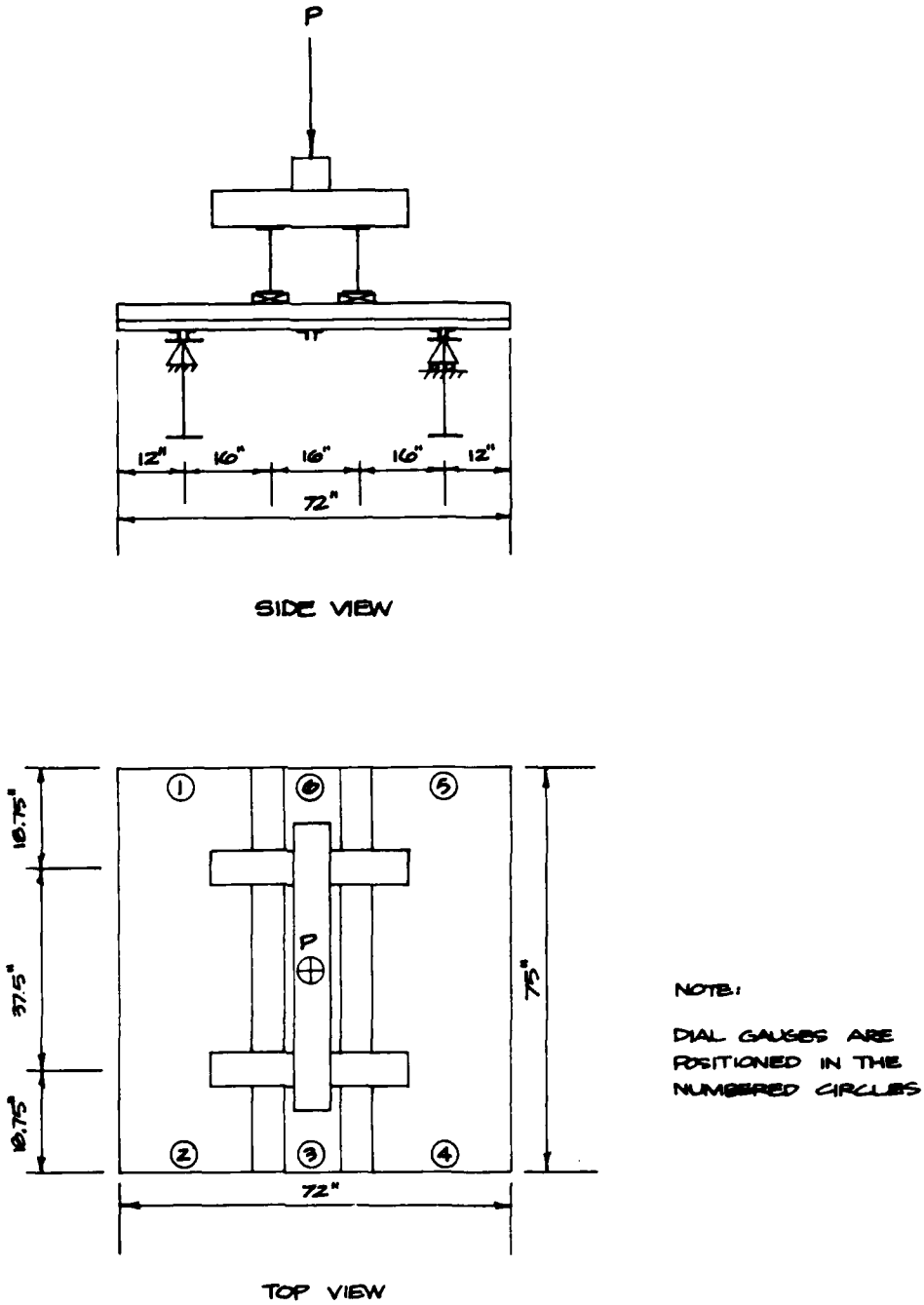

Fig. 2-41. Test Arrangement for Test No. 80-5.

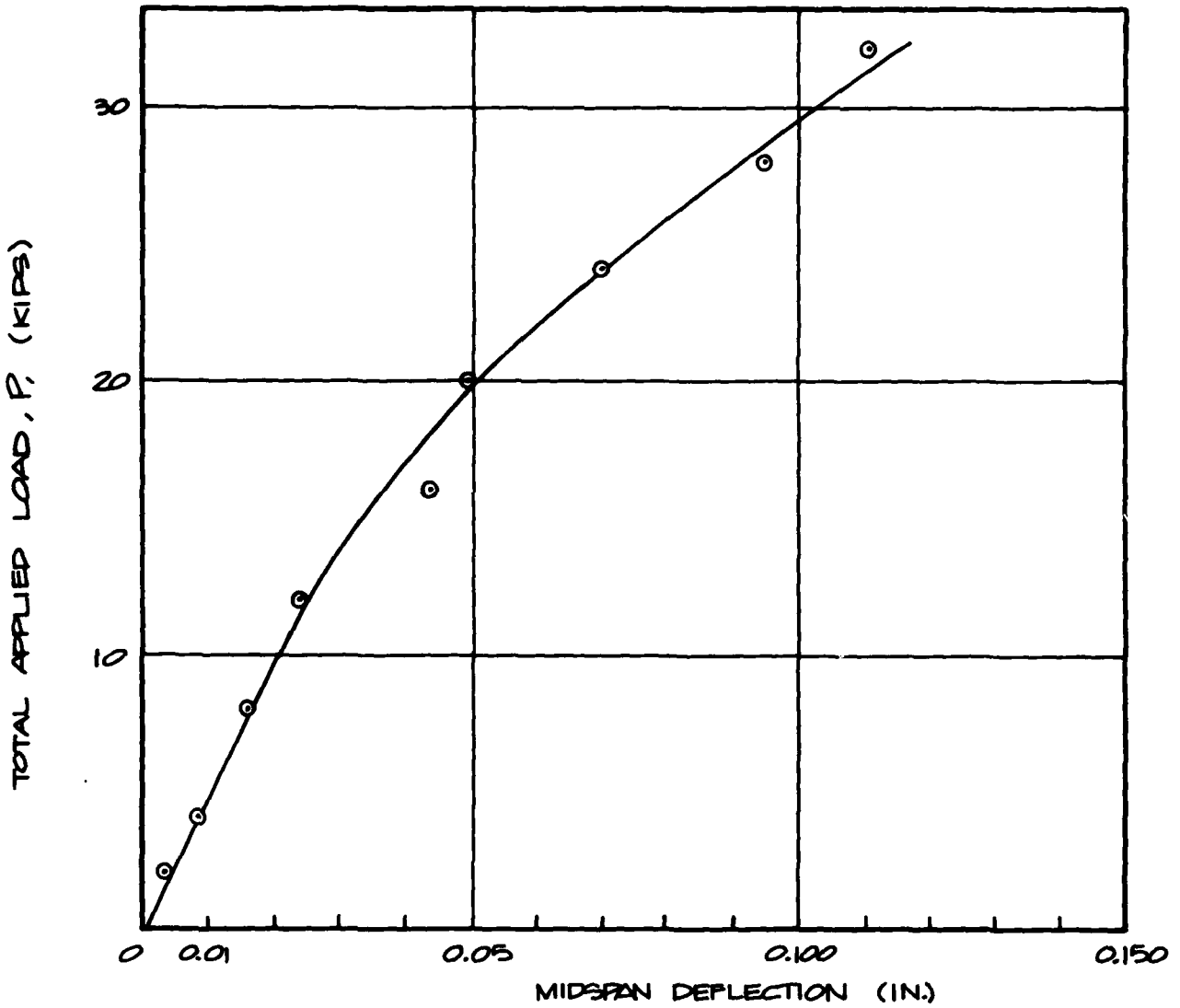

Fig. 2-42. Load vs Deflection for Test No. 80-5.

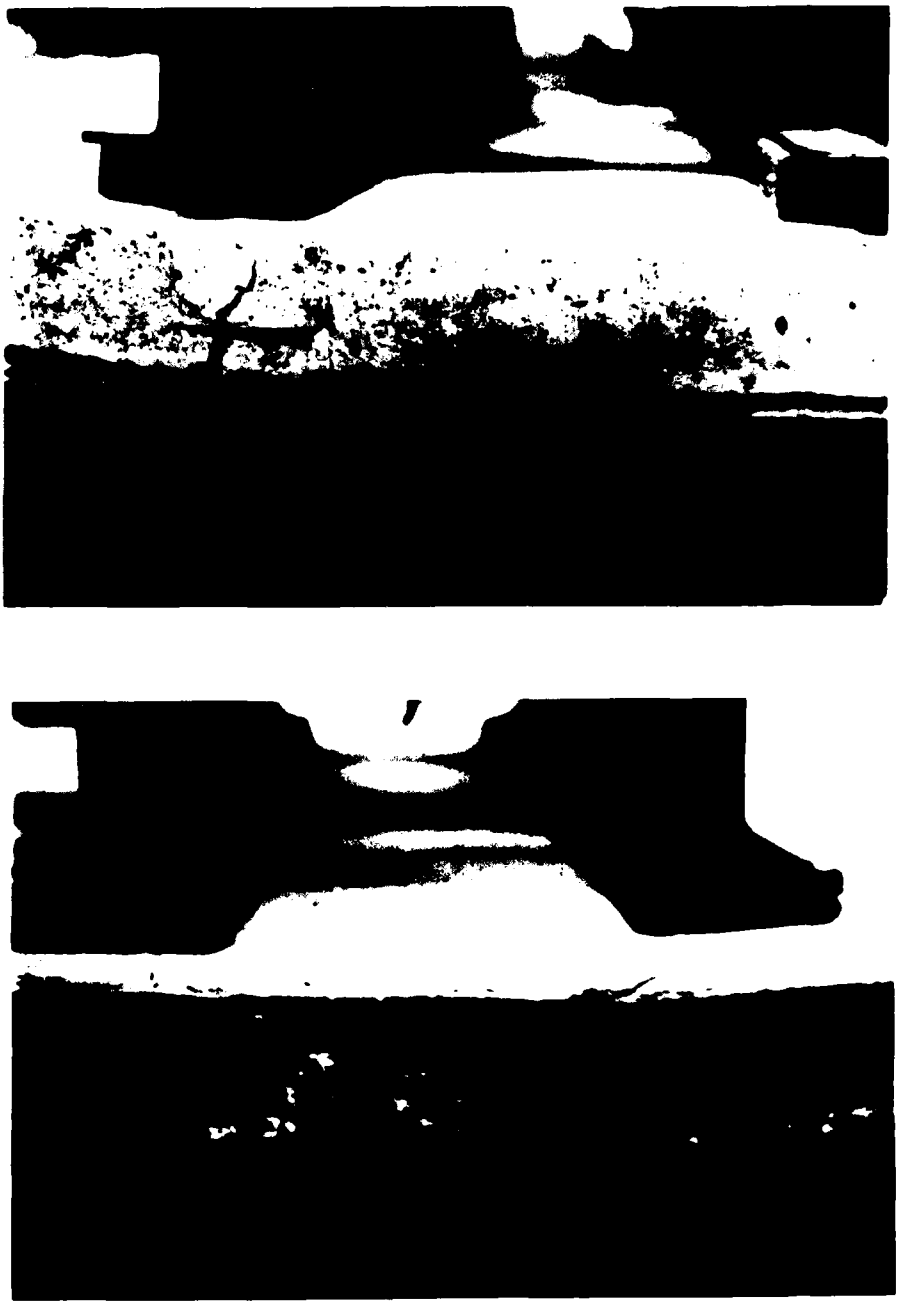

Fig. 2-43. Posttest Photographs, Test No. 80-5.

RESULTS AND CONCLUSIONS

The ultimate moment capacity of the top chord assembly for the test configurations is listed in Table 2-4.

TABLE 2-4: ULTIMATE MOMENT CAPACITY OF FLUTED METAL DECK WITH CONCRETE TOPPING

Test No.	Test Description	Ultimate Moment Capacity
80-3	Ultimate positive moment capacity of top chord assembly in the longitudinal direction	$+M_u$ = +74.7 kip-in./joist
80-4	Ultimate negative moment capacity of concrete decking in transverse direction	$-M_u$ = -1,400 lb-in./in.
80-5	Ultimate positive moment capacity of concrete decking in the transverse direction	$+M_u$ = +3,200 lb-in./in.

The manufacturer* recommends using span (i.e., joist spacing) from 6 ft 0 inches to 12 ft 0 inches for the type of decking used in this test program. The ultimate failure load for both of these spans was determined by using plastic analysis.** The plastic analysis for the 6 ft 0 inch span is shown in Figure 2-44.

Table 2-5 compares the manufacturer's recommended load to the predicted failure load. The prediction was based on the tested ultimate

* VERCO Manufacturing, Inc., Cat. V14, Table 12.

** Sometimes referred to as limit analysis.

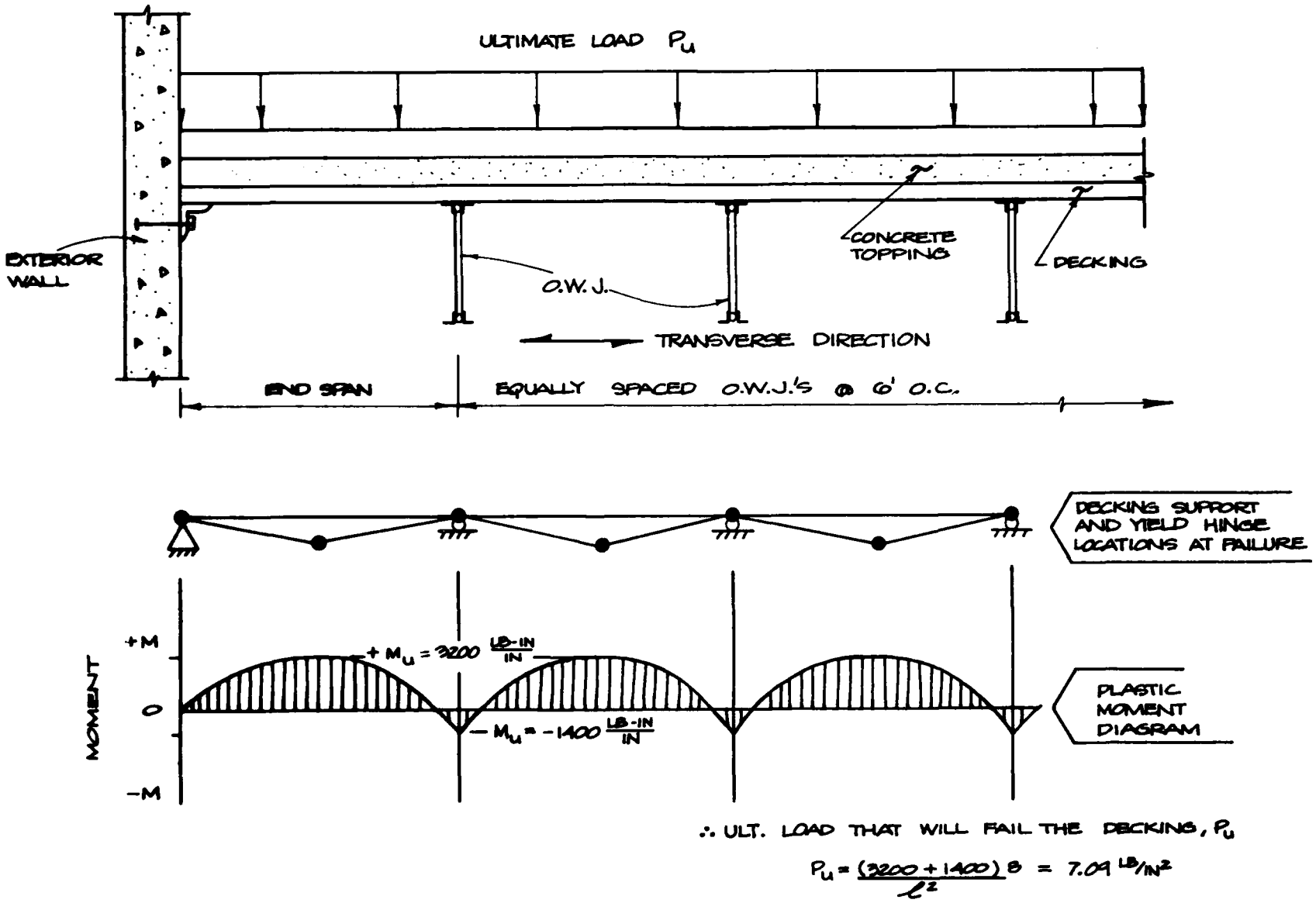

Fig. 2-44. Failure Prediction of Top Chord Assembly Loaded in the Transverse Direction.

capacity of the slabs in conjunction with plastic analysis. The factor of safety against failure of 1.45 to 2.4 is lower than expected.

TABLE 2-5: DECKING LOAD-CARRYING CAPACITY IN THE TRANSVERSE DIRECTION

Decking Span	Manufacturer's Recommended Load	Predicted Ultimate Load Based on Tests 80-4 & 80-5	Factor of Safety Against Failure
6' - 0"	426 psf (2.96 psi)	7.09 psi	2.4
12' - 0"	177 psf (1.23 psi)	1.78 psi	1.45

The low value(s) of the factor of safety suggest that the specimens, which were taken from previously tested full-scale floor tests, may not have been undamaged as originally hoped in the planning for the tests. Although damage was not evident prior to testing, bond between the concrete and decking was apparently weakened during the previous testing. The strength of the decking and concrete floor slab comes from the composite action between the concrete and steel and requires an effective chemical bond between the two materials. If this bond is broken or damaged, as is believed to be the case, the ultimate moment capacity will be substantially reduced.

A conservative factor of safety, which would be consistent with current building codes, would be 1.7 times the allowable load (i.e., the manufacturer's recommended load). Using this factor of safety and the manufacturer's recommended loads in conjunction with plastic analysis, the full range of composite construction for concrete and fluted metal deck can be analyzed for almost all commercial buildings using this type of construction.

Section 3
PRESTRESSED CONCRETE HOLLOW-CORE SLAB TESTS

INTRODUCTION

This is the second series of concrete floor tests conducted and reported in this program. The first series consisted of three tests representing portions of reinforced concrete slabs from typical beam, slab, and girder buildings. These tests were reported in Refs. 3 and 4, and a summary of the test results from these references is shown below:

Specimen	Hardening Technique	W_{peak} (KSF)	(psi)
1 (Ref. 3)	base case	0.875	6.08
2 (Ref. 3)	single shore	2.58	17.92
3 (Ref. 4)	double shores	5.24	36.4

During this phase of the program the major analytical and experimental efforts were devoted to prestressed concrete hollow-core slabs. The purpose of this work was to develop data in all three load categories — "light", "medium", and "heavy" — for this type of construction. These slabs are widely used throughout the country in motel and apartment structures, retail stores, manufacturing buildings, and warehouses. They are commonly used where fire-resistant separations are required, such as a floor separating underground parking from living quarters.

There are a number of manufacturers of this type of product throughout the United States. The particular slabs used in these tests were produced by a national manufacturer who accounts for a significant portion of the hollow-core production in the country. Further, the tests slabs were deemed to be representative of products of this type produced by the other manufacturers.

MANUFACTURE OF TEST SLABS

The prescast prestressed hollow-core concrete slabs used for these tests were 40 inches in width and 4, 8, and 10 inches thick. (This type of slab is available in thicknesses of 4, 6, 8, 10, and 12 inches.) The slab units are produced from high strength, zero slump concrete placed with a machine that deposits, compacts, and finishes the concrete in three immediately successive layers by an extrusion process in one complete operation, resulting in a monolithic slab section. The length of the completed slab is the full length of the casting bed (750 ft). The slabs are cured and saw cut to the required lengths, at which time the transfer of the prestress force is accomplished. The reinforcing consists entirely of longitudinal prestressing strands, which were pretensioned between abutments, located at each end of the casting bed, prior to concrete placement.

DESIGN OF TEST SLABS

The slabs were designed in accordance with the 1976 Uniform Building Code (Ref. 5) and ACI Standard 318-71 (Ref. 6). The design section properties, unit weights, concrete strengths, size, number, and location of strands, and design spans are shown for the 4-, 8-, and 10-inch-thick slabs in Figures 3-1, 3-2, and 3-3. The prestressing strand used was uncoated, seven-wire, stress-relieved strand with ultimate strengths of 250,000 lb/in.^{2} or 270,000 lb/in.^{2} and conformed to the requirements of ASTM A 416.

4" PRESTRESSED PRECAST HOLLOW-CORE PLANK

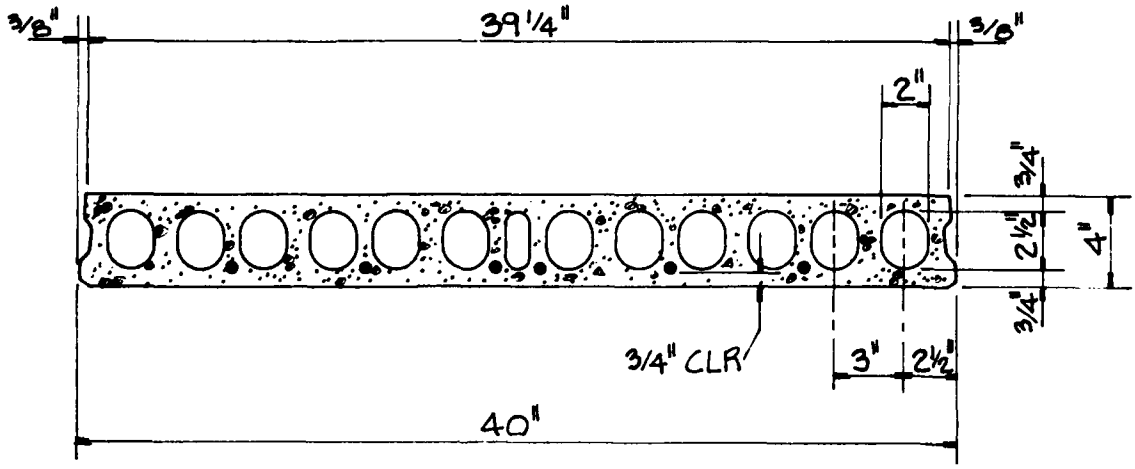

SECTION PROPERTIES

$A = 132\ in^2$	$I = 205\ in^4$
$Y_T = 1.98\ in$	$Y_B = 2.02\ in$
$S_T = 104\ in^3$	$S_B = 101\ in^3$

DESIGN SPAN = 12ft 8in
f'c = 5000 psi
WGT = 35 lbs/ft²
STRANDS = 6-1/4 in dia -250ᵏ
LIGHT DESIGN LOAD = 70 lbs/ft²

Fig. 3-1. Design Properties of 4-inch Prestressed Precast Hollow-Core Plank.

8" PRESTRESSED PRECAST HOLLOW-CORE PLANK

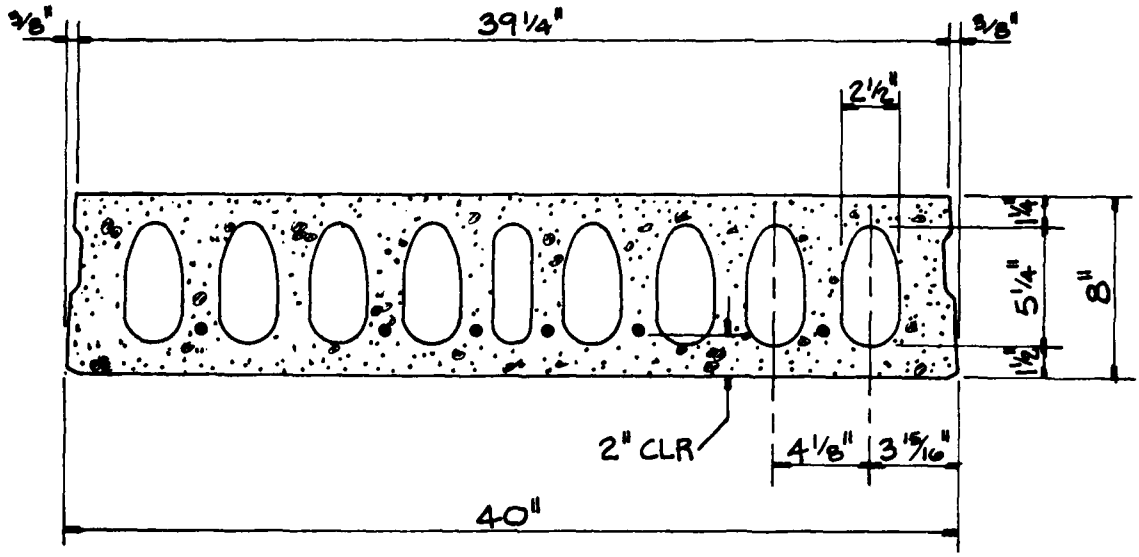

SECTION PROPERTIES

$A = 218\ IN^2$	$I = 1515\ IN^4$
$Y_T = 4.02\ IN$	$Y_B = 3.98\ IN$
$S_T = 377\ IN^3$	$S_B = 380\ IN^3$

DESIGN SPAN = 18 ft 0 in
$f'c$ = 5000 PSI
WGT = 60 lbs/ft²
STRANDS = 6 - 3/8 in dia - 270K
MEDIUM DESIGN LOAD = 165 lbs/ft²

Fig. 3-2. Design Properties of 8-inch Prestressed Precast Hollow-Core Plank.

10" PRESTRESSED PRECAST HOLLOW-CORE PLANK

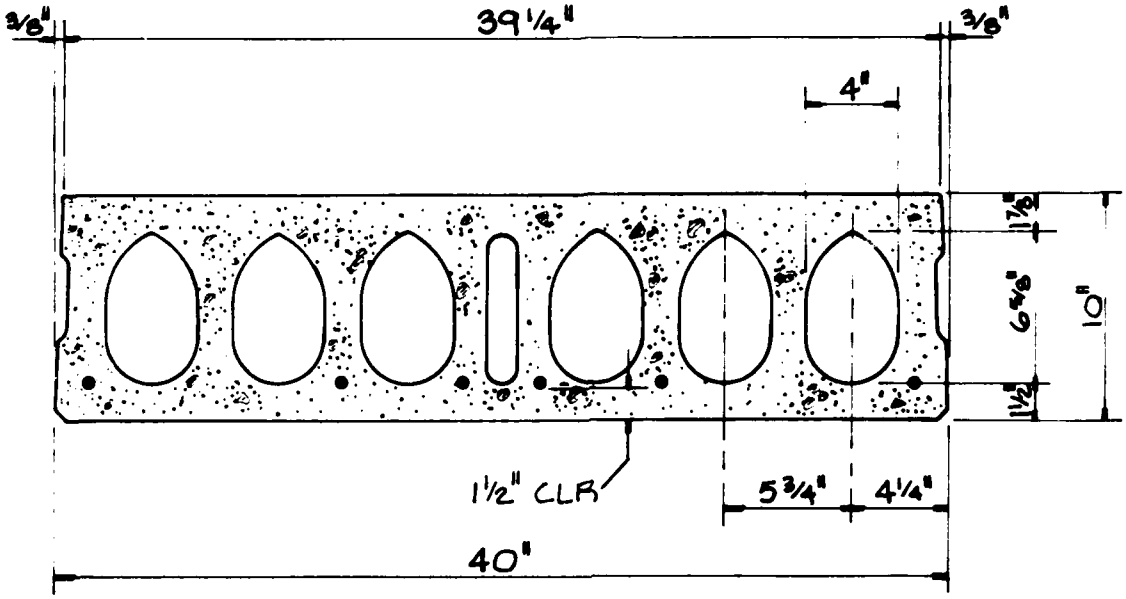

SECTION PROPERTIES

$A = 272\ IN^2$	$I = 2970\ IN^4$
$Y_T = 5.09\ IN$	$Y_B = 4.91\ IN$
$S_T = 585\ IN^3$	$S_B = 604\ IN^3$

DESIGN SPAN = 18 ft 0 in
f'c = 5000 PSI
WGT = 75 lbs/ft²
STRANDS = 6-3/8 in dia -270K
HEAVY DESIGN LOAD = 265 lbs/ft²

Fig. 3-3. Design Properties of 10-inch Prestressed Precast Hollow-Core Plank.

The calculated design loads for each test slab are shown on Figures 3-1, 3-2, and 3-3. The calculations used to determine these design ultimate load capacities are presented in Appendix B.

TEST PROGRAM

This program consisted of load tests to failure on 15 prestressed concrete slabs, manufactured and designed as previously outlined in this section. Three thicknesses of plank were used for the tests — 4, 8, and 10 inches, and in all cases the plank was 40 inches wide. The cross-section of each of the planks was as shown in Figures 3-1, 3-2, and 3-3. The test spans were : 12 ft 8 in. for the 4-inch-thick units, and 18 ft 0 in. for the 8- and 10-inch-thick units, center to center of bearing.

Four tests were conducted on the 4-inch-thick units, five tests on the 8-inch-thick units, and six tests on the 10-inch-thick units. A detailed outline of each test, including the load and shoring configurations used, and the respective results are presented below.

Tests Nos. 1 and 2 (Base Case, 4-inch Slab)

Both of these tests were conducted on identical slabs simply supported. The load was applied in both tests at two locations by a single hydraulic ram in the configuration shown in Figure 3-4. The vertical deflection was measured and recorded at midspan and at the one-third points.

The load was applied at a slow rate in 500 lb increments and the deflection recorded at each increment. Both test slabs failed when the applied ram load reached 6,500 lb (3,250 lb at each one-third point). The calculated uniform load at failure was 205 psf (1.4 psi). The uniform load vs midspan deflection curves are shown in Figures 3-5 and 3-6 for Tests Nos. 1 and 2, respectively.

The failure occurred in a similar manner in both tests. Vertical

AD-A100 490 SCIENTIFIC SERVICE INC REDWOOD CITY CA F/G 13/13
UPGRADING OF EXISTING STRUCTURES. PHASE III. SHELTER DESIGN OPT--ETC(U)
MAY 81 R S TANSLEY, B L GABRIELSEN EMW-C-0153
UNCLASSIFIED SSI-8012-6 NL

2 OF 3
AD
A100490

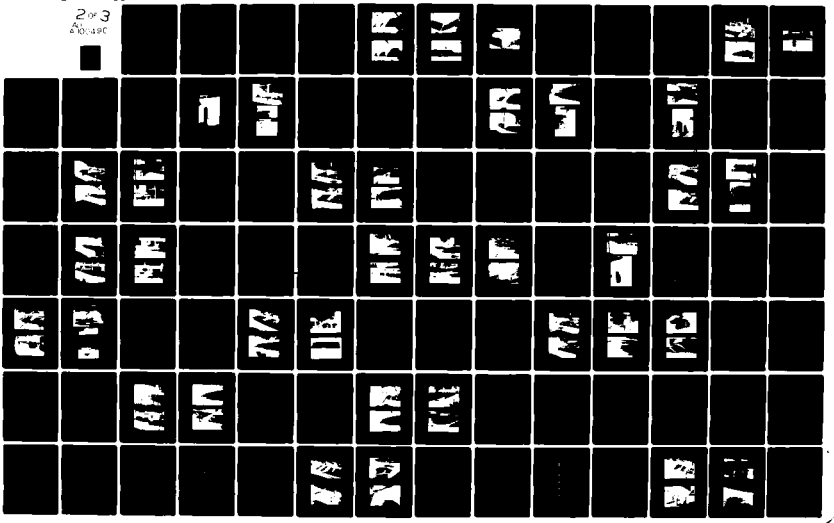

tension cracks were first noted between the load points at approximately 110 psf (0.8 psi), and the slabs failed suddenly in flexure at their approximate midspan after supporting the 205 psf (1.4 psi) load for several minutes. The failed slabs were completely separated at midspan, and an abrupt tension failure of the strands occurred with little or no indication of yield. An inspection of the ends of the slabs after testing did not indicate any evidence of strand bond failure in either of the tests.

Figure 3-7 shows the 4-inch slabs prior to testing. Figure 3-8 shows Test No. 1 after test. Figure 3-9 is of Test No. 2 during test and shows the tension cracks forming; and Figure 3-10 shows Test No. 2 after test.

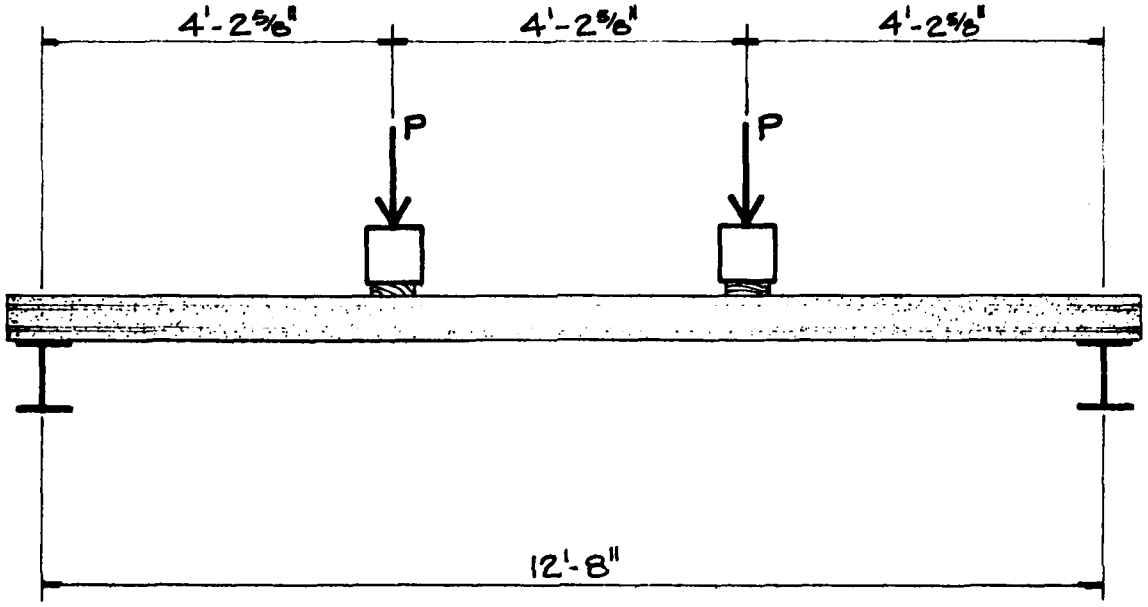

Fig. 3-4. Loading Configuration — Base Case, 4-inch Slab, Tests Nos. 1 and 2.

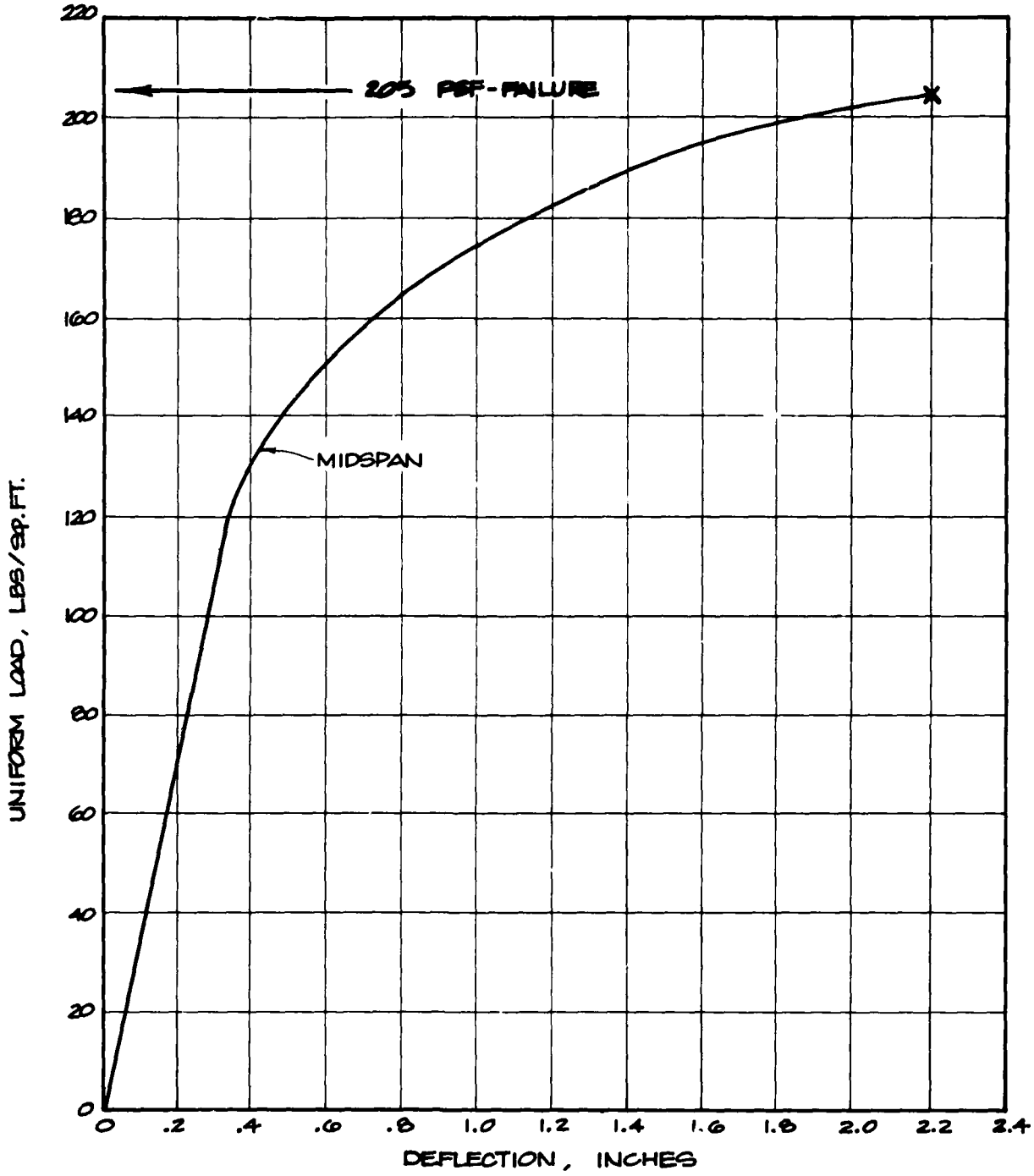

Fig. 3-5. Uniform Load vs Deflection, Test No. 1, Base Case, 4-inch Slab.

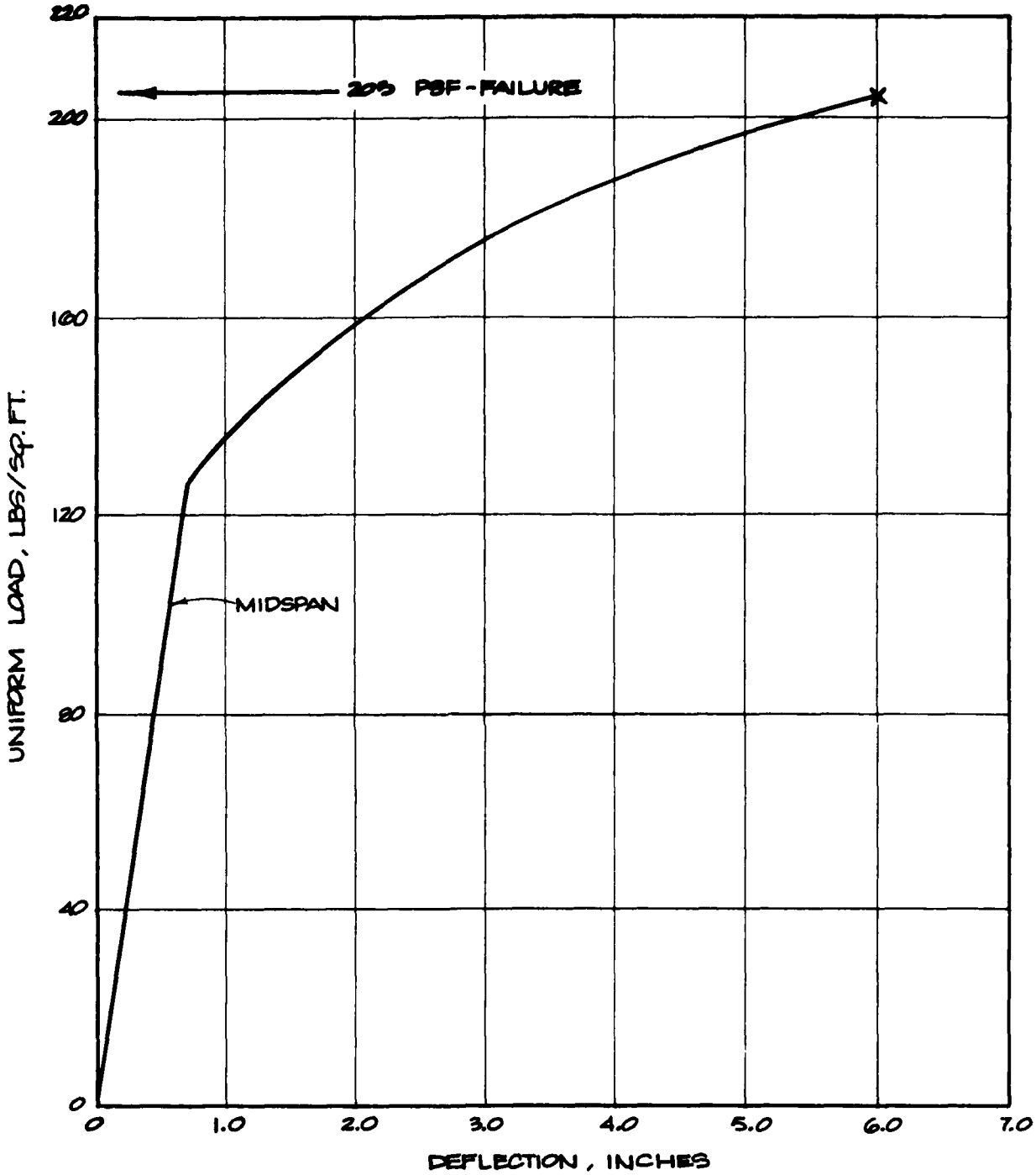

Fig. 3-6. Uniform Load vs Deflection, Test No. 2, Base Case, 4-inch Slab.

A. Test No. 1.

B. Test No. 2.

Fig. 3-7. Pretest Photographs of 4-inch Slabs, Tests Nos. 1 and 2.

Fig. 3-8. Test No. 1, After Test.

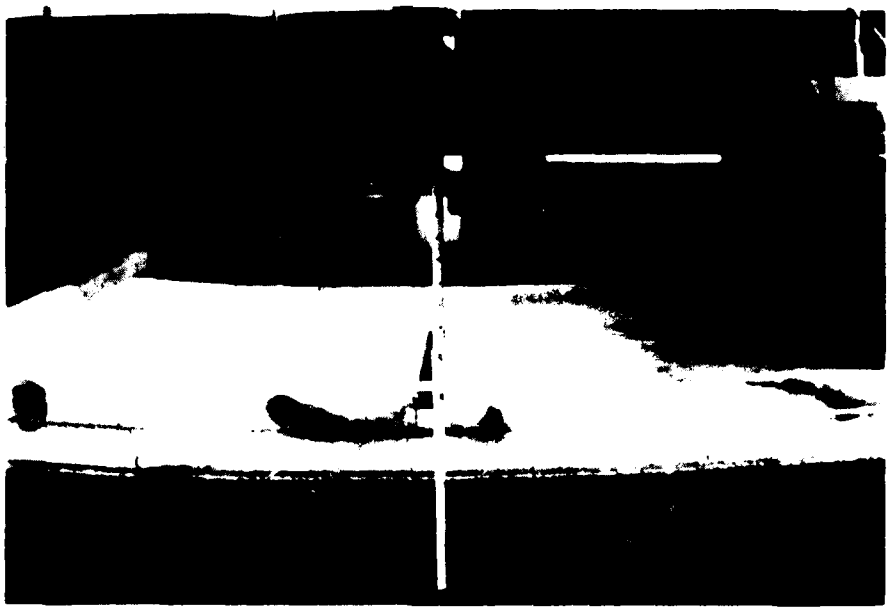

Fig. 3-9, Test No. 2, During Test.

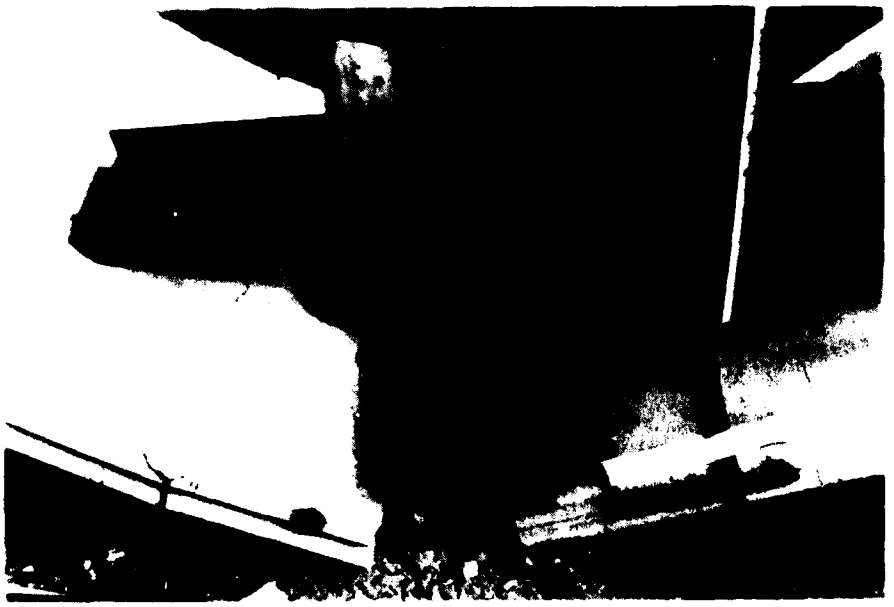

Fig. 3-10. Test No. 2, After Test.

Test No. 3 (Shored at Midspan, 4-inch Slab)

The slab used for this test was simply supported at its ends and shored at midspan with a timber shore shimmed tightly against the bottom of the slab. The load was applied at four locations by two hydraulic rams in the configuration shown in Figure 3-11. The vertical deflection was measured and recorded at midspan (over the shore) and at the one-quarter points.

The load was applied at a slow rate in 1000 lb/ram increments and the deflection recorded at each increment.

The test slab failed when the applied load reached 16,000 lb/ram. The calculated uniform load at failure was 1,012 psf (7.0 psi). The uniform load vs deflection curve for each span is shown in Figure 3-12.

Positive moment tension cracks* near the center of each span and a negative moment tension crack* over the shore were noted in the slab at approximately 822 psf (5.7 psi). The failure occurred in flexure near the center of each of the spans.

Figure 3-13 shows the 4-inch slab, shore in place, before and after test; Figure 3-14 shows the negative moment tension crack, which occurred over the shore, after test.

---

* Note: Positive moment tension cracks are those that occur on the bottom of the test slabs, and negative moment tension cracks are those that occur on the top.

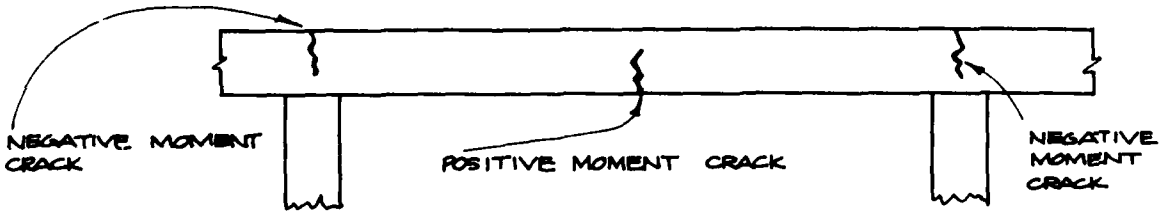

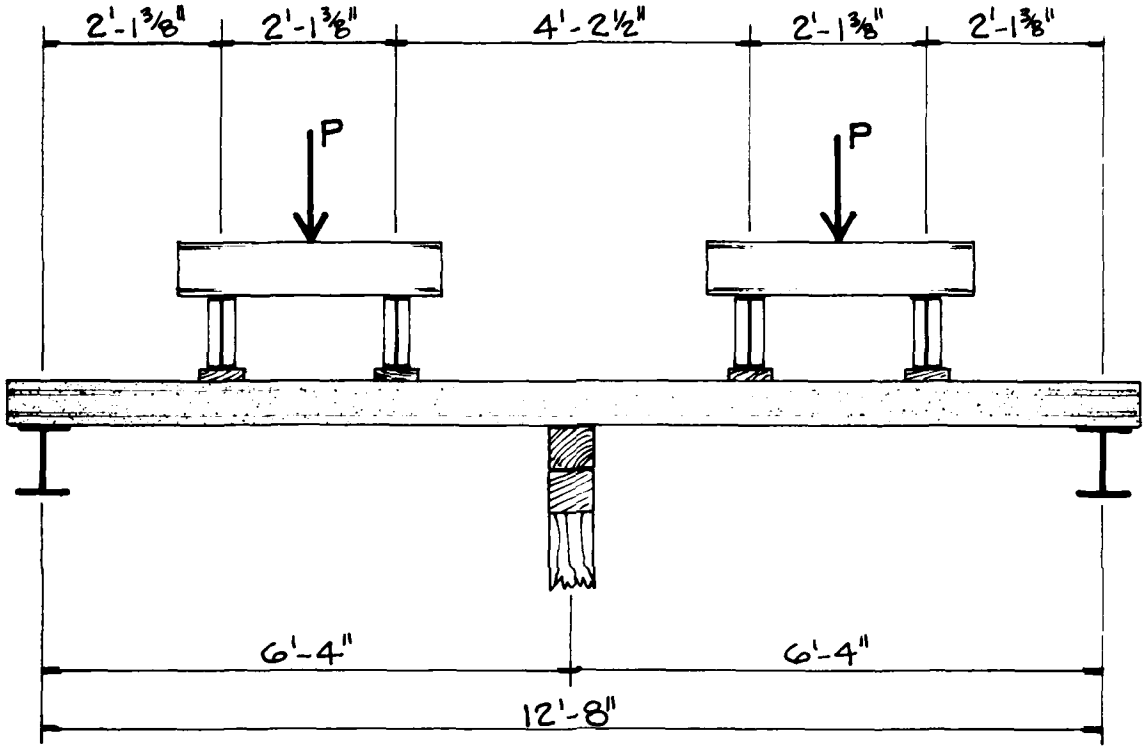

Fig. 3-11. Loading Configuration — Shored at Midspan, 4-inch Slab, Test No. 3.

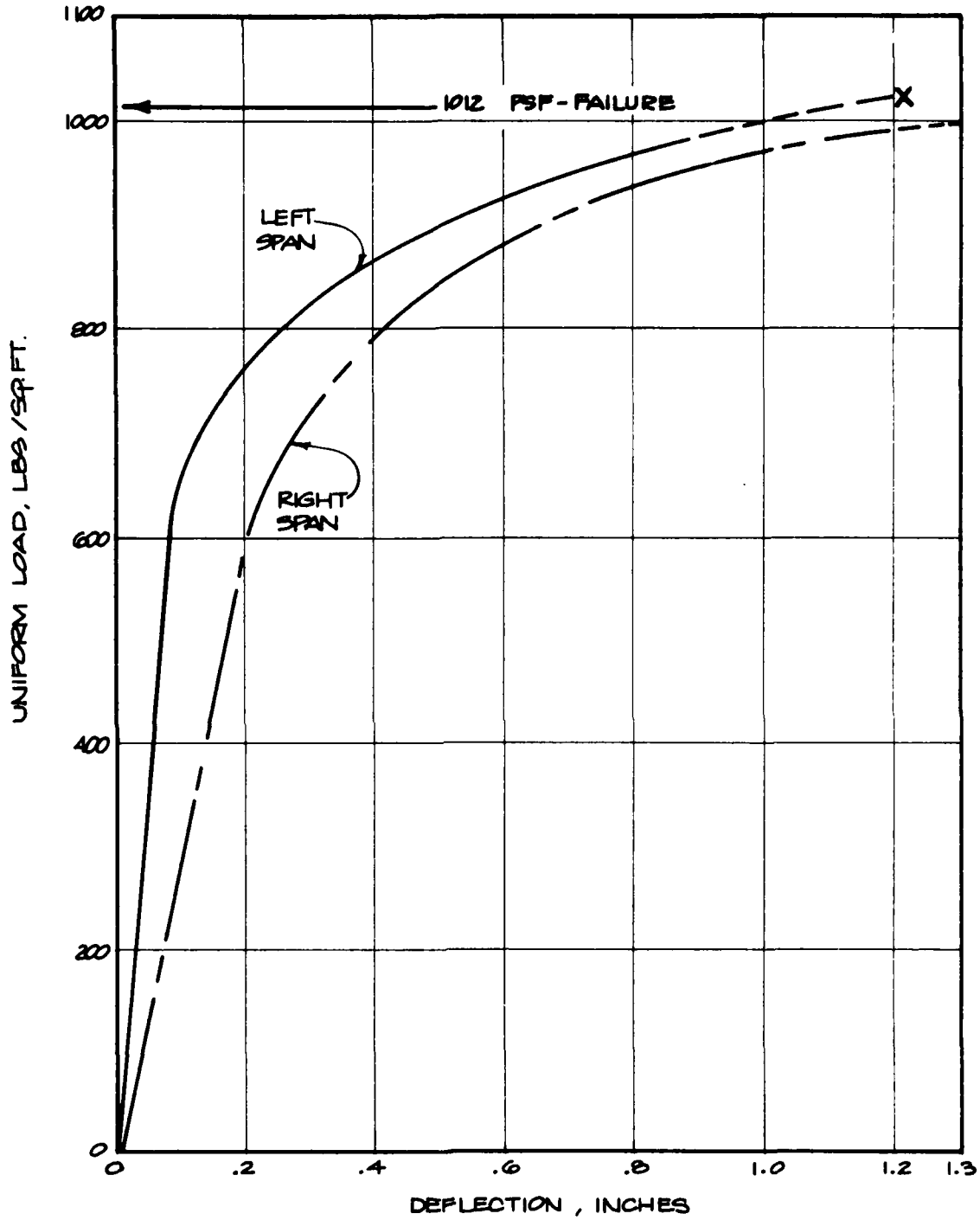

Fig. 3-12. Uniform Load vs Deflection, Test No. 3, Shored at Midspan, 4-inch Slab.

Fig. 3-13. Pre- and Posttest Photographs, Test No. [illegible]

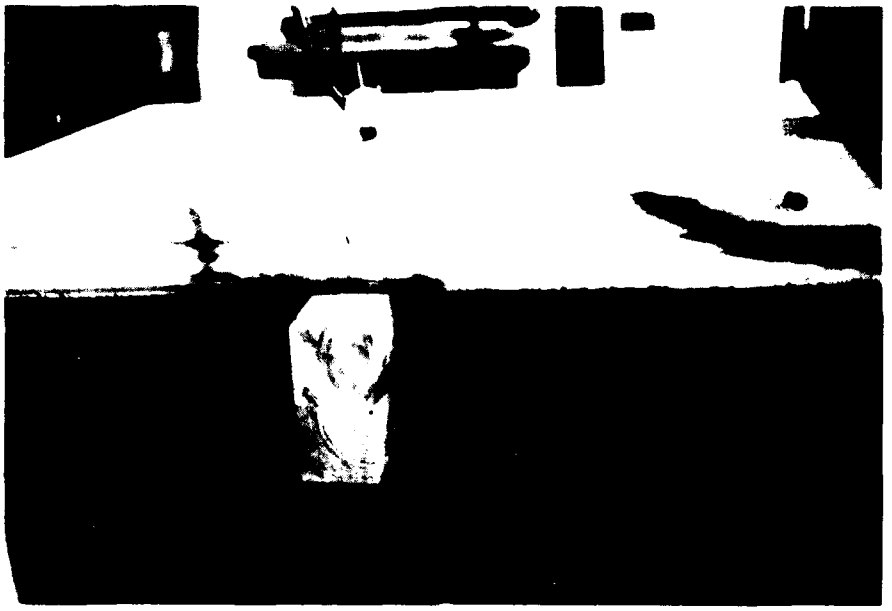

Fig. 3-14. Negative Moment Tension Crack, Test No. 3, After Test.

Test No. 4 (Shored at One-Third Span, 4-inch Slab)

The slab used for this test was simply supported at its ends and shored at the one-third points with timber shores shimmed tightly against the bottom of the slab. The load was applied at six locations by three hydraulic rams in the configuration shown in Figure 3-15. The vertical deflection was measured and recorded at the one-third points (over the shores) and at three locations midway between each support.

The load was applied at a slow rate in 1,000 lb/ram increments and the deflection recorded at each increment. The test slab failed when the applied load reached 25,500 lb/ram. The calculated uniform load at failure was 2,431 psf (16.9 psi). The uniform load vs relative deflection curves for the left and right spans are shown in Figure 3-16.

Positive moment tension cracks first occurred at the center of the spans at 1,811 psf (12.6 psi), and the first negative moment crack occurred over a shore at 2,002 psf (13.9 psi). The slab failed when bond failure of the prestressing strands occurred, resulting in a shear/flexure failure of the end spans.

Figure 3-17 shows one of the shores used, prior to test. The post-test photographs in Figure 3-18 shows the full test assembly and loading configuration, and one of the negative moment tension cracks after test.

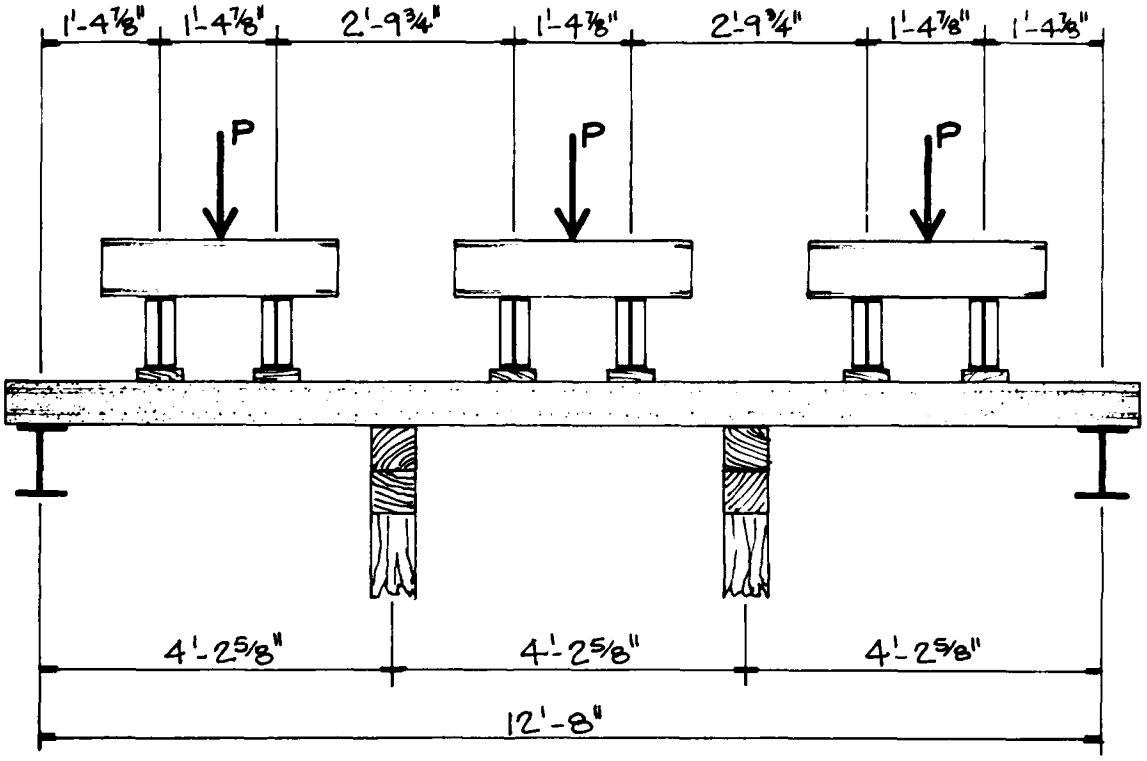

Fig. 3-15. Loading Configuration — Shored at One-Third Points, 4-inch Slab, Test No. 4.

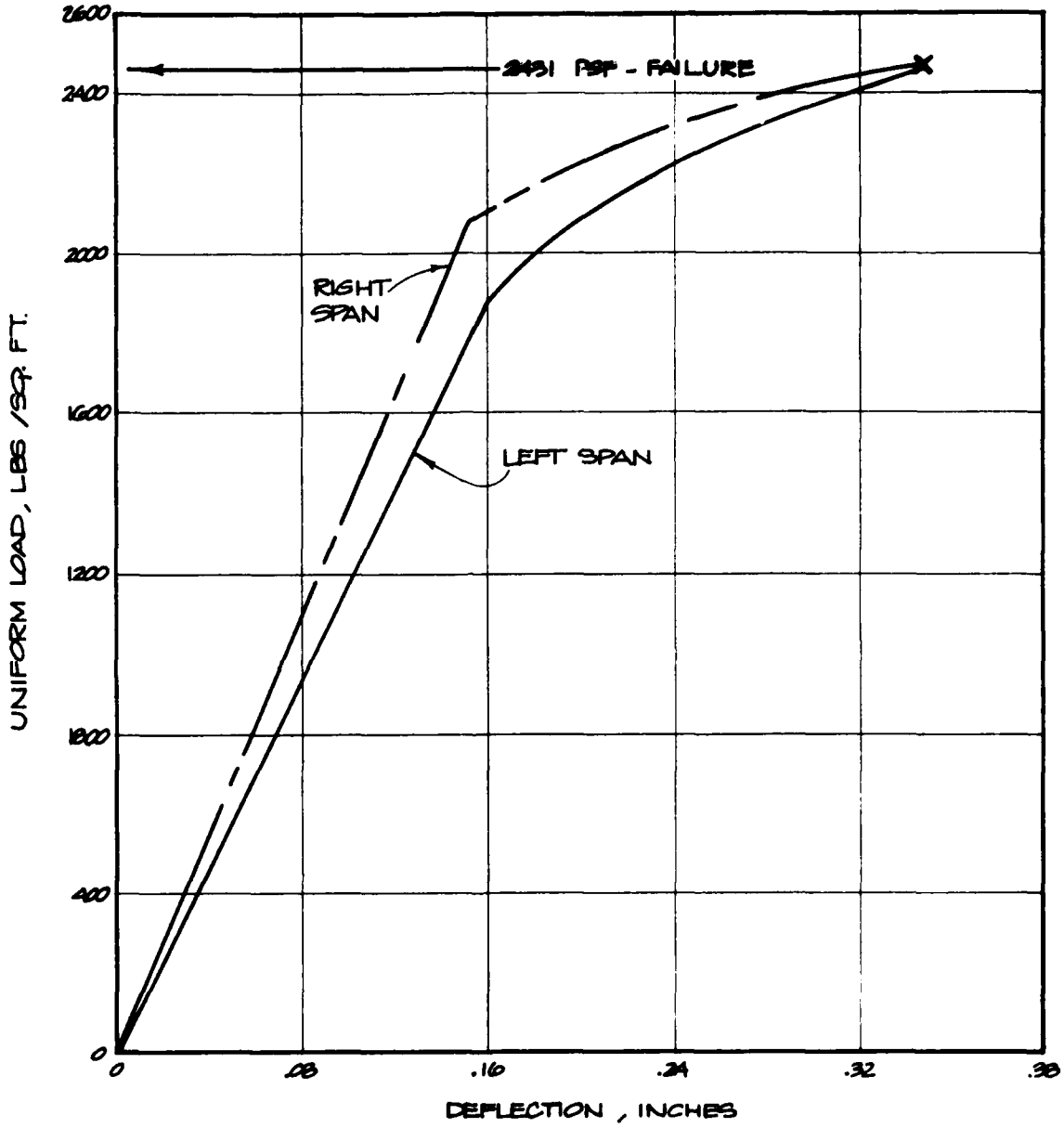

Fig. 3-16. Uniform Load vs Deflection, Test No. 4, One-Third Shoring, 4-inch Slab.

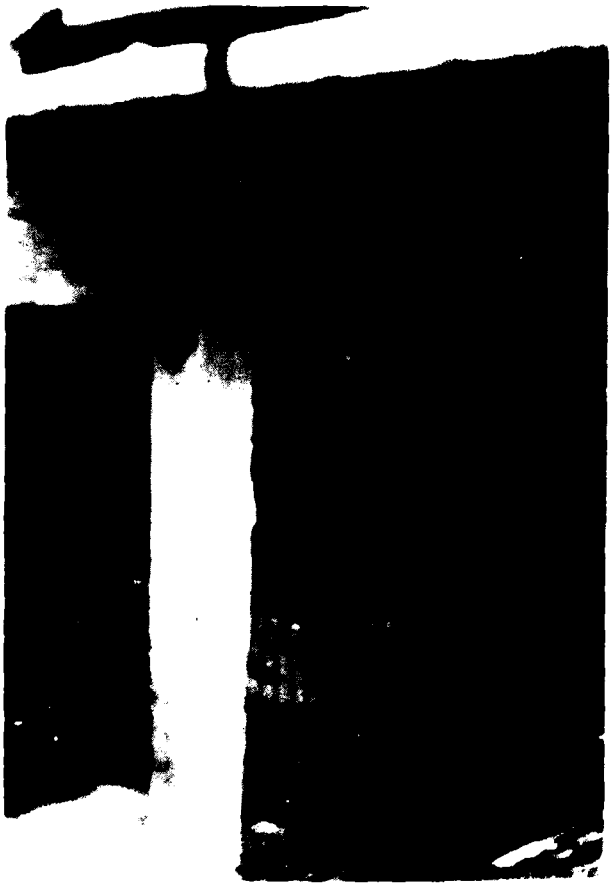

Fig. 3-17. Shoring Details, Test No. 4, Before Test.

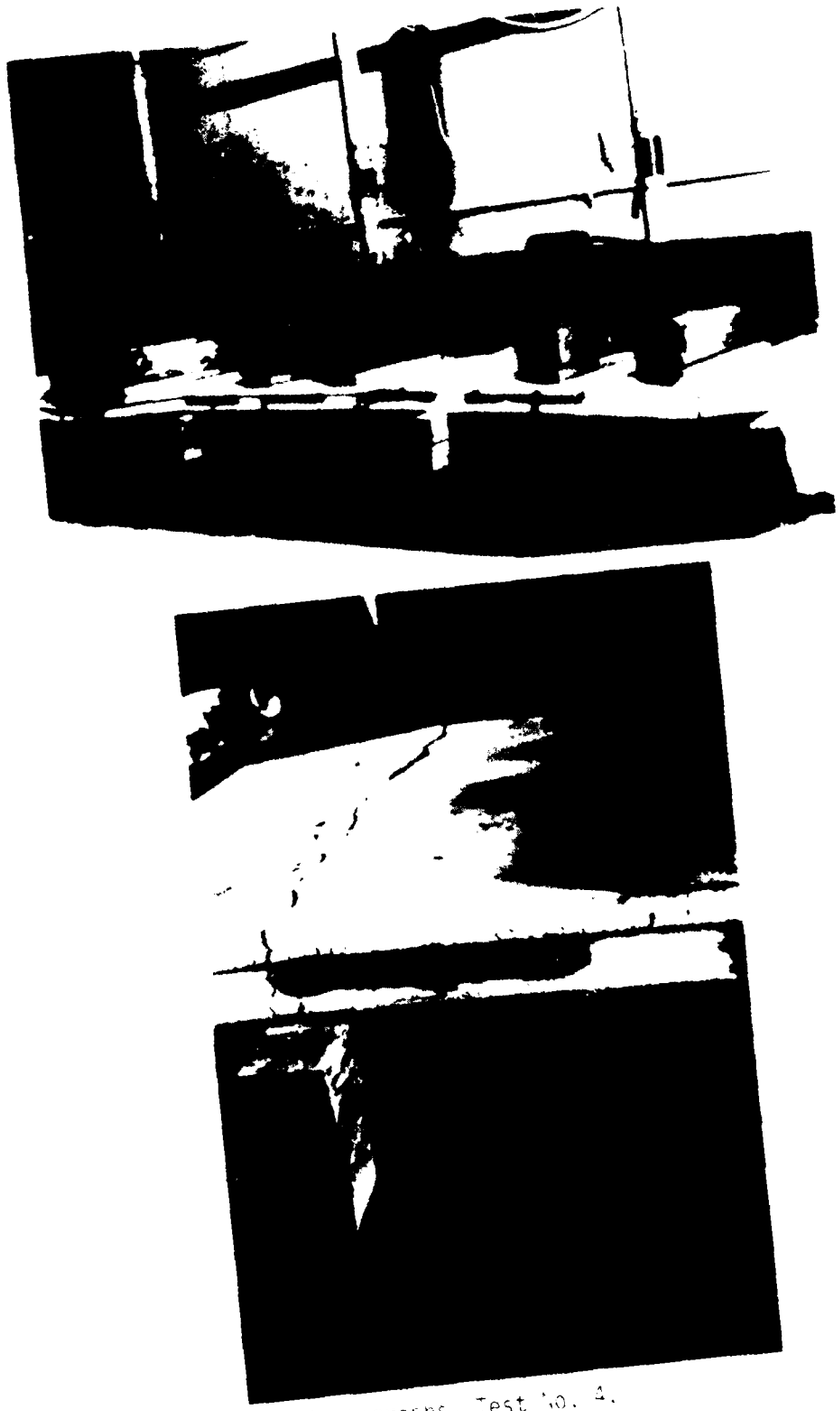

Fig. 3-18. Posttest Photographs, Test No. 4.

Test No. 5 (Base Case, 8-inch Slab)

The slab in this test was simply supported. The load was applied at two locations by two hydraulic rams in the configuration shown in Figure 3-19. The vertical deflection was measured and recorded at midspan and at the one-third points.

The load was applied at a slow rate in 1,000 lb/ram increments and the deflection recorded at each increment. The slab failed when the applied load reached 9,000 lb/ram. The calculated uniform load at failure was 400 psf (2.8 psi). The uniform load vs deflection curve for midspan is shown in Figure 3-20.

Positive moment tension cracks were first noted under each load point at approximately 178 psf (1.2 psi). The failure occurred in flexure at these locations. A careful inspection of the slab after test indicated bond failure of the strands at each end had also occurred.

Figure 3-21 shows the slab before and after test. The posttest photographs in Figure 3-22 show one of the positive moment tension cracks after test and the distress caused by a compression failure of the concrete.

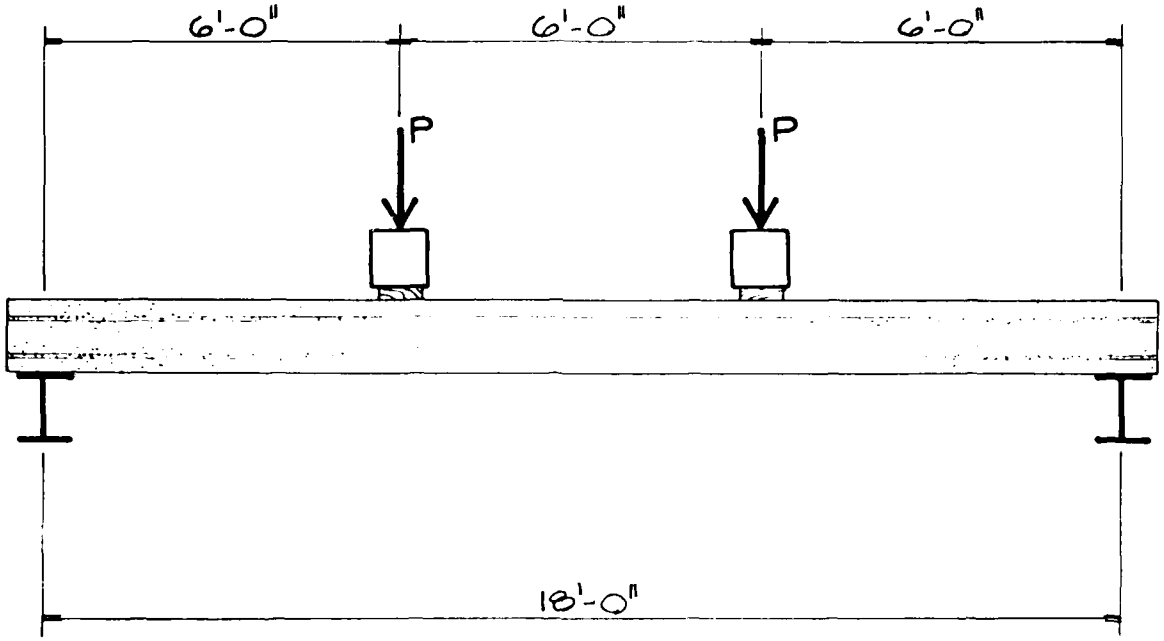

Fig. 3-19. Loading Configuration, Base Case, 8-inch Slab, Test No. 5.

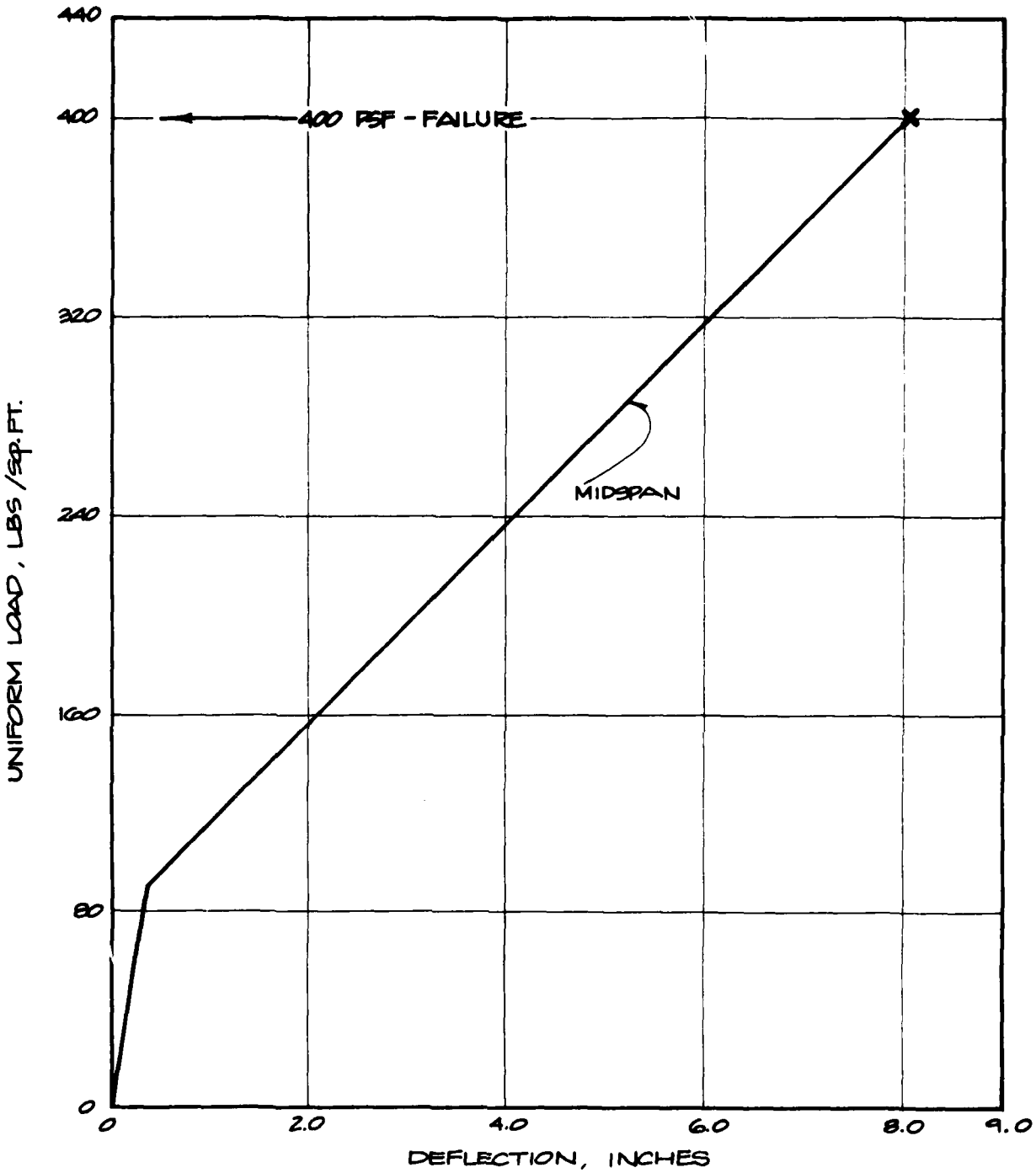

Fig. 3-20. Uniform Load vs Deflection, Test No. 5, Base Case, 8-inch Slab.

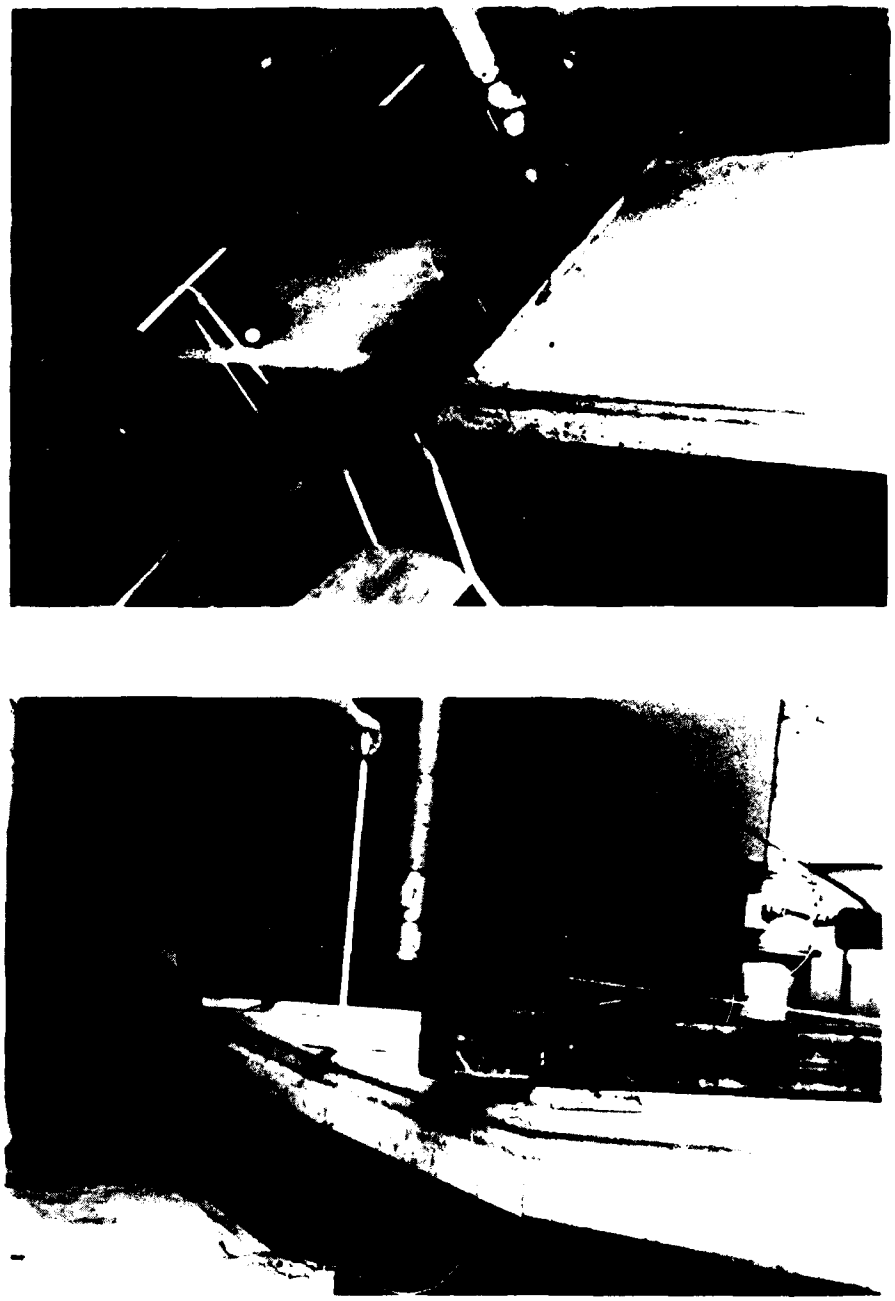

Fig. 3-21. Pre- and Posttest Photographs, Test No. 5.

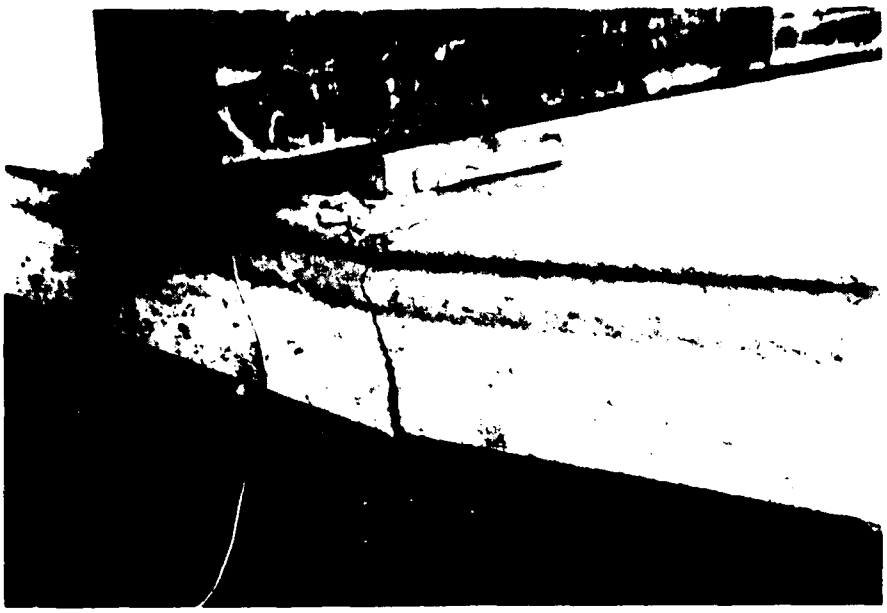

Fig. 3-22. Posttest Photographs, Test No. 5.

Tests Nos. 6 and 7 (Shored at Midspan, 8-inch Slabs)

Both of these tests were conducted on identical slabs simply supported and shored at midspan. The two tests differed in the type and method of shoring. In Test No. 6, the shore consisted of a structural steel tube shimmed tightly against the bottom of the slab. Figure 3-23 shows this shore in position prior to test. Test No. 7 utilized a shore constructed of heavy timber in such a manner as to permit the slab to deflect 1½ inches prior to picking up any load. This gap was achieved by shimming the shore tightly against the bottom of the slab with the 1½-inch gap at the bottom, and securing it in place with lightly nailed boards on either side of the base. This shore, in position prior to test, is shown in Figure 3-24.

The purpose of the two different types of shore systems was to determine if the performance varied between these two extremes in shoring; i.e., one permitting no vertical moment at midspan (Test No. 6) and the other permitting substantial vertical movement — 1½ inches plus the normal crushing of the timber (Test No. 7).

The load was applied in both tests at four locations by two hydraulic rams in the configurations shown in Figure 3-25. The vertical deflection was measured and recorded at the quarter points and at midspan (over the shores). In both tests, the load was applied at a slow rate of 2,000 lb/ram increments and the deflection recorded at each increment.

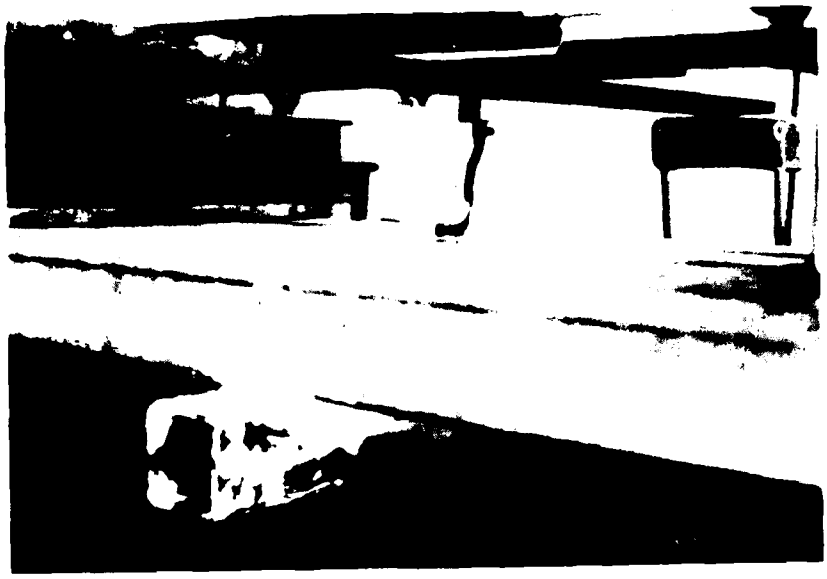

Fig. 3-23. Test No. 6, Steel Shore.

Fig. 3-24. Test No. 7, Timber Shore With 1½-inch Gap.

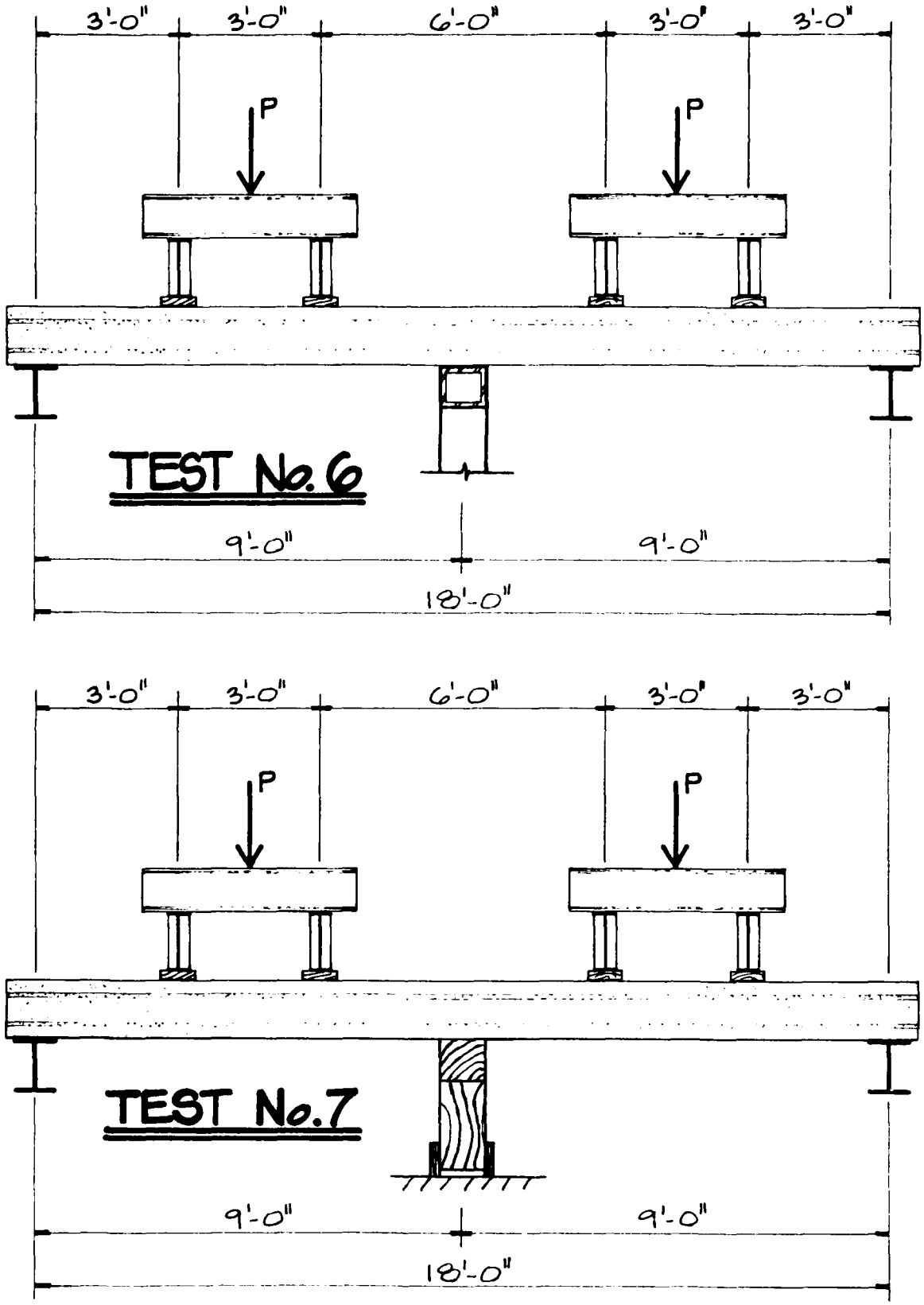

Fig. 3-25. Loading Configuration — Shored at Midspan, 8-inch Slabs, Tests Nos. 6 and 7.

In Test No. 6, the slab failed when the applied load reached 35,000 lb/ram. The calculated uniform load at failure was 1,557 psf (10.8 psi). The uniform load vs relative deflection curve for each span is shown in Figure 3-26.

A negative moment tension crack at midspan, over the shore, and positive moment tension cracks at the approximate quarter points occurred at 1,068 psf (7.4 psi), and failure occurred as a result of bond failure and flexure.

Figure 3-27 shows the slab before and after test. Figure 3-28A shows the negative moment tension crack after test, and Figure 3-28B shows one of the positive moment flexure cracks after test.

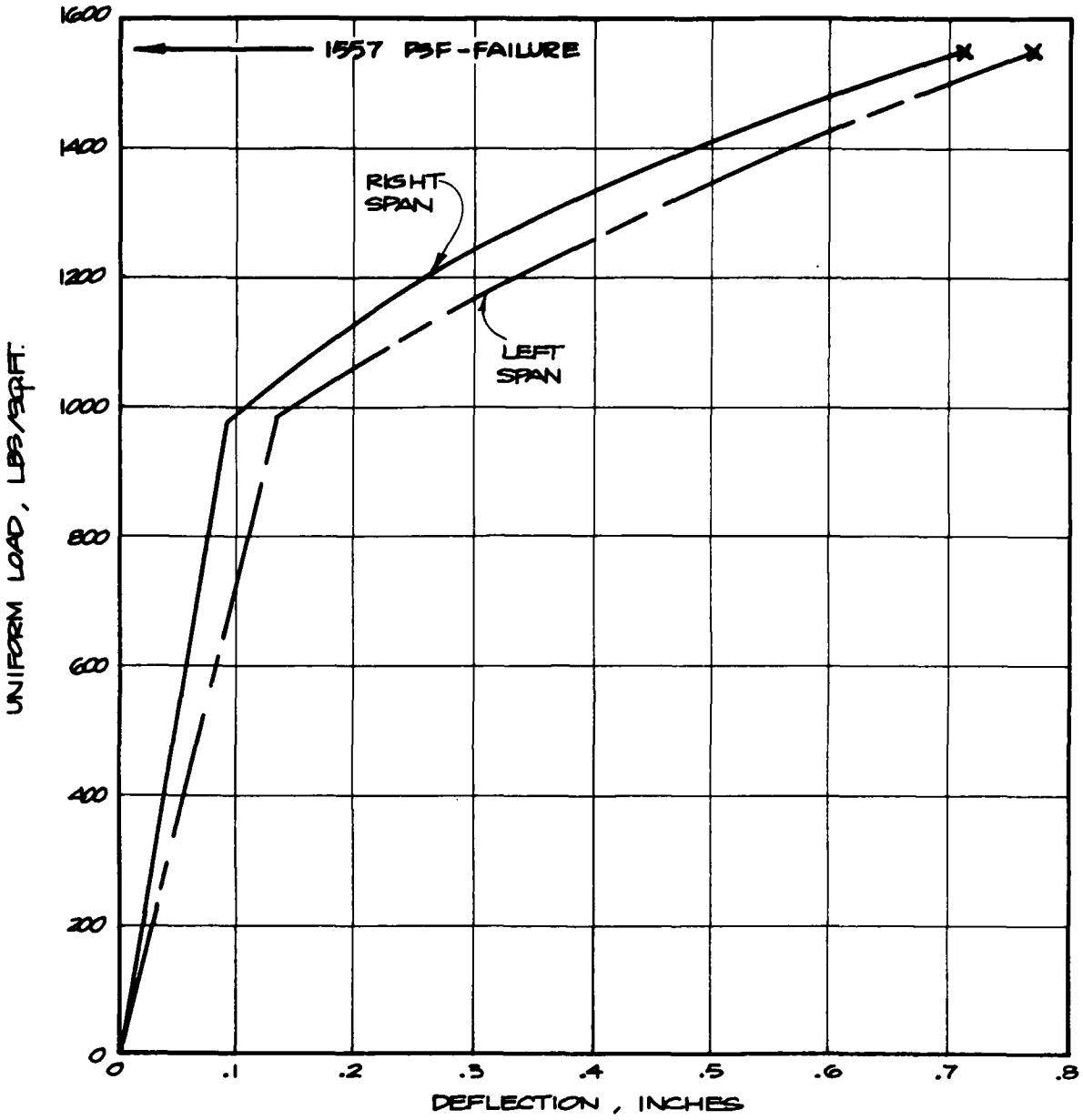

Fig. 3-26. Uniform Load vs Deflection, Test No. 6, Midspan Shoring, 8-inch slab.

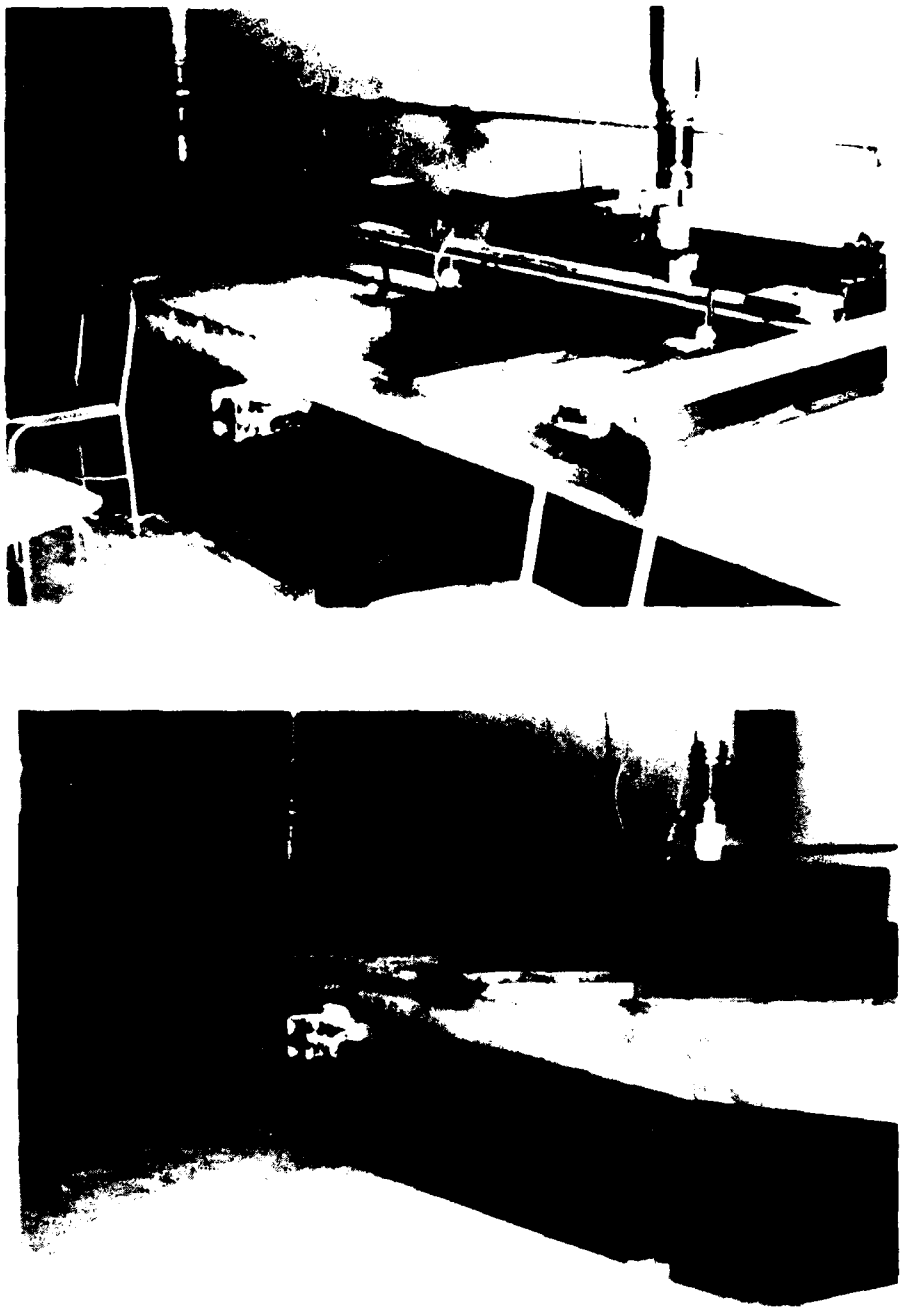

Fig. 3-27. Pre- and Posttest Photographs, Test No. 6.

A

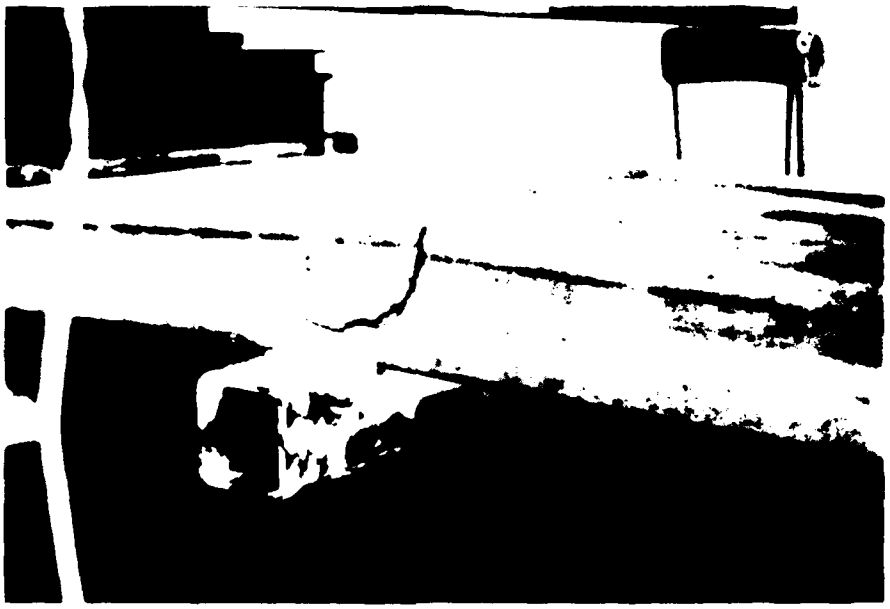

B

Fig. 3-28. Posttest Photographs, Test No. 6.

In Test No. 7, the slab failed when the applied load reached 37,000 lb/ram. The calculated uniform load at failure was 1,646 psf (11.4 psi). The uniform load vs relative deflection curve for each span is shown in Figure 3-29.

The first positive moment tension crack was noted near a quarter point at 356 psf (2.5 psi). The negative moment tension crack occurred at 1,157 psf (8.0 psi). The failure occurred as a result of bond failure in the prestressing strands, causing loss of load-carrying capacity by shear/flexure.

Figure 3-30 shows the slab before and after test. Figure 3-31 shows the failure near the left support and the right span failure.

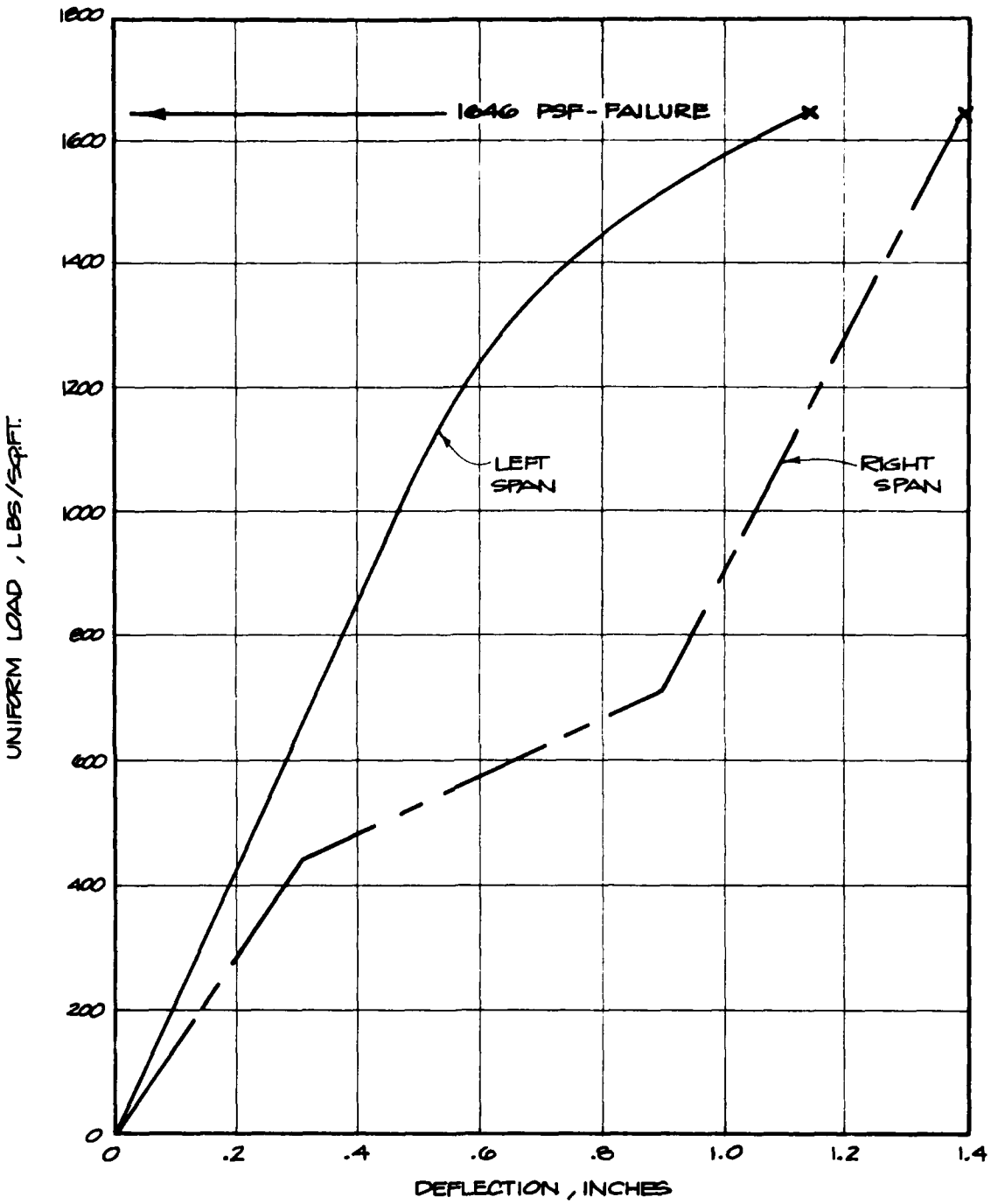

Fig. 3-29. Uniform Load vs Deflection, Test No. 7, Midspan Shoring, 8-inch Slab.

Fig. 3-30. Pre- and Posttest Photographs, Test No. 7.

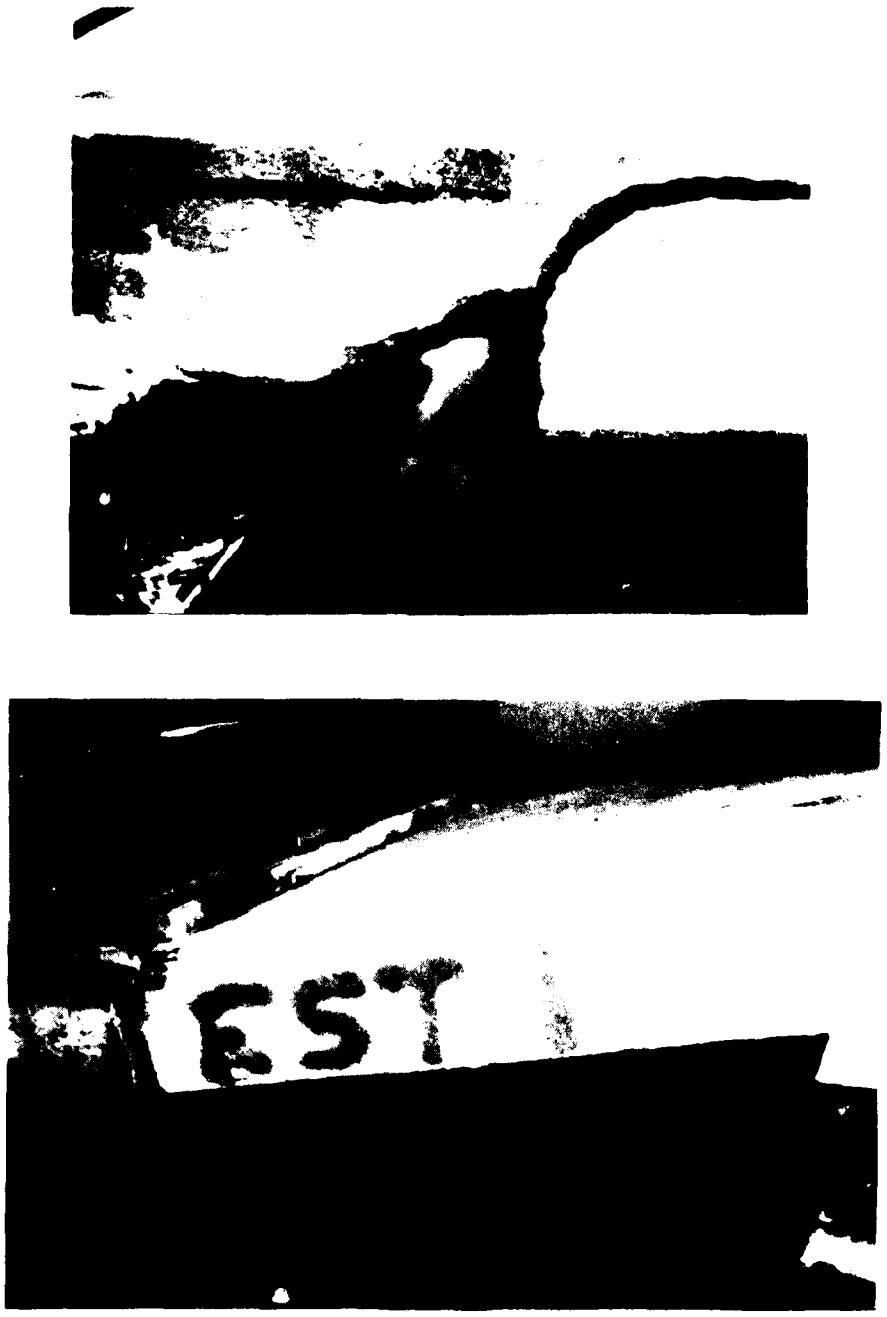

Fig. 3-31. Left and Right Span Failures, Test No. 7.

Tests Nos. 8 and 9 (Shored at Two Locations, 8-inch Slabs)

These two tests were conducted on identical slabs simply supported and shored at two locations with timber shimmed tightly against the bottom of the slabs. The only variable in the two tests was the shore location. In Test No. 8, the shores were located at the one-third points. In Test No. 9, the two shores were positioned at the outside one-quarter points. The shoring and loading configurations are shown in Figure 3-32. The purpose of varying the shoring configuration in each test was to determine the effect of this dimensional change on the performance of the system.

In Test No. 8, the load was applied at six locations by three hydraulic rams, and in Test No. 9 at eight locations by four rams. Figure 3-32 shows these loading configurations. The vertical deflection in each test was measured midway between each of the supports and over each of the shores.

In both tests, the load was applied at a slow rate of 4,000 lb/ram increments and the deflection recorded at each increment.

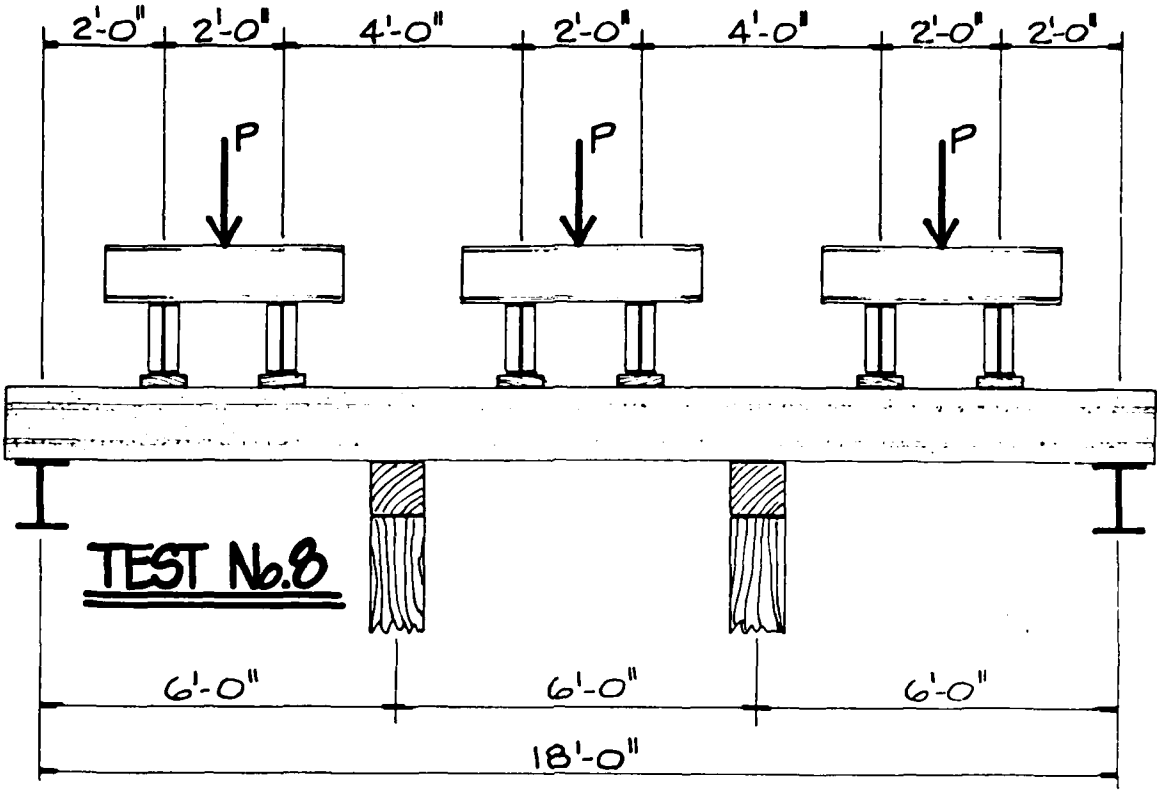

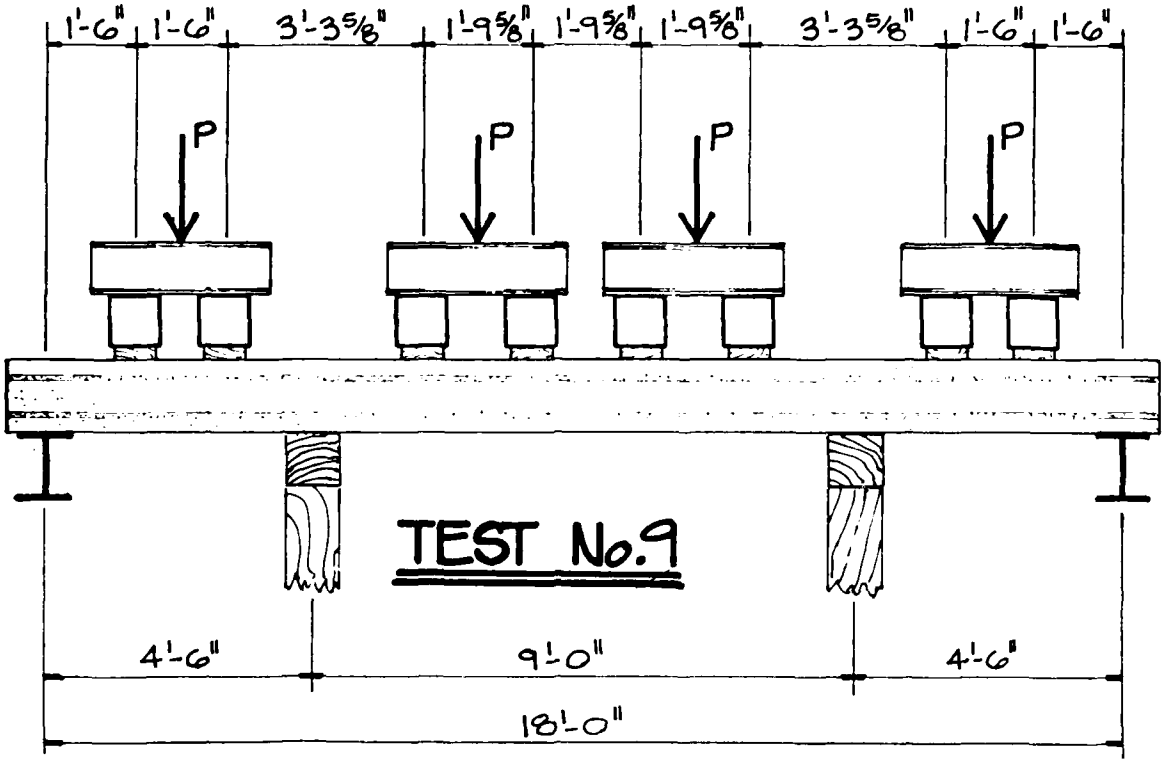

Fig. 3-32. Loading Configuration — Two Shores, 8-inch Slabs, Tests Nos. 8 and 9.

In Test No. 8, the slab failed when the applied load reached 44,000 lb/ram. The calculated uniform load at failure was 2,936 psf (20.4 psi). The uniform load vs relative deflection curve for each span is shown in Figure 3-33.

The first positive moment tension crack occurred in an end span at 1,868 psf (13.0 psi), and negative moment tension cracks were noted over both shores at 2,669 psf (18.5 psi). The failure occurred in shear/flexure in the right span as a result of bond failure of the prestressing strands. The loads continued to be applied to the center and left spans until failure. The left span failed at 3,870 psf (26.9 psi), and the center span failed at 5,072 psf (35.2 psi).

Figure 3-34 shows the slab before and after test. Figure 3-35A shows the failure of the right span, and Figure 3-35B shows the failure of the center span, which occurred just left of the right shore.

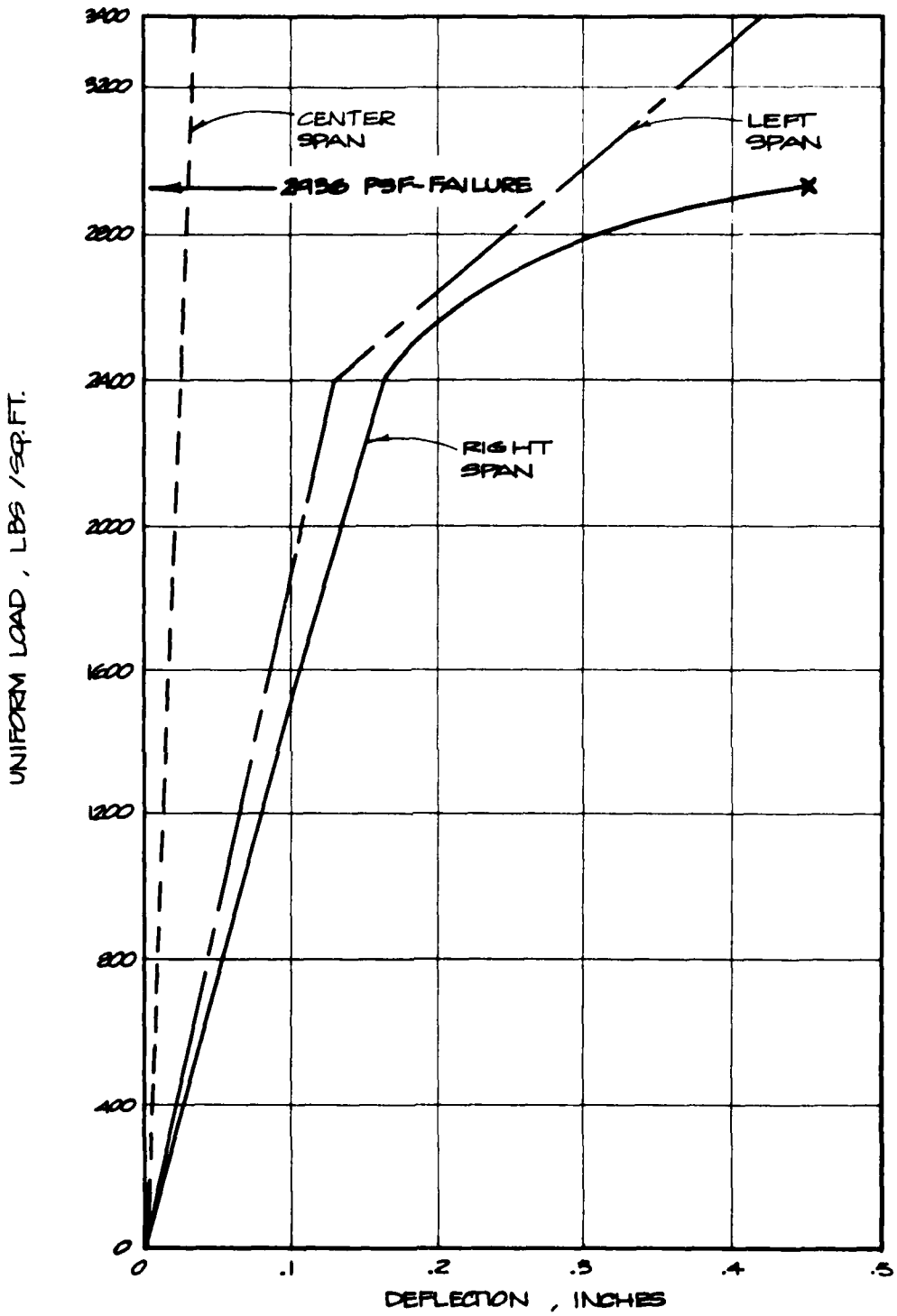

Fig. 3-33. Uniform Load vs Deflection, Test No. 8, One-Third Point Shores, 8-inch Slab.

Fig. 3-34. Pre- and Posttest Photographs, Test No. 8.

A

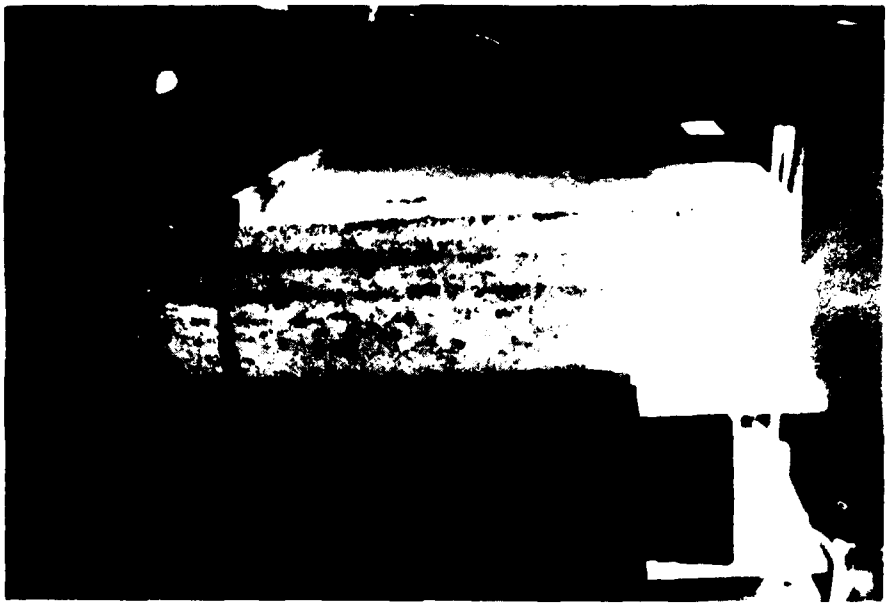

B

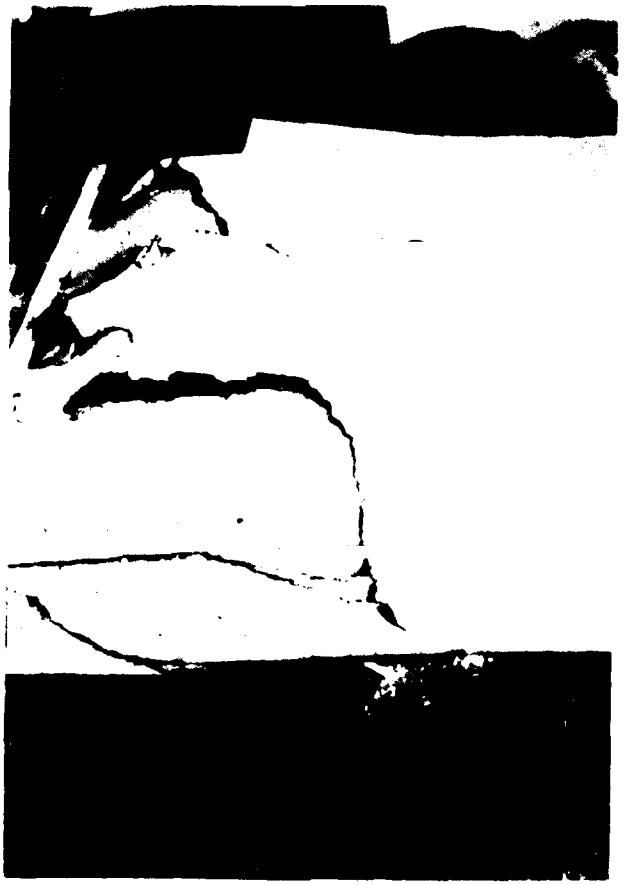

Fig. 3-35. Posttest Photographs, Test No. 8.

In Test No. 9, the slab failed when the applied load reached 38,000 lb/ram. The calculated uniform load at failure was 3,043 psf (21.1 psi). The uniform load vs relative deflection curve for each span is shown in Figure 3-36.

The first positive moment tension crack occurred in the center span at 1,121 spf (7.8 psi), and negative moment tension cracks were noted over both shores at 1,361 psf (9.4 psi). The failure occurred in the center span as a result of shear/flexure. The load continued to be applied to the two end spans until failure. Both spans failed as a result of bond failure at 3,915 psf (27.2 psi).

Figure 3-37 shows the test slab after test, with the center span failure. Figure 3-38 shows the left and right span failures.

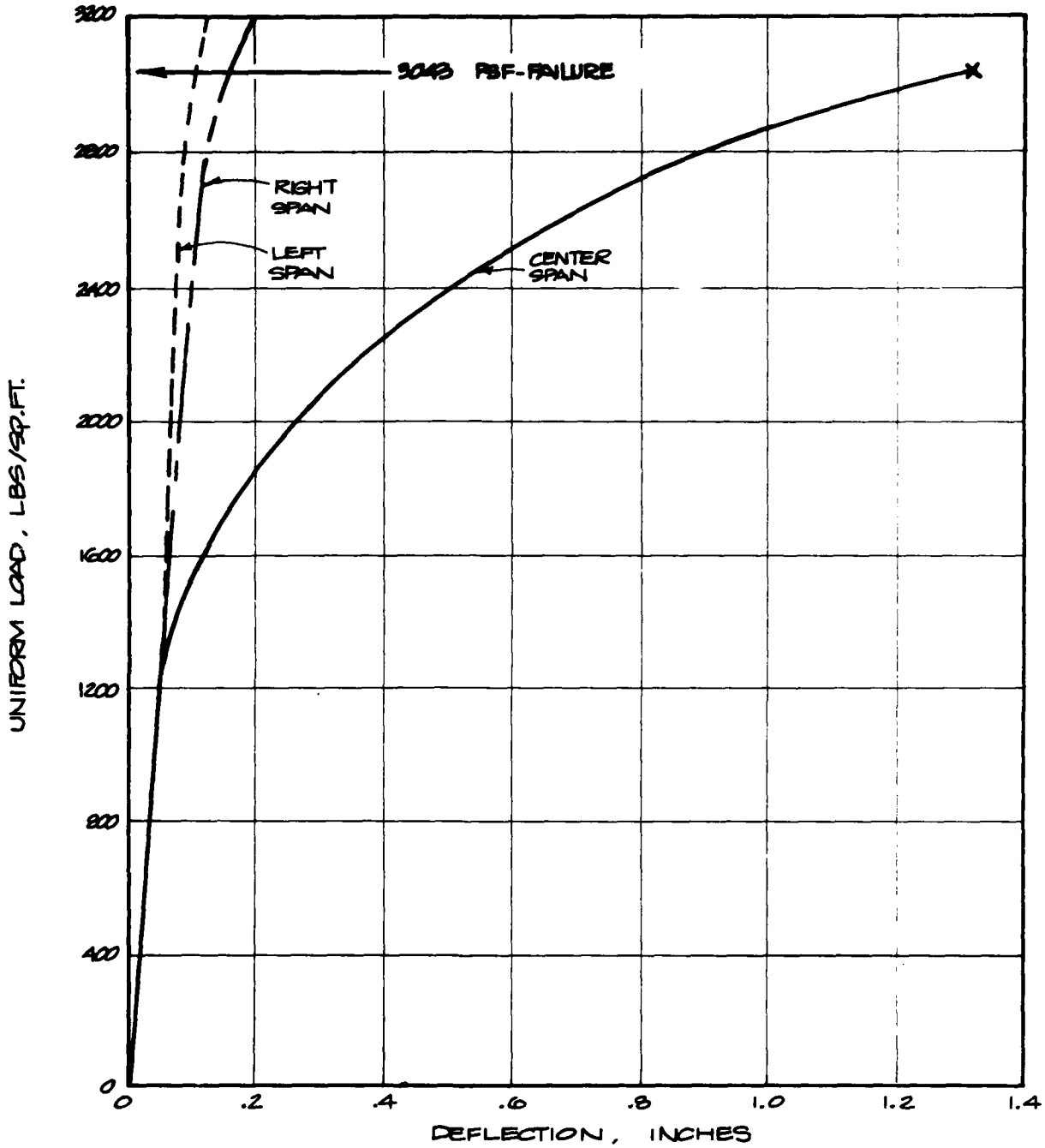

Fig. 3-36. Uniform Load vs Deflection, Test No. 9, One-Quarter Point Shores, 8-inch Slab.

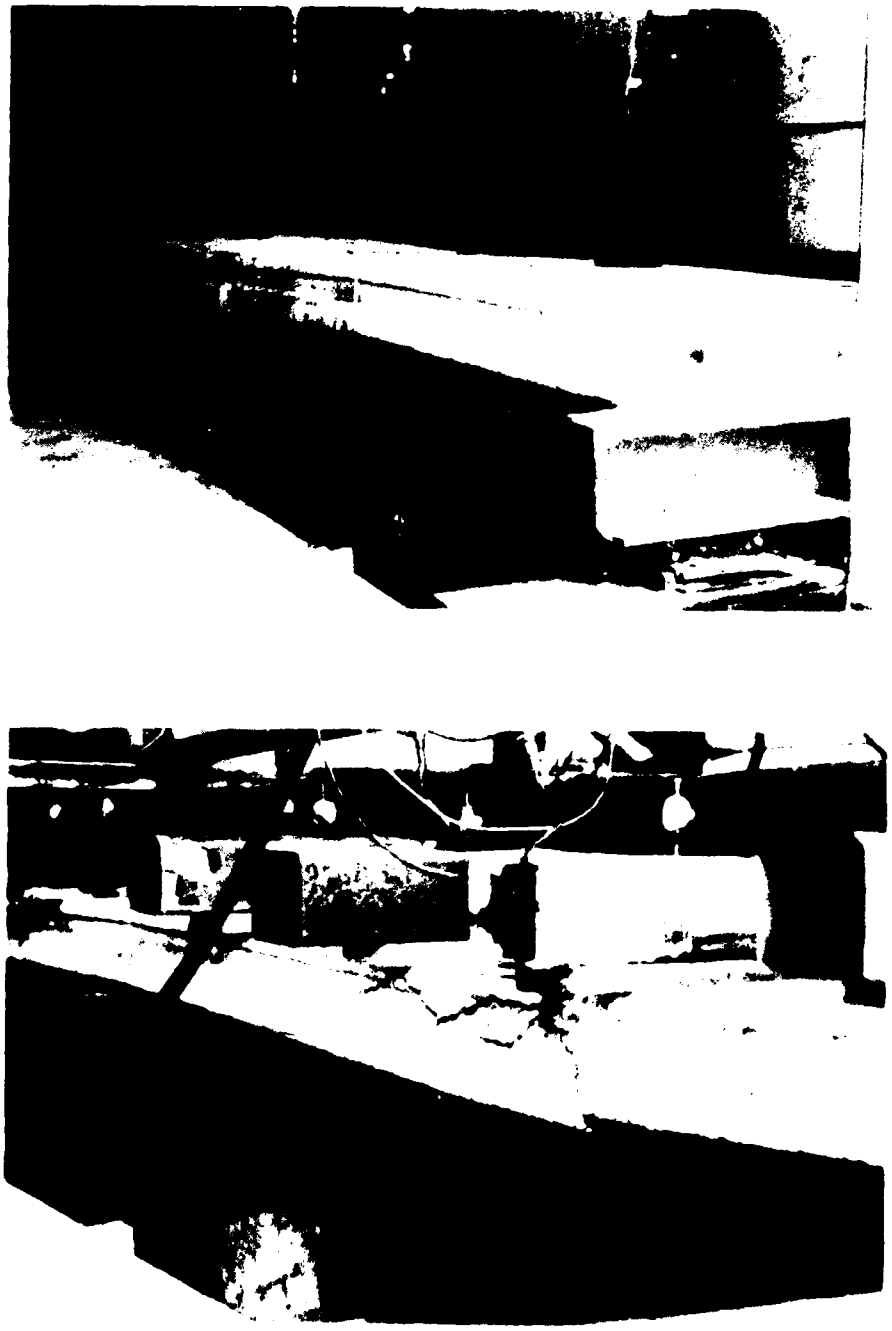

Fig. 3-37. Test No. 9 After Test, Showing Center Span Failure.

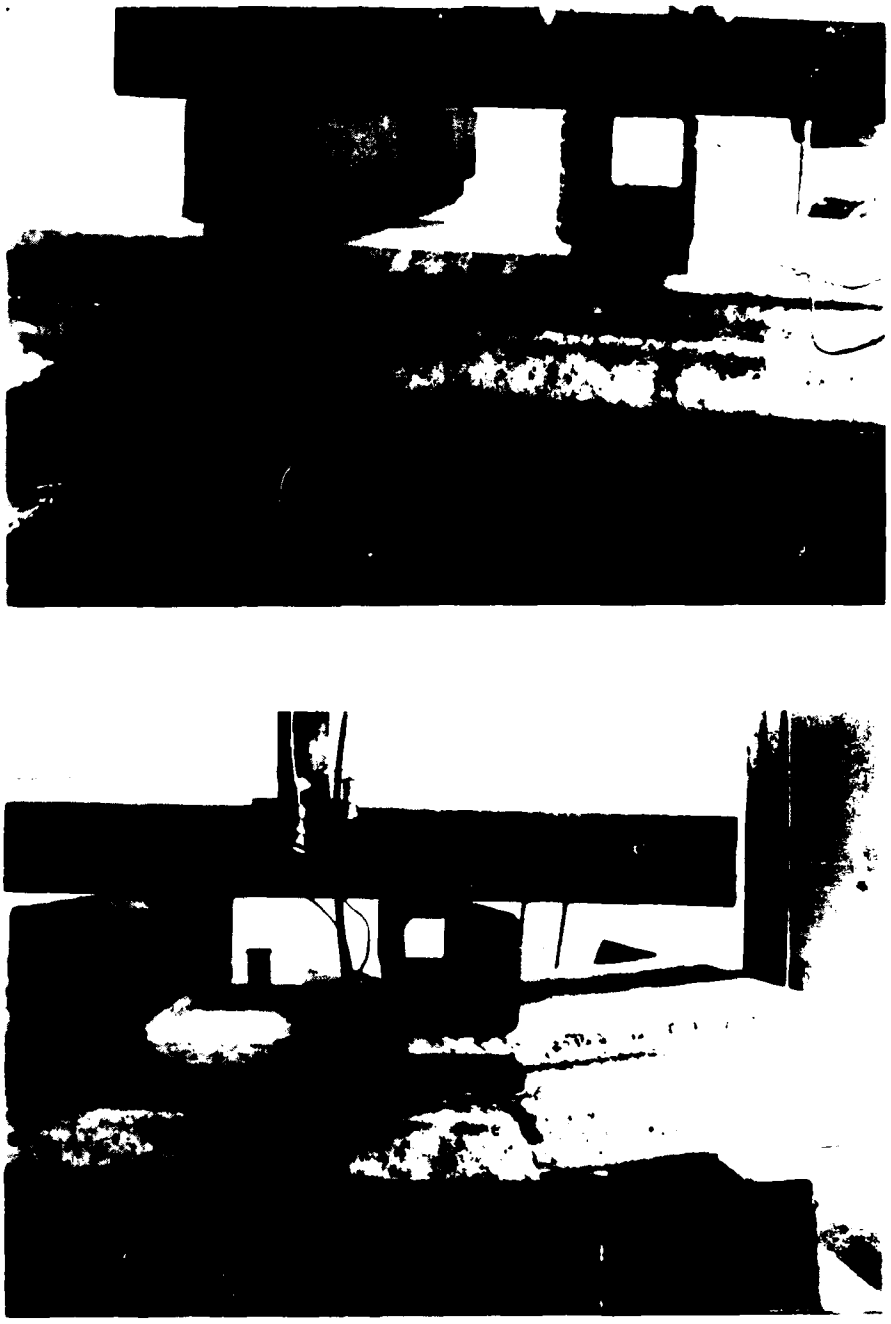

Fig. 3-38. Left and Right Span Failures, Test No. 9.

Test No. 10 (Base Case, 10-inch Slab)

The slab used in this test was simply supported. The load was applied at two locations by two hydraulic rams in the configuration shown in Figure 3-39. The vertical deflection was measured and recorded at midspan and at the one-third points.

The load was applied at a slow rate in 1,000 lb/ram increments and the deflection recorded at each increment. The slab failed when the applied load reached 18,500 lb/ram. The calculated uniform load at failure was 823 psf (5.7 psi). The uniform load vs deflection curve for midspan is shown in Figure 3-40.

A positive moment tension crack was first noted under the right loading point at approximately 400 psf (2.8 psi). The failure occurred in flexure at the location of this first crack, simultaneously with a prestressing strand bond failure at the right end of the slab.

Figure 3-41 shows the slab prior to test. Figure 3-42 shows the tension cracks under the right load point during test. Figure 3-43 shows the failed slab after test. Figure 3-44A shows a closeup of the failed section after test. Figure 3-44B is a closeup of the right end of the slab after test and shows a small hole where one of the prestressing strands failed in bond and has been drawn in. This bond failure occurred in all six strands.

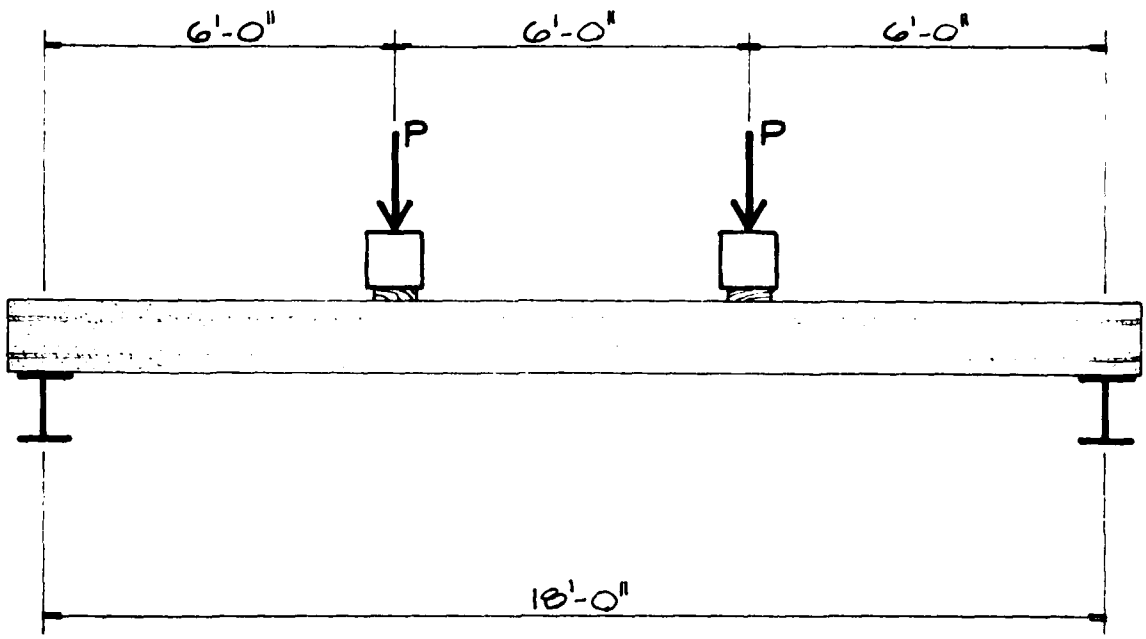

Fig. 3-39. Loading Configuration — Base Case, 10-inch Slab, Test No. 10.

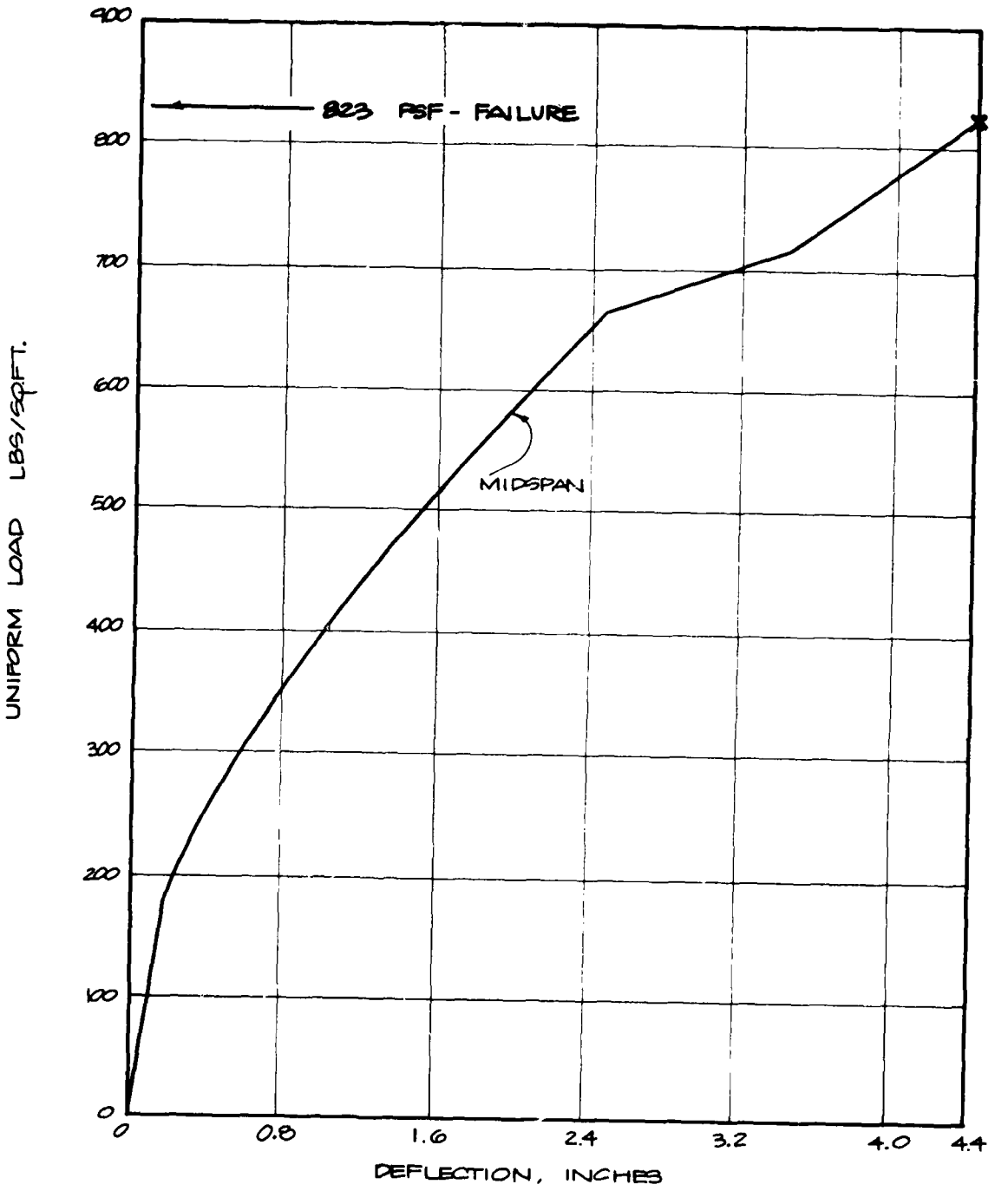

Fig. 3-40. Uniform Load vs Deflection, Test No. 10, Base Case, 10-inch Slab.

Fig. 3-41. Test No. 10, Before Test.

Fig. 3-42. Test No. 10, During Test.

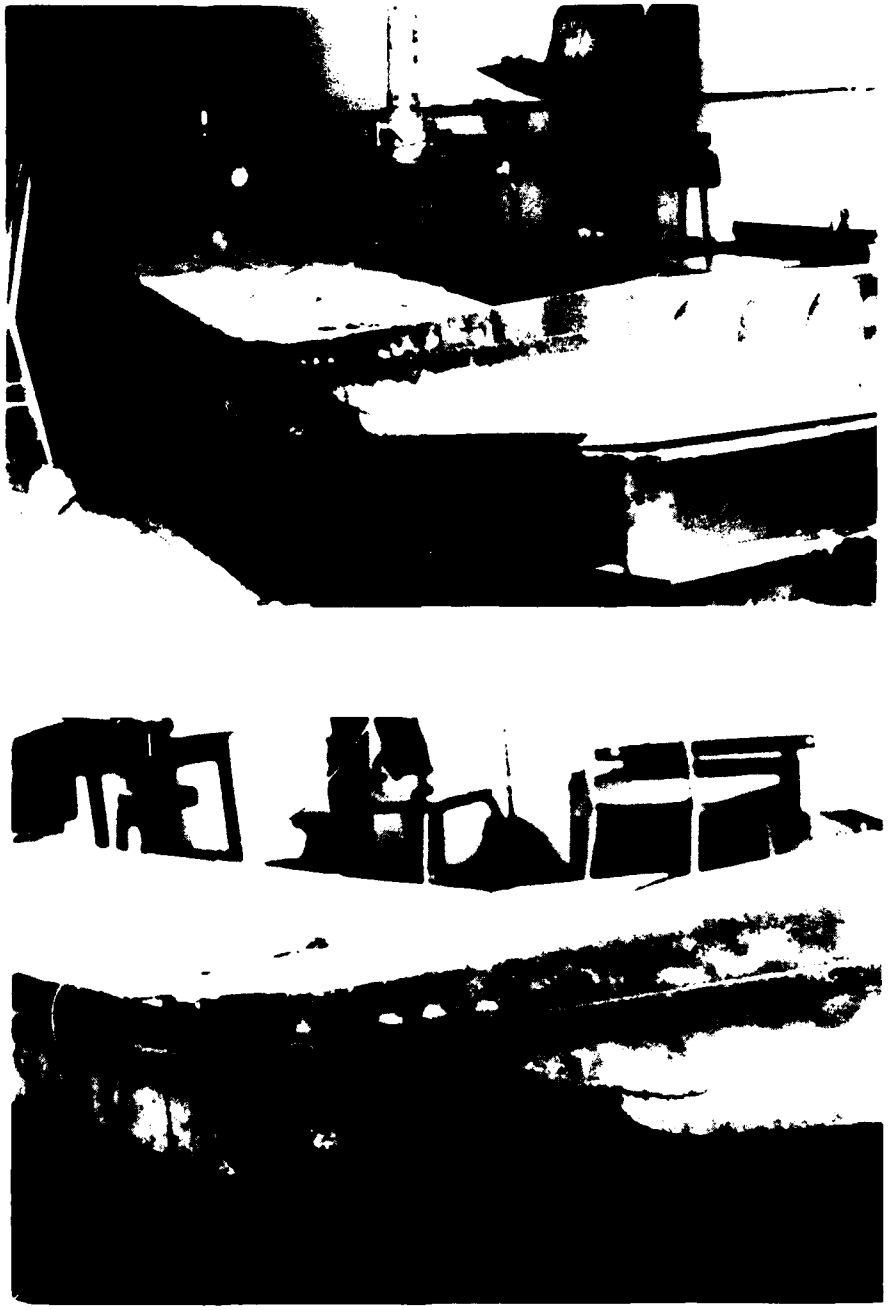

Fig. 3-43. Test No. 10, After Test.

A

B

Fig. 3-44. Closeup Photographs of Test No. 10 After Test.

Tests Nos. 11 and 12 (Shored at Midspan, 10-inch Slabs)

Both of these tests were conducted on identical slabs simply supported and shored at midspan. The two tests differed in the type of shoring used. In Test No. 11, the shore consisted of a structural steel tube and in Test No 12, heavy timber. The steel and timber shores were both shimmed tightly against the bottom of the test slabs, as shown in Figure 3-45.

The purpose of testing the two different types of shores was to see if a variance in performance exists between a shore that permits no vertical movement (steel in Test No. 11) and a shore that permits some vertical movement (timber in Test No. 12), because of the normal crushing of the timber. It might be pointed out that these tests are similar to Tests Nos. 6 and 7 that were conducted on the 8-inch slabs, except that in Test No. 7 the timber shore provided a 1½-inch gap. In Tests Nos. 11 and 12, as mentioned above, both shores are shimmed tightly.

The load was applied in both tests at four locations by two hydraulic rams in the configurations shown in Figure 3-46. The vertical deflection was measured an recorded at the quarter points and at midspan (over the shores).

In both tests, the load was applied at a slow rate of 4,000 lb/ram increments and the deflection recorded at each increment.

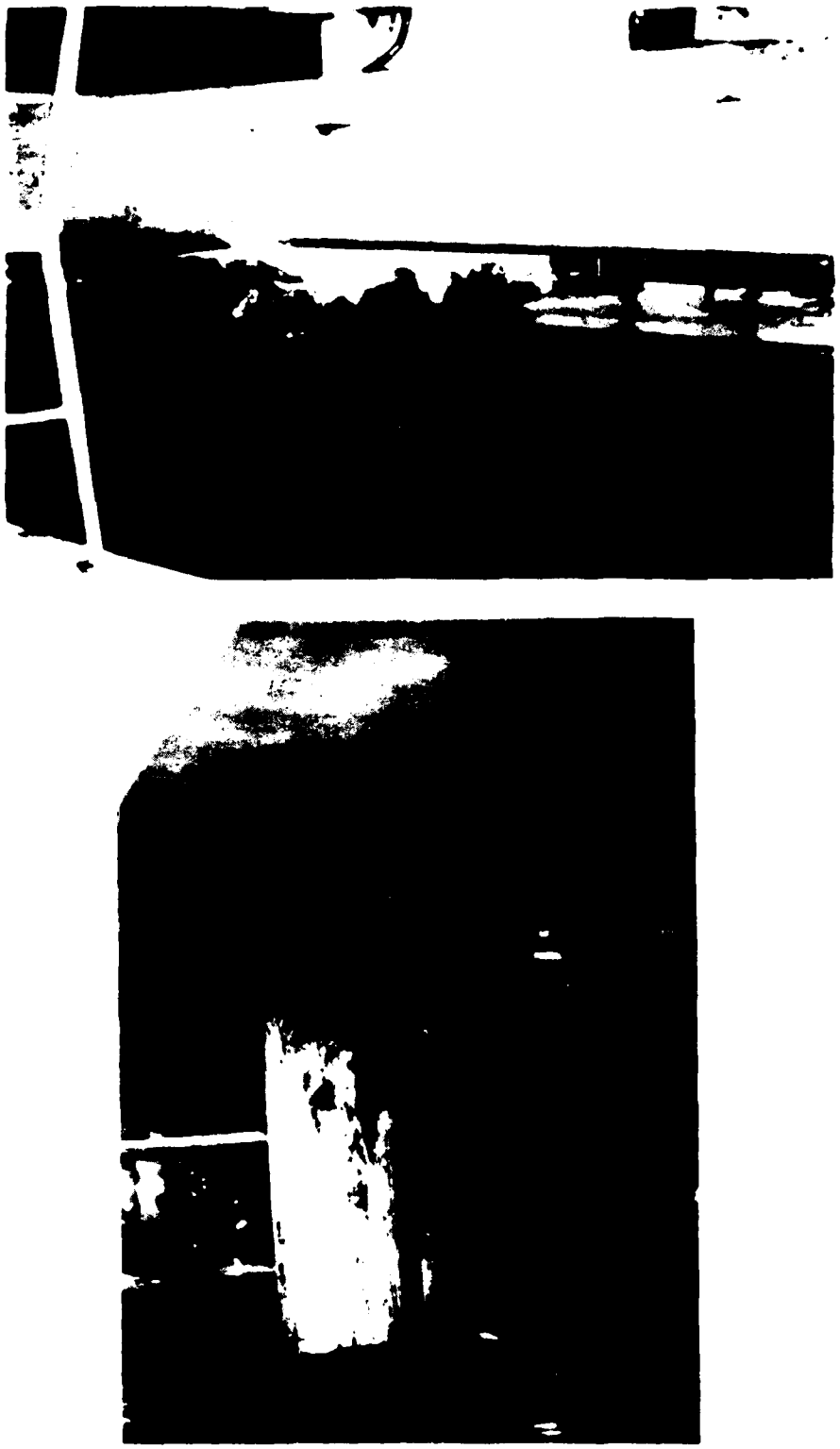

Fig. 3-45. Steel Shore (Test No. [illegible]) and Timber Shore (Test No. 12), Prior to Test.

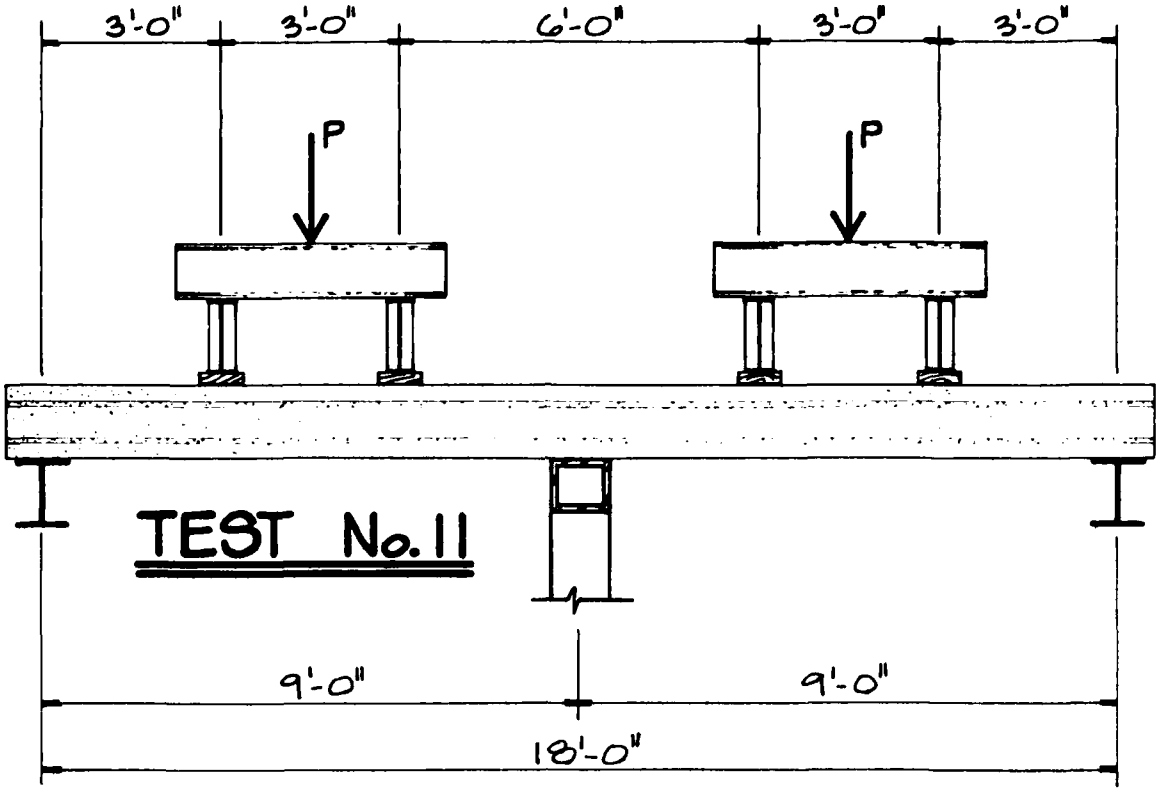

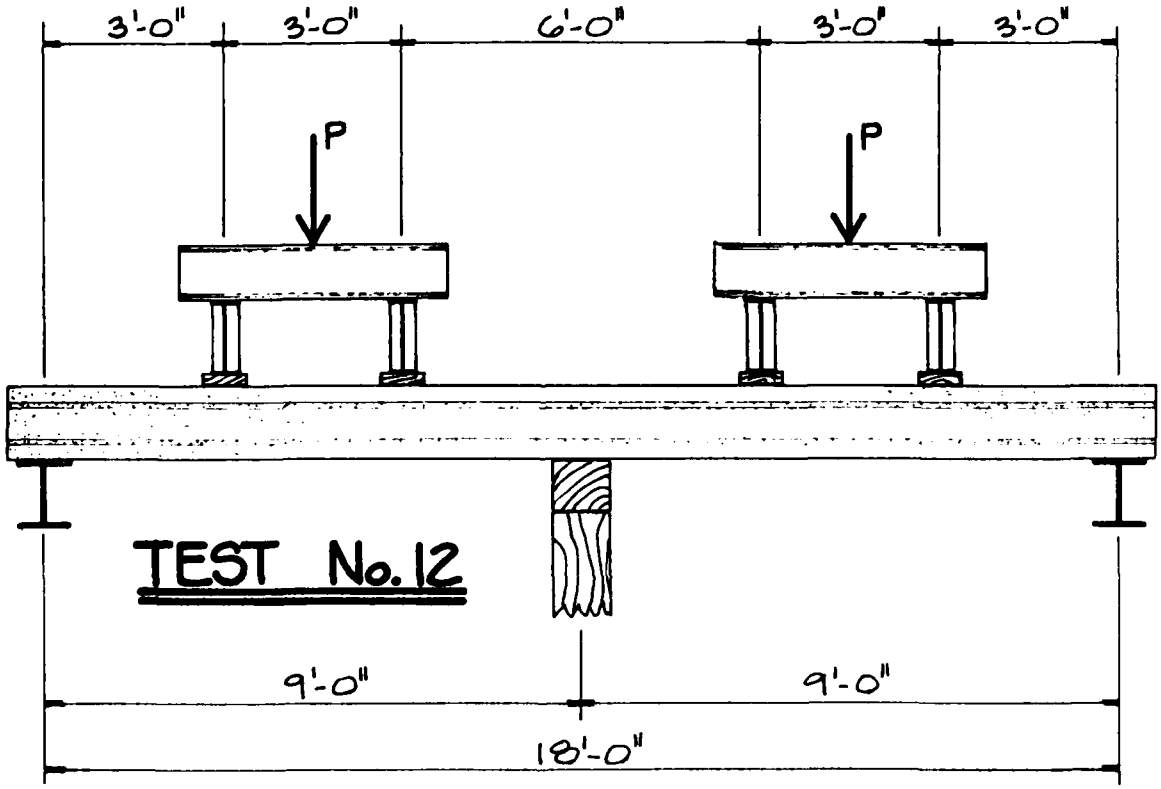

Fig. 3-46. Loading Configuration — Shored at Midspan, 10-inch Slabs, Tests Nos. 11 and 12.

In Test No. 11, the slab failed when the applied load reached 68,000 lb/ram. The calculated uniform load at failure was 3,025 psf (21.0 psi). The uniform load vs relative deflection curve for each span is shown in Figure 3-47.

A negative moment tension crack at midspan over the shore occurred at 1,602 psf (11.1 psi). Positive moment tension cracks were first noted at 1,780 psf (12.4 psi). The failure occurred as a result of bond failure of the prestressing strands, causing a sudden shear/flexure failure in the left span.

Figure 3-48A shows the slab prior to test. Figure 3-48B shows the left end of the slab after test. Figure 3-49A shows a closeup of the failed portion of the slab, and Figure 3-49B, the negative moment tension crack over the shore after test.

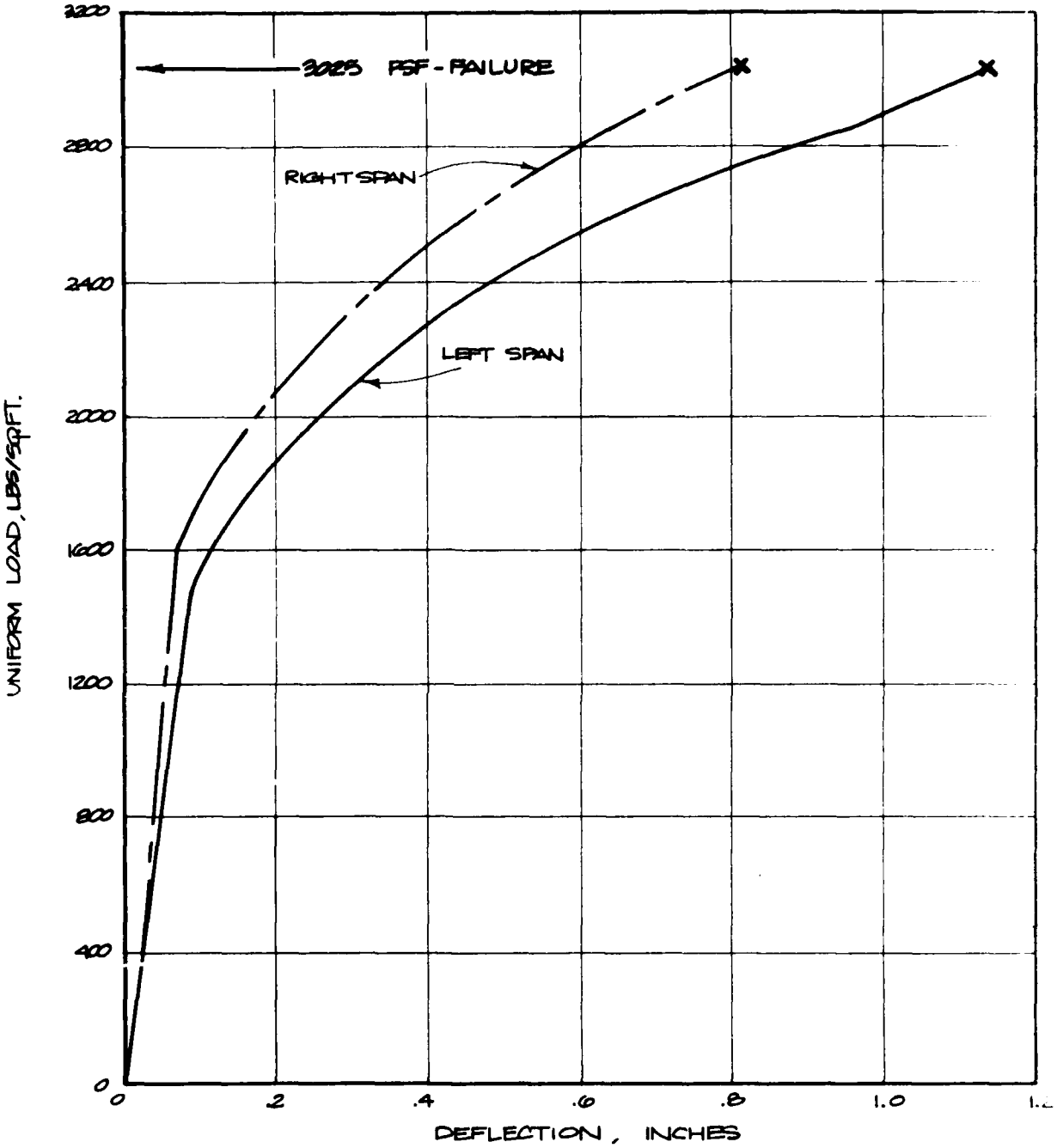

Fig. 3-47. Uniform Load vs Deflection, Test No. 11, Midspan Shoring, 10-inch Slab.

A

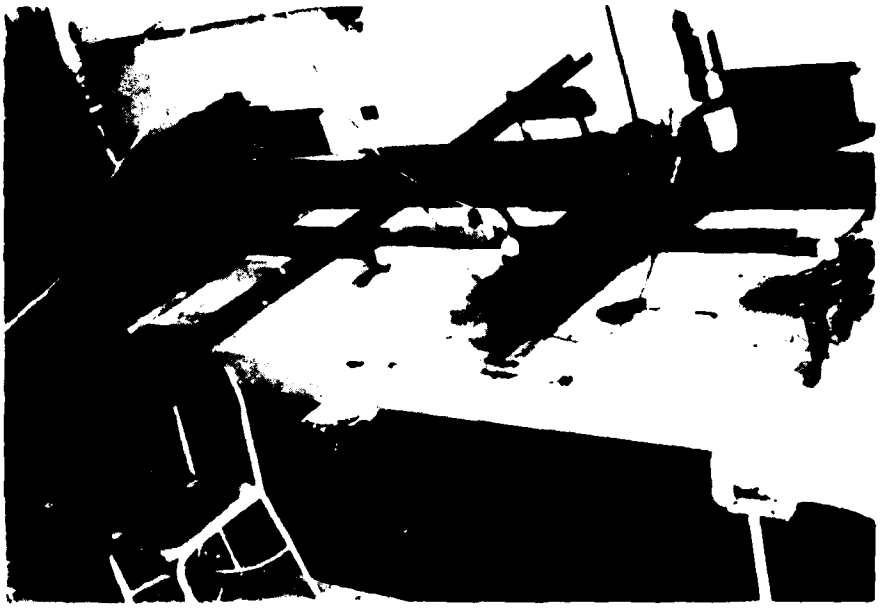

B

Fig. 3-48. Pre- and Posttest Photographs, Test No. 11.

A

B

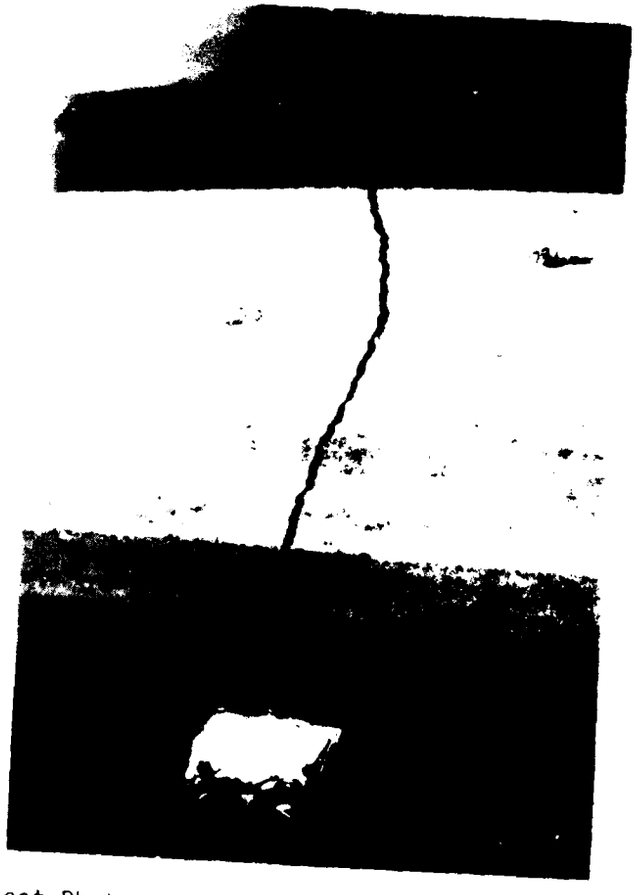

Fig. 3-49. Posttest Photographs, Test No. 11.

In Test No. 12, the slab failed when the applied load reached 66,000 lb/ram. The calculated uniform load at failure was 2,937 psf (20.4 psi). The uniform load vs relative deflection curve for each span is shown in Figure 3-50.

A negative moment tension crack at midspan over the shore occurred at 1,958 psf (13.6 psi). Positive moment tension cracks were first noted at 2,135 psf (14.8 psi). The failure occurred as a result of bond failure of the prestressing strands, causing a sudden shear failure near the left support.

Figure 3-51A shows the slab during test, immediately after the formation of the negative moment tension crack. Figure 3-51B shows the left end of the slab after test. The closeup photographs in Figure 3-52 show the failed portion of the slab and the left end after test. The bond failure of the prestressing strands is evident in this figure.

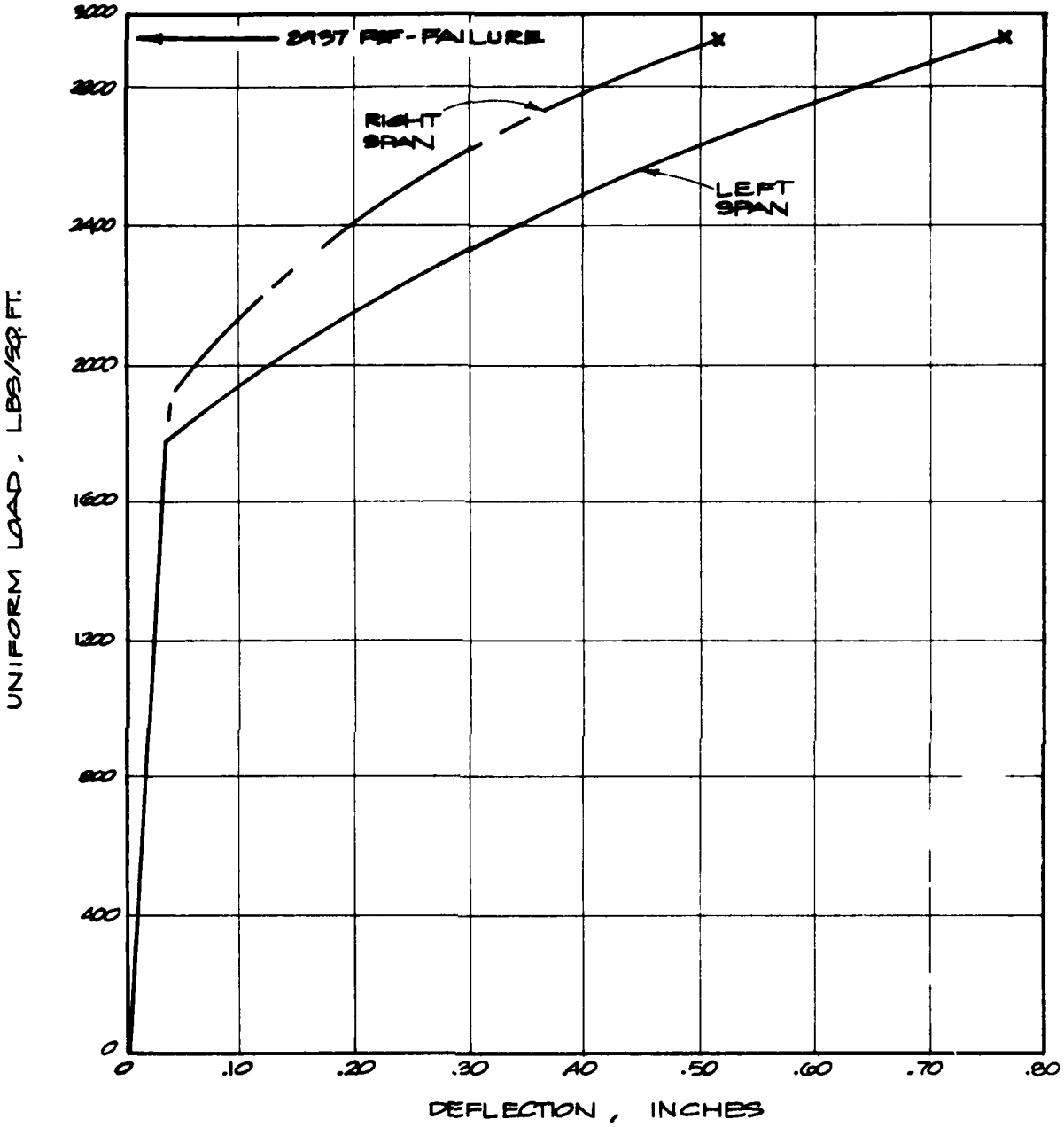

Fig. 3-50. Uniform Load vs Deflection, Test No. 12, Midspan Shoring, 10-inch Slab.

A

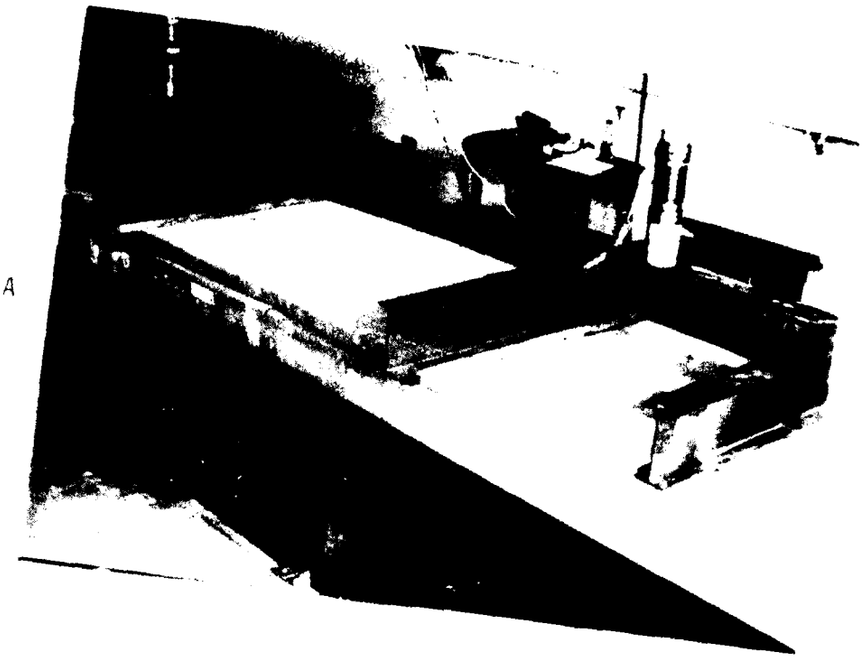

B

Fig. 3-51.

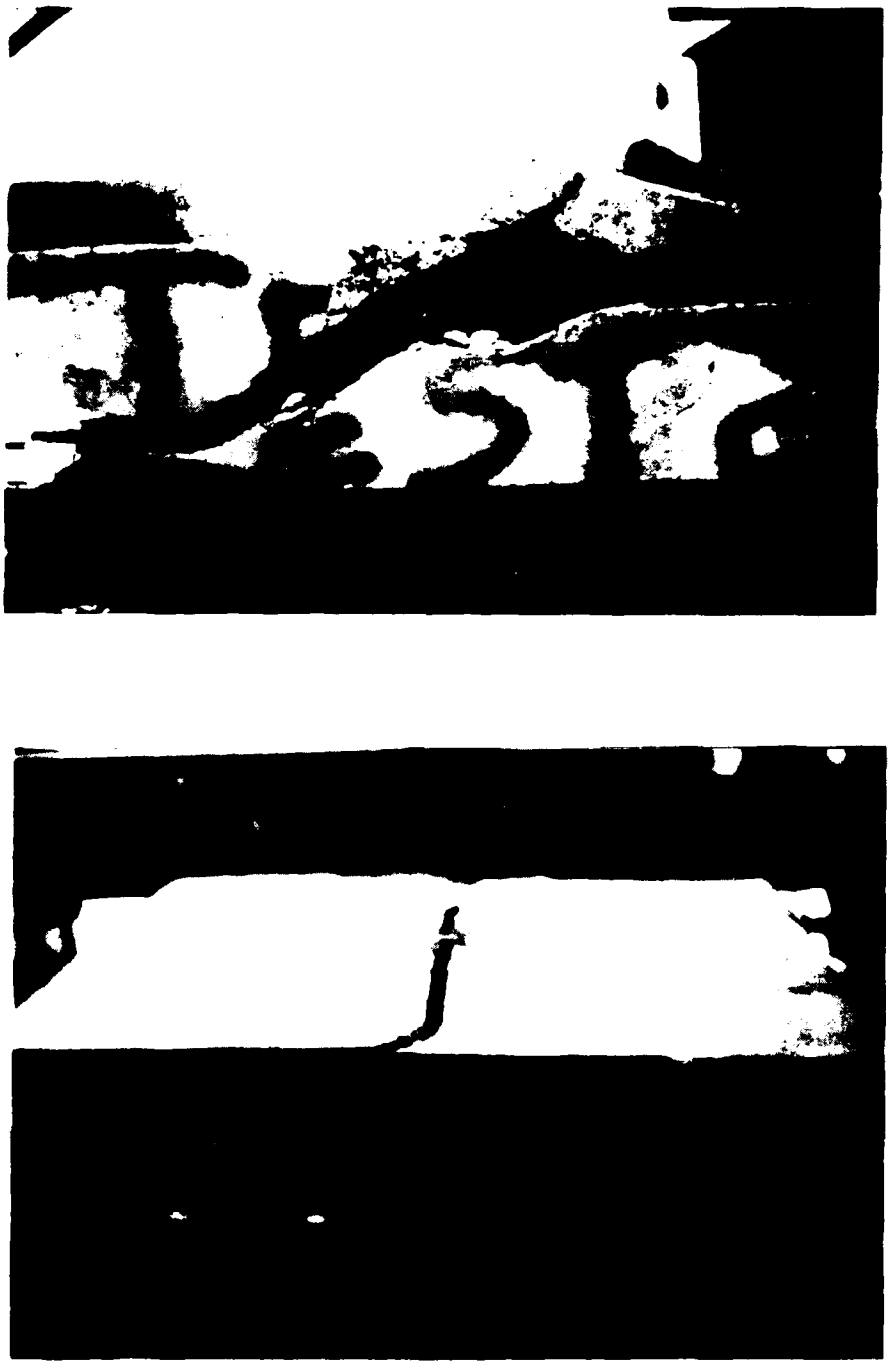

Fig. 3-[illegible]. Closeup Photographs of Test No. 1[illegible] After Test.

Test No. 13 (Shored at One-Third Span, 10-inch Slab)

The slab used for this test was simply supported at its ends and shored at the one-third points with timber shoring shimmed tightly against the bottom of the slab. The load was applied at six locations by three hydraulic rams in the configuration shown in Figure 3-53. The vertical deflection was measured and recorded at the one-third points (over the shores) and at three locations midway between each support.

The load was applied at a slow rate in 8,000 lb/ram increments and the deflection recorded at each increment. The test slab failed when the applied load reached 72,000 lb/ram. The calculated uniform load at failure was 4,805 psf (33.4 psi). The uniform load vs relative deflection curve for each span is shown in Figure 3-54.

Positive moment tension cracks first occurred at the center of the spans at 2,669 psf (18.5 psi), and the first negative moment tension crack occurred over a shore at 4,004 psf (27.8 psi). The slab failed when bond failure of the prestressing strands occurred at the slab ends, resulting in a shear/flexure failure near the end supports. The center span continued to be loaded until failure, which occurred at 7,474 psf (51.9 psi) and was the result of a shear/flexure failure adjacent to the right shore.

Figure 3-55 shows the slab before and after test. Figure 3-56 shows the failure near the left and right supports. Figure 3-57A shows the negative moment tension crack over the left shore after test, and Figure 3-57B shows the failure adjacent to the right shore after test.

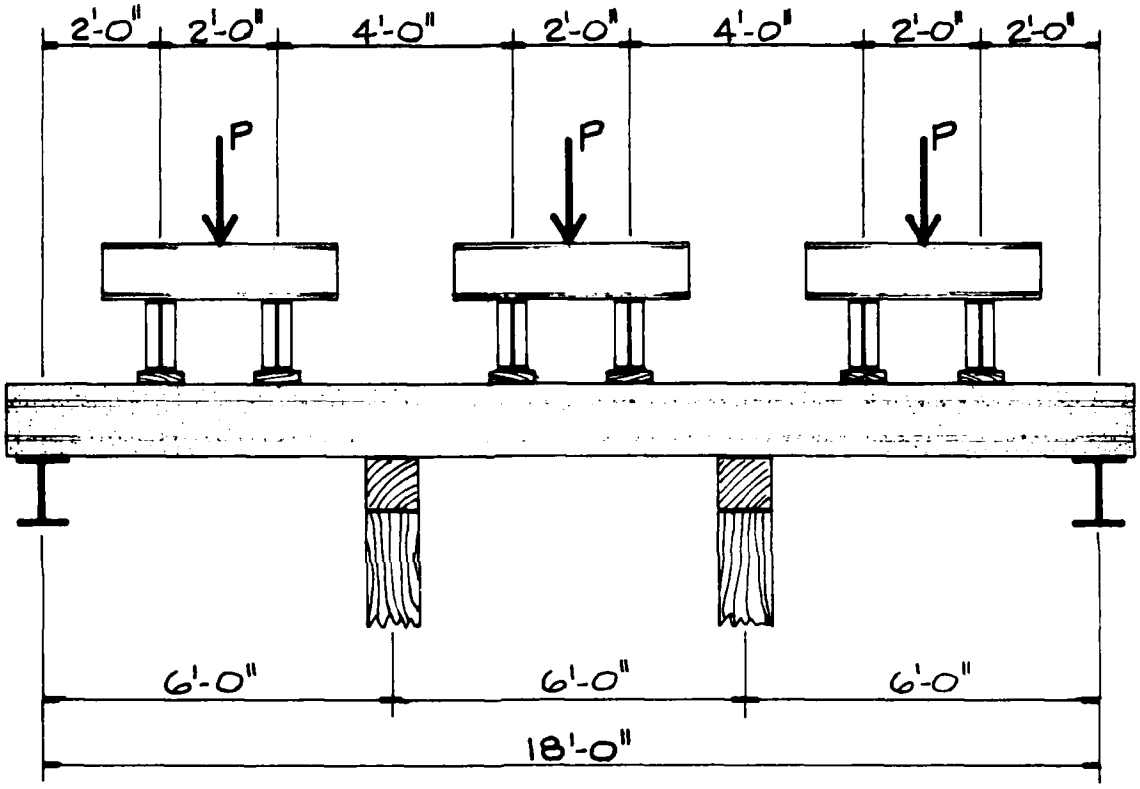

Fig. 3-53. Loading Configuration — Shored at One-Third Points, 10-inch Slab, Test No. 13.

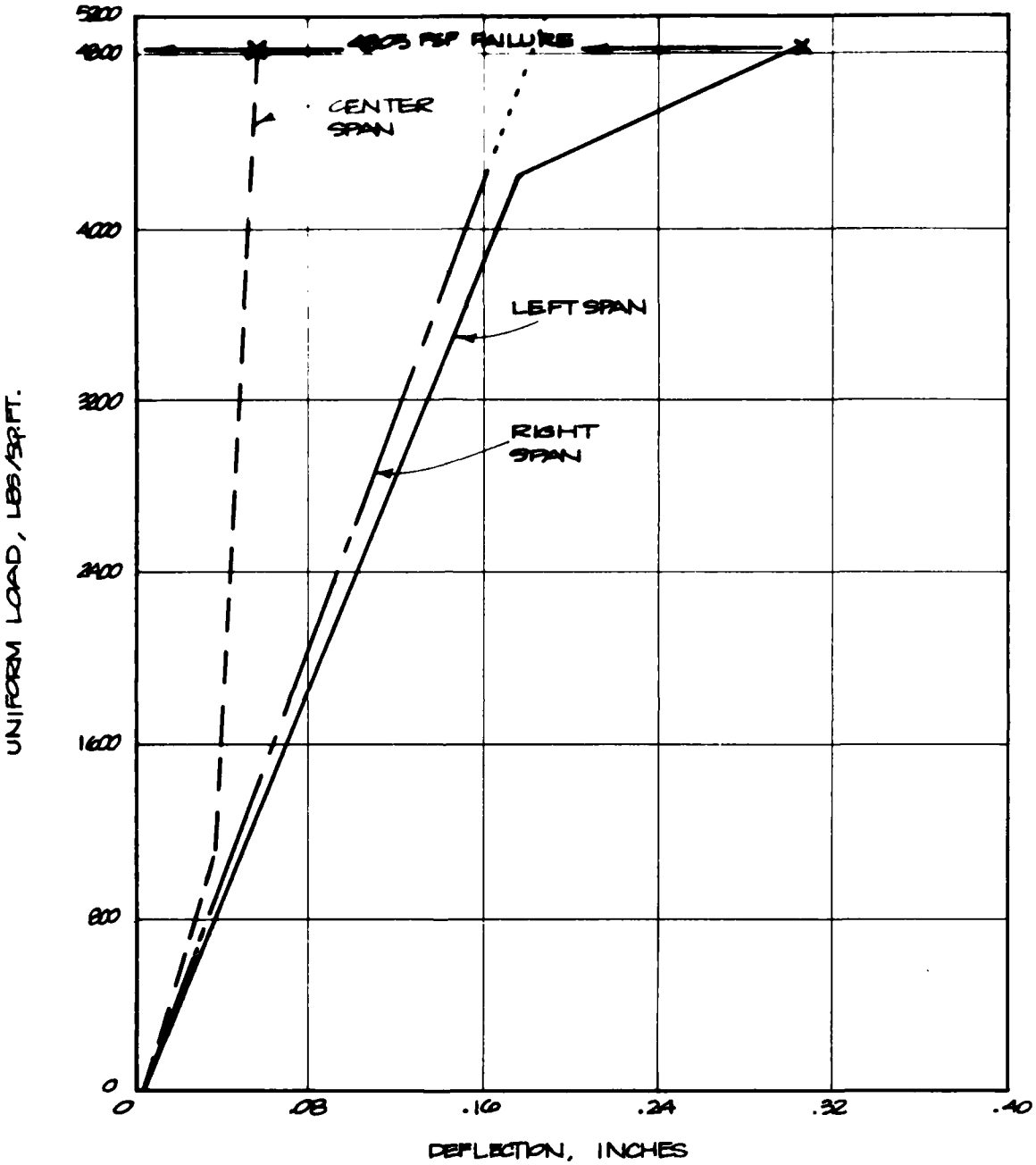

Fig. 3-54. Uniform Load vs Deflection, Test No. 13, One-Third Point Shoring, 10-inch Slab.

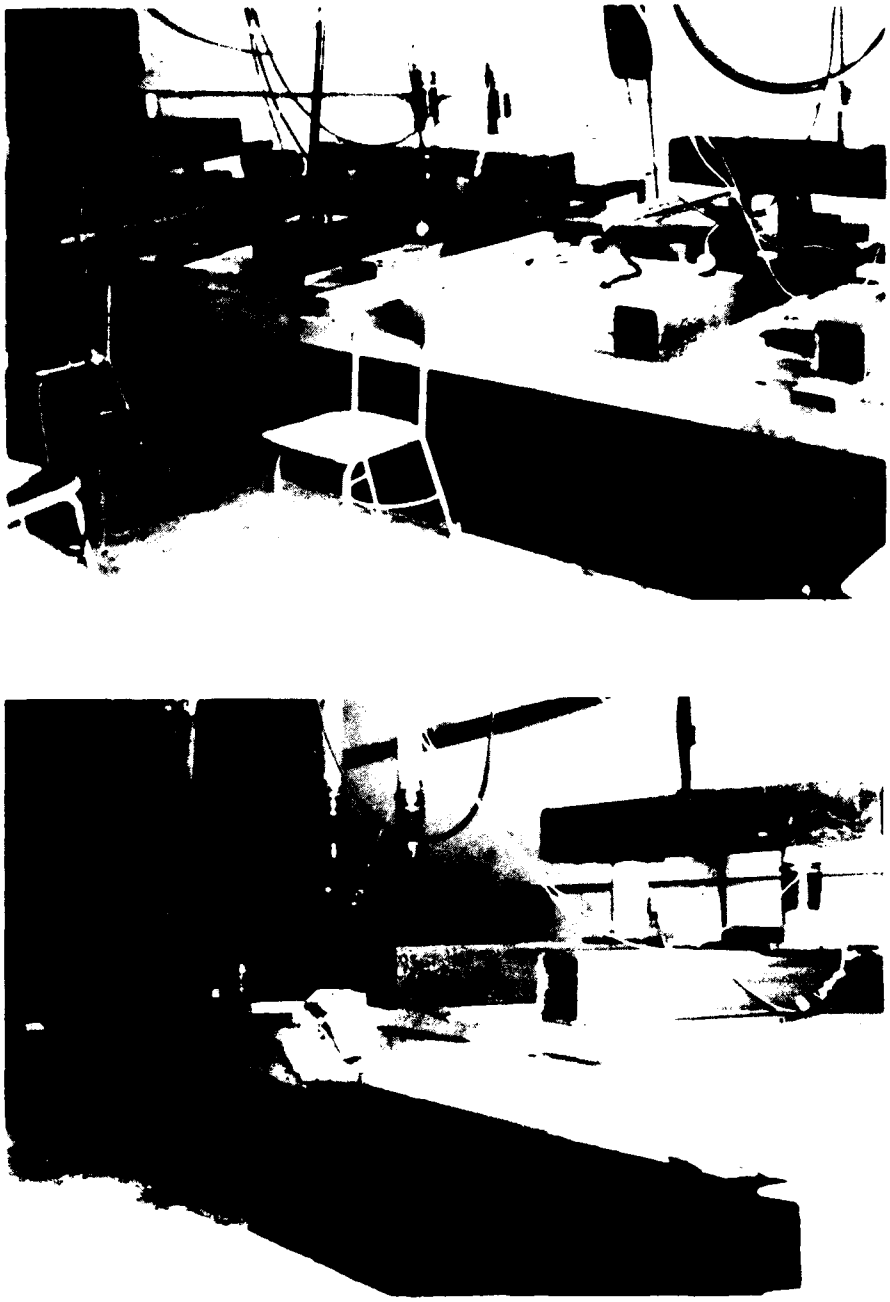

Fig. 3-55. Pre- and Posttest Photographs, Test No. 13.

Fig. 3-56. Test No. 13, Failure Near Left and Right Supports.

A

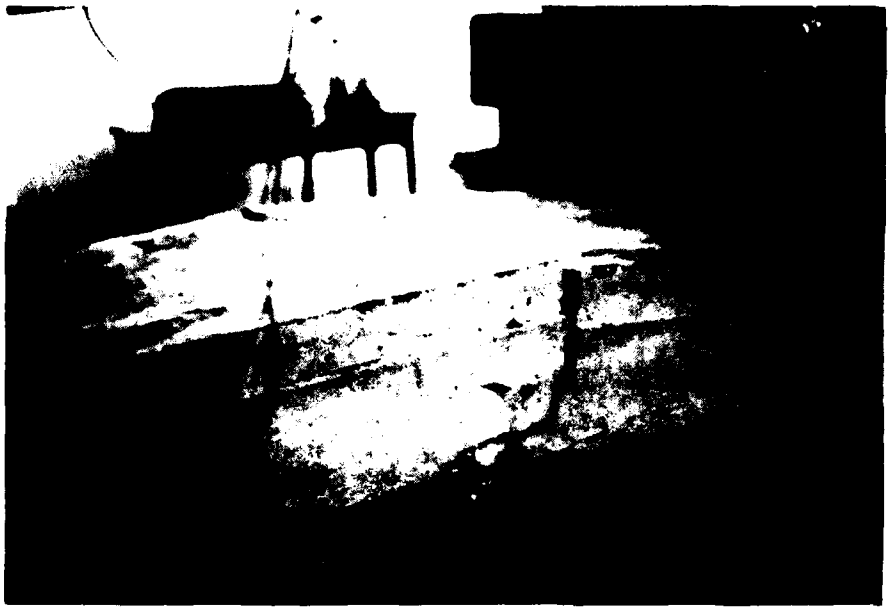

B

Fig. 3-57. Test No. 13, After Test.

Tests Nos. 14 and 15 (Shored at Two Locations, 10-inch Slab)

These two tests were conducted on identical slabs simply supported and shored with timber at the outside one-quarter points. The shoring and loading configuration for both tests are shown in Figure 3-58. The purpose of these tests was to vary the two shore configurations with respect to Test No. 13, in order to determine the effect of this dimensional change on the system's performance. The reason for duplicating Test No. 14 with Test No. 15 was to verify the collapse loads and modes of failure.

In both tests, the load was applied at eight locations by four rams, and the vertical deflection was measured midway between each of the supports and over each of the shores. The loads were applied at a slow rate in varying increments of 4,000 to 8,000 lb/ram and the deflection recorded at each increment.

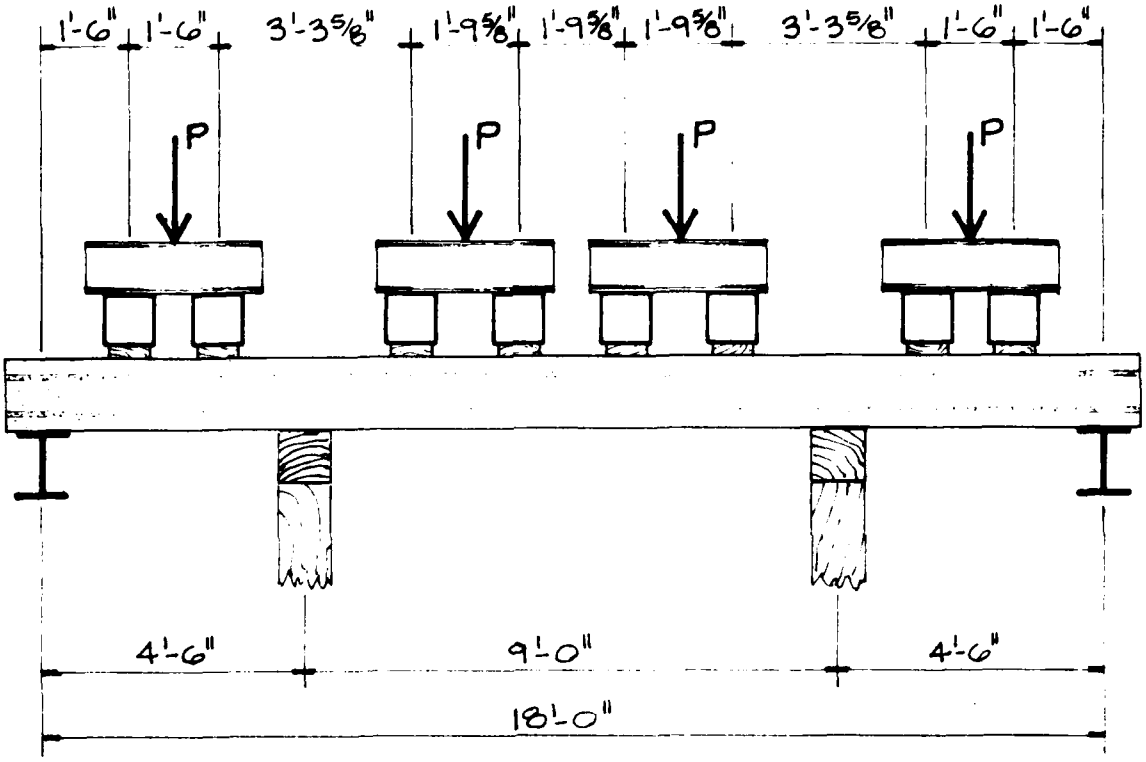

Fig. 3-58. Loading Configuration — Two Shores, 10-inch Slabs, Tests No. 14 and 15.

In Test No. 14, the slab failed when the applied load reached 50,000 lb/ram. The calculated uniform load at failure was 4,004 psf (27.8 psi). The uniform load vs relative deflection curve for each span is shown in Figure 3-59.

The first positive moment tension crack occurred in the center span at 1,602 psf (11.1 psi), and negative moment tension cracks were noted over both shores at 2,883 psf (20.0 psi). The failure occurred in shear/flexure in the center span, just inside the left shore. An examination of the failed area indicated considerable loss of bond in the prestressing strands.

Figure 3-60A shows the slab prior to test. Figure 3-60B shows the failed area immediately after test and before unloading. Figure 3-61A shows the slab after test and after unloading. Figure 3-61B shows a closeup of the failed section.

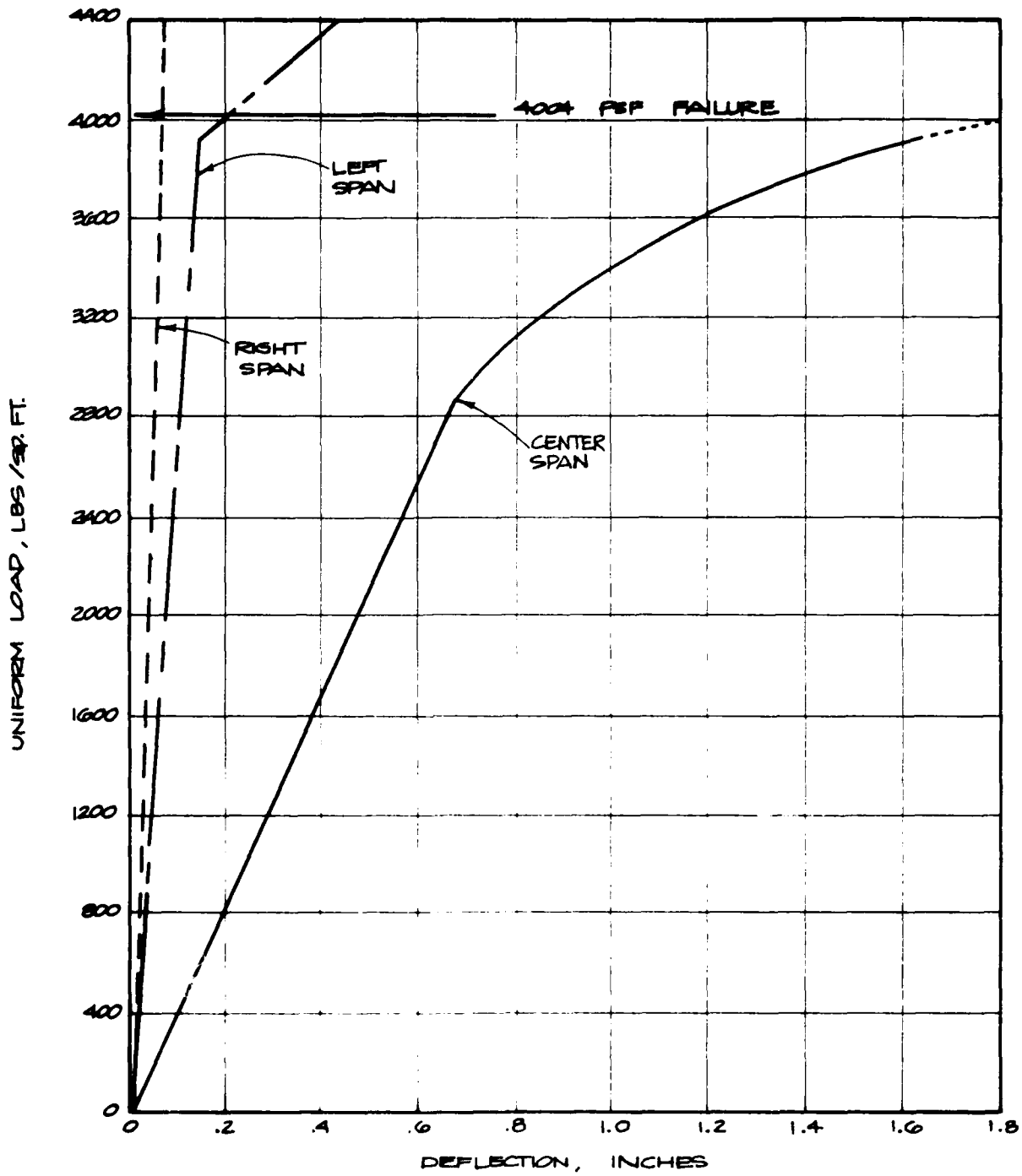

Fig. 3-59. Uniform Load vs Deflection, Test No. 14, Shored at One-Third Points, 10-inch Slab.

A

B

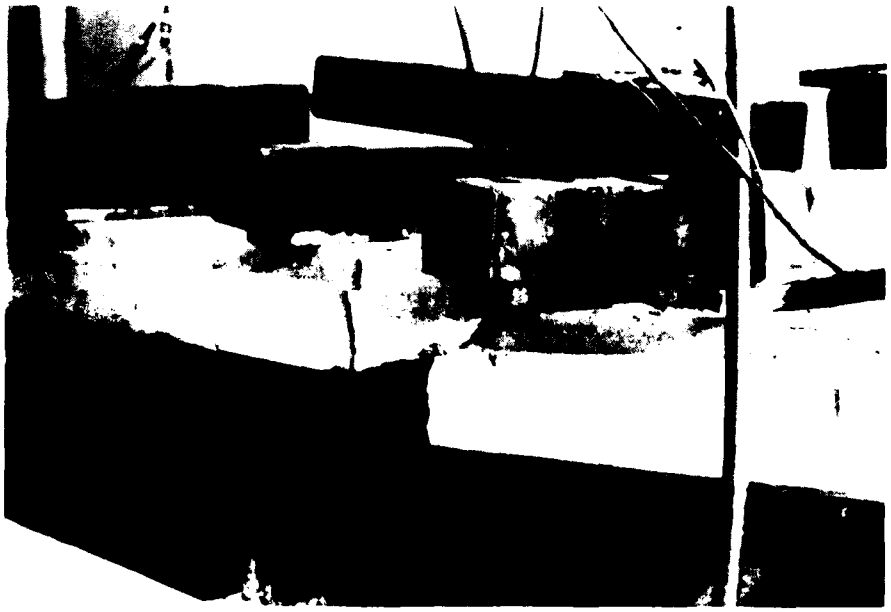

Fig. 3-60 Pre- and Posttest Photographs, Test No. 14.

A

B

Fig. 3-61. Posttest Photographs, Test No. 14.

In Test No. 15, The slab failed when the applied load reached 46,000 lb/ram. The calculated uniform load at failure was 3,687 psf (25.6 psi). The uniform load vs relative deflection curve for each span is shown in Figure 3-62.

The first positive moment tension crack occurred in the center span at 1,281 psf (8.9 psi), and negative moment tension cracks were noted over both shores at 2,883 psf (20.0 psi). The failure occurred in the center span as a result of shear/flexure. Evidence of strand bond failure was again present at the failed section.

Figure 3-63 shows the slab before and after test. Figure 3-64 shows closeup photographs of the failed section of the slab.

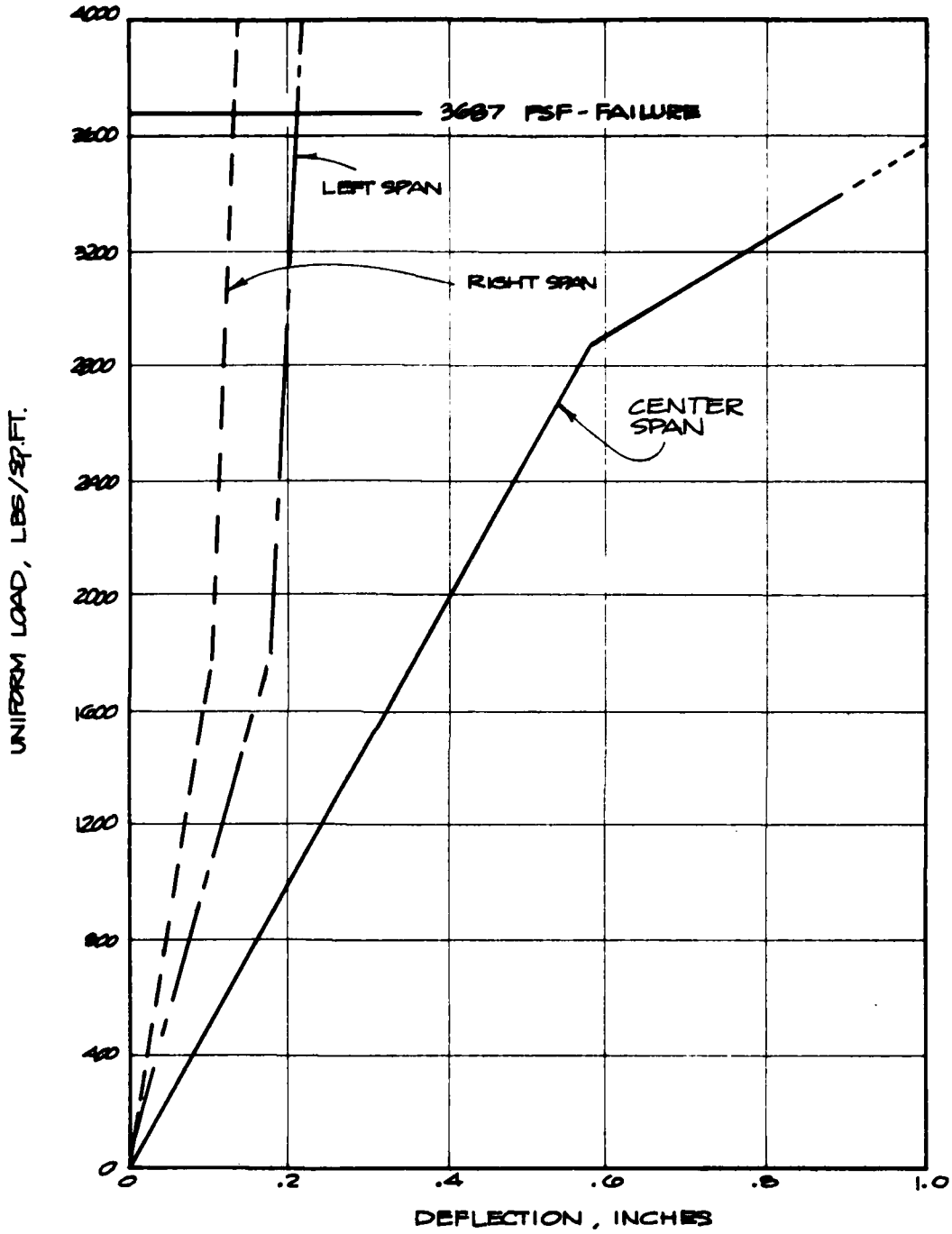

Fig. 3-62. Uniform Load vs Deflection, Test No. 15, Shored at One-Quarter Points, 10-inch Slab.

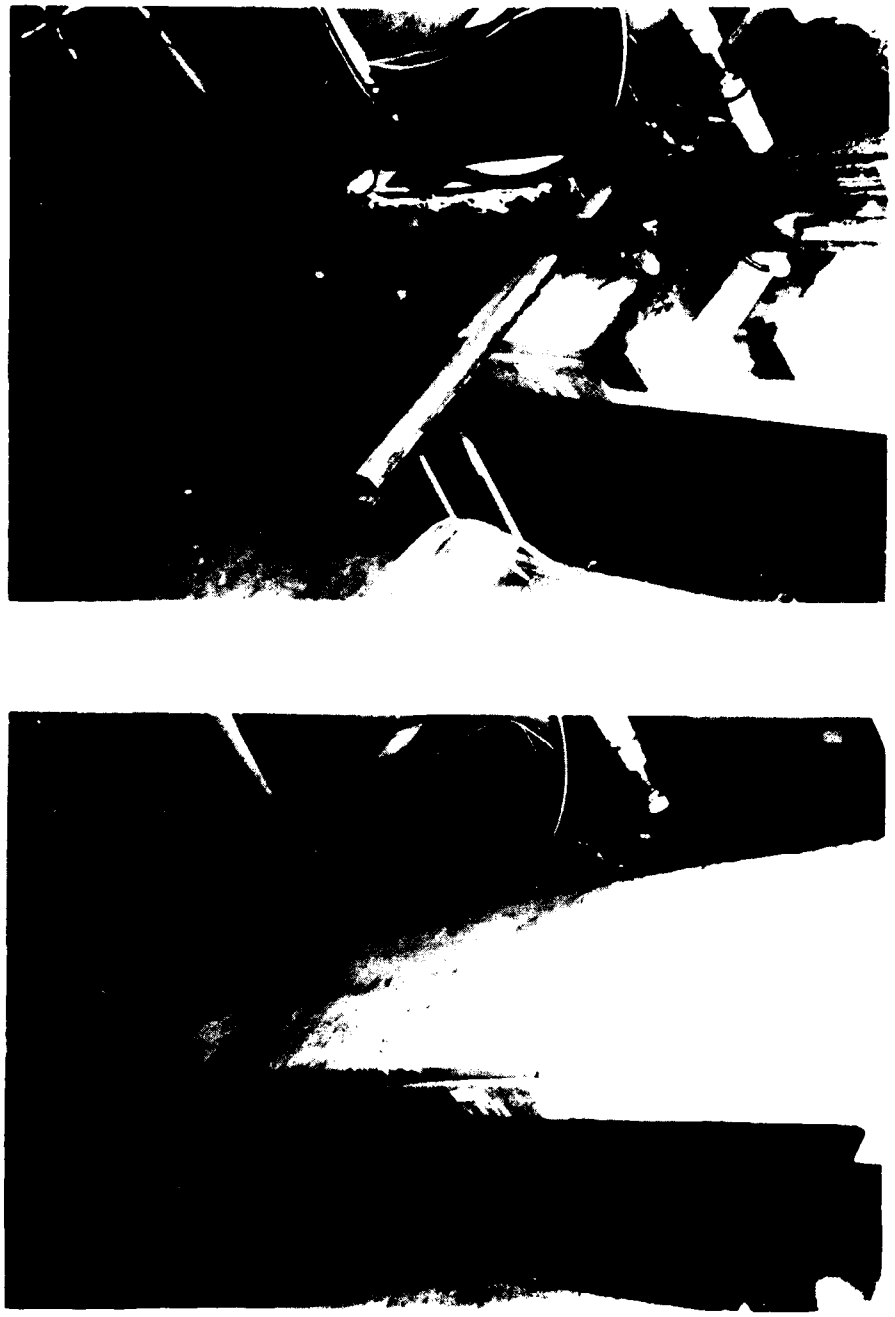

Fig. 3-63. Pre- and Posttest Photographs, Test No. 15.

Fig. 3-64. Posttest Photographs, Test No. 15.

SUMMARY

Below is a summary of the precast concrete hollow-core slab tests discussed in this section of the report.

TABLE 3-1

PRESTRESSED CONCRETE HOLLOW-CORE SLABS — SUMMARY OF TEST DATA

Test No.	Slab Thickness	Design Live Load (psf)	Upgrading	Failure Load (psf)	Failure Load (psi)
1	4 in.	70	None	205	1.4
2	4 in.	70	None	205	1.4
3	4 in.	70	Midspan — Timber	1,012	7.0
4	4 in.	70	One-third span — Timber	2,431	16.9
5	8 in.	165	None	400	2.8
6	8 in.	165	Midspan — Steel	1,557	10.8
7	8 in.	165	Midspan — Timber, 1½-in. gap	1,646	11.4
8	8 in.	165	One-third span — Timber	2,936	20.4
9	8 in.	165	Two shores, one each at one-quarter span from support	3,043	21.1
10	10 in.	260	None	823	5.7
11	10 in.	260	Midspan — Steel	3,025	21.0
12	10 in.	260	Midspan — Timber	2,937	20.4
13	10 in.	260	One-third span — Timber	4,805	33.4
14	10 in.	260	Two shores, one each at one-quarter span from support	4,004	27.8
15	10 in.	260	Two shores, one each at one-quarter span from support	3,687	25.6

Several interesting variations were introduced into this test program for evaluation. One was the shoring of identical test assemblies with different shoring systems and materials, and another was varying the shore locations in the two-shore upgrading configurations from the traditional one-third span positions, a comparison again conducted on identical test assemblies. An analysis of these data indicates the following:

Comparison of Shore Types

In this case the tests referred to are Tests Nos. 6 and 7 and Tests Nos. 11 and 12 (see Table 3-1). Tests Nos. 6 and 7 were identical assemblies shored at the same location, but the shore in Test No. 7 was constructed to permit a 1½-inch deflection at midspan prior to picking up load, while in Test No. 6 the shore was steel tubing shimmed tightly to the bottom of the slab. The failure loads were 10.8 psi in Test No. 6 and 11.4 psi in Test No. 7 — not significantly different.

In Tests Nos. 11 and 12, identical assemblies were shored at midspan with shores of different materials. Test No. 11 was shored with steel tubing, while Test No. 12 used conventional wood shores; both types of shores were shimmed tightly to the bottom of the test slabs. Obviously the wood shores would permit some deflection from the crushing of the timber, while the steel shores would permit little, if any, deflection. The failure loads were 21.0 psi in Test No. 11 and 20.4 psi in Test No. 12 — again, virtually no significant difference.

Accordingly it may be concluded that, with respect to prestressed concrete, the degree of tightness of the shore to the slabs, and the material the shore is made of, are not significant factors in the performance of the upgraded system.

Varying Shore Locations

In the second case the tests referred to for comparison purposes are Tests Nos. 8, 9, 13, 14, and 15. Tests Nos. 8 and 9 were 8-inch slabs — No. 8 shored at the one-third span locations and No. 9 also with two shores,

but with the shores located at the outside one-quarter points, thus creating a longer center span. The failure loads of Tests Nos. 8 and 9 were 20.4 psi and 21.1 psi, respectively — not significantly different. Tests Nos. 13, 14, and 15 were 10-inch slabs, with No. 13 shored at the one-third points and Nos. 14 and 15 shored at the outside one-quarter points with two shores. The failure loads were 27.8 psi for Test No. 14 and 25.6 psi for Test No. 15, both slightly lower than Test No. 13 at 33.4 psi.

It was observed that the one-third span failures (Tests Nos. 4, 8, and 13) consistently occurred in the end spans, while the center span indicated little or no distress. The end span failures appeared to be primarily the result of shear and were directly related to the loss of bond in the prestressing tendons. It should be noted that the tendons do not become fully developed for approximately 24 to 30 inches from the end, and thus do not transmit significant compression to the concrete in the high shear zones. It was believed that, by moving the shores closer to the slab ends (thus decreasing the end span and therefore the shear — and moment — in these spans) and increasing the center span (and accordingly the moment and shear in this span), the failures of each span would approximate each other and thereby increase the upgrading capability of the system. Although this may be theoretically true at some division of span between one-quarter point and one-third point, the test results do not indicate a significant difference. This could be quite important since it suggests that extreme accuracy in the placement of the shores is not required for upgrading procedures to be effective.

The failure modes and the predictability of these modes are discussed in detail in Appendix B of this report. The results of all of the tests reported in this section, as listed in Table 3-1, were consistent with the prediction methodology previously used and with the values listed in the Preliminary Survival Matrix for Floors, Table 7-1 of this report.

Section 4
WOOD FLOOR TESTS

INTRODUCTION

This is the third series of wood floor tests reported in this program. The first series consisted of eleven tests directed toward the development of base data on typical floor systems found in residential and commercial structures, the upgrading of these floor systems by various methods, and the correlation of the tests and results with work performed by others. This first series was also instrumental in providing data to assist in development of a failure prediction theory for timber structures (Ref. 3).

The second series consisted of two full-scale tests devoted to developing drop test procedures for simulating dynamic failures (Ref. 4).

The series investigated this year was primarily concerned with the development of base case and upgrading data for the "medium" wood joist category; i.e., the floors designed for 125 psf live load. This loading is typical of floors used for light storage, a common construction type not previously tested.

TEST PROGRAM

The program consisted of load tests to failure of three identical test assemblies. The assemblies were similar to those tested and reported previously (Refs. 3 and 4), except that deeper joists (2x12's instead of 2x10's) were used. These deeper joists were required because of the increased design live loading. The framing and construction details are shown in Figures 4-1, 4-2, and 4-3.

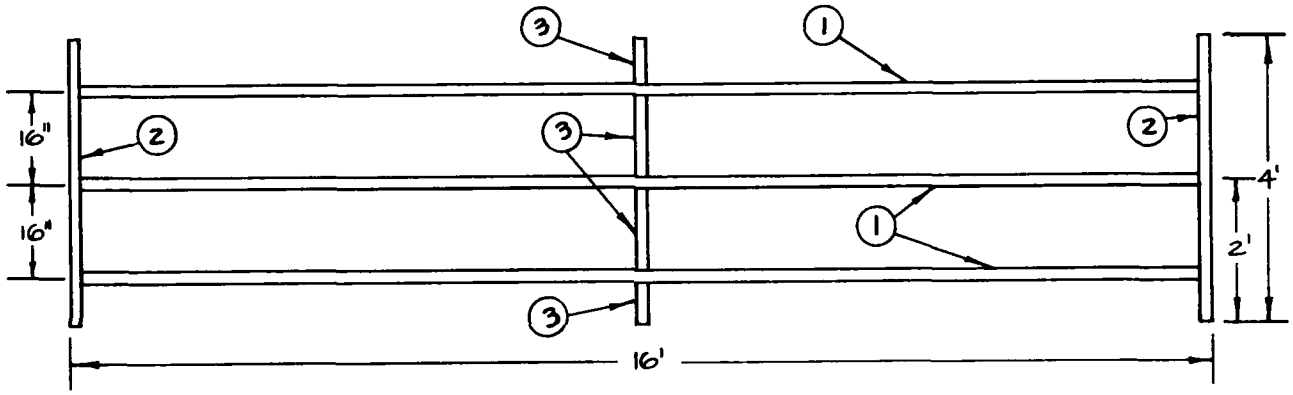

1 2" x 12" x 15'9" JOIST ON 16" CENTERS

2 2" x 12" x 4' HEADER

3 2" x 12" BLOCKING

ALL FRAMING MATERIAL IS:

- DOUGLAS FIR
- SELECT STRUCTURAL

HEADERS AND BLOCKING NAILED TO JOISTS WITH THREE 16d COMMON NAILS/ JOIST

Fig. 4-1. Framing Detail for All Floor Assemblies.

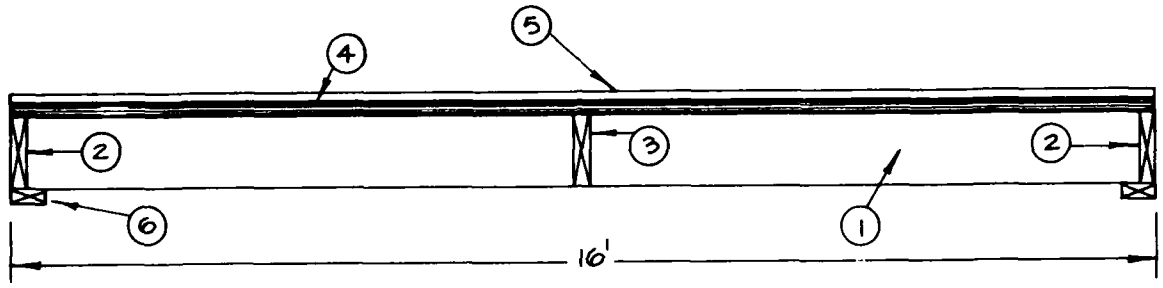

1. 2" x 12" x 15'9" JOIST
2. 2" x 12" x 4' END BLOCK
3. 2" x 12" BLOCKING
4. 3/4" 4' x 8' PLYWOOD SUBFLOOR (C-D EXTERIOR)
5. 3/8" PARTICLE BOARD
6. 2" x 4" x 4' SILL

Fig. 4-2. Construction Details for All Floor Assemblies.

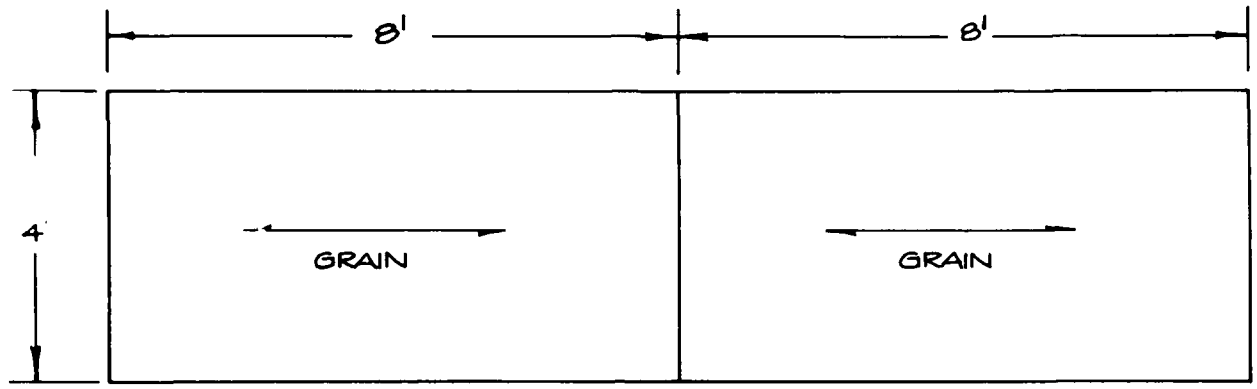

SUBFLOOR

FIRST LAYER : 3/4" C-D EXTERIOR PLYWOOD
8d COMMON NAILS ON 6" CENTERS

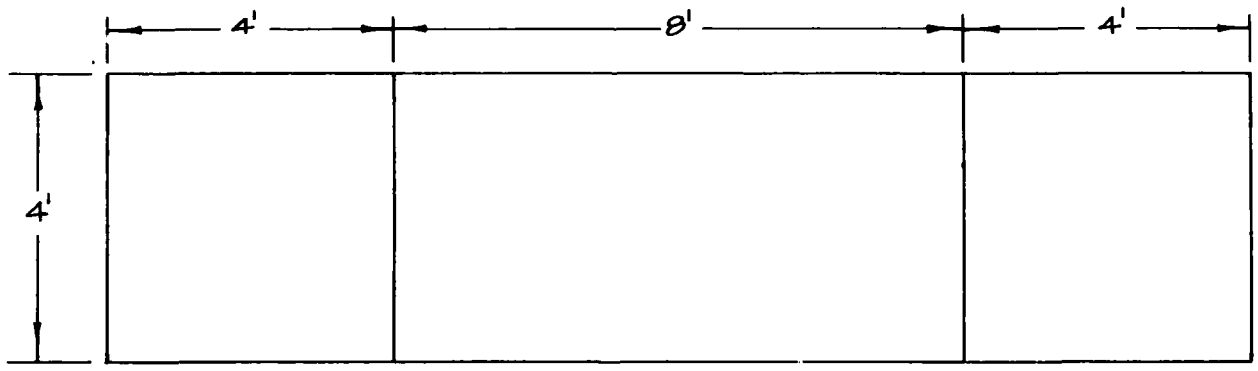

FLOOR

SECOND LAYER : 3/8" PARTICLE BOARD
6d COMMON NAILS ON 12" CENTERS

Fig. 4-3. Flooring Details for All Floor Assemblies.

In order to be consistent with the previously conducted test programs and the "Summary of Test Data" presented in Table 4-1, Ref. 4, these three tests are designated as Group 7, assemblies 14, 15, and 16. (This table is included at the end of this section as Table 4-1.)

The first assembly tested in the current program, No. 14, was the base case, and the test was conducted without any shoring or upgrading modifications. The second test assembly, No. 15, was upgraded by shoring at midspan. The third test assembly, No. 16 in Group 7, was upgraded by locating shores at one third the span.

The remainder of this section reports the test method, loading arrangement, and test results for each of the assemblies.

Assembly No. 14 (Base Case)

This test was conducted with the assembly simply supported. The load was applied at six locations by hydraulic rams in the configuration shown in Figure 4-4. The vertical deflection was measured and recorded at midspan and over each end support. The moisture content of the joists was measured at 11.9%. The load was applied at a slow rate in 500 lb/ram increments, and the deflection recorded at each increment.

The assembly failed with the two outside rams applying loads of 6,000 lb each and the center ram applying a load of 6,500 lb. The calculated uniform load at failure was 368 psf (2.6 psi). The relative midspan deflection, as measured immediately prior to failure, was 2.78 inches. The uniform load vs midspan deflection curve is shown in Figure 4-5.

The failure occurred when one of the outside joists split longitudinally approximately three-quarters of its length. Inspection of the failed joist after test indicated that the joist had failed first in bearing at the sill, and that the crack had progressed diagonally from the bearing failure toward the center of the assembly. This mode of failure was confirmed by personnel observing the assembly at the time of failure.

The remainder of the joists were examined with respect to their degree of bearing on the sill, and in all cases it was found that a small amount of clearance was present between the bottom of the joists and the sills. These clearances were not more than 1/8 inch, but were large enough to prevent the joists from fully transmitting the bearing loads to the sills.

Figure 4-6 shows two views of the assembly after test. Figure 2-7 shows the sill where the crack initiated and the bearing failure occurred. Figure 4-8 shows the failed joist in the direction of crack propagation.

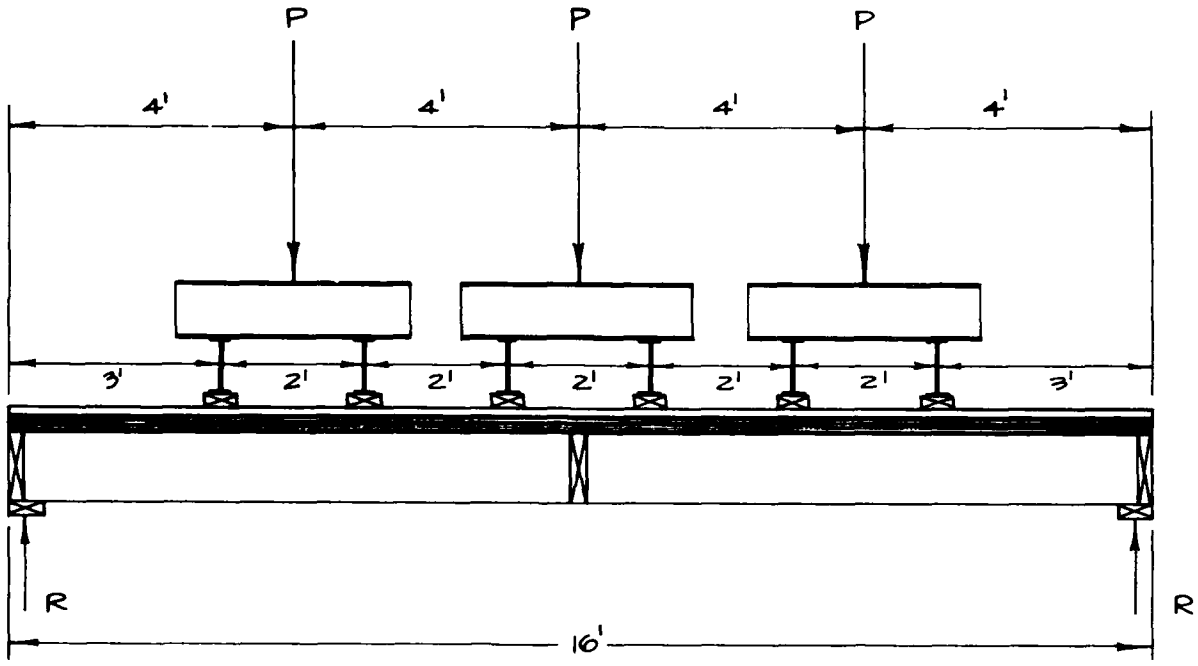

Fig. 4-4. Loading Configuration - Base Case, Assembly No. 14.

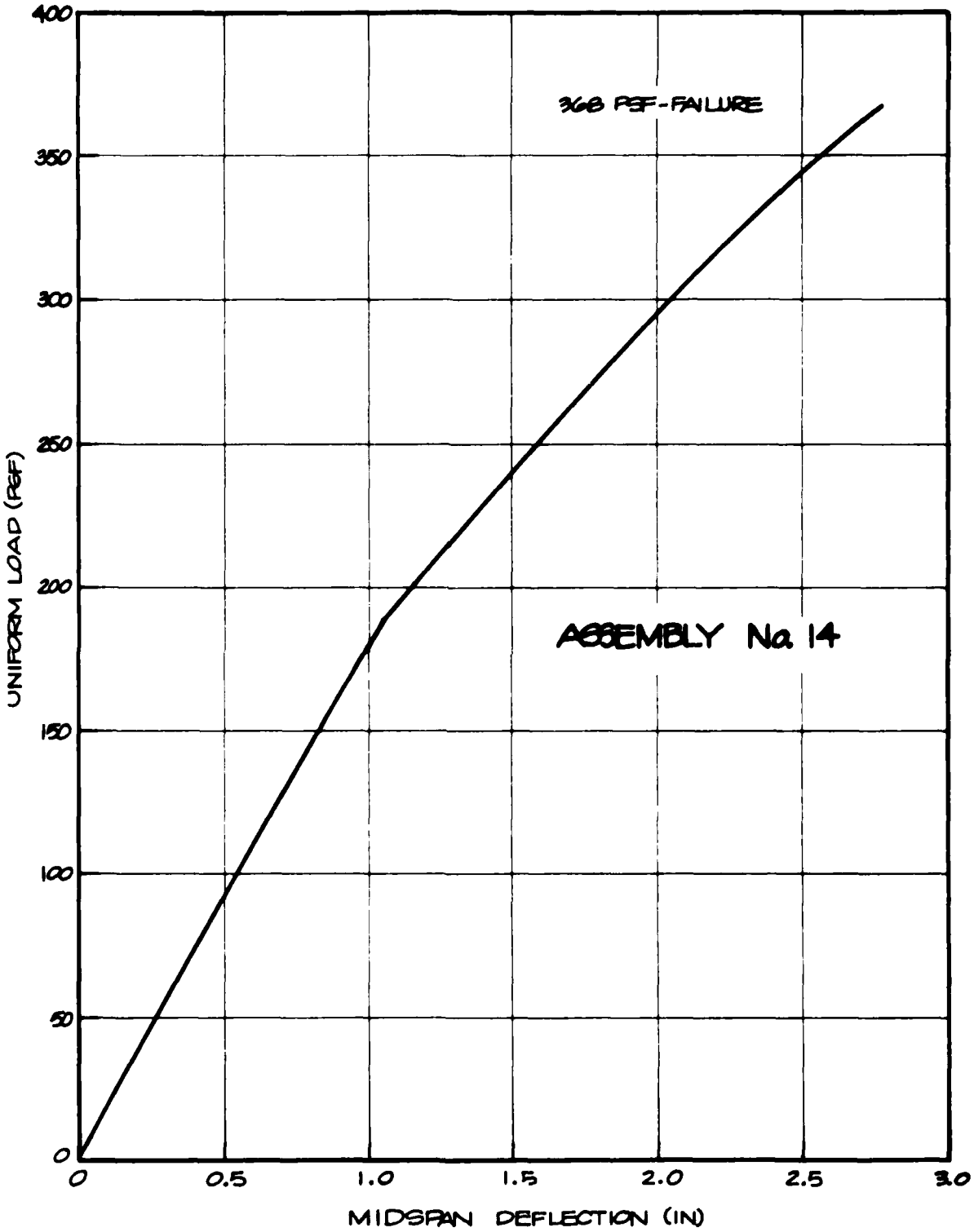

Fig. 4-5. Uniform Load vs Deflection, Assembly No. 14.

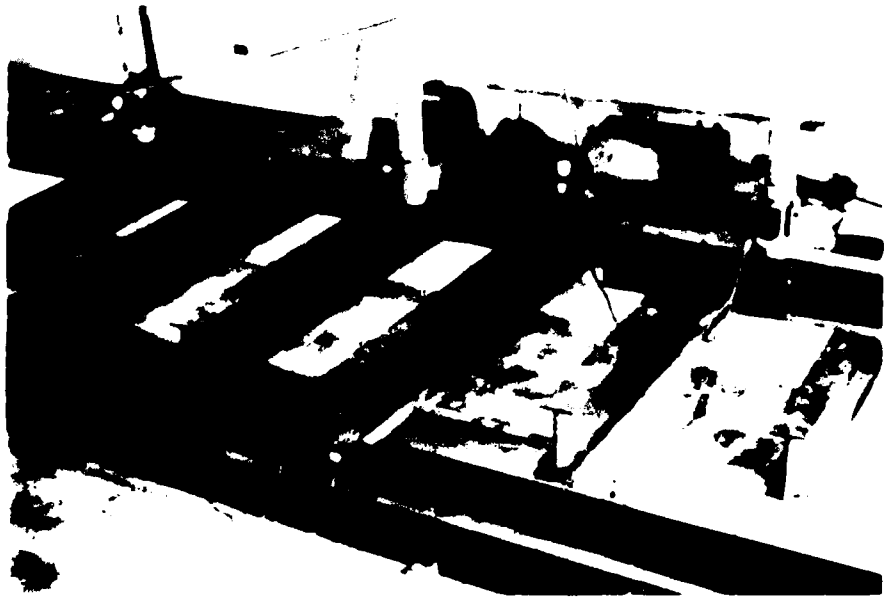

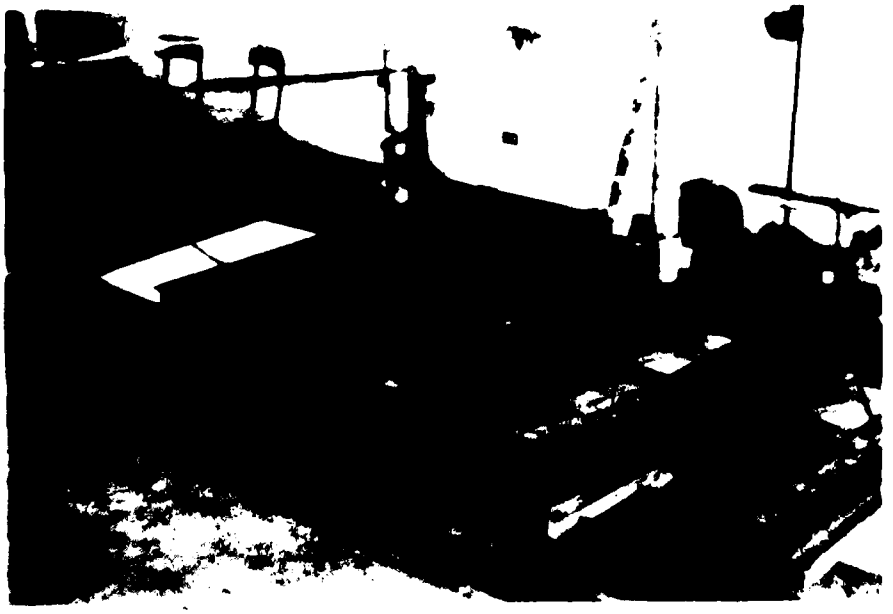

Fig. 4-6. Assembly No. 14 After Test.

Fig. 4-7. [illegible]
Asser[illegible]

Fig. 4-8. Failed [illegible] Propagation,
Asser[illegible]

Assembly No. 15 (Shored at Midspan)

The assembly in this test was simply supported at its ends and shored at midspan. The shore was constructed as shown in Figure 4-9 and shimmed tightly against the bottom of the joists. The load was applied at four locations by hydraulic rams in the configuration shown in Figure 4-10. The vertical deflections were measured and recorded at the center of the spans on either side of the shore, over the shore at midspan, and over each end support. The moisture content of the joists was measured at 12.3%.

The load was applied at a slow rate in 1,000 lb/ram increments and the deflections recorded at each increment.

The assembly failed with each ram applying a load of 31,000 lb. The calculated uniform load at failure was 1,320 psf (9.2 psi). The relative deflections, as measured immediately prior to the failure, were 1.38 inches at the center of the left span and 0.78 inches at the center of the right span. The uniform load vs deflection curve for each span is shown in Figure 4-11.

The failure occurred as a result of the crushing of the 4x4 horizontal shore member at the locations of the vertical 4x4 supports. This bearing failure caused subsequent rotation of the shore, thus rendering it ineffective for support, and resulted in an immediate flexural failure at midspan of one of the joists in the test assembly.

Figure 4-12 shows a top view of the assembly prior to test. Figure 4-13 shows the shore in place prior to test. Figure 4-14 shows the top portion of the shore after test and depicts the bearing failure of the horizontal member. Figure 4-15 shows the flexural failure of the joist at midspan.

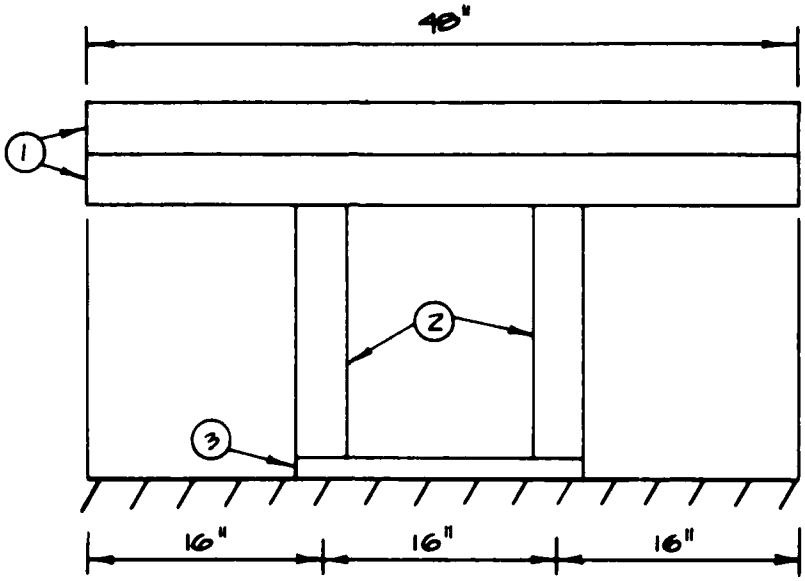

① 4"x4"x4' NAILED TOGETHER WITH FOUR 8d COMMON NAILS (TOENAILED).

② 4"x4"x17" NAILED TO THE 4"x4"x4' WITH TWO 8d COMMON NAILS EACH (TOENAILED).

③ 2"x12"x19" NOT NAILED.

Fig. 4-9. Shore Used at Midspan, Assembly No. 15.

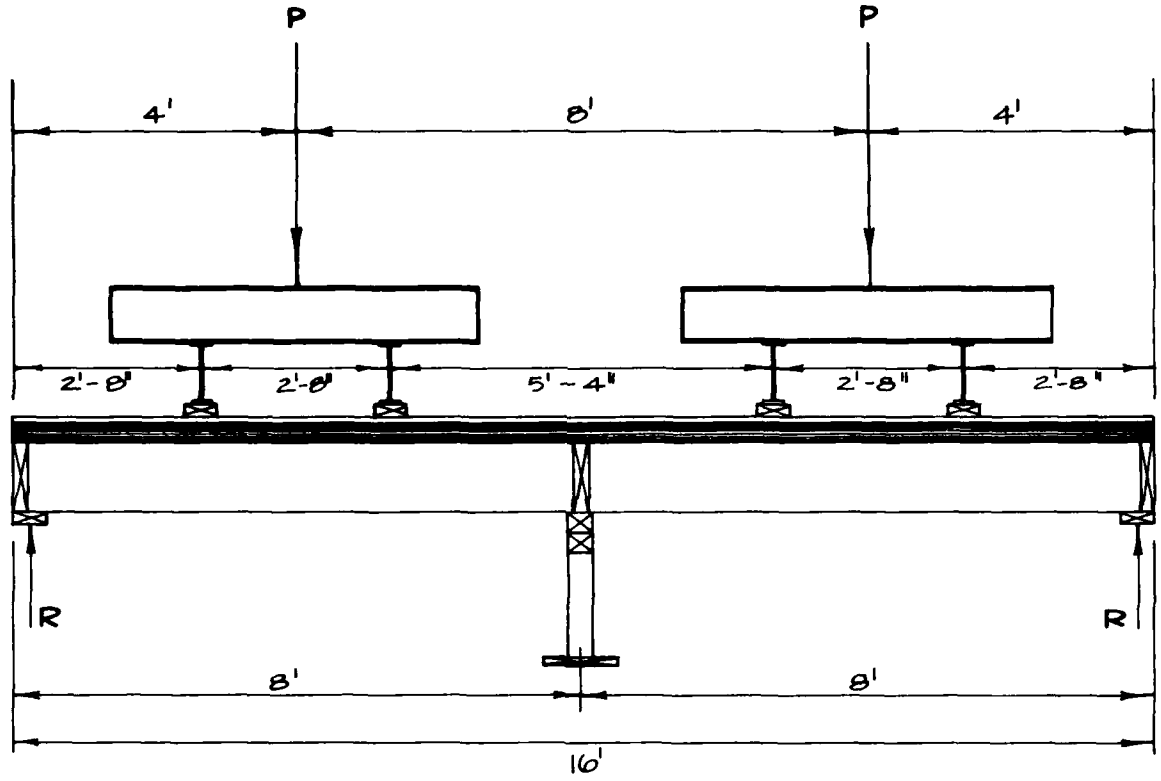

Fig. 4-10. Loading Configuration, Shored at Midspan, Assembly No. 15.

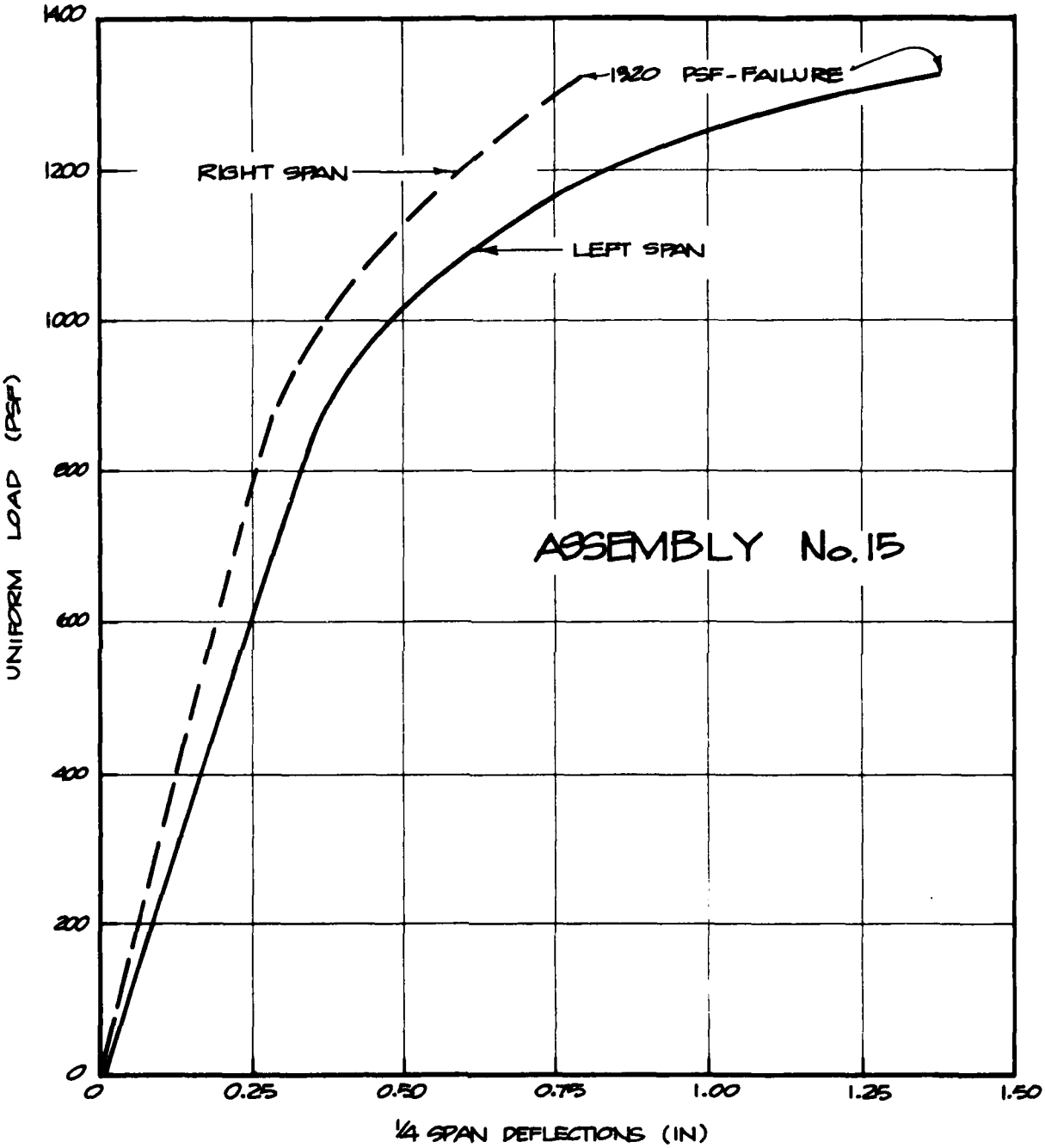

Fig. 4-11. Uniform Load vs Deflections, Assembly No. 15.

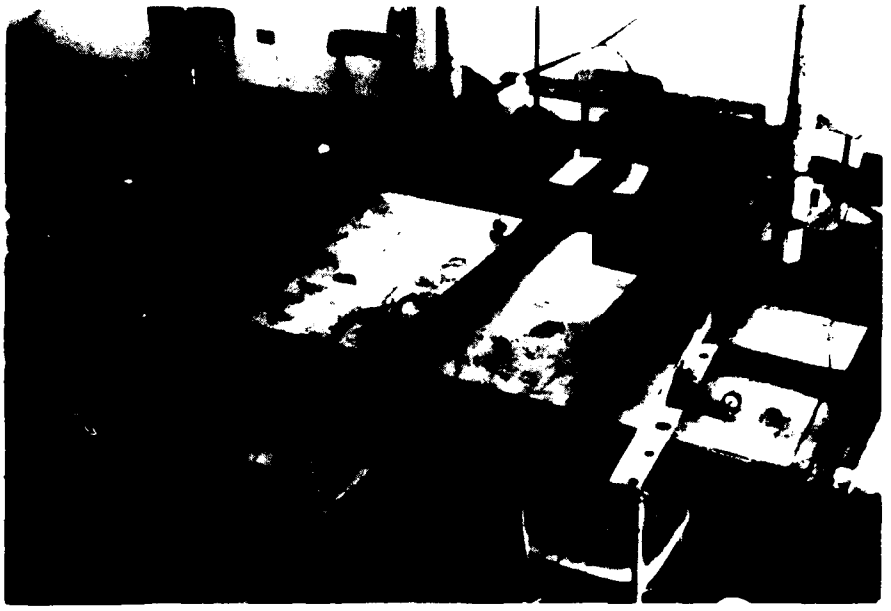

Fig. 4-12. Assembly No. 15 Before Test.

Fig. 4-13. Shore Before Test, Assembly No. 15.

Fig. 4-14. Shore Atten Test, [illegible] Horizontal Member, [illegible]

Fig. 4-15. Midspan [illegible]

Assembly No. 16 (Shored at One-Third Span)

The assembly in this test was again simply supported at its ends. The shores were located at the one-third points of the span. Both shores were constructed as shown in Figure 4-16 and were shimmed tightly against the bottom of the joists. [Note: The shore detail differs from the single shore test (No. 15) in that metal post caps were used.] The load was applied at six locations by hydraulic rams in the configuration shown in Figure 4-17. The vertical deflections were measured and recorded at the center of each of the three spans, over both shores, and over each end support. The moisture content of the joists was measured at 10.0%.

The load was applied at a slow rate in 1,000 lb/ram increments and the deflections recorded at each increment.

The assembly failed with each ram applying a load of 32,000 lb. The calculated uniform load at failure was 2,005 psf (13.9 psi). The relative deflections, as measured immediately prior to the failure, were 0.59 inches at the center of the left span and 0.05 inches at the center of the right span. The uniform load vs deflection curve for this test is shown in Figure 4-18.

The failure occurred initially in shear near one end of an outside joist. This failure evidenced itself by a longitudinal crack, apparently starting at the end of the joist approximately 4 inches from the bottom, and progressing toward the first shore.

Figure 4-19 shows a top view of the assembly prior to test. Figure 4-20 shows one of the shores in place prior to test. Figure 4-21 shows the shores after test. Figure 4-22 shows the flexure failure in the end of the joist.

AD-A100 490 SCIENTIFIC SERVICE INC REDWOOD CITY CA F/G 13/13
UPGRADING OF EXISTING STRUCTURES. PHASE III. SHELTER DESIGN OPT--ETC(U)
MAY 81 R S TANSLEY, B L GABRIELSEN EMW-C-0153
UNCLASSIFIED SSI-8012-6 NL

3 OF 3
AD
A100490

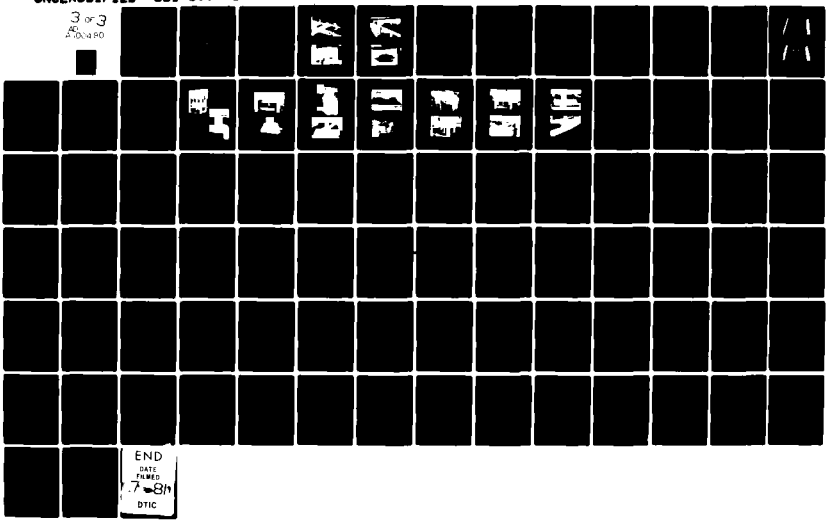

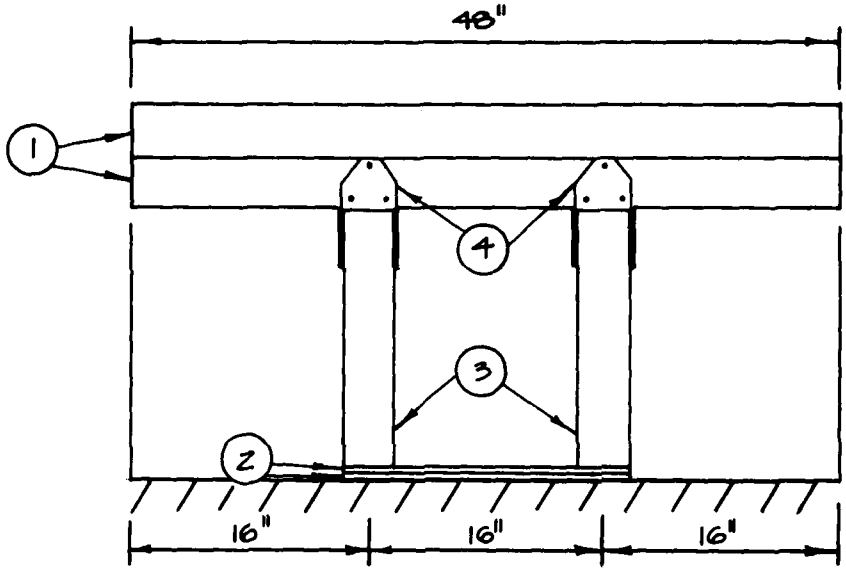

1. 4" x 4" x 4'
2. ½" x 12" x 19" PLYWOOD
3. 4" x 4" x 17½"
4. 4" x 4" POST CAP/BASE CONNECTORS, 18 GAUGE GALVANIZED STEEL

4"x4"x4' ARE NAILED TOGETHER WITH FOUR 8d COMMON NAILS (TOENAILED).

POST CAP/BASE CONNECTORS ATTACHED WITH THREE 16d NAILS TO EACH SURFACE.

THE PLYWOOD WAS NOT NAILED.

Fig. 4-16. Shores Used at One-Third Span, Assembly No. 16.

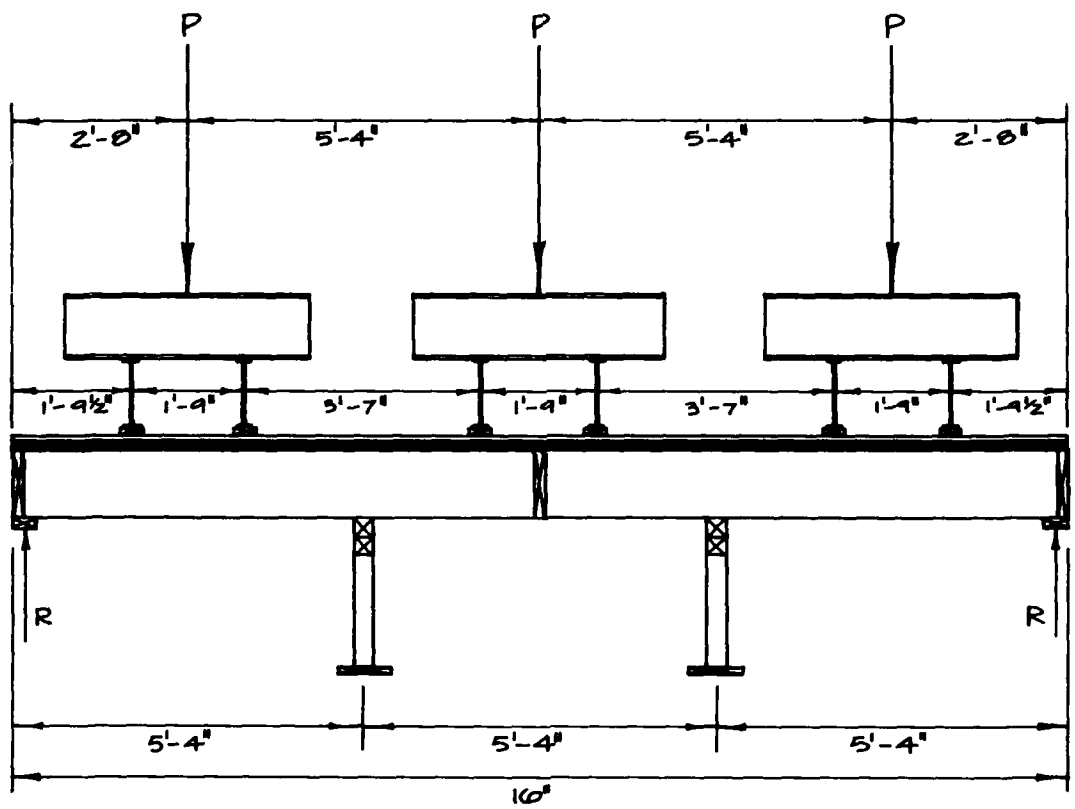

Fig. 4-17. Loading Configuration, Shored at One-Third Span, Assembly No. 16.

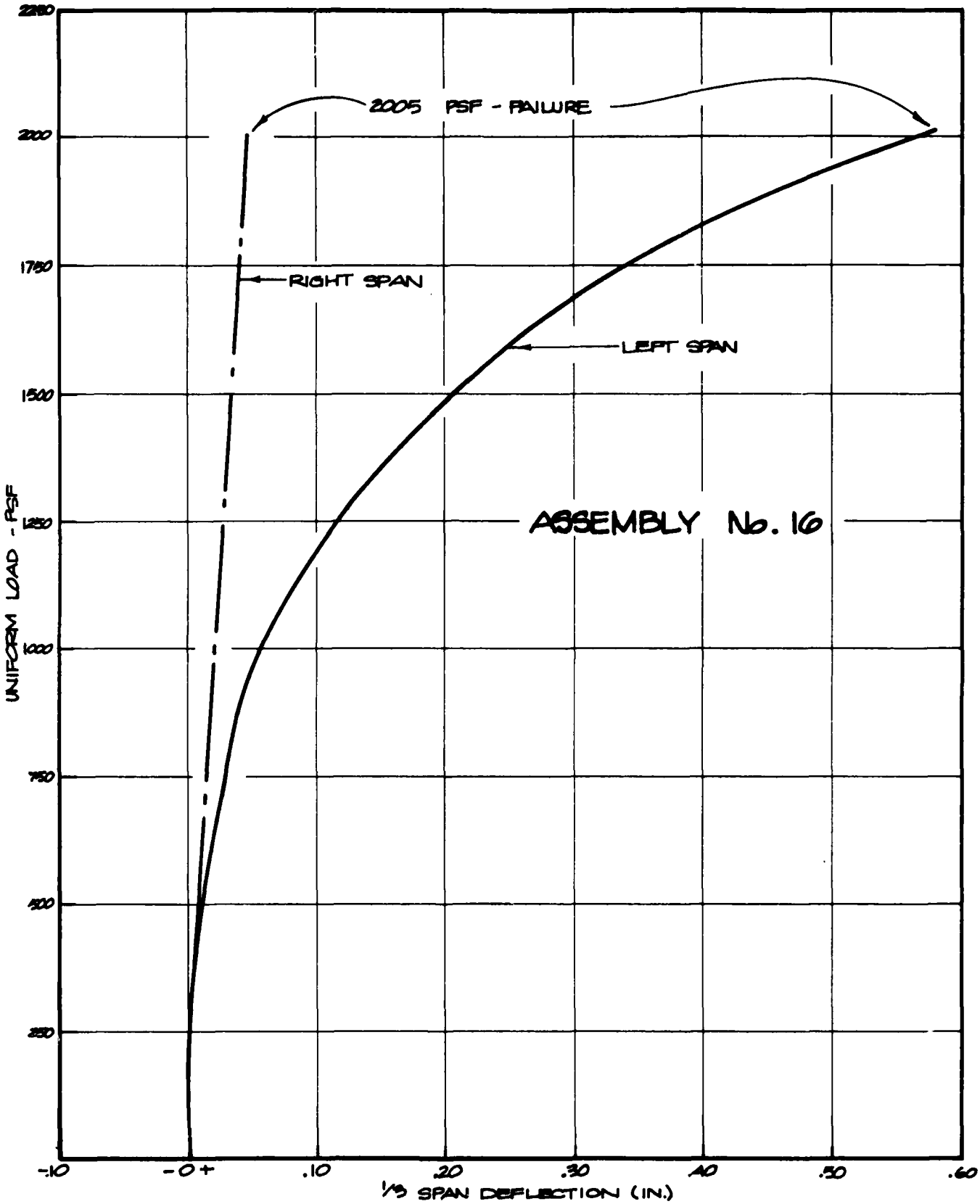

Fig. 4-18. Uniform Load vs Deflection, Assembly No. 16.

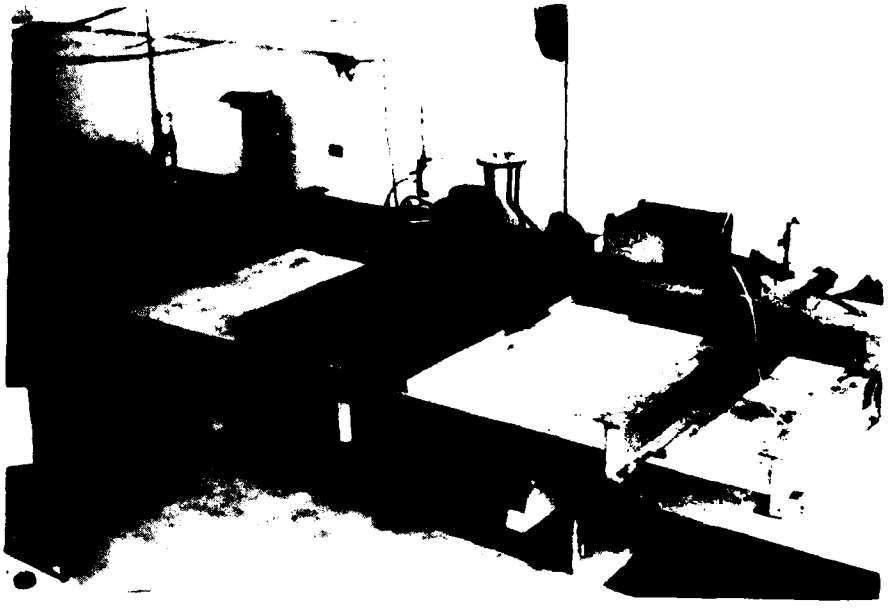

Fig. 4-19. Assembly No. 16 Before Test.

Fig. 4-20. Shore Before Test, Assembly No. 16.

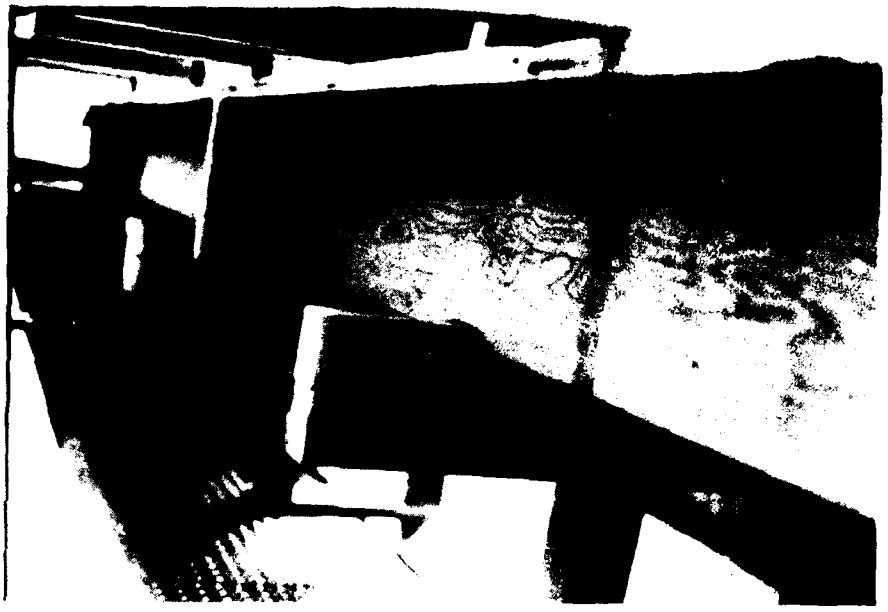

Fig. 4-21. Shores After Test, Assembly No. 16.

Fig. 4-22. Failed Joist, Assembly No. 16.

SUMMARY OF TEST DATA

The failure overpressures for the three tests herein reported were:

Assembly No. 14 (base case)	2.56 psi
Assembly No. 15 (shored at midspan)	9.17 psi
Assembly No. 16 (shored at one-third span)	13.92 psi

These values have been added to Table 4-1, which is a summary of all wood floor test data. The data developed in the current series (1980) are underlined.

TABLE 4-1: WOOD FLOORS — SUMMARY OF TEST DATA

Group	Specimen Number	Design Service Load (PSF)	Hardening Technique	W_{peak} (KSF)	t_{peak} (seconds)	F_b (psi)	P (psi)
1	1	50	Base case	0.166	0.8	3,973	1.15
	4	50	Base case	0.224	1.28	5,362	1.56
	12	50	Base case	0.189	–	4,525	1.31
	13	50	Base case	0.225	–	5,386	1.56
2	3	50	2 x 6 glued to bottom of joists	0.310	2.9	4,210	2.15
	6	50		0.472	3.0	6,410	3.28
3	5	50	2 layers of plywood on bottom	0.479	20.0	—	3.33
	9	50		0.456	8.5	—	3.17
4	10	50	Shores (single)	1.13	4.5	—	7.85
5	2	50	Shores (double)	1.47	2.25	—	10.21
6	7	50	King-Post	0.411	6.0	—	2.85
	8	50	King-Post	0.636	26.0	—	4.42
	11	50	King-Post	0.527	8.5	—	3.66
7	14	125	Base case	0.368	–	5,727	2.56
	15	125	Shores (single)	1.320	–	—	9.17
	16	125	Shores (double)	2.005	–	—	13.92

Section 5
CONCRETE SLAB PUNCHING SHEAR TESTS

INTRODUCTION

One of the most practical methods for upgrading existing structures is by the use of shores or posts. There is, however, very little data on the punching shear capability of the slab above, when that slab is reinforced concrete, or the concrete slab on grade below, when these types of shores are used. In order to obtain preliminary data in this area, a limited test series was conducted during this program.

The test specimens were manufactured with varying reinforcing steel patterns in order to simulate the types of slabs that would be shored as well as slabs on grade. Two different types of shores (timber and steel) were used in the investigation. The typical blast load condition of a shore-supported roof slab and slab on grade is shown in Figure 5-1.

These tests were conducted in order to evaluate the following strength properties and conditions:

A: Location of reinforcing steel —

1) Reinforcing steel located at slab face adjacent to support — representing the roof slab with positive moment (bottom) steel at location of shore support.

2) Reinforcing steel located at slab face away from the shore support — representing the floor slab with positive moment (bottom) steel at location of shore support.

B: Variations in amounts of reinforcing steel—

1) No steel

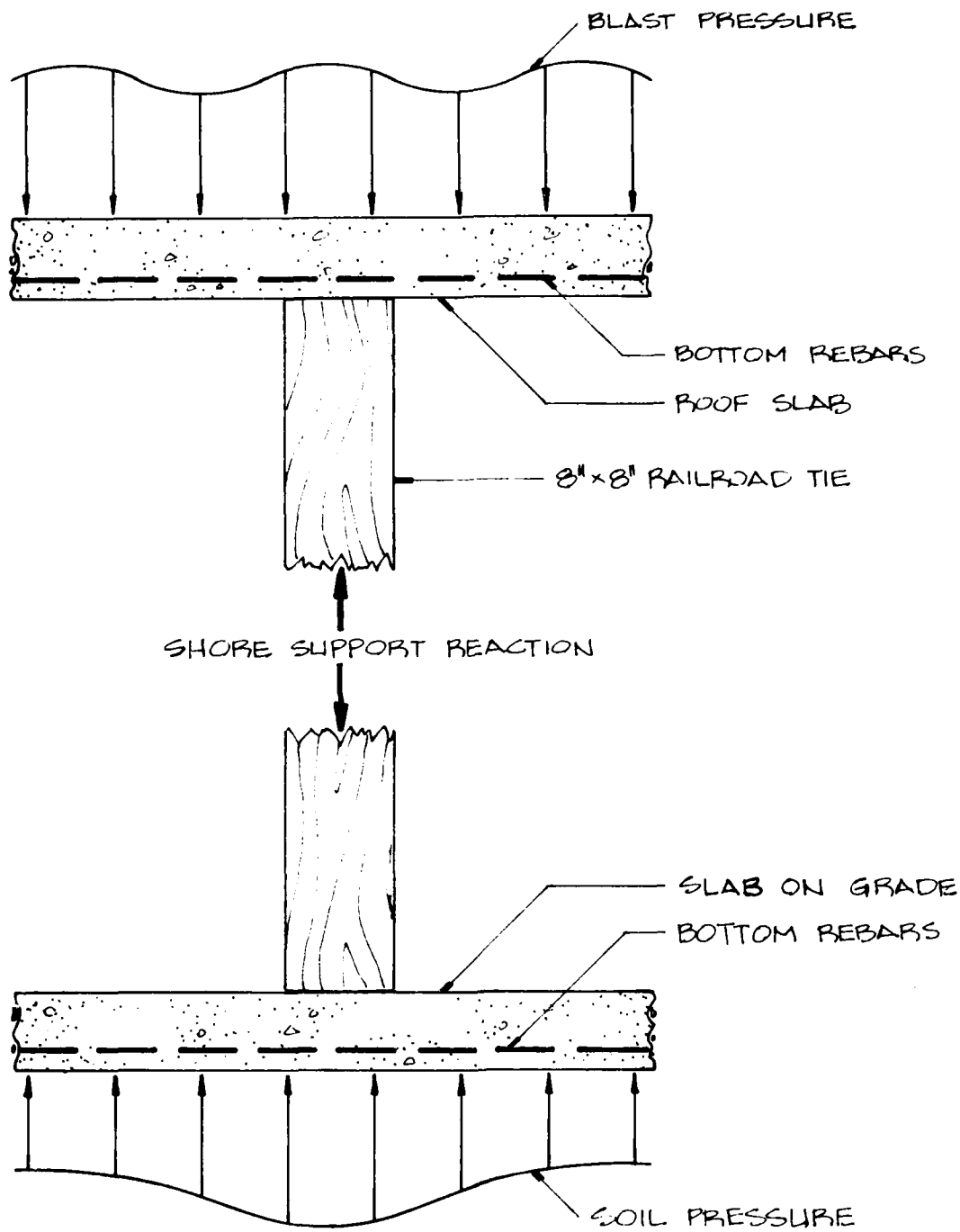

Fig. 5-1. Load Conditions for Shore-Supported Roof Slab and Slab on Grade.

2) Two-way steel

3) One-way steel

C: Bearing —

1) 8-inch-by-8-inch-by-1/2-inch steel plate bearing pad

2) Rough saw cut end bearing of 8x8 shore directly on slab.

DESIGN AND MANUFACTURE OF TEST SLABS

All of the concrete test slabs were 3 ft 10 inches by 3 ft 10 inches by 5 - 3/4 inches. A total of 16 were cast: two without reinforcing, four reinforced as one-way slabs, and ten reinforced as two-way slabs. The reinforcement layout for the one-way slabs consisted of No. 4 bars 12 inches on center in one direction and 16 inches on center in the other. The two-way slabs had No. 4 bars 12 inches on center in both directions. In both cases the reinforcing bars were located so that the clear concrete cover was 1¼ inches. Figure 5-2 shows the reinforcement layout for both types of slabs.

The reinforcing steel in all of the slabs was No. 4, GRADE 60, ASTM A 615. The concrete strength was determined by manufacturing six 6-inch-by-12-inch compression test cylinders from a representative sampling of the pour and testing them to failure in compression after 28 days. The results of the 28-day tests ranged from 3,383 psi to 3,887 psi and averaged 3,650 psi.

Figure 5-3 shows the one-way and two-way slab forms with the steel in place prior to casting.

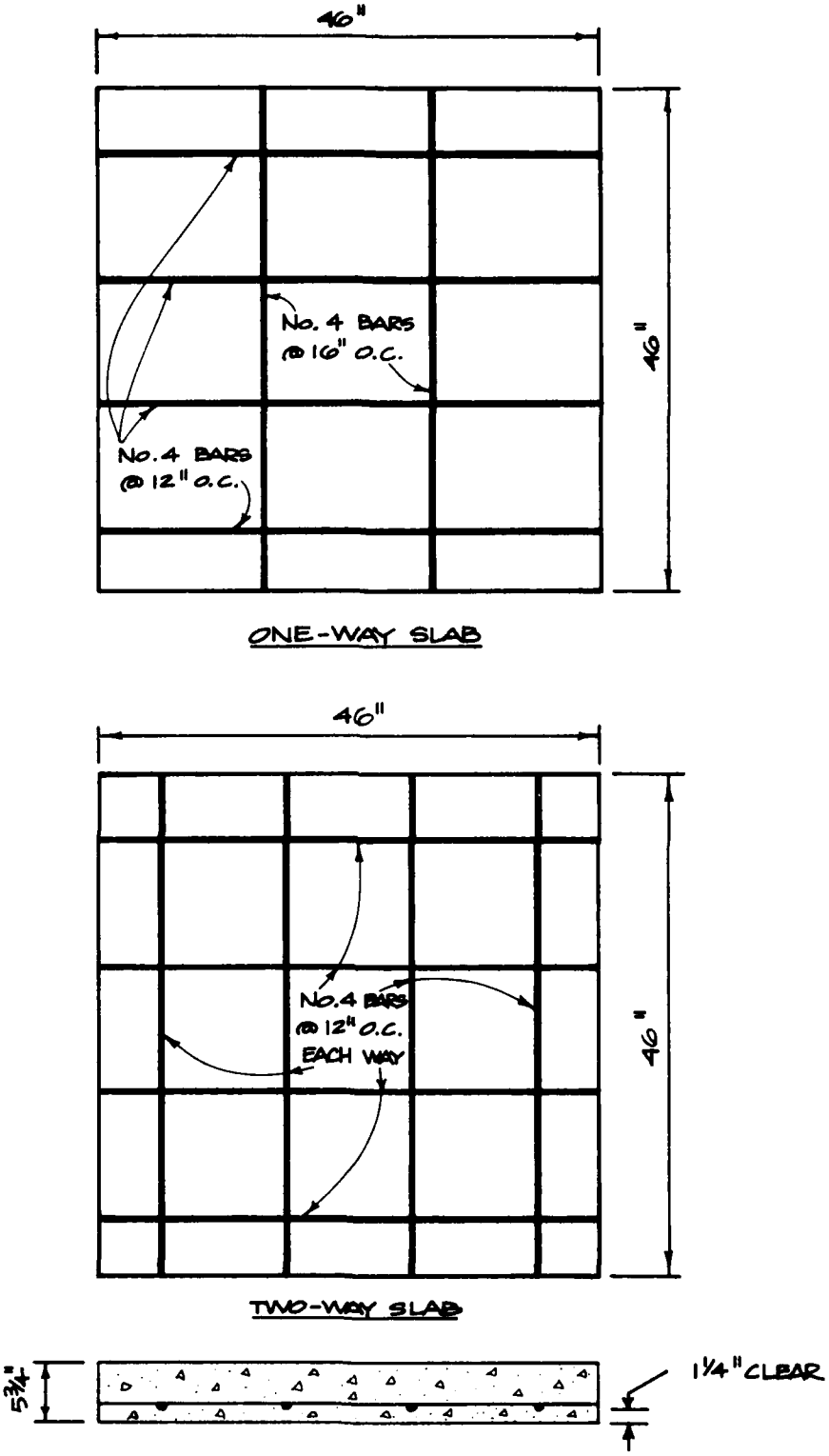

Fig. 5-2. Test Slabs, Reinforcing Steel Layout.

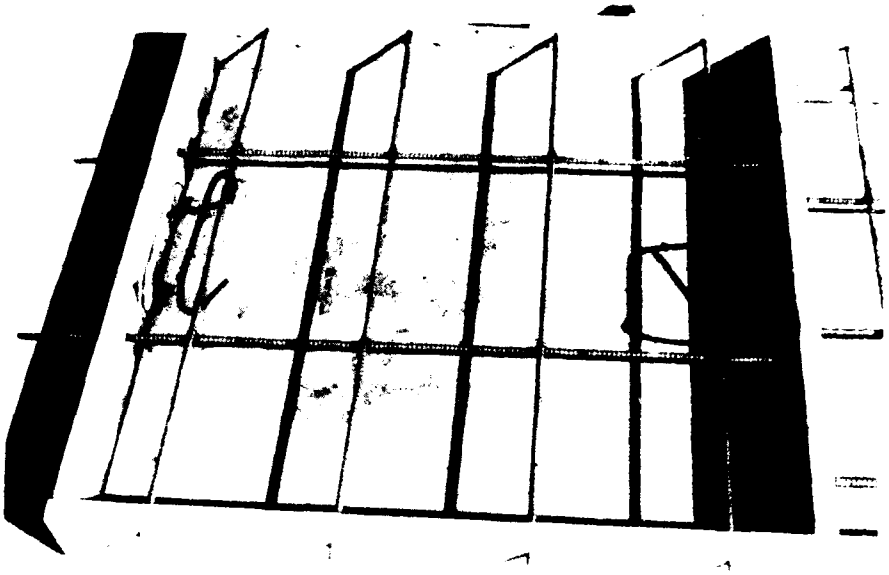

One-Way Slab

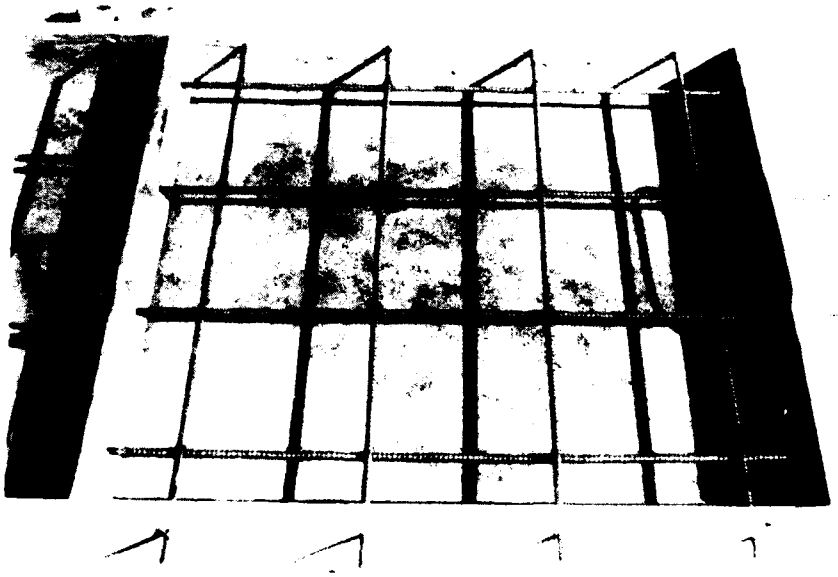

Two-Way Slab

Fig. 5-3. Forms Prior to Casting.

TEST PROGRAM

The testing program consisted of 16 tests. Eight slabs — five one-way, two two-way, and one unreinforced — were tested by applying load to an 8-inch-by-8-inch timber centered on the slabs. The other eight slabs, identical to those above, were loaded by applying load to an 8-inch-by-8-inch steel plate centered on the slab. In all 16 tests, the slab was supported below by a timber frame with inside dimensions of 24 inches by 24 inches. (The 2-foot dimension of the frame was selected in order to closely approximate the distance between inflection points to either side of a shore spaced 5 feet on center.

The load was always applied from the top. In order to simulate slabs with top steel, the test slabs were turned upside down so that the reinforcing steel was near the top surface of the slab.

Figure 5-4 shows a sketch of the typical test setup with the load and support conditions. Figure 5-5 shows a typical test setup with the timber post loading, and Figure 5-6, a typical test setup with the steel plate loading.

TEST RESULTS

A list of all the test results is presented in Table 5-1. Figures 5-7 through 5-11 show a representative sampling of the slabs after test.

TABLE 5-1: PUNCHING SHEAR TESTS

Test No.	Load Type	Slab Description	Failure Load (lb)
1	8" x 8" timber	Unreinforced	24,000
2	"	One-way slab bottom steel	40,400
3	"	One-way slab top steel	35,200
4	"	Two-way slab bottom steel	60,400
5	"	Two-way slab top steel	32,800
6	8" x 8" steel plate	Unreinforced	22,000
7	"	One-way slab bottom steel	50,200
8	"	One-way slab top steel	41,450
9	"	Two-way slab bottom steel	78,520
10	"	Two-way slab top steel	43,200
11	8" x 8" timber	Two-way slab bottom steel	78,500
12	"	Two-way slab bottom steel	72,400
13	"	Two-way slab bottom steel	78,000
14	8" x 8" steel plate	Two-way slab bottom steel	85,900
15	"	Two-way slab bottom steel	75,100
16	"	Two-way slab bottom steel	88,880

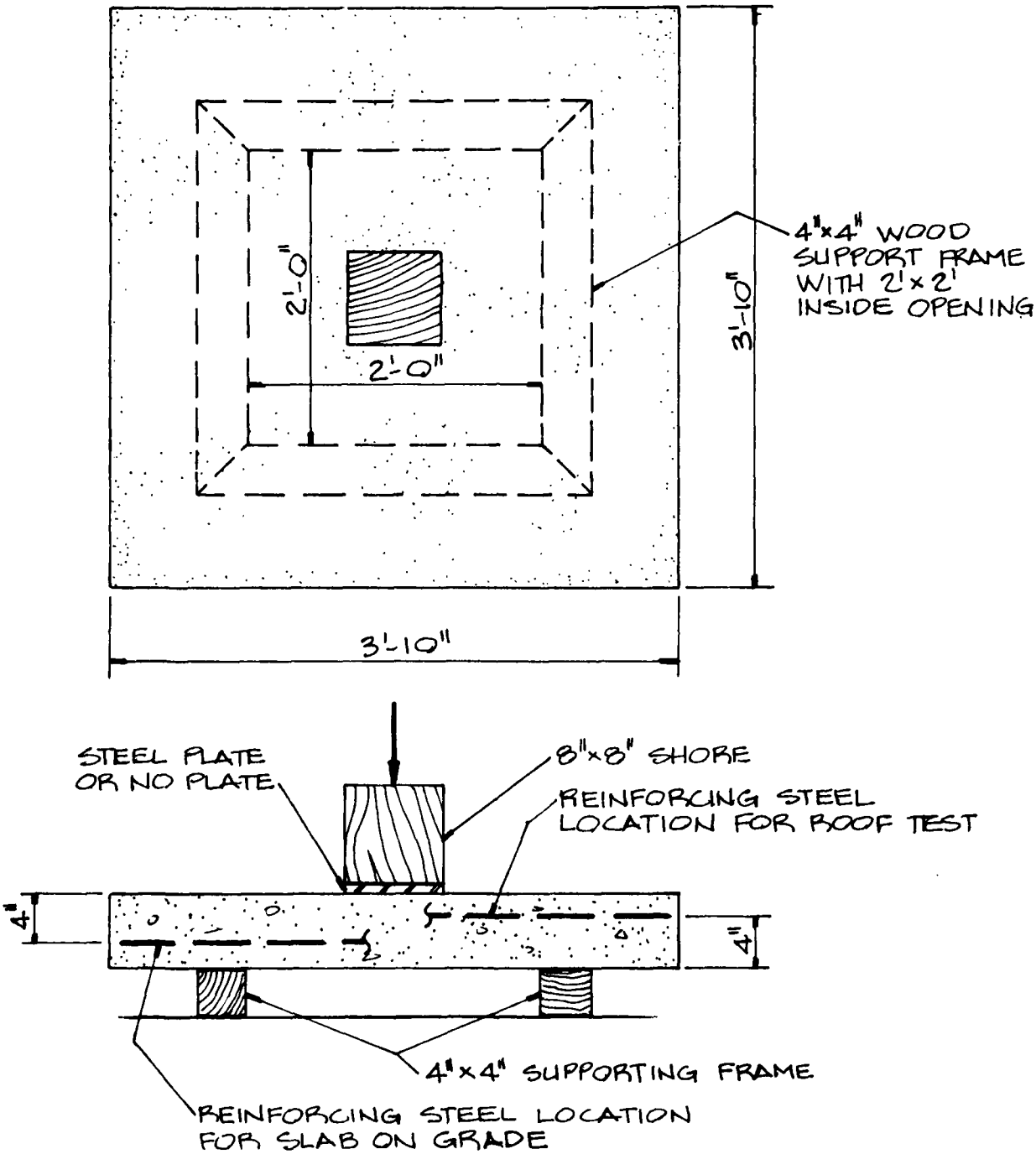

Fig. 5-4. Typical Test Setup With Load and Support Conditions.

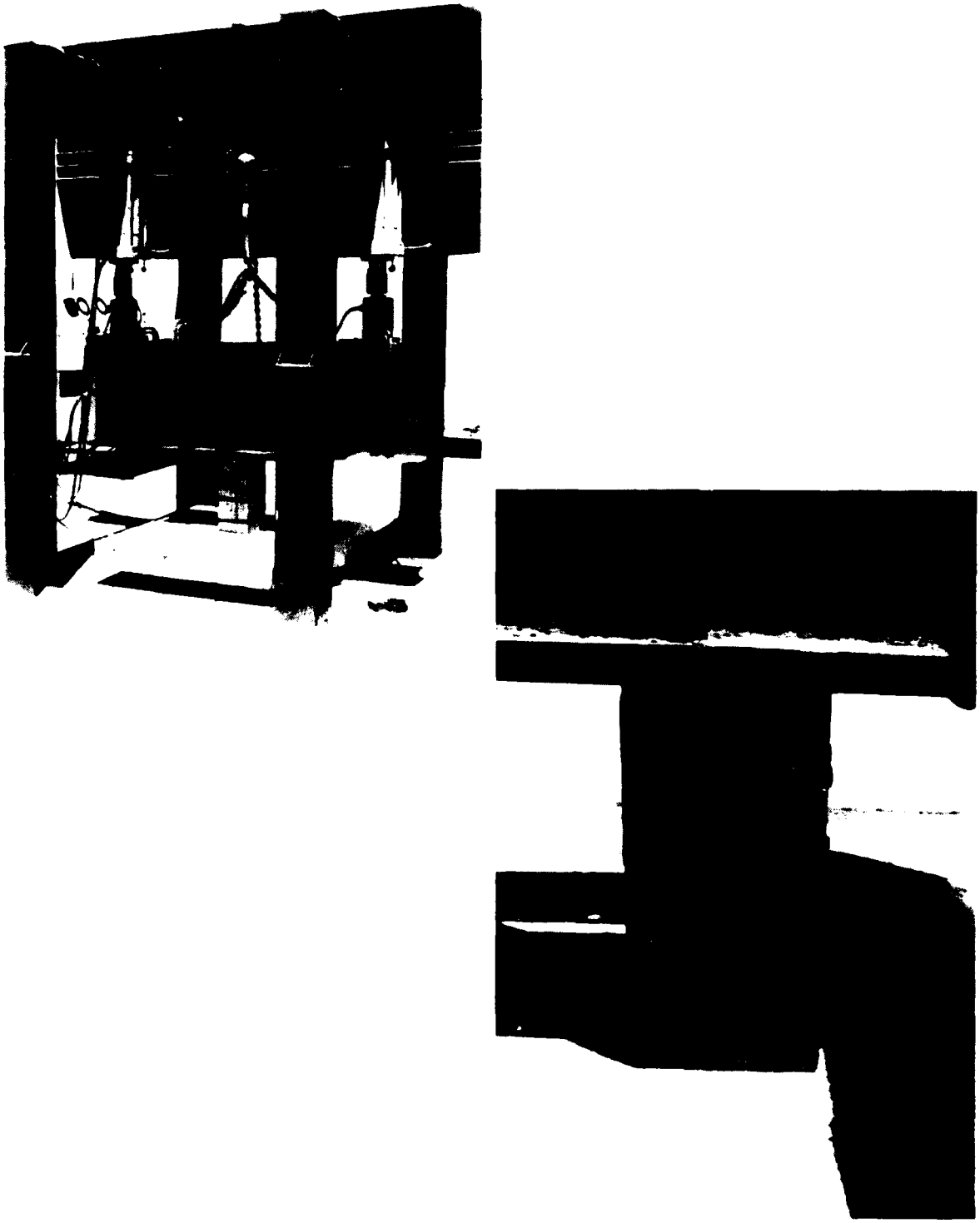

Fig. 5-5. Timber Post Test Setup.

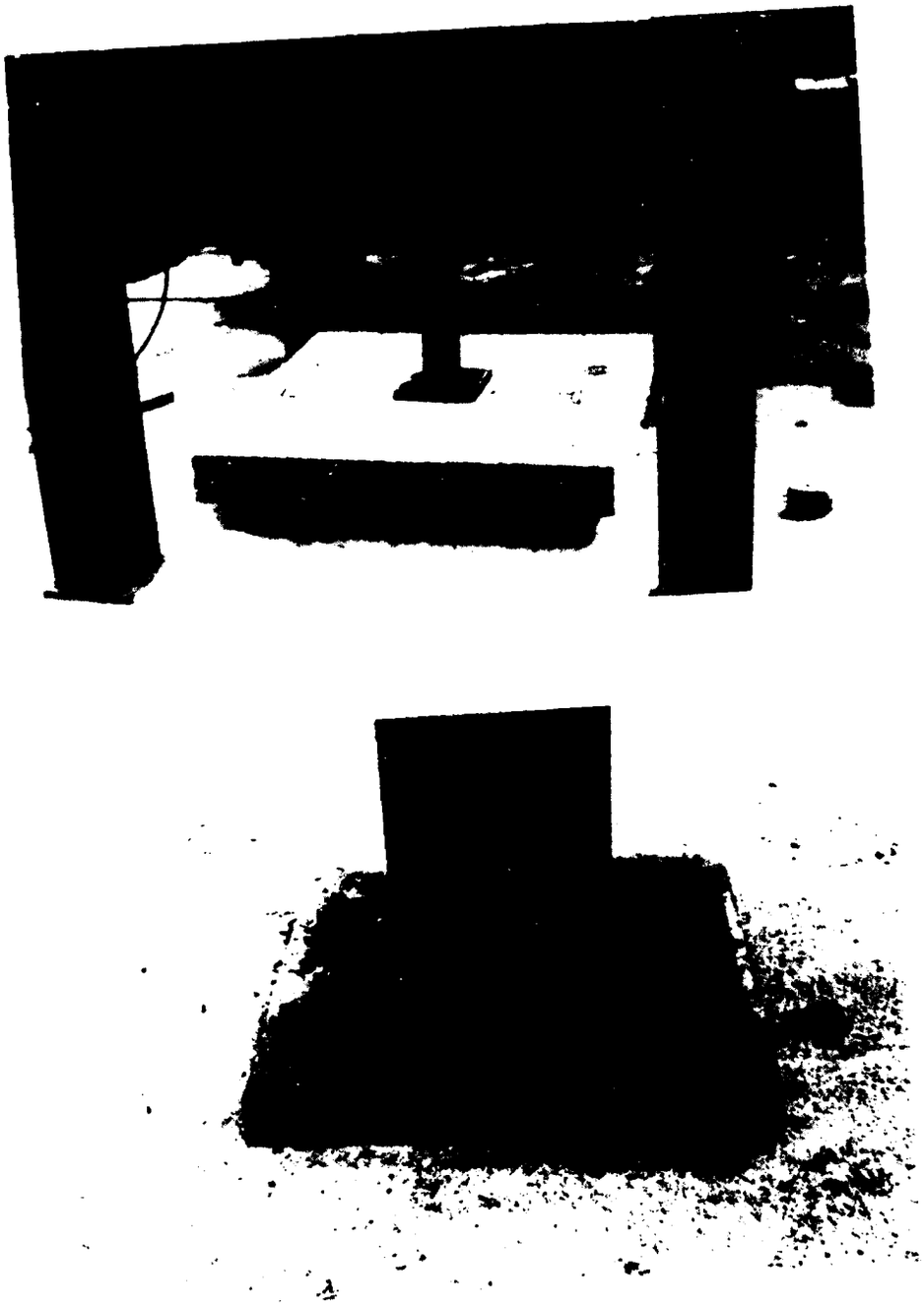

Fig. 5-6. Steel Plate Test Setup.

Test No. 1

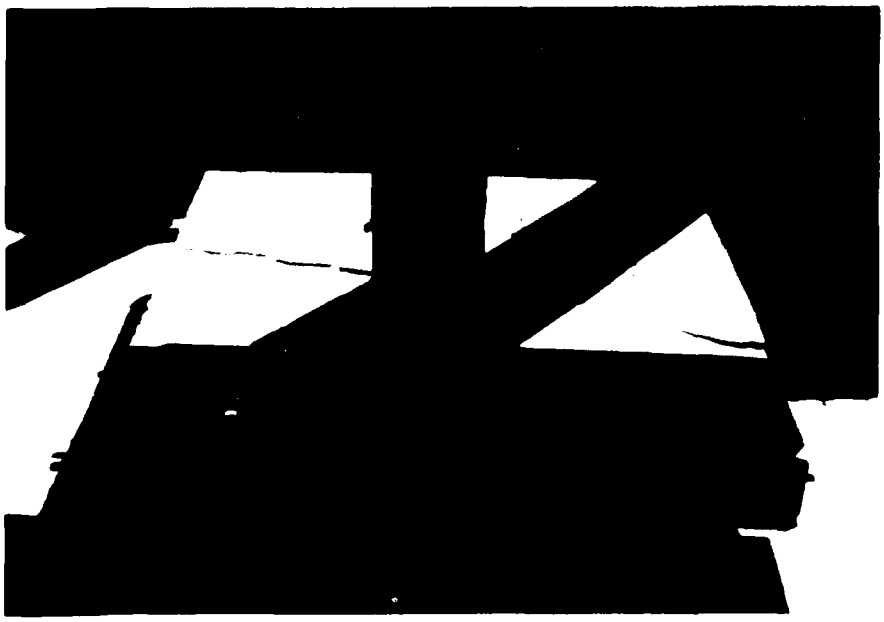

Test No. [illegible]

Fig. 5-7. Posttest Photographs, Tests Nos. 1 and [illegible].

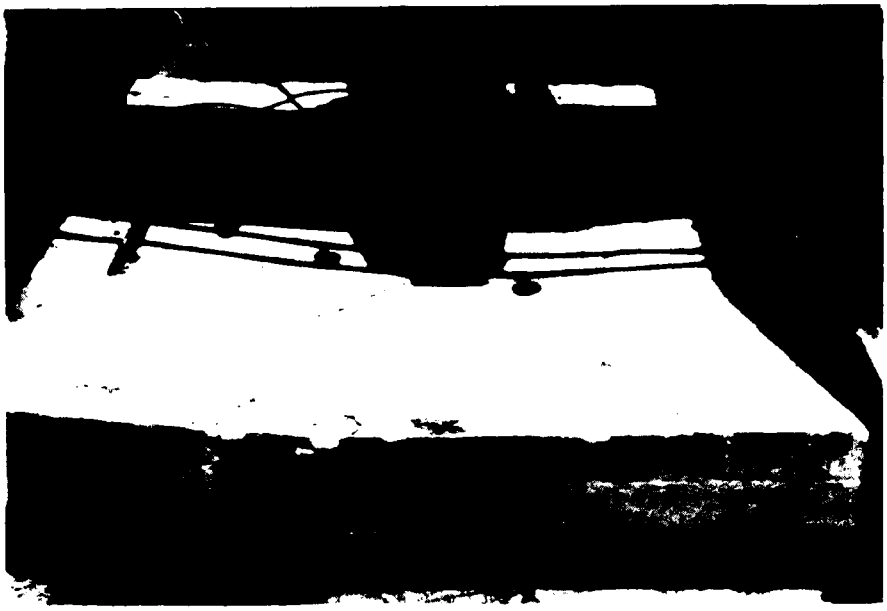

Test No. 3

Test No. 3

Fig. 5-6. Posttest Photographs, Test No. 3

Test No. 4

Test No. 6

Fig. 5-9. Posttest Photographs, Tests Nos. 4 and 6.

Test No. 7

Test No. 8

Fig. 5-10. Posttest Photographs, Tests Nos. 7 and 8.

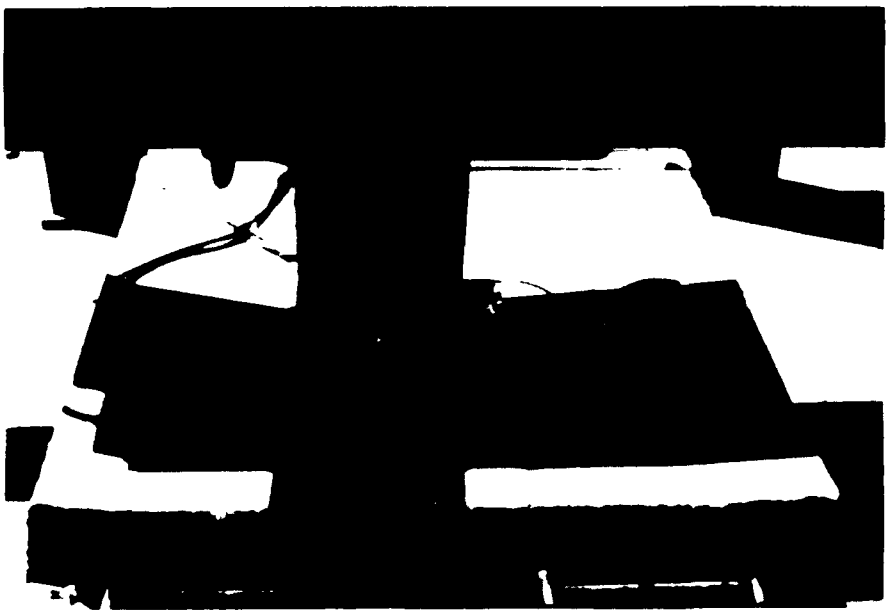

Test No. 9

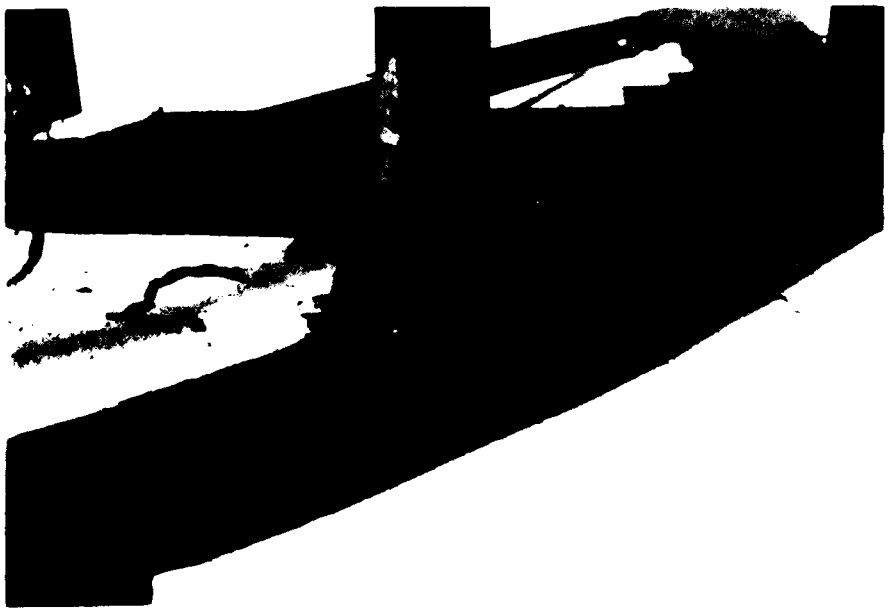

Test No. 10

Fig. 5-11. Posttest Photographs, Tests Nos. 9 and 10.

PREDICTION ANALYSIS

Slab Without Reinforcing and Slab With Top Reinforcing (Roof Slab Condition)

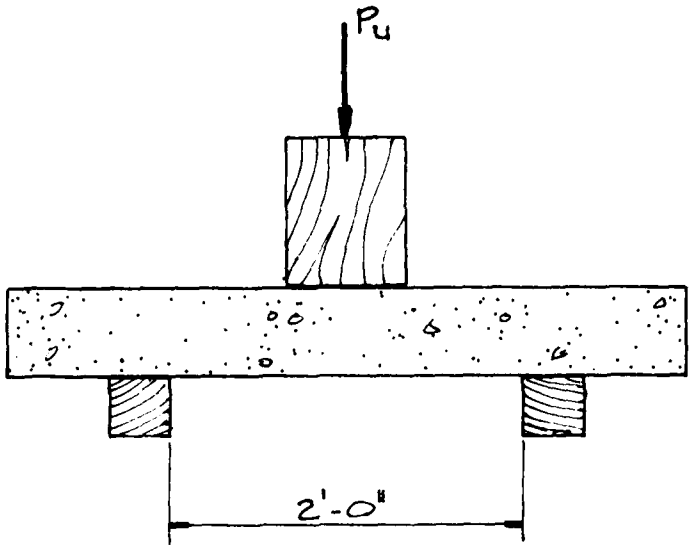

Strength prediction model: A low bound estimate of failure load, P_u, may be obtained by assuming that the slab spans as a simple beam over the 2-foot clear span of the 4-inch-by-4-inch support frame; then failure occurs when this simple beam moment, $P_u(1\ ft)/2$, creates tensile failure stress

$$f_t = 8\sqrt{f'_c} \simeq 500\ PSI$$

in the gross section of the 3-ft-10-inch-by-5.75-inch slab cross-section.

$$\text{SECTION MODULUS, } S = \frac{(46\ in.)(5.75\ in.)^2}{6} = 253\ in^3$$

$$M_u = (P_u/2)(1)(12) = S\,f_t = (253)(500)$$

$$P_u = 21\ KIPS$$

This simple beam assumption is considered here as reasonably applicable if it is recognized that the slab is not really uniformly supported by the

wooden support frame. It raises at its corners so as to rest on an equivalent two-support set of high spots on the uneven wood frame.

Another alternative method of modeling this slab and its support condition can be based on analysis of the slab by a simple yield-line procedure. The simple 45 degree diagonal yield line pattern actually results in an identical numerical solution.

This strength prediction was also employed for slabs with top reinforcing, since it was felt that tensile concrete failure would be the controlling mode. However, as can be seen in the summary table at the end of this section (Table 5-2), that is a lower bound prediction for this type of slab. Evidently, a type of dowel action and/or membrane effect is provided by the top reinforcing. This is an area that requires further investigation.

Reinforcing Steel At Face Away From Shore Support (Floor Slab Condition)

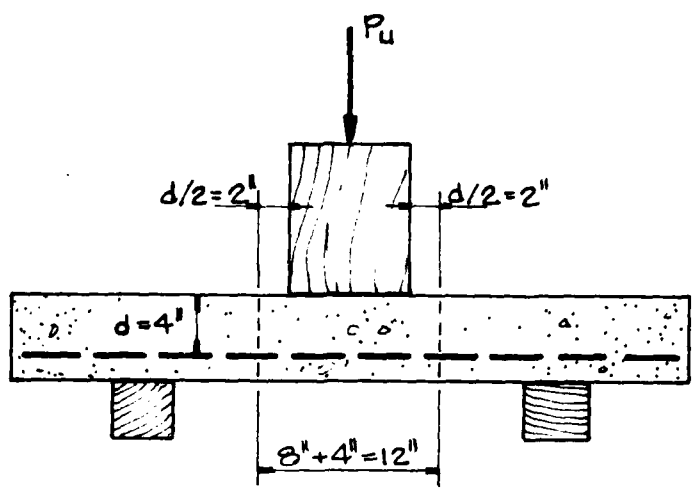

Predicted load, P_u, is based on v_u on perimeter $d/2$ from shore face, where,

$$v_u = 4\sqrt{f'_c} = 250 \text{ PSI}$$

$$P_u = 4(12)(4)(0.250) = 48 \text{ KIPS}$$

Shore Bearing Effect on Strength

Test No.	Description	FAILURE LOAD IN KIPS Steel Plate	Timber Post	Steel Plate / Timber Post
1, 6	No reinforcing steel	22.0	24.0	0.92
2, 7	One-way bottom	50.2	40.4	1.25
3, 8	One-way top	41.4	35.2	1.18
4, 9	Two-way bottom	78.5	60.4	1.30
5,10	Two-way top	43.2	32.8	1.32
11,14	Two-way bottom	85.9	78.5	1.10
12,15	Two-way bottom	75.1	72.4	1.04
13,16	Two-way bottom	88.9	78.0	1.14
	Average	83.2	76.5	1.10

In all but the non-reinforced slab, there is a significant 10% to 30% extra strength when the steel bearing pad is used. One reason for the lower capacity of the wood bearing (without plate) might be that slight "out-of-flat", or non-uniform, bearing of the wood causes a more concentrated punching effect — somewhat like that of a beveled end of a chisel.

SUMMARY

A summary of the slab strength predictions and the test results is presented in Table 5-2.

The use of the American Concrete Institute (ACI 318-77) equation for punching shear:

$$V_u = 4\sqrt{f'_c}$$

does not permit consideration of the following important factors related

TABLE 5-2: SUMMARY OF SLAB STRENGTH PREDICTIONS AND TEST RESULTS

Test No.	Description	Test (kips)	Prediction (kips)
1	Unreinforced	24	21.0
6	"	22	21.0
3	One-way top steel	35.2	21.0
8	"	41.4	21.0
5	Two-way top steel	32.8	21.0
10	"	43.2	21.0
2	One-way bottom steel	40.4	48.0
7	"	50.2	48.0
4	Two-way bottom steel	60.4	48.0
9	"	78.5	48.0
11	"	78.5	48.0
12	"	72.4	48.0
13	"	78.0	48.0
14	"	85.9	48.0
15	"	75.1	48.0
16	"	88.9	48.0

to actual punching shear capacity of slabs:

a) Intensity of bending moment, or M/V ratio.

b) Presence of arching action between load and slab supports.

c) Steel ratio.

A simple relation including all of the factors is definitely required in order to better predict the corresponding extra strengths or weaknesses. One such relation being developed is

V_u on perimeter $d/2$ out from face of shore is

$$V_u = 160 \left[f'_c \rho \left(\frac{2h}{c-r} \right) \right]^{1/3}$$

where c = support span

r = shore size

h = slab thickness.

This relation applied for long shear-span (large M/V) ratios of

$$\frac{2h}{c-r} \leq 0.4$$

For short spans where arching effects can occur between the shore and the slab support, then use

$$V_u = 160 \left[f'_c \rho \left(\frac{2h}{c-r} \right) \right]^{1/3} \frac{\left(\frac{2h}{c-r} \right)}{0.4}$$

to reflect the extra strength effect.

It should be mentioned that previous researchers have developed similar types of slab equations; however, these are quite complex and do not have the accuracy that would be merited by the complexity of the relation.

SLABS ON GRADE

Further work is required to assess the effects of soil modulus and strength on the punching capacity of shores bearing on foundation slabs. Since punching load produces a failure cone with bearing on the soil of about 50 ksf, it is not likely that soil strength could provide any significant support (soil capacities are 5 to 10 ksf). Therefore, the most important factor would be the soil modulus. It is proposed that several finite element slab analyses be performed for differing soil moduli and slab boundary conditions. The primary effect would be the variation in bending moment in the slab, where a low modulus would create the larger moment effects. Then with the appropriate punching shear equation, this moment effect can be entered into the strength prediction.

Section 6
SUMMARY OF PHASE III

This report presents a summary of the technical work performed during Phase III of a program to develop upgrading techniques for existing structures. This investigation has included the development of failure prediction methodologies for the most common construction types, in both "as built" and upgraded configurations. The prediction methodologies are founded on engineering mechanics, limit theory, and statistical approaches to failure analysis that enable realistic assessment to be made of failure probabilities based on the combined effects of statistical variation in materials, structural elements, and construction practices. These analysis and prediction techniques have been applied to wood, steel, and concrete roof and floor systems; both full- and small-scale verification tests, to failure, have been performed statically, dynamically, and in combination.

To date, Scientific Service, Inc., has conducted full-scale loading tests to failure on 16 wood joist floors, 3 one-way reinforced concrete floors, 15 prestressed concrete hollow-core slabs, and 3 open-web steel joist floors with metal decking and structural concrete topping. Each type of construction tested included a minimum of one base case test; that is, "as built" without any upgrading. The additional tests in each group incorporated various upgrading schemes appropriate to the construction type.

These full-scale tests have been complemented by a variety of small-scale tests that investigated punching shear of concrete floors and the contribution of the metal decking and structural concrete topping on open-web steel joist floors.

The results of the analytical and experimental program have been used to develop a preliminary survival matrix for floors, which is presented in Table 7-1. This matrix indicates the overpressure, in psi, at which 95% of the floor systems are better than the rating provided; i.e., it has been assumed that a 5% probability of collapse is an acceptable risk level. The test values obtained from the experimental program are indicated on the matrix. Also included is a preliminary survival matrix for roofs (Table 7-2). The roof matrix does not contain any test values.

The survival pressures indicated for the various types of construction were determined by assuming the dead loads (load of structure itself) and increasing the design live loads by the safety factors required for the design, as outlined in the applicable codes, for the particular construction considered.

Although the overpressure values indicated do not consider any superimposed live loads, it is assumed that some radiation protection would be required. Accordingly, the survival overpressures included the fallout radiation protection necessary to achieve a protection factor (P_f) of 100; i.e., 18 inches of earth (assumed density = 100 pcf) or other materials of comparable density. The weight of this radiation protection has been deducted from the survival overpressure when the floor or roof is in both the shored and the "as built" configurations. The test values (*italics)* have also been reduced for comparison purposes to include this radiation protection.

The basic construction type groups in Table 7-1 for floors are further divided into categories of light, medium, and heavy. These categories are based on the allowable live loads for types of occupancy, as specified in the building codes, and are defined as follows:

Light	40 to 60 psf
Medium	80 to 125 psf
Heavy	150 to 250 psf

The midspan, one-third span, and one-quarter span shoring may be lines of shoring, such as posts and beams or stud walls, placed transverse to one-way structural systems (open-web josts, double tees, etc.), or it may be post shores, located symmetrically under two-way structural systems (flat slabs, waffle slab, etc.). The king post truss shoring consists basically of cables or rods secured parallel to joists or beams and tensioned to form a king post truss configuration. The flange system consists of attaching bottom flanges to wood joists, while the boxed beam system involves "boxing" the entire ceiling system (wood joists) by attaching a plywood diaphragm, secured to the joists, under the entire ceiling.

The results of this Phase III effort have confirmed some of the survival estimates in Table 7-1 (which was first published in 1978) and have caused some modification to others. For example, the original estimates for concrete floors seem to be very close. The estimates for wood, however, will be reduced in the future. The reason for this is twofold: First, test data indicate that, as the heavier floor systems are shored, the mode of failure changes from flexure to much lower bearing failures. Second, as more and more published and unpublished data from graded sawn lumber are analyzed, it appears that the traditionally used dynamic increase of 100% for allowable stresses in timber will be more like 60% and the commonly used increase of 25% for seasoning should not be used at all. The changes in prediction for timber structures will be made when enough test data from the industry become available. The estimates for open-web joist floors, on the other hand, have been increased because of favorable test results and a revised prediction procedure that takes into account the contribution of the steel decking and concrete topping.

Section 7
PROGRAM SUMMARY

This section presents a compilation of significant portions of the technical work performed by Scientific Service, Inc., with respect to the program to develop upgrading techniques for existing structures. The data presented are a result of prediction methodologies founded on engineering mechanics, limit theory, and statistical approaches, and in many cases, verified by both small- and full-scale tests to failure. This summary includes charts and data from a number of SSI reports and manuals, which were developed as part of this program, as it was determined that this information should be compiled and presented in one location in order to increase its availability and usefulness.

Tables 7-1 and 7-2 are preliminary survival matrices for floors and roofs, respectively. (Table 7-1 was initially published in the Phase II report, Ref. 4, and updated in this Phase III report.) The data were developed as a result of the work and analysis presented in both these reports as well as in SSI Report No. 7719-4 (Ref. 3). These matrices indicate the overpressure in psi at which 95% of the floor of roof systems are predicted to survive "as built" and with various types of shoring. Those which have been tested are also indicated in the tables.

The survival pressures indicated for the various types of construction were determined by assuming the dead loads (load of structure itself) and increasing the design live loads by the safety factors required for the design, as outlined in the applicable codes, for the particular construction considered. The "as built" survival overpressure considers the floor "as is" with no superimposed live loads, but with all safety factors removed. However, all the survival overpressures assume radiation protection equal to a P_f of 100 (18 inches of earth of equivalent) superimposed on the floor.

Table 7-3 is a survival matrix for walls, which was determined by combining the data presented in SSI Report No. 7618-1 (Ref. 7). The survival pressures indicated are those at which 90% of the walls would survive. These values are based on both theoretical and experimental results.

Table 7-4 on expedient shelters was derived from combining the data presented in SSI reports No. 8012-7 (Ref 1) and No. 8012-8 (Ref.8). The values shown in this table are estimated by using the information supplied by various manufacturers in their literature and a review of some preliminary test data provided by them. None of the values indicated has been verified by test for use as expedient shelters.

Table 7-5, Punching Shear, is a reproduction of Table 5-1 presented previously in this report, and is included here in order to obtain completeness in this section. This table indicates values obtained by punching through 5-3/4-inch concrete slabs with two different types of posts (timber and steel). The slabs had various reinforcing steel configurations or were unreinforced.

TABLE 7-1: PRELIMINARY SURVIVAL MATRIX FOR FLOORS

Overpressure at Which 95% of Floors Will Survive "As Built" and With Various Types of Shoring
(All values in psi.)

Type of Floor Construction and Dead Load	As Built		Shoring Required											
			Midspan		1/3 Span		1/4 Span		King-Post Truss		Flange		Boxed Beam	
	Pred.	Test	Pred	Test	Pred	Test	Pred	Test	Pred	Test	Pred	Test	Pred	Test
WOOD D.L. = 20 psf														
Light — Joist, Glulam*	†	*0.4*	3.3	*6.8*	8.6	*9.2*	—		1.6	*1.8*	1.1	*1.1*	1.1	*2.1*
Medium — Joist, Glulam	0.9	*1.5*	6.7	*8.1*	16.4	*12.9*	—		3.8		2.8		2.8	
Heavy — Plank	2.6		13.7		32.1		—		8.2		—		—	
STEEL, LIGHT D.L. = 30 psf														
Light — Open-Web Joist	0.2	*0.3*	1.0	*1.2*	2.8	*3.5*	—		1.0		—		—	
Medium — Open-Web Joist	1.4	*1.6*	3.0	*3.4*	6.6	*8.0*	—		2.5		—		—	
STEEL, HEAVY D.L. = 80 psf														
Light — Beam and Slab	0.1		3.1		7.9		—		—		—		—	
Medium — Beam and Slab	0.8		5.5		13.3		—		—		—		—	
Heavy — Beam and Slab	2.0		10.3		24.0		—							

Note: Overpressure values assume radiation protection equal to a P_f of 100 (18 in. of earth or equivalent) superimposed on floor. Assumed density of earth = 100 pcf.

* Glulam not tested. † — Required radiation protection ($P_f = 100$) would cause floor to collapse.

TABLE 7-1: PRELIMINARY SURVIVAL MATRIX FOR FLOORS (contd)

Overpressure at Which 95% of Floors Will Survive "As Built" and With Various Types of Shoring
(All values in psi.)

Type of Floor Construction and Dead Load	As Built		Shoring Required											
			Midspan		1/3 Span		1/4 Span		King-Post Truss		Flange		Boxed Beam	
	Pred.	Test	Pred	Test	Pred	Test	Pred	Test	Pred	Test	Pred	Test	Pred	Test
CONCRETE D.L. = 100 psf														
Light – Single and Double Tees, One-Way Joists	0.6		4.7		11.7		–		–		–		–	
Light – Hollow-Core Slabs	0.6	*0.6*	4.8	*6.2*	11.7	*16.1*	–		–		–		–	
Light – One-Way Solid Slabs	0.9		5.0		12.0		–		–		–		–	
Light – Flat Slab, Flat Plate - Two-Way	0.9		5.0		12.0		21.7		–		–		–	
Light – Waffle Slab	0.6		4.7		11.7		21.4		–		–		–	
Medium – Single and Double Tees, One-Way Joists	1.3		7.6		18.0		–		–		–		–	
Medium – Hollow-Core Slabs	1.5	*2.2*	7.8	*10.2*	18.2	*19.8*	–		–		–		–	
Medium – One-Way Solid Slabs	1.7		8.0		18.4		–		–		–		–	
Medium – Flat Slab, Flat Plate - Two-Way	1.7		8.0		18.4		33.0		–		–		–	
Medium – Waffle Slab	1.3		7.6		18.0		32.6	*43.0**	–		–		–	

Note: Overpressure values assume radiation protection equal to a P_f of 100 (18 in. of earth or equivalent) superimposed on floor. Assumed density of earth = 100 pcf.

* Waterways Experiment Station Test

TABLE 7-1: PRELIMINARY SURVIVAL MATRIX FOR FLOORS (contd)

Overpressure at Which 95% of Floors Will Survive "As Built" and With Various Types of Shoring
(All values in psi.)

Type of Floor Construction and Dead Load	Shoring Required													
	As Built		Midspan		1/3 Span		1/4 Span		King-Post Truss		Flange		Boxed Beam	
	Pred.	Test	Pred	Test	Pred	Test	Pred	Test	Pred	Test	Pred	Test	Pred	Test
CONCRETE D. L = 100 psf														
Heavy — Single and Double Tees, One-Way Joists	2.8		13.2		30.6		—		—		—		—	
Heavy — Hollow-Core Slabs	3.0	*5.3*	13.4	*19.9*	30.8	*30.1*	—		—		—		—	
Heavy — One-Way Solid Slabs	3.3	*5.9*	13.7	*17.7*	31.1	*36.2*	—		—		—		—	
Heavy — Flat Slab, Flat Plate - Two-Way	3.3		13.7		31.1		55.4		—		—		—	
Heavy — Waffle Slab	2.8		13.2		30.6		54.9		—		—		—	

Note: Overpressure values assume radiation protection equal to a P_f of 100 (18 in. of earth or equivalent) superimposed on floor. Assumed density of earth = 100 pcf.

TABLE 7-2: PRELIMINARY SURVIVAL MATRIX FOR ROOFS

Overpressure at Which 95% of Roofs Will Survive
"As Built" and With Various Types of Shoring. All values in psi.

Type of Roof Construction and Dead Load	As Built	Shoring Required		
		Midspan	1/3 Span	1/4 Span
WOOD D.L. = 15 psf				
Joist, Glulam	†	0.6	2.7	–
STEEL, LIGHT D.L. = 25 psf				
Open-Web Joist, Plywood Deck	†	†	0.2	–
STEEL, HEAVY D.L. = 60 psf				
Open-Web Joist, Metal Deck	†	†	0.8	–
CONCRETE D.L. = 80 psf				
Single & Double Tees, One-Way Joists	0.0	2.2	6.0	–
Hollow-Core Slabs	0.0	2.3	6.1	–
One-Way Slabs	0.2	2.5	6.4	–
Flat Plate & Flat Slabs	0.2	2.5	6.4	11.7
Waffle Slabs	0.0	2.2	6.0	11.4

Note: Overpressure values assume radiation protection equal to a P_f of 100 (18 in. of earth or equivalent) superimposed on roof. Assumed density of earth = 100 pcf.

All values are predicted values.

† – Required radiation protection (P_f = 100) would cause roof to collapse.

TABLE 7-3: SURVIVAL PRESSURE MATRIX FOR WALLS

Incident Overpressures at which 90% of Walls Will Survive (all tabulated values are in psi)

Wall Material and Thickness / Support Condition	Brick			Concrete Block	Composite Concrete Block/ Brick
	4-in.	8-in.	12-in.	8-in.	10-in.
Solid Walls					
SIMPLE BEAM	0.1	0.4	1.0	0.1	0.7
FIXED BEAM	0.2	0.7	1.4	0.2	1.0
ARCHED BEAM	0.8	4.3	7.7	2.6	3.7
ARCHED BEAM W/GAP	0.2	1.1	1.9	0.6	0.9
Window Walls					
SIMPLE BEAM	0.2	0.8	1.9	0.4	1.3
FIXED BEAM	0.4	1.3	2.9	0.5	2.0
ARCHED BEAM	0.8	5.3	9.8	3.2	4.5
ARCHED BEAM W/ GAP	0.3	0.6	2.5	0.8	1.3

TABLE 7-3: SURVIVAL PRESSURE MATRIX FOR WALLS (contd)

Incident Overpressures at which 90% of Walls Will Survive (all tabulated values are in psi)

Wall Material and Thickness / Support Conditions	Brick			Concrete Block	Composite Concrete Block/ Brick
	4-in.	8-in.	12-in.	8-in.	10-in.
Doorway Walls					
SIMPLE BEAM	0.2	0.7	1.5	0.3	1.0
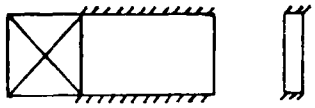 FIXED BEAM	0.3	0.4	2.3	0.5	1.6
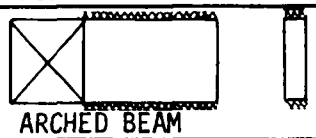 ARCHED BEAM	1.5	7.7	14.0	4.6	6.7
ARCHED BEAM W/GAP	0.4	2.0	3.5	1.2	1.7

TABLE 7-3: SURVIVAL PRESSURE MATRIX FOR WALLS (contd)

Incident Overpressures at which 90% of Walls Will Survive (all tabulated values are in psi)

Wall Material and Thickness / Support Conditions	Brick			Concrete Block	Composite Concrete Block/ Brick
	4-in.	8-in.	12-in.	8-in.	10-in.
PLATES					
Solid Walls					
SIMPLE PLATE 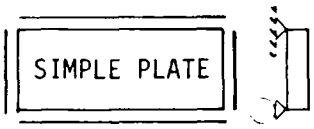	0.2	0.7	1.6	0.3	1.1
FIXED PLATE 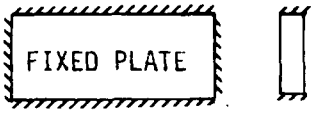	0.4	1.5	3.4	0.6	2.3
ARCHED PLATE	1.5	7.7	13.3	2.6	3.7
Window Walls					
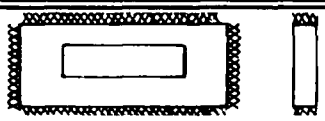 ARCHED PLATE	1.8	9.3	17.1	3.2	4.5
Doorway Walls					
ARCHED PLATE	1.8	9.2	16.8	4.6	6.7

TABLE 7-4: EXPEDIENT SHELTER SURVIVAL MATRIX
ALL VALUES IN PSI

SHELTER OPTION DESCRIPTION	OVERPRESSURE RESISTANCE (ESTIMATED VALUES-NOT VERIFIED BY TEST)			
	UNBURIED	BURIED	SHORED & BURIED	LIMITATIONS AND DESCRIPTION
TANKS				
Pressure Vessels	-	>40	(a)	New tanks only.
Fiberglas (CEMO MK II)	-	>40	(a)	Tested to 50 psi under laboratory conditions.
Fiberglas Fuel Tanks	1±	3 to 5	(b)>5	Information based on one manufacturer's specifications.
Steel Fuel Tanks	>1	>5	(b)	Overpressure resistance is a function of shell thickness.
RAILCARS				
Tank Cars	-	>40	(b)	Tank cars have limited availability due to high demand.
Hopper Cars (closed)	-	>40	(b)	False floors must be constructed over hopper bottoms. It is estimated that over 3,000 are available annually.
Hopper Cars (open)	-	>40	(b)(c)	Cars are buried upside down and thus an earth floor may be used. It is estimated that over 6,000 are available annually.
Gondolas	-	>40	(b)(c)	Cars are buried upside down and an earth floor may be used. It is estimated that over 3,000 are available on an annual basis.
Refrigerator & Box Cars	1 to 2	2 to 4	(b) >4	Based on obtaining steel car bodies. It is estimated that over 10,000 are available annually.

TABLE 7-4: EXPEDIENT SHELTER SURVIVAL MATRIX
ALL VALUES IN PSI (contd)

SHELTER OPTION DESCRIPTION	OVERPRESSURE RESISTANCE (ESTIMATED VALUES-NOT VERIFIED BY TEST)			
	UNBURIED	BURIED	SHORED & BURIED	LIMITATIONS AND DESCRIPTION
RAILCARS (contd)				
Caboose & Passenger Cars	0.25 to 0.5	1 to 2	(b)(d)>3	Fewer than 400 available on an annual basis.
STORM DRAIN SYSTEMS				
Large Pipes & Box Culverts	-	>40	(a)	Limited to arid climates in most instances. Extensive closures required to prevent longitudinal blast effects. Temporary raised floors may be constructed in culverts with low flow volumes.
Storm Manholes	-	>40	(a)	Manholes are available on nearly every storm drainage system and they are not limited to major box culverts. False floors are easily constructed and they provide easy access to major culverts.
OTHER OPTIONS				
Concrete Utility Vaults	-	>40	(b)	Unshored vaults may be implemented for host area locations. Upgrading of some components for closures is necessary.
Maritime Shipping Containers	0.5 to 1.7	1.0 to 3.4	(e)>4	Overpressure resistance values shown are for top and side walls only. These values do not reflect the additional resistance of frame members, or floors rated at approximately 26 psi. Containers are available at nearly every major port facility and from manufacturers.

TABLE 7-4: EXPEDIENT SHELTER SURVIVAL MATRIX
ALL VALUES IN PSI (contd)

SHELTER OPTION DESCRIPTION	OVERPRESSURE RESISTANCE (ESTIMATED VALUES-NOT VERIFIED BY TEST)			
	UNBURIED	BURIED	SHORED & BURIED	LIMITATIONS AND DESCRIPTION
OTHER OPTIONS (contd)				
Truck Van Bodies	≈1	≈2	(b)(f)	Truck van bodies are constructed without stiff frame members above floor level.

KEY:

(a) Shoring not required.

(b) Shoring methods have not been developed, upper limit of overpressure resistance to be investigated.

(c) False floors may be constructed in lieu of earth floor with upside-down burial.

(d) Caboose and passenger cars have significant areas of glass that require closures.

(e) Preliminary design analysis indicates post and beam shores at 30 inches on center may be used up to 4 psi overpressures.

(f) Preliminary design analysis indicates post and beam shores may be used. Shore spacing and upgrading potential will depend upon manufacturer and method of construction.

TABLE 7-5: PUNCHING SHEAR TESTS

Test No.	Load Type	Slab Description	Failure Load (lb)
1	8" x 8" timber	Unreinforced	24,000
2	"	One-way slab bottom steel	40,400
3	"	One-way slab top steel	35,200
4	"	Two-way slab bottom steel	60,400
5	"	Two-way slab top steel	32,800
6	8" x 8" steel plate	Unreinforced	22,000
7	"	One-way slab bottom steel	50,200
8	"	One-way slab top steel	41,450
9	"	Two-way slab bottom steel	78,520
10	"	Two-way slab top steel	43,200
11	8" x 8" timber	Two-way slab bottom steel	78,500
12	"	Two-way slab bottom steel	72,400
13	"	Two-way slab bottom steel	78,000
14	8" x 8" steel plate	Two-way slab bottom steel	85,900
15	"	Two-way slab bottom steel	75,100
16	"	Two-way slab bottom steel	88,880

Section 8

REFERENCES

1. Tansley, R.S. and R.D. Bernard, Shelter Upgrading Manual: Key Worker Shelters, SSI Report No. 8012-7, May 1981.

2. Wilton,C., B.L. Gabrielsen, and R.S. Tansley, Shelter Upgrading Manual: Host Area Shelters, SSI Report No. 7815-8, March 1980.

3. Gabrielsen, B.L., G. Cuzner, R. Lindskog, Blast Upgrading of Existing Structures, SSI Report No. 7719-4, January 1979.

4. Gabrielsen, B.L., R.S. Tansley, and G. Cuzner, Upgrading of Existing Structures Phase II, SSI Report No. 7910-5, June 1980.

5. Uniform Building Code, 1976 Edition, International Conference of Building Officials, Whittier California, 1976.

6. Building Code Requirements for Reinforced Concrete (ACI 318-71), American Concrete Institute, Detroit, Michigan.

7. Wilton, C., K. Kaplan, and B.L. Gabrielsen, The Shock Tunnel: History and Results, (five volumes), SSI Report No 7618-1, March 1978.

8. Revisions and additions to SSI Report No. 7815-8, Shelter Upgrading Manual: Host Area Shelters, SSI Report No. 8012-8, May 1981.

Appendix A

Open-Web Steel Joist Floor Test Failure Prediction

OPEN-WEB STEEL JOIST FLOOR TEST FAILURE PREDICTION

In Phase I of this program (Ref. 1), a 20-foot long 18H8 open-web joist was analyzed to determine upgrading techniques for this type of structure. This preliminary analysis indicated that shoring was the best means, but the analysis also indicated that, if a rigid shore were used, the lower chord of the open-web joist would go into compression and fail prematurely because of buckling. Thus, the concept of stress control was utilized, where an intentional gap was left on top of the shore to ensure that the lower chord would remain in tension until ultimate failure occurred.

On the basis of the preliminary analysis, a testing program was conducted to determine experimentally the increased load-carrying capacity of shored floor systems vs unshored systems. Three full-scale tests to failure on open-web joists were conducted, and the results are listed in Section 2, Table 2-2. The preliminary analysis underestimated the ultimate failure load by 32% to 53% for the shored and unshored floors tested.

This section of the report is directed toward improving the failure prediction by developing a finite element model that can analytically duplicate the structural load-deflection response of the actual test floors and can accurately predict the ultimate failure load for these floors. Having an accurate computer model will permit inexpensive analyses to be performed instead of tests.

COMPUTER MODEL

A computer model was used to develop an analytical method for failure prediction. Control Data Corporation's MRI version of STARDYNE was the computer code used for this structural analysis.

Preliminary analysis conducted prior to testing (see Refs. 1 and 2) modeled only the open-web joist behavior and neglected the concrete topping and fluted metal deck contribution. Additonally, the previous analysis assumed idealized truss behavior, which did not account for any secondary effects that were due to joint rotations in the open-web joist or the fixity of the members (effective length, $K\ell$). Both of these original simplifications resulted in a more flexible and weaker model than actual test data now indicate.

The analytical model developed in this phase of the study accounts for both secondary effects and the portion of composite behavior that was developed between the top chord of the 18H8 open-web joist and the decking.

To determine the structural effectiveness of the concrete topping, the load vs deflection data for base case Test No. 80-1 was used (see Figure A-1). The analytical model was then analyzed using STARDYNE. The concrete thickness was varied until the computer model deflection equaled that of the test floor under the same applied load.

BASE CASE PREDICTION

To predict the ultimate failure load for the simply supported unshored floor, a uniform load was introduced into the computer model. This uniform load was increased analytically until one member (web member 22)*

* Note, the buckling stress for the web member(s) is based on an effective length of 0.79ℓ, which was analytically and experimentally verified.

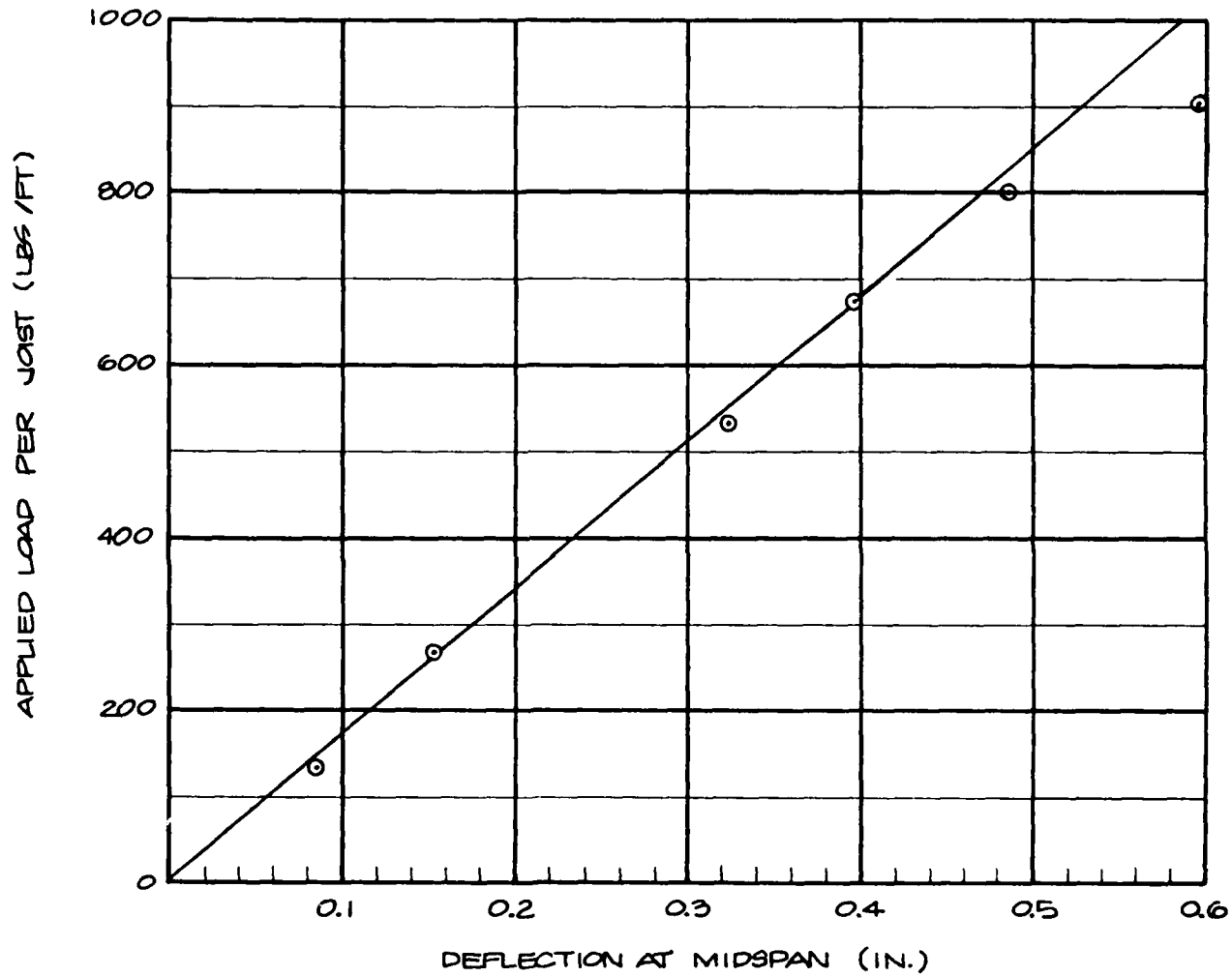

Fig. A-1. Load vs Deflection, Test No. 80-1.

in this case) reached its ultimate stress. Web member 22 was the first structural member to indicate failure at an ultimate buckling stress of 30.3 kips/in., or at a load of 1,070 plf/joist. Figure A-2 shows the computer predicted axial stresses in the web members at the predicted load of 1,070 plf/joist, which compares well with Test No. 80-1 (1,160 plf). This comparison shows that the computer model predicts the failure load at 92% of the actual failure load.

DOUBLE SHORED FAILURE PREDICTION

The computer model of the floor, developed earlier in this section, was used to predict failure for the double shored floor tests.

Shoring, especially by the method used in these tests, complicates the prediction analysis because of the stress control gap over the shores. The actual floor system deflects like an unshored floor until there is a load of about 600 plf/joist and the floor comes in contact with the shore and seats itself. Subsequent increases in load will result in a change of slope (stiffer) in the load deflection curve. Figure A-3 shows this relationship.

Failure prediction was an iterative process using the method of superposition and is outlined in the following steps:

1. Assume a load.

2. Determine the deflection of the actual floor in Test No. 79-2 at a location over the shore using Figure A-3.

3. Determine the deflection of the unshored floor under the assumed load at the same location.

4. Apply an upward unit load at the two shore locations and determine the resulting deflection.

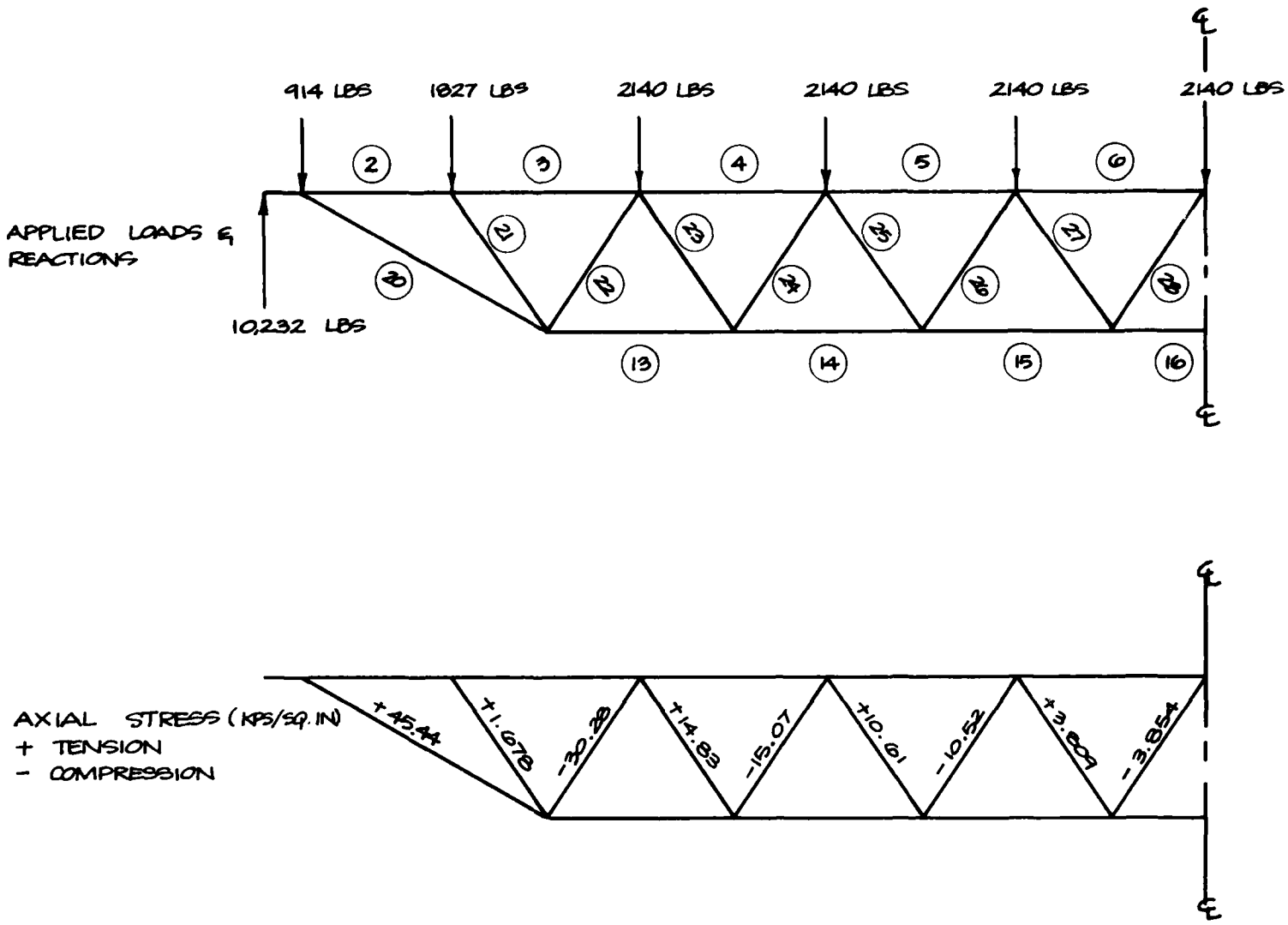

Fig. A-2. Computer Model Analysis Results of 18H8, Open-Web Steel Joist (Failure Load, w_u = 1,070 plf/joist).

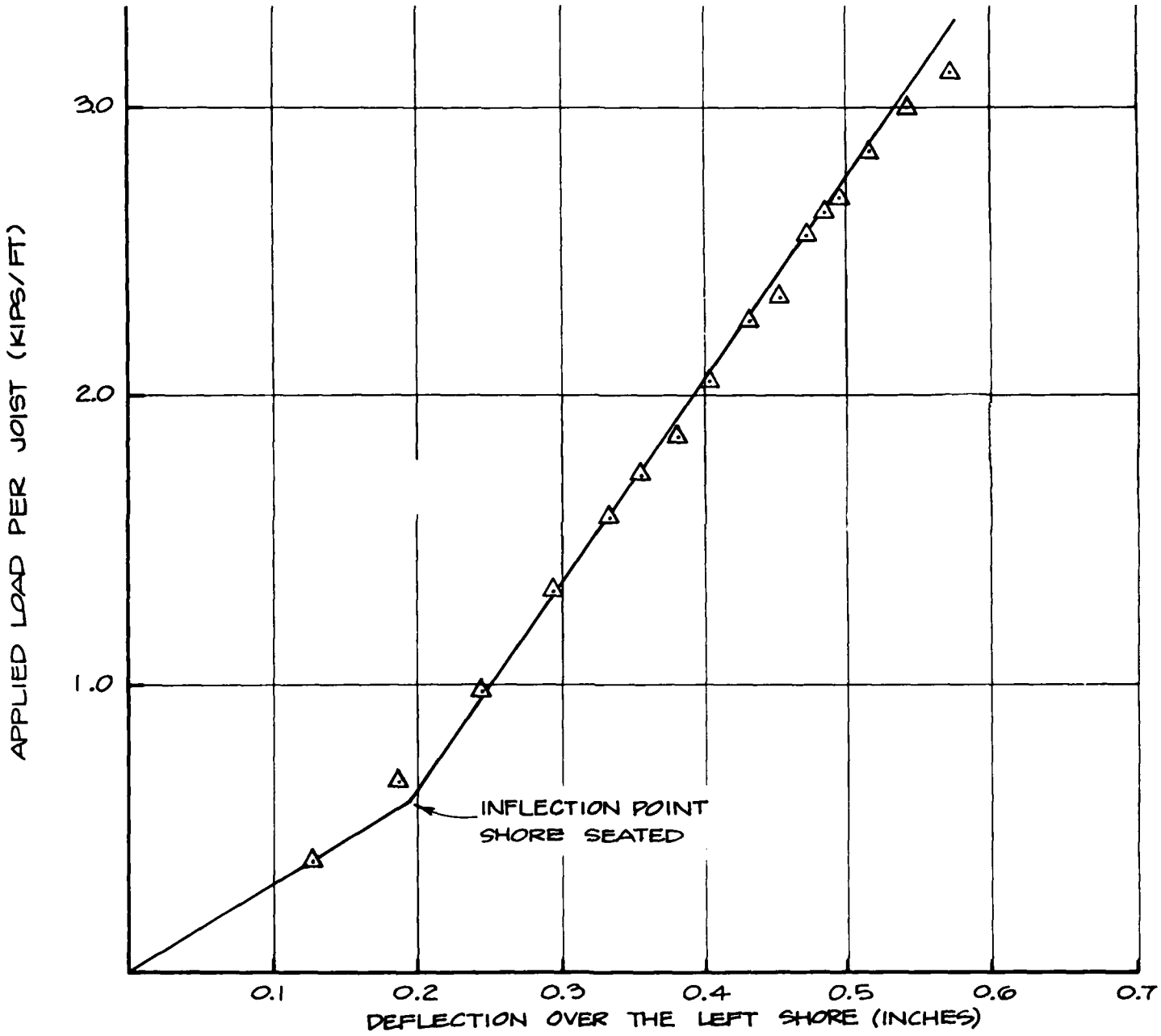

Fig. A-3. Load vs Deflection, Test No. 79-2.

5. Using superposition, increase the upward load until the sum of deflections in steps 3 and 4 equal the actual deflection determined in step 2.

6. Compute the member stresses.

7. Check the member stresses found in step 6 and determine if any member exceeds ultimate stress. If not, assume a larger load, step 1, and proceed as before.

Failure is predicted at a load of 3,300 plf/joist. Floor Test No. 79-2 failed in one or both of the following modes:

1) The left shore failed due to combined bearing and shear failure in the wood beam supporting the floor.

2) The top chord failed in flexure as a result of web member 20 yielding in tension leading to a redistribution of the load.

The analysis indicates a tensile stress of 60,000 psi in web member 20 at failure, exceeding the yield stress of 50,000 psi, but less than the ultimate stress of 76,000 psi.

In Figure A-4 the predicted axial stress for each of the web members is shown. The analysis predicts failure at 3,300 plf; in Test No. 79-2 the failure load was 3,920 plf; the prediction is 84% of the test value.

SINGLE SHORED FAILURE PREDICTION

The same method used to predict ultimate failure load for the double shored open-web joist floors was used to predict failure for the single shored floors. The load vs deflection data from Test No. 79-3 (see Figure A-5) was used to determine the shoring reaction.

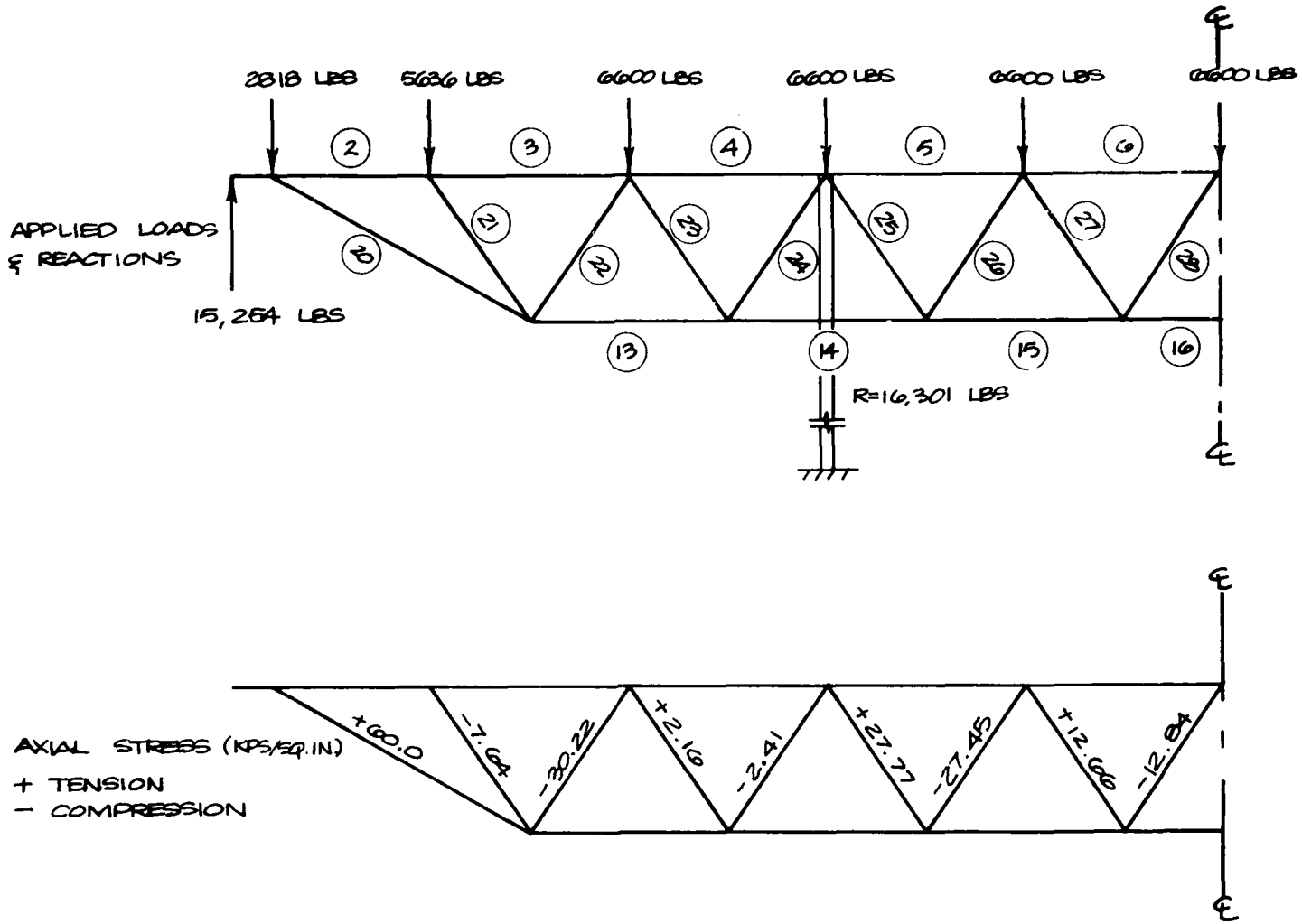

Fig. A-4. Computer Model Analysis Results for a Double Shored, 18H8 Open-Web Steel Joist. (Ultimate Failure Load, w_u = 3,300 plf/joist).

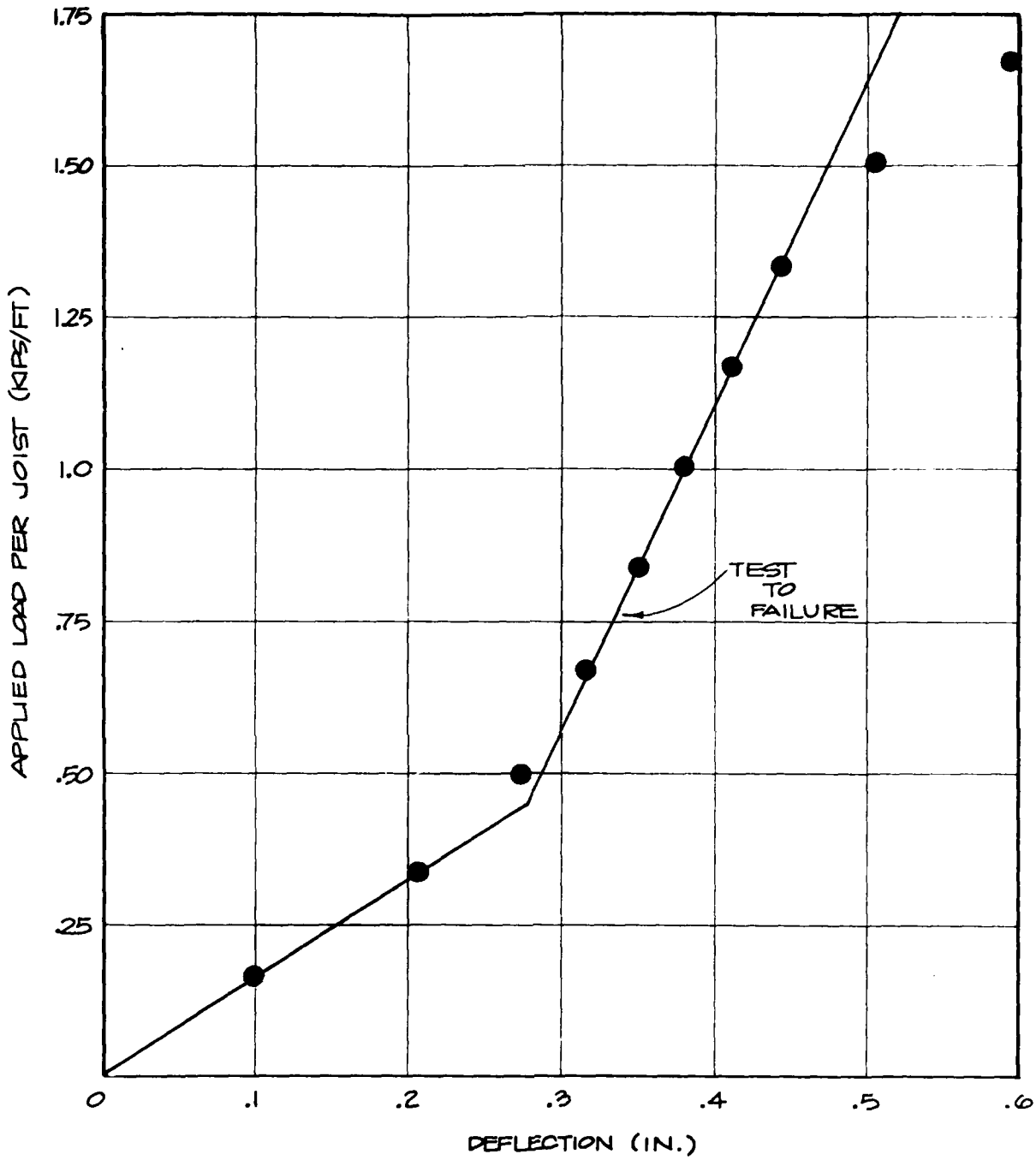

Fig. A-5. Load vs Deflection, Test No. 79-3.

The prediction indicates a floor failure at 1,750 plf/joist. Analysis predicts web members 22 and 20 to be critical. Figure A-6 shows the predicted axial stresses for the web members. Web member 22 is at the calculated ultimate buckling stress and web member 20 is at the calculated maximum yield stress in tension.

The prediction of 1,750 plf was 9% below the actual failure load of 1,928 plf.

CONCLUSIONS AND RECOMMENDATIONS

The computer model analysis closely predicted open-web joist floor behavior and provided a reasonable prediction of ultimate load capacity. This type of analysis capability provides a means of studying the effects that varying stress control gaps and shoring methods have on the ultimate load carrying capacity of open-web joist structures. On the tests performed to date, the stress control gaps were selected on the basis of the following criteria:

1) Single shore, at midspan; 1/16-inch of gap per 5 feet of span.

2) Double shored, at one-third points; use three-quarter the gap in step 1.

For example, a 20-foot span would have a 1/4-inch gap for the single shored condition and a 3/16-inch gap for the double shored floors.

Thus far, only wood shoring has been used to upgrade open-web joist floor systems. One of the inherent problems and virtues with using wood has been bearing failures in the wood which cause additional deflection.

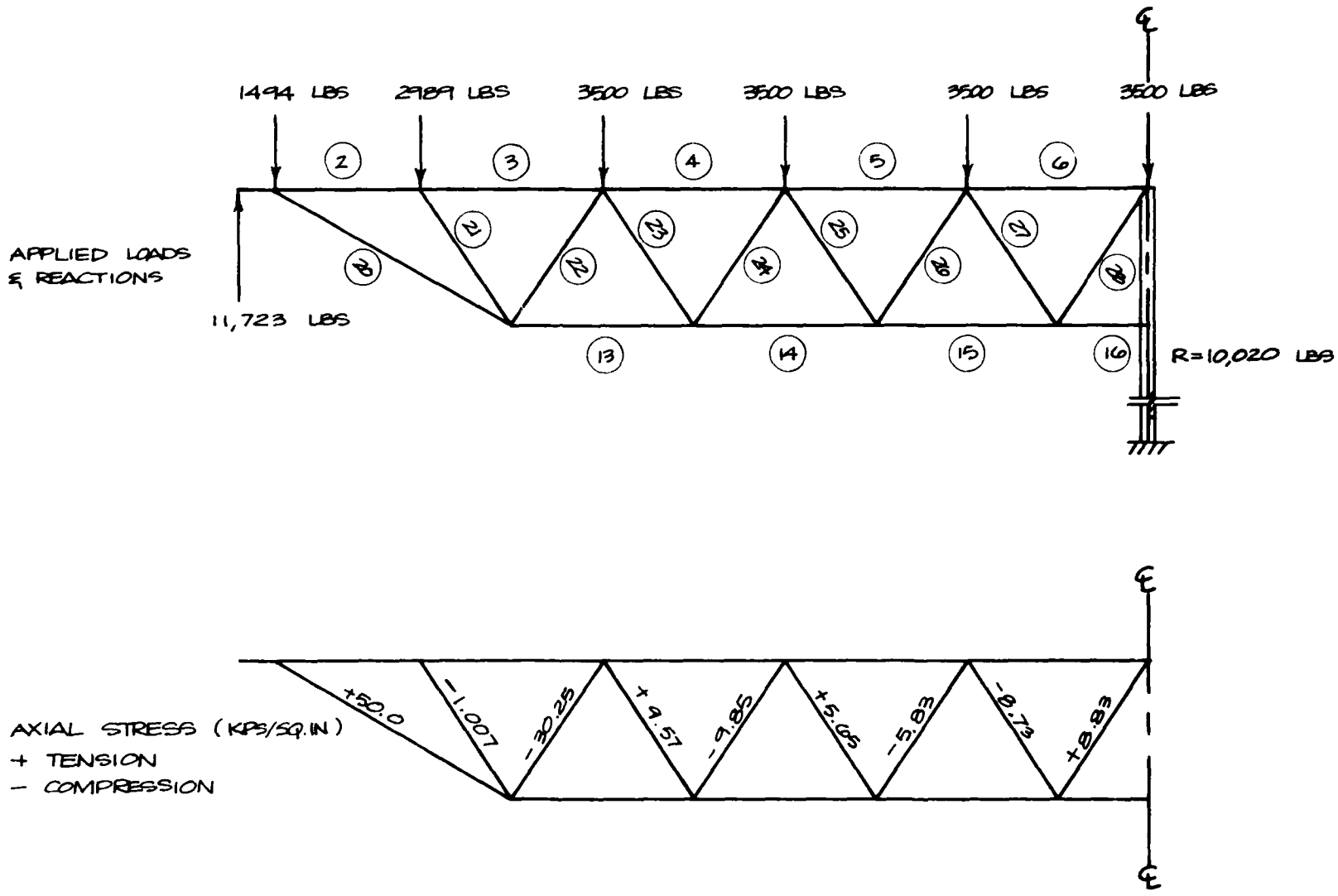

Fig. A-6. Computer Model Analysis Results for a Single Shored, 18H8 Open-Web Steel Joist. (Ultimate Failure Load, w_u = 1,750 plf/joist).

It is, therefore, recommended that total deflection be limited in some future tests to the recommended stress control gap. This could be achieved through the use of a more rigid steel shore, rather than wood.

Table A-1 summarizes the tests and predictions conducted to date for a typical floor system designed for an allowable live load of 125 psf (i.e. a floor in the medium load category).

REFERENCES

1. Gabrielsen, B.L., G. Cuzner, R. Lindskog, Blast Upgrading of Existing Structures, SSI Report No. 7719-4, January 1979.

2. Gabrielsen, B.L., R.S. Tansley, and G. Cuzner, Upgrading of Existing Structures Phase II, SSI Report No. 7910-5, June 1980.

TABLE A-1: REVISED PERFORMANCE PREDICTIONS COMPARED WITH TEST DATA

Open-Web Joist, H-Series, 18H8, 20-ft Span, Spaced 3 ft on Center, Simply Supported

Test No.	Type of Shoring	Tested Ultimate Failure Load		Predicted Ultimate Failure Load	
		(plf/Joist)*	(psi)**	(plf/Joist)*	(psi)**
80-1	None — Base Case	1,160	2.4	1,070	2.2
79-3	Shore at center with 1/4-in. gap	1,928	4.2	1,750	3.8
79-2	Shores at third points with 0.11-in. gap	3,920	8.8	3,300	7.4

* Includes dead load of floor.

** Determined using a joist spacing of 3 ft on center (2 ft on center tested). Floor dead load effects have been subtracted out.

APPENDIX B

Prestressed Concrete

PRESTRESSED CONCRETE

INTRODUCTION

This section of the report contains the calculations used to determine the design ultimate load capacity of each of the precast prestressed slabs tested and reported in Section 3. Also included is a description of the different modes of failure exhibited by these test slabs and how each mode can be predicted in terms of the location in the slab span and the shear-to-moment ratio.

DESIGN OF TEST SLABS

The slabs were designed in accordance with ACI Standard 318-71 (Ref. 1). The design section properties, unit weights, concrete strengths, size, number, and location of strands, and design spans are shown for the 4-inch, 8-inch, and 10-inch-thick slabs in Figures B-1, B-2, and B-3. The prestressing strand used was uncoated, seven-wire, stress-relieved strand with properties as shown in the following chart:

Nominal Diameter of Strand (in.)	Nominal Steel Area of Strand A_{ps} (sq in.)	Breaking Strength of Strand (min. lb)	Ultimate Strength f_{pu} (psi)
1/4 (0.250)	0.036	9,000	250,000
3/8 (0.375)	0.085	23,000	270,000

The following calculations indicate the design methods used for each of the test slabs. The notation used is defined in Table B-1.

4" PRESTRESSED PRECAST HOLLOW-CORE PLANK

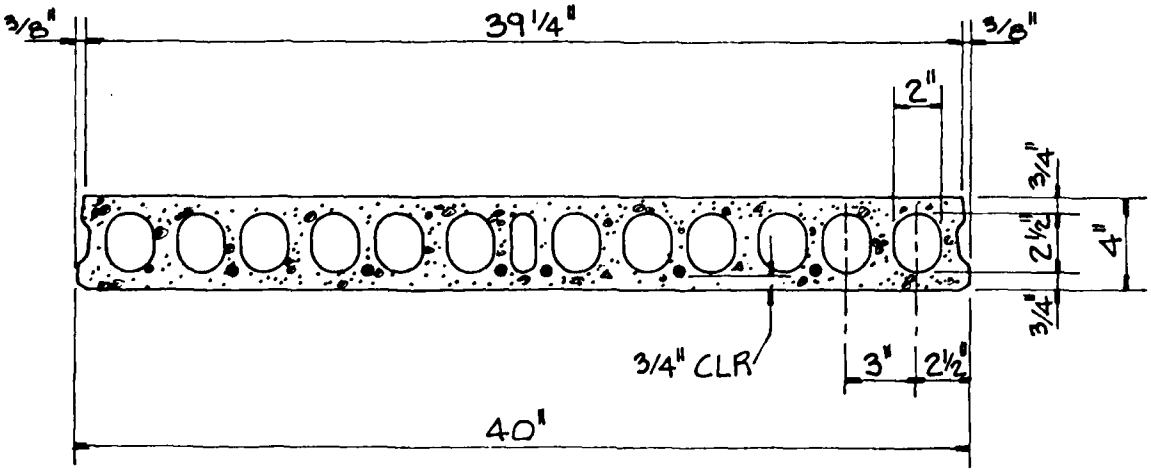

SECTION PROPERTIES

$A = 132 \text{ IN}^2$ $\qquad$ $I = 205 \text{ IN}^4$

$Y_T = 1.98 \text{ IN}$ $\qquad$ $Y_B = 2.02 \text{ IN}$

$S_T = 104 \text{ IN}^3$ $\qquad$ $S_B = 101 \text{ IN}^3$

DESIGN SPAN = 12ft 8in

f'c = 5000 PSI

WGT = 35 lbs/ft²

STRANDS = 6-1/4 in dia -250ᵏ

LIGHT DESIGN LOAD = 70 lbs/ft²

Fig. B-1. Design Properties of 4-inch Prestressed Precast Hollow-Core Plank.

8" PRESTRESSED PRECAST HOLLOW-CORE PLANK

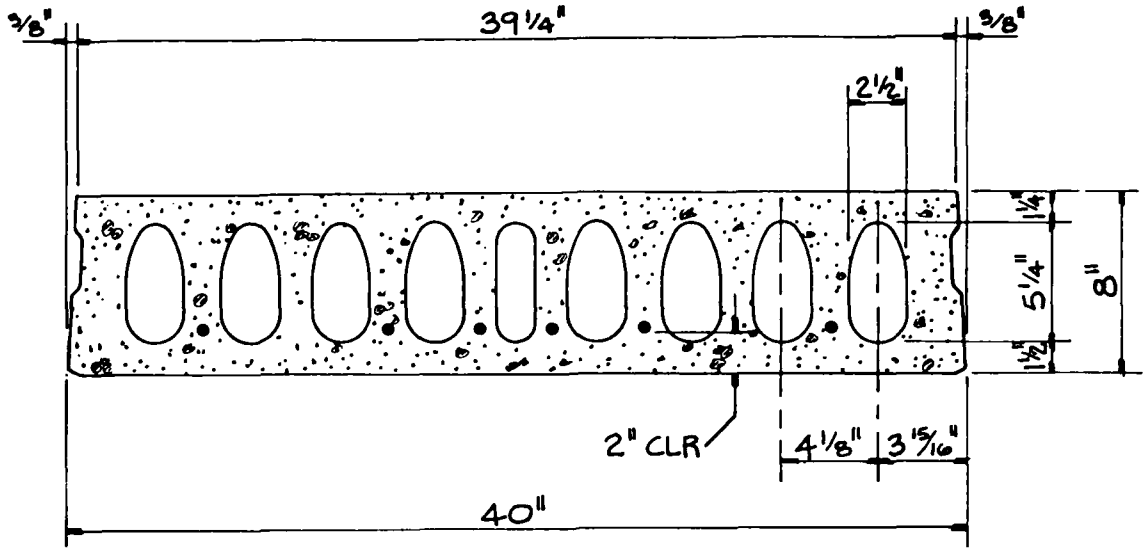

SECTION PROPERTIES

$A = 218\ IN^2$	$I = 1515\ IN^4$
$Y_T = 4.02\ IN$	$Y_B = 3.98\ IN$
$S_T = 377\ IN^3$	$S_B = 380\ IN^3$

DESIGN SPAN = 18 ft 0 in
f'c = 5000 PSI
WGT = 60 lbs/ft²
STRANDS = 6 - 3/8 in dia - 270K
MEDIUM DESIGN LOAD = 165 lbs/ft²

Fig B-2. Design Properties of 8-inch Prestressed Precast Hollow-Core Plank.

10" PRESTRESSED PRECAST HOLLOW-CORE PLANK

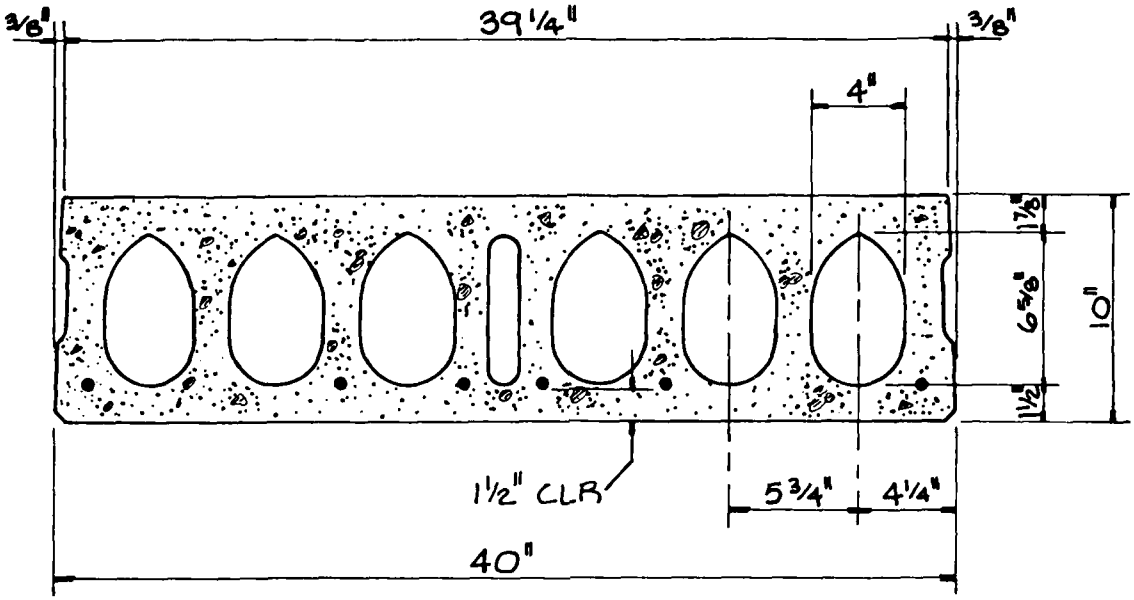

SECTION PROPERTIES

$A = 272\ IN^2$	$I = 2970\ IN^4$
$Y_T = 5.09\ IN$	$Y_B = 4.91\ IN$
$S_T = 585\ IN^3$	$S_B = 604\ IN^3$

DESIGN SPAN = 18 ft 0 in
f'c = 5000 PSI
WGT = 75 lbs/ft²
STRANDS = 6-3/8 in dia -270K
HEAVY DESIGN LOAD = 265 lbs/ft²

Fig. B-3. Design Properties of 10-inch Prestressed Precast Hollow-Core Plank.

TABLE B-1: NOTATION

A = cross sectional area

A_{ps} = area of prestressed reinforcement

a = depth of equivalent rectangular stress block

a_s = shear span

b = width of compression face of member

d = distance from extreme compression fiber to centroid of tension reinforcement

d' = distance from bottom fiber to centroid of reinforcement

e = eccentricity of design load or prestress force parallel to axis measured from the centroid of the section

f_b = stress in the bottom fiber of the cross section

f'_c = specified compressive strength of concrete

f_{ps} = stress in prestressed reinforcement at nominal strength

f_{pu} = ultimate strength of prestressing steel

f_{se} = effective stress in prestressing steel after losses

f_t = stress in top fiber of the cross section

h = overall depth of member

I = moment of inertia

j = for resisting lever arm used in jd

M = service load moment

M_{max} = maximum factored moment at section due to externally applied loads

M_p = prestressing moment

M_u = applied factored moment at a section

P = prestress force after losses

P_u = ultimate force in prestressing strands

S_b = section modulus with respect to the bottom fiber of a cross section

S_T = section modulus with respect to the top fiber of a cross section

u_F = flexural bond stress

u_t = transfer bond stress

V = total shear

V_d = dead load shear (unfactored)

V_i = factored shear force at section due to externally applied loads occurring simultaneously with M_{max}

V_p = vertical component of the effective prestress force at the section considered

V_u = factored shear force at section

v_u = factored shear stress

Y_b = distance from bottom fiber to center of gravity of the section

Y_t = distance from top fiber to center of gravity of the section

$\rho_p = A_{ps}/bd$ = ratio of prestressed reinforcement

Σ_o = perimeter of all effective steel

ϕ = strength reduction factor

4 IN. THICK SLAB

THE SECTION PROPERTIES USED IN THIS DESIGN ARE SHOWN IN FIG. B-1, SPAN = 12.67 FT.

DESIGN LOADS

OFFICE OCCUPANCY, 50 PSF LIVE LOAD PARTITIONS, 20 PSF DEAD LOAD.

MOMENTS

		$M^{K\text{-}IN}$	× L.F.	=	$M_u^{K\text{-}IN}$
4 IN. SLAB	$= 0.035 \times 3.33 \times \overline{12.67}^2 \times 1.5 =$	28.1	× 1.4	=	39.3
LIVE LOAD	$= 0.050 \times 3.33 \times \overline{12.67}^2 \times 1.5 =$	40.1	× 1.7	=	68.1
DEAD LOAD	$= 0.020 \times 3.33 \times \overline{12.67}^2 \times 1.5 =$	16.0	× 1.4	=	22.4
		$84.2^{K\text{-}IN}$			$129.8^{K\text{-}IN}$

PRESTRESSING FORCE REQUIRED

ASSUME 1/4 IN. DIAMETER STRAND WITH 3/4 IN. CLEAR BOTTOM COVER, THEREFORE

$$e = Y_b - 0.75 - 0.25/2 = 2.02 - 0.88 = 1.14 \text{ IN.}$$

$$f_b = 6\sqrt{f'_c} = 6\sqrt{5000} = 0.424 \text{ KSI}$$

$$P_{REQ} = \frac{\frac{M}{S_b} - f_b}{\frac{1}{A} + \frac{e}{S_b}} = \frac{\frac{84.2}{101} - 0.424}{\frac{1}{132} + \frac{1.14}{101}} = \frac{0.410}{0.0189} = 21.7^K$$

USING 1/4 IN. DIAMETER - 250^K STRANDS

$A_{ps} = 0.036 \quad P_u = 9$ K/STRAND

ASSUME 22% PRESTRESS LOSSES AND $f_{se} = 0.7\ f_{pu}$

$P = 9 \times 0.7 \times 0.78 = 4.9$ K/STRAND

STRAND REQ'D $= \frac{21.7}{4.9} = 4.4$

∴ USE 6-1/4 IN. DIAMETER - 250^K STRANDS = 29.4^K

$A_{ps} = 6 \times 0.036 = .216 \text{ IN}^2$

CHECK SERVICE LOAD STRESSES @ ℄ SPAN

(-) TENSION
(+) COMPRESSION

$$f_t = \frac{29.4}{132} - \frac{(29.4)(1.14)}{104} + \frac{84.2}{104} = +0.710 < 0.45\ f'_c = +2.250 \quad \underline{\text{O.K.}}$$

$$f_b = \frac{29.4}{132} + \frac{(29.4)(1.14)}{101} - \frac{84.2}{101} = -0.279 < 0.6\sqrt{f'_c} = -0.424 \quad \underline{\text{O.K.}}$$

CHECK ULTIMATE STRENGTH

$P_u = 6 \times 9^K = 54^K$, $d = 1.98 + 1.14 = 3.12$ IN.
$b = 40$ IN.

$$A_{ps} f_{ps} = P_u \left(1 - 0.5 \rho_p \frac{f_{pu}}{f'_c}\right), \quad \rho_p = \frac{A_{ps}}{bd}$$

$$A_{ps} f_{ps} = 54 \left(1 - 0.5 \frac{.216}{40 \times 3.12} \times \frac{250}{5}\right) = 51.7^K$$

$$a = \frac{A_{ps} f_{ps}}{0.85 f'_c b} = \frac{51.7}{(.085)(5)(40)} = 0.304 \text{ IN.}$$

$$M_{MAX} = \phi A_{ps} f_{ps} (d - a/2), \quad \phi = 0.9$$

$$M_{MAX} = 0.9 \times 51.7 \left(3.12 - \frac{0.304}{2}\right) = 138.1^{K\text{-}IN} > 129.8^{K\text{-}IN} \quad \underline{O.K.}$$

8 IN. THICK SLAB

THE SECTION PROPERTIES USED IN THIS DESIGN ARE SHOWN IN FIG. B-2. SPAN = 18.0 FT.

DESIGN LOADS

HEAVY MANUFACTURING, 125 PSF LIVE LOAD
PARTITIONS, 20 PSF DEAD LOAD
MECHANICAL, MISC., 20 PSF DEAD LOAD

MOMENTS

		$M^{K\text{-}IN}$	× L.F.	= $M_u^{K\text{-}IN}$
8 IN. SLAB	$= 0.060 \times 3.33 \times \overline{18.0}^2 \times 1.5 =$	97.1	× 1.4	= 135.9
LIVE LOAD	$= 0.125 \times 3.33 \times \overline{18.0}^2 \times 1.5 =$	202.3	× 1.7	= 343.9
DEAD LOAD	$= 0.040 \times 3.33 \times \overline{18.0}^2 \times 1.5 =$	64.7	× 1.4	= 90.6
		$364.1^{K\text{-}IN}$		$570.4^{K\text{-}IN}$

PRESTRESSING FORCE REQUIRED

ASSUME 3/8 IN. DIAMETER STRAND WITH 2 IN. CLEAR BOTTOM COVER, THEREFORE

$$e = Y_b - 2 - \frac{0.375}{2} = 3.98 - 2.19 = 1.79 \text{ IN.}$$

$$f_b = 6\sqrt{f'_c} = 6\sqrt{5000} = 0.424 \text{ KSI}$$

$$P_{REQ} = \frac{\frac{M}{S_b} - f_b}{\frac{1}{A} + \frac{e}{S_b}} = \frac{\frac{364.1}{380} - 0.424}{\frac{1}{218} \quad \frac{1.79}{380}} = \frac{0.534}{0.0093} = 57.4^K$$

USING 3/8 IN. DIAMETER - 270^K STRANDS

$A_{ps} = 0.085 \text{ IN}^2$ $\quad P_u = 23 \text{ K/STRAND}$

ASSUME 22% PRESTRESS LOSSES AND $f_{se} = 0.7 f_{pu}$

$P = 23 \times 0.7 \times 0.78 = 12.56^K/\text{STRAND}$

STRAND REQ'D $\frac{57.4}{12.56} = 4.6$

$\therefore$ USE 6-3/8 IN. DIAMETER - 270^K STRANDS $= 75.4^K$

$A_{ps} = 6 \times 0.085 = 0.510 \text{ IN}^2$

CHECK SERVICE LOAD STRESSES AT ℄ SPAN

(-) TENSION
(+) COMPRESSION

$$f_t = \frac{75.4}{218} - \frac{(75.4)(1.79)}{377} + \frac{364.1}{377} = +0.954 < 0.45 f'_c = +2.250 \quad \underline{\text{O.K.}}$$

$$f_b = \frac{75.4}{218} + \frac{(75.4)(1.79)}{380} - \frac{364.1}{380} = -0.257 < 6\sqrt{f'_c} = -0.424 \quad \underline{\text{O.K.}}$$

CHECK ULTIMATE STRENGTH

$P_u = 6 \times 23^K = 138^K$, $d = 4.02 + 1.79 = 5.81$ IN.
$b = 40$ IN.

$$A_{ps} f_{ps} = P_u \left(1 - 0.5 \rho_p \frac{f_{pu}}{f'_c}\right) , \quad \rho_p = \frac{A_{ps}}{bd}$$

$$A_{ps} f_{ps} = 138 \left(1 - 0.5 \frac{0.510}{40 \times 5.81} \times \frac{270}{5}\right) = 129.8^K$$

$$a = \frac{A_{ps} f_{ps}}{0.85 f'_c b} = \frac{129.8}{(0.85)(5)(40)} = 0.764 \text{ IN.}$$

$$M_{MAX} = \phi A_{ps} f_{ps} \left(d - \frac{a}{2}\right) , \quad \phi = 0.9$$

$$M_{MAX} = 0.9 \times 129.8 \left(5.81 - \frac{0.764}{2}\right) = 634.1^{K\text{-}IN} > 570.4^{K\text{-}IN} \quad \underline{\text{O.K.}}$$

10 IN. THICK SLAB

THE SECTION PROPERTIES USED IN THIS DESIGN ARE SHOWN IN FIG. B-3. SPAN = 18.0 FT.

DESIGN LOADS

HEAVY STORAGE, 250 PSF LIVE LOAD
MECHANICAL, MISC., 10 PSF DEAD LOAD

MOMENTS

		$M^{K\cdot IN}$	$\times$ L.F.	$= M_u^{K\cdot IN}$
10 IN. SLAB	$= 0.075 \times 3.33 \times \overline{18.0}^2 \times 1.5 =$	121.4	$\times$ 1.4	$=$ 169.9
LIVE LOAD	$= 0.250 \times 3.33 \times \overline{18.0}^2 \times 1.5 =$	404.6	$\times$ 1.7	$=$ 687.8
DEAD LOAD	$= 0.010 \times 3.33 \times \overline{18.0}^2 \times 1.5 =$	16.2	$\times$ 1.4	$=$ 22.6
		542.2 K·IN		880.3 K·IN

PRESTRESSING FORCE REQUIRED

ASSUME 3/8 IN. DIAMETER STRAND WITH 1½ IN. CLEAR BOTTOM COVER, THEREFORE

$$e = Y_b - 1.5 - \frac{0.375}{2} = 4.91 - 1.69 = 3.22 \text{ IN.}$$

$$f_b = 6\sqrt{f'_c} = 6\sqrt{5000} = 0.424 \text{ KSI}$$

$$P_{REQ} = \frac{\frac{M}{S_b} - f_b}{\frac{1}{A} + \frac{e}{S_b}} = \frac{\frac{542.2}{604} - 0.424}{\frac{1}{272} + \frac{3.22}{604}} = \frac{0.474}{0.0090} = 52.6^K$$

USING 3/8 IN. DIAMETER - 270^K STRANDS

$A_{ps} = 0.085 \text{ IN}^2$ $\qquad P_u = 23^K/\text{STRAND}$

ASSUME 22% PRESTRESS LOSSES AND $f_{se} = 0.7\, f_{pu}$

$P = 23 \times 0.7 \times 0.78 = 12.56^K/\text{STRAND}$

$$\text{STRAND REQ'D} = \frac{52.6}{12.56} = 4.2$$

$\therefore$ USE 6 - 3/8 IN. DIAMETER - 270^K STRAND $= 75.4^K$

$A_{ps} = 6 \times 0.085 = 0.510 \text{ IN}^2$

CHECK SERVICE LOAD STRESSES AT ℄ SPAN

$$f_t = \frac{75.4}{272} - \frac{(75.4)(3.22)}{585} + \frac{542.2}{585} = 0.789 < .45\, f'_c = +2.250 \quad \underline{\text{O.K.}}$$

$$f_b = \frac{75.4}{272} + \frac{(75.4)(3.22)}{604} - \frac{542.2}{604} = -0.218 < 6\sqrt{f'_c} = -0.429 \quad \underline{\text{O.K.}}$$

CHECK ULTIMATE STRENGTH

$P_u = 6 \times 23^K = 138^K$, $d = 5.09 + 3.22 = 8.31$ IN.
$b = 40$ IN.

$$A_{ps} f_{ps} = P_u \left(1 - 0.5 \rho_p \frac{f_{pu}}{f'_c}\right), \quad \rho_p = \frac{A_{ps}}{bd}$$

$$A_{ps} f_{ps} = 138 \left(1 - 0.5 \frac{0.510}{40 \times 8.31} \times \frac{270}{5}\right) = 132.3^K$$

$$a = \frac{A_{ps} f_{ps}}{0.85 f'_c b} = \frac{132.3}{(0.85)(5)(40)} = 0.778$$

$$M_{MAX} = \phi A_{ps} f_{ps} \left(d - \frac{a}{2}\right), \quad \phi = 0.9$$

$$M_{MAX} = 0.9 \times 132.3 \left(8.31 - \frac{0.778}{2}\right) = 943.1^{K\text{-}IN} > 880.3^{K\text{-}IN}$$

FAILURE MODES OF PRESTRESSED CONCRETE SLABS ON CONTINUOUS SUPPORTS

The purpose of this section is to describe the different modes of failure as exhibited by load tests on shore-supported prestressed concrete slabs. It will be shown that each mode can be predicted in terms of the location on the slab span and the shear-to-moment ratio. Figure B-4 shows a typical test slab with a given arrangement of loads and intermediate shore supports. The possible failure modes, as indicated on Figure B-4, and strength prediction equations are described as follows.

① Pure Flexure

This is failure by strand yield or rupture in a section under pure positive bending moment, $M_{①}$, with no shear. The prediction equation is

$$M_{①} = P_u\left(1 - .5\rho\frac{f_{pu}}{f'_c}\right)\left(d - \frac{a}{2}\right)$$

② Negative Moment Flexure

This is the flexural strength of the portion of the beam section at and below the level of the prestressing strand.

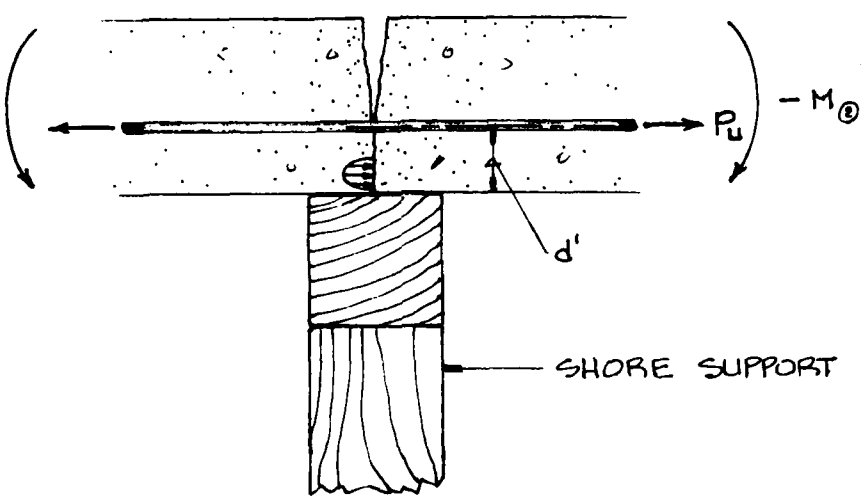

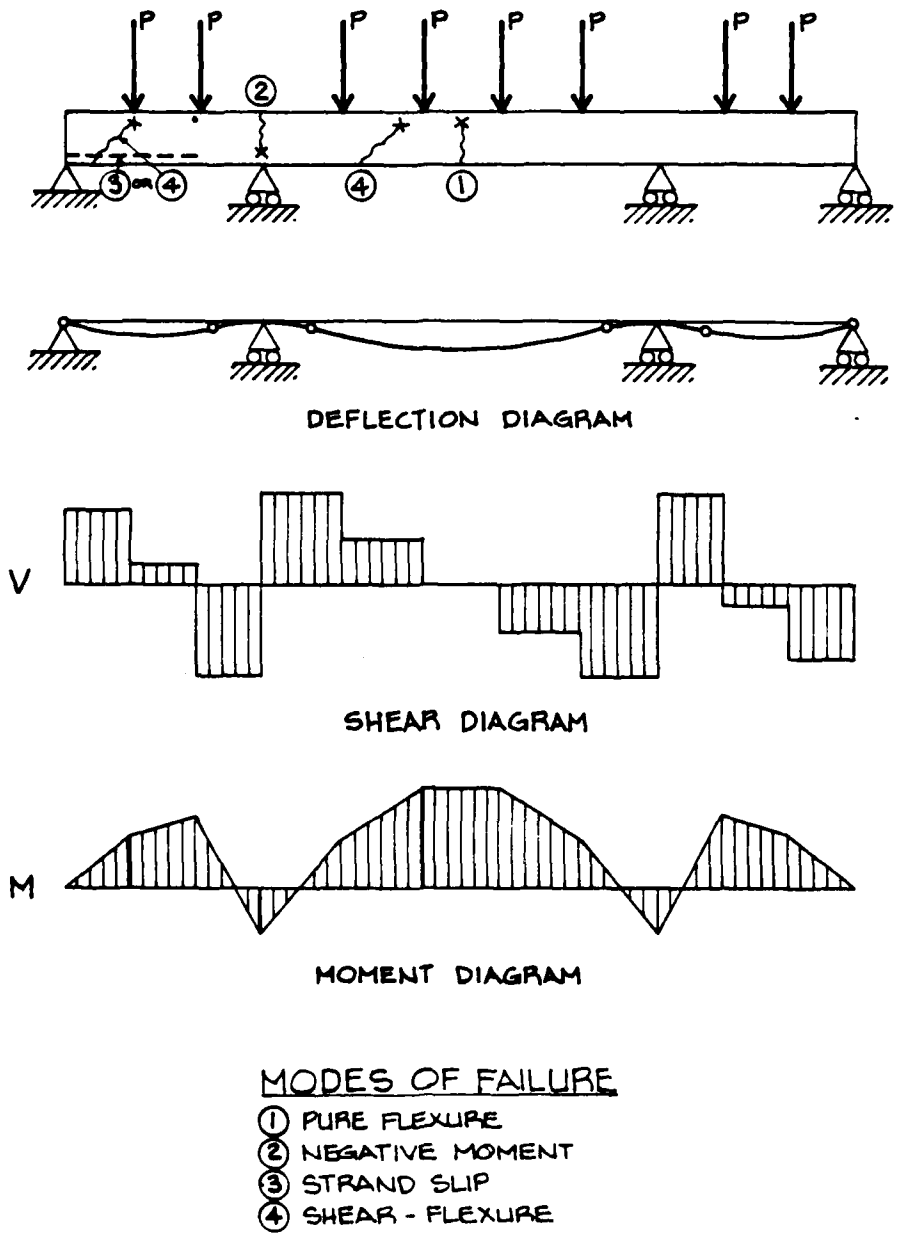

Fig. B-4. Description of Failure Modes.

It is a "broken back" type of failure and is predicted by $P_u d'$

However, during testing, it was found that this mode did not lead to a loss of load-carrying capacity for the supported slab. The mode behavior is of a stable yield hinge, such that the continuous slab span is transformed into a system of three simple spans. The resisting moment, $M_{②}$, is a restraining moment couple for these simple spans.

③ Strand Slip

This mode occurs when the flexural bond stress $u_F = \frac{V}{\Sigma o j d}$ adds to the existing strand transfer bond stress in the outer end spans of the slab. When this combined bond stress exceeds the strand bond capacity, then strand slip, $R_{③}$, occurs and the now "unreinforced" beam section fails in tension cracking or in shear.

The general function of bond in prestressed members is well explained in Janney (Ref. 2):

> "Pre-tensioned steel in prestressed concrete members serves a dual function. Part of the available tensile strength of the steel is used first to establish a compressive prestress in the concrete. Secondly, if a member is loaded beyond cracking, all or part of the steel tensile strength may be utilized to assist the concrete in resisting the externally applied bending moment.
>
> A bond between concrete and steel must exist if concrete is to be prestressed by the pre-tensioning method for with this method the steel is tensioned before the concrete is placed and is released after the concrete has developed sufficient strength. The tension in the steel is transferred to the concrete entirely by bond. The bond which accomplishes this function is referred to herein as the "prestress transfer bond."
>
> Prestress transfer bond is present from the ends of a prestressed member to the beginning of a region in which the steel tension is constant. When the pre-tension force was released slowly, the length required to transfer the pre-tension force to the concrete varied from about 1 to 3 ft from the ends of the members.
>
> The prestressing element in a pre-tensioned flexural member also serves a function similar to that of ordinary reinforcement in concrete which has not been prestressed, that is, it develops

bond stresses as a direct consequence of flexure. The increase in steel stress resulting from flexure of a prestressed member is usually unimportant under normal service conditions, that is, in an uncracked condition. But if cracking occurs, the bond between steel and concrete in the flexure region plays an important part in governing the subsequent performance of the member. Bond which develops as a result of flexure, as distinct from that required to establish the prestress, is referred to as "flexural bond" throughout this report.

In the failure tests of center-loaded beams reported in this paper, flexural bond stresses were relatively low until flexural cracks occurred in the concrete. High steel stresses occurred at these cracks, and in consequence the maximum values of flexural bond stress were found initially adjacent to such cracks in the midspan regions of the beams. As loading continued, however, the high steel stresses spread outward from the crack and the maximum values of flexural bond stress moved from the center toward the beam ends.

Since prestress transfer bond occurred only in the end regions of the beams there was little interaction between flexural bond and prestress bond when cracking first took place. Even at final bond failure, as evidenced by end-slip of the prestressing element, the maximum values of flexural bond stress had moved outward only to a region just overlapping that of the prestress transfer bond. Failure occurred in all cases before high flexural bond stresses developed in the end regions where the maximum prestress transfer bond stresses prevailed."

There is an important interaction between the increase in steel stress due to moment in the transfer length and the transfer bond capacity. One component of transfer bond resistance is the friction as provided by the "Poisson Effect" expansion of the strand against the surrounding concrete cover; this occurs when the strand prestress is initially transferred into the slab. When the slab is loaded, as in these tests, with high flexural steel stress in the transfer zone, then this stress reduces the strand diameter (reverse Poisson effect) and hence also reduces the friction resistance of the strand against the concrete cover. In a simple explanation, the flexural steel stress shrinks the diameter of the strand away from the walls of the concrete duct in which it is embedded. Once separated from contact with these duct walls, the strand is easily drawn through the duct, and strand slip is the result. It is interesting to note that this process of stress-diameter decrease is used to break the adhesion and withdraw

the plastic post-tensioning duct liners from the post-tensioned slabs.

Ref. 3 by Hanson and Kaar offers a reasonable method of predicting the beam strength (shear) at which strand slip may occur in the transfer length portion of the beam. However, it should be recognized that the Ref. 3 recommendations are based on solid rectangular beam sections under laboratory fabrication conditions. Bond slip values may be expected to be lower and certainly more variable for the hollow-core slab sections, as fabricated under mass-production conditions, and with varying amounts of concrete cover (3/4 inch to 2 inches) for the strands. Otherwise, the bond slip curves of Figure 5 from Ref. 3 (see Figure B-5) are reasonably applicable to the slab properties of concrete strength and strand capacities. The value for $u_F = 400$ psi is applicable for all strand sizes.

Mode ③ occurs when the flexural bond stress in strand transfer length is greater than average transfer bond stress:

$$u_F = \frac{V}{\Sigma o\, jd} \geq u_t = 0.40 \text{ ksi}$$

Therefore, $R_{③}$ is $V = \Sigma o\, jd\,(0.40)$

④ Shear Flexure

This is shear failure in a section carrying both shear and positive bending moment. Prediction of the strength of this failure mode depends upon the existence of the prestressing force in the section. Therefore, this mode must be considered for both end span and interior span conditions.

End Span Condition

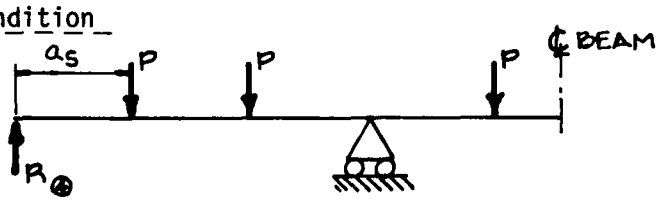

In the end span, shear intensities necessary for shear failure are also large enough to create flexural bond stresses in excess of transfer bond capacity. Hence strand slip and subsequent prestress loss occurs.

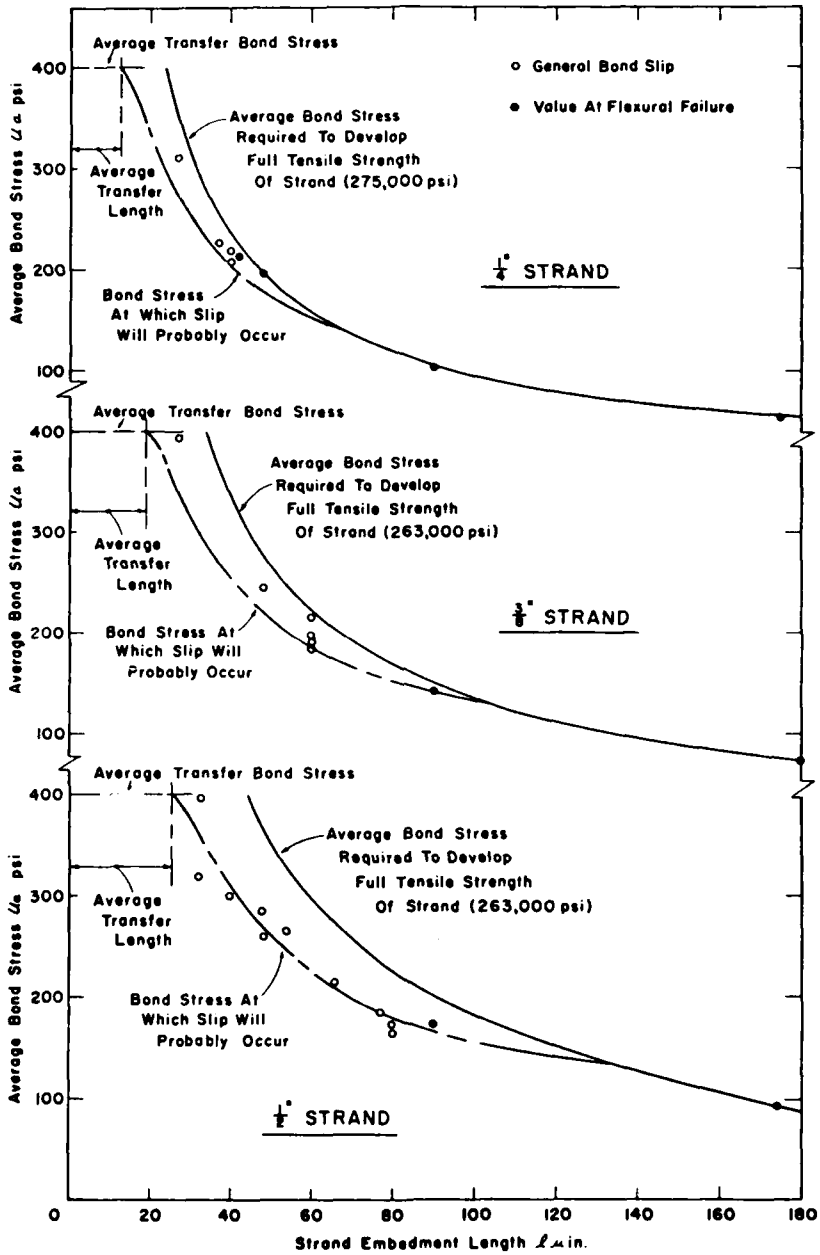

Fig. 5—Relation of average bond stress u_a to strand embedment length

Fig. B-5. Relation of Average Bond Stress to Strand Embedment Length (from Ref. 3).

The resulting end span sections are therefore ordinary reinforced concrete, and the shear failure stress is predicted by

$$v_u = \frac{R_{\oplus}}{A} = 60\left[f'_c\,\rho\,\frac{d}{a_s}\right]^{1/3}$$

$$R_{\oplus} = A v_u$$

(see Ref. 4)

Interior Span Condition

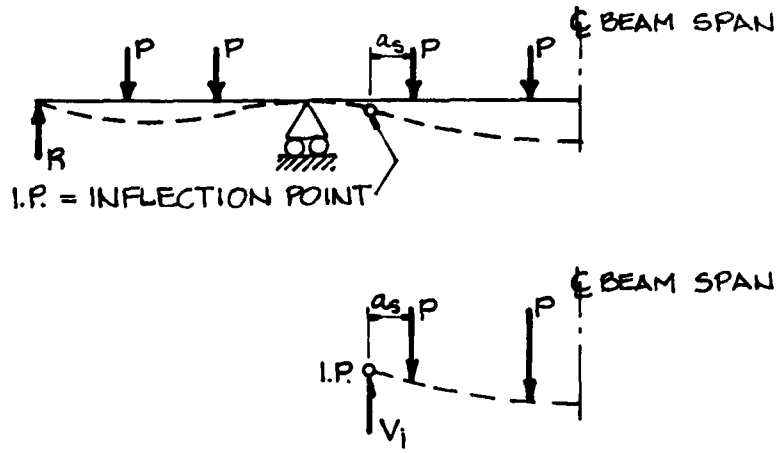

In the interior span there is no possibility of strand slip, and shear strength prediction must include the beneficial effect of the prestressing moment, M_p, on the section. This beneficial effect can be represented by a load-resisting shear, V_p, equal to that shear necessary to cancel out the prestress moment, M_p, in the shear span a_s.

$$V_p = \frac{M_p}{a_s}$$

where a_s is measured from the estimated location of the inflection point to the first interior load point. Then with the prestress moment canceled out by V_p, the remainder of the shear resistance is given by

$$V_u = A(60)\left[f'_c\,\rho\,\frac{d}{a_s}\right]$$

Total interior span shear strength is given by

$$V_{\oplus} = V_u + V_p$$

SUMMARY

The predicted strength for each of the test slabs was calculated, based on the equations presented herein, for each of the applicable failure modes and compared to the actual test value observed for each failure mode. These data are presented in Table B-2. No data are listed for mode $M_{②}$, negative moment flexure, since none of the test slabs failed, nor was predicted to fail, in this mode. The predicted mode of failure (*) on the table was selected by using the ratio value (P_{min}/P_{test}) nearest unity.

In the last column of Table B-2, the values of the ratio of minimum predicted failure load to actual load (P_{min}/P_{test}) are seen to be reasonably close to unity. The low values (0.69, 0.77) indicate that the test slab somehow developed extra high strength, probably caused by extra prestress or by arching effects between load and support pads. The ratios greater than unity (1.06, 1.09) indicate a slightly non-conservative prediction, where the test slab failed early, perhaps because of loss of prestress or a concrete weakness.

It is worthwhile to remark that strand slip in the anchorage zone was a common occurrence in short shear span; it is felt this type of failure might be less likely to occur under uniformly distributed (rather than concentrated) loads.

Finally, the success in strength prediction was largely due to the availablility of the shear stress equation

$$v_u = 60\left[f'_c \rho \frac{d}{a_s}\right]^{1/3}$$

The existing American Concrete Institute Code (ACI 313-77) equation

$$v_u = 1.9\sqrt{f'_c} + 2500\rho \frac{V_u d}{M_w}$$

does not adequately represent the important effects of high moment, M, and low steel percentage, ρ, on the shear strength.

TABLE B-2: CALCULATED VS ACTUAL FAILURE MODE CAPACITIES

Predicted Failure Load, K / Actual Failure Load, K

* Predicted Failure Mode

Test No.	Strand Slip R③	Pure Flexure M①	End Span Shear R④	Interior Span Shear V④	Actual Failure Mode	P_{min} / P_{test}
1	5.1 / 3.25	12.8 / 13.7*	na	na	M①	0.94
2	5.1 / 3.25	12.8 / 13.7*	na	na	M①	0.94
3	5.1 / 7.31	12.8 / 15.4*	8.2 / 7.31	na	M①	0.84
4	5.1 / 11.6*	12.8 / 16.3	9.2 / 11.6*	na	R③ R④	0.79
5	15.2 / 9.0	58.8 / 54.0*	na	na	R③ M①	1.09
6	15.2 / 14.9	58.8 / 44.8	15.7 / 14.9*	na	R③ R④	1.06
7	15.2 / 15.8	58.8 / 47.5	15.7 / 15.8*	na	R③ R④	0.99
8	15.2 / 18.2	58.8 / 36.4	18.3 / 18.2*	na	R③ R④	1.01
9	15.2 / 13.9	58.8 / 79.0*	20.5 / 13.9	34.4 / 38.0*	V④ M①	0.91
10	21.6 / 18.5	87.1 / 111*	na	na	M①	0.77
11	21.6 / 31.2*	87.1 / 89.5*	19.8 / 31.2*	na	R③ R④	0.97
12	21.6 / 32.2*	87.1 / 92.5*	19.8 / 32.2*	na	R③ R④	0.94
13	21.6 / 33.0*	87.1 / 66.0	22.8 / 33.0*	na	R③ R④	0.69
14	21.6 / 21.4	87.1 / 118.0*	25.3 / 21.4	48.8 / 50.0*	V④	0.98
15	21.6 / 19.7	87.1 / 109.0	25.3 / 19.7	48.8 / 46.0*	V④	1.06

References

1. Building Code Requirements for Reinforced Concrete (ACI 318-71, American Concrete Institute, Detroit Michigan.

2. Janney, Jack R., "Nature of Bond in Pre-Tensioned Prestressed Concrete," Journal of the American Concrete Institute, V. 25, No. 9, May 1954, reprinted by Portland Cement Association.

3. Hans , Norman W. and Paul H. Kaar, "Flexural Bond Tests of Pre-Tensioned Pres essed Beams," Journal of the American Concrete Institute, January 1959, reprinted by Portland Cement Association.

4. Suggested Revisions to Shear Provisions for Building Codes, ACI Committee Report, American Concrete Institute, Detroit, Michigan.

DISTRIBUTION LIST

(one copy each unless otherwise specified)

Federal Emergency Management Agency
Mitigation and Research
Attn: Administrative Officer
Washington, D.C. 20472 (60)

Assistant Secretary of the Army (R&D)
Attn: Assistant for Research
Washington, D.C. 20301

Chief of Naval Research
Washington, D.C. 20360

Mr. Phillip M. Smith
Associate Director,
Natural Resources and Commercial Services
Office of Science and Technology Policy
Executive Office Bldg
Washington, D.C. 20500

Defense Technical Information Center
Cameron Station
Alexandria, VA 22314 (12)

Civil Defense Research Project
Oak Ridge National Laboratory
Attn: Librarian
P.O. Box X
Oak Ridge, TN 37830

Mr. Edward L. Hill
Research Triangle Institute
Post Office Box 12194
Research Triangle Park
North Carolina 27709

Commanding Officer
U.S. Naval Civil Engineering Laboratory
Attn: Document Library
Port Hueneme, CA 93041

AFWL/Civil Engineering Division
Attn: Technical Library
Kirtland Air Force Base
Albuquerque, NM 87117

Director, U.S. Army Engineer Waterways Experiment Station
Post Office Box 631
Vicksburg, MS 39180

Dikewood Corporation
1613 University Blvd, N.E.
Albuquerque, NM 39180

Department of Energy
Office of Environment
Operational and Environmental Safety Division (EV131)
Environmental Protection and Public Safety Branch
Attn: L.J. Deal
Dr. Rodolf J. Englemann
Washington, D.C. 20545

GARD, Inc.
7449 North Natchez Avenue
Niles, IL 60648

Director
Ballistic Research Laboratory
Attn: Document Library
Aberdeen Proving Ground, MD 21005

Civil Engineering Center/AF/PRECET
Attn: Technical Library
Wright-Patterson Air Force Base
Dayton, OH 45433

Director, Army Materials and
Mechanics Research Center
Attn: Technical Library
Watertown, MA 02170

The Rand Corporation
Attn: Document Libarary
1700 Main Street
Santa Monica, CA 90401

Director, U.S. Army Engineer
Waterways Experiment Station
Attn: Document Library
Post Office Box 631
Vicksburg, MS 39180

Mr. Donald A. Bettge
Mitigation and Research
Federal Emergency Management Agency
1725 I Street, N.W.
Washington, D.C. 20472

Dr. Lewis V. Spencer
Radiation Theory Section 4.3
National Bureau of Standards
Washington, D.C. 20234

Mr. Anatole Longinow
IIT Research Institute
10 West 35th Street
Chicago, IL 60616

Mr. Chuck Wilton
Scientific Service, Inc.
517 East Bayshore
Redwood City, CA 94063

Mr. Samuel Kramer, Chief
Office of Federal Building Technology
Center for Building Technology
National Bureau of Standards
Washington, D.C. 20234

Dr. Clarence R. Mehl
Department 5230
Sandia Corporation
Box 5800, Sandia Base
Albuquerque, NM 87115

Director, Defense Nuclear Agency
Attn: Mr. Tom Kennedy
Washington, D.C. 20305

Director, Defense Nuclear Agency
Attn: Technical Library
Washington, D.C. 20305

Emergency Technology Division
Oak Ridge National Laboratory
Post Office Box X
Oak Ridge, TN 37830
Attn: Librarian

Technology & Management Consultants
1850 N. Whitley Avenue
Suite 916
Hollywood, CA 90028

Defense Logistics Agency
Civil Preparedness Office
Richmond, VA 23297

H.L. Murphy Associates
Box 1727
San Mateo, CA 94401

Department of Energy
Headquarters Library, G-49
Washington, D.C. 20545

Disaster Research Center
Ohio State University
404B West 17th Avenue
Columbus, OH 43210

Dr. Charles Fritz
National Academy of Sciences
2101 Constitution Avenue
Washington, D.C. 20418

Dr. Leon Goure
Science Applications, Inc.
1710 Goodridge Dr.
P.O. Box 1303
McLean, VA 22102

Agbabian Associates
250 North Nash Street
El Segundo, CA 90245

Bell Telephone Laboratories
Whippany Road
Whippany, NJ 07981
Attn: Mr. E. Witt
Mr. R. May
Mr. J. Foss

Ballistic Research Library
Attn: Librarian
Aberdeen Proving Ground, MD 21005

Mr. Jack C. Greene
Greenewood
Route 4 - Box 85A
Bakerville,NC 28705

Dr. William Chenault
Human Science Research
Westgate Industrial Park
P.O. Box 370
McLean, VA 22010

University of Florida
Civil Defense Technical Services Center
College of Engineering
Department of Engineering
Gainesville FL 32601

Dr. Leo Schmidt
Institute for Defense Analysis
400 Army-Navy Drive
Arlington, VA 22202

Mr. James E Beck and Associates
4216 Los Palos Avenue
Palo Alto, CA 94306

Science Applications, Inc.
1710 Goodridge Drive
P.O. Box 1303
McLean, VA 22102

Mr. Kenneth Kaplan
Management Science Associates
P.O. Box 239
Los Altos, CA 94022

Research Institute of Protective Construction
Attn: Mr. J. Gut
2 AUF DER NAUER
CH — 8001 Zurich
SWITZERLAND

Sandia National Laboratory
Box 5800
Albuquerque, NM 87185

Los Alamos Scientific Laboratory
Attn: Document Library
Los Alamos, NM 87544

Mr. Richard. K. Laurino
Center for Planning and Research, Inc.
2483 E. Bayshore Road
Palo Alto, CA 94303

Nuclear Engineering Department
Duncan Annex
Purdue University
Lafayette, IN 47907

UPGRADING OF EXISTING STRUCTURES: PHASE III Unclassified
SHELTER DESIGN OPTIONS

Scientific Service, Inc., Redwood City, CA, May 1981
Contract No. EMW-C-0153, Work Unit 1128A 262 pages

This report presents the results of an investigation of blast upgrading of existing structures, which consisted of developing failure prediction methodologies for various structure types, both in "as built" and in upgraded configurations, and verifying these prediction techniques with full-scale load tests.

These upgrading schemes were developed for use as shelters in support of Civil Defense crisis relocation planning. Structure types investigated included wood, steel, and concrete floor and roof systems.

The results of this study are being used in the development of a shelter manual presenting the various upgrading concepts in an illustrative workbook form for use in the field.

UPGRADING OF EXISTING STRUCTURES: PHASE III Unclassified
SHELTER DESIGN OPTIONS

Scientific Service, Inc., Redwood City, CA, May 1981
Contract No. EMW-C-0153, Work Unit 1128A 262 pages

This report presents the results of an investigation of blast upgrading of existing structures, which consisted of developing failure prediction methodologies for various structure types, both in "as built" and in upgraded configurations, and verifying these prediction techniques with full-scale load tests.

These upgrading schemes were developed for use as shelters in support of Civil Defense crisis relocation planning. Structure types investigated included wood, steel, and concrete floor and roof systems.

The results of this study are being used in the development of a shelter manual presenting the various upgrading concepts in an illustrative workbook form for use in the field.

UPGRADING OF EXISTING STRUCTURES: PHASE III Unclassified
SHELTER DESIGN OPTIONS

Scientific Service, Inc., Redwood City, CA, May 1981
Contract No. EMW-C-0153, Work Unit 1128A 262 pages

This report presents the results of an investigation of blast upgrading of existing structures, which consisted of developing failure prediction methodologies for various structure types, both in "as built" and in upgraded configurations, and verifying these prediction techniques with full-scale load tests.

These upgrading schemes were developed for use as shelters in support of Civil Defense crisis relocation planning. Structure types investigated included wood, steel, and concrete floor and roof systems.

The results of this study are being used in the development of a shelter manual presenting the various upgrading concepts in an illustrative workbook form for use in the field.

UPGRADING OF EXISTING STRUCTURES: PHASE III Unclassified
SHELTER DESIGN OPTIONS

Scientific Service, Inc., Redwood City, CA, May 1981
Contract No. EMW-C-0153, Work Unit 1128A 262 pages

This report presents the results of an investigation of blast upgrading of existing structures, which consisted of developing failure prediction methodologies for various structure types, both in "as built" and in upgraded configurations, and verifying these prediction techniques with full-scale load tests.

These upgrading schemes were developed for use as shelters in support of Civil Defense crisis relocation planning. Structure types investigated included wood, steel, and concrete floor and roof systems.

The results of this study are being used in the development of a shelter manual presenting the various upgrading concepts in an illustrative workbook form for use in the field.

LMED

8